Semiconductor Polymer Architectures using Click Chemistry and Controlled Radical Polymerization

DISSERTATION

zur Erlangung des akademischen Grades
eines Doktors der Naturwissenschaften (Dr. rer. nat.)
im Fach Chemie der Fakultät für
Biologie, Chemie und Geowissenschaften der Universität Bayreuth

vorgelegt von
Andreas Sebastian Lang

Geboren in Naila / Deutschland

Bayreuth, 2011

Die vorliegende Arbeit wurde in der Zeit von November 2008 bis Juli 2011 am Lehrstuhl für Angewandte Funktionspolymere/Makromolekulare Chemie I unter der Betreuung von Prof. Dr. Mukundan Thelakkat angefertigt.

Vollständiger Abdruck der von der Fakultät für Biologie, Chemie und Geowissenschaften der Universität Bayreuth genehmigten Dissertation zur Erlangung des akademischen Grades eines Doktors der Naturwissenschaften (Dr. rer. nat.)

Dissertation eingereicht am: 01.August 2011
Wissenschaftliches Kolloquium: 07. Dezember 2011

Prüfungsausschuss:

Erstgutachter: Prof. Dr. Mukundan Thelakkat
Zweitgutachter: Prof. Dr. Axel H. E. Müller
Vorsitzender: Prof. Dr. Georg Papastavrou
Prof. Dr. Birgit Weber

Amtierende Dekanin: Prof. Dr. Beate Lohnert

Jeder sieht, was du scheinst. Nur wenige fühlen, wie du bist.

Niccolò Machiavelli

Meiner Familie

Table of Content

1.	**Summary**	**1**
2.	**Zusammenfassung**	**5**
3.	**Introduction**	**9**
	3.1 Motivation	9
	3.2 Controlled Radical Polymerization	10
	3.3 Click Chemistry	17
4.	**Overview**	**33**
	Individual Contributions to Joint Publications	53
5.	**NMRP versus "Click" Chemistry for the Synthesis of Semiconductor Polymers Carrying Pendant Perylene Bisimides**	**57**
6.	**Modular Synthesis of Poly(perylene bisimides) using "Click" Chemistry: A Comparative Study**	**85**
7.	**Highly Efficient Electron-Transport Side-Chain Perylene Polymers**	**111**
8.	**Semiconductor Nanoparticles from Donor-Acceptor Dual Brush Block Copolymers**	**127**
9.	**Semiconductor Dendritic-Linear Block Copolymers by Nitroxide Mediated Radical Polymerization**	**145**
10.	**"Click" Chemistry for p-Type Semiconductor Materials**	**159**
11.	**Semiconductor Block Copolymers: The Influence of Polar Substitution on Microphase Separation**	**169**
	List of Publications	**181**
	Danksagung	**183**
	Erklärung	**187**

Chapter 1

Summary

This thesis deals with the synthesis and characterization of side-chain semiconductor homopolymers and block copolymers for the application in organic photovoltaics (OPV). Special attention lies on the development and application of modern synthetic techniques for the easy and reproducible synthesis of such polymers, also in higher quantities. Controlled radical polymerization, such as nitroxide mediated radical polymerization (NMRP) and reversible addition-fragmentation chain transfer polymerization (RAFT), and its combination with polymer analogous reactions, such as copper-catalyzed azide-alkyne cycloaddition (CuAAC, "click" chemistry), was applied successfully to develop new complex semiconductor polymer architectures. With this method, a general approach for the synthesis of side-chain semiconductor polymers could be generated. Two kinds of scaffold polymers, poly(propargyl acrylate) and poly(propargyl oxystyrene) were used. "Click" chemistry allows the tuning of the thermal, structural, electrical and optical properties by modular substitution with different semiconductor moieties. We analyzed thermotropic phase behavior and structural properties of the synthesized polymers extensively by different methods like differential scanning calorimetry (DSC), temperature-controlled polarized optical microscopy (POM) and temperature-controlled X-ray diffraction (XRD) experiments. Nanostructured assemblies were studied by transmission electron microscopy (TEM) and atomic force microscopy (AFM).

In the first part of this work, the general principle of attaching the n-type semiconductor perylene bisimide (PBI) to a polymer backbone by azide-alkyne "click" chemistry was studied. Here, an azide functionalized PBI was "clicked" to poly(propargyl acrylate). We were able to resolve the fundamental question of the comparability of the resulting "clicked" polymer with polymers having similar structure, but which were directly synthesized by controlled radical polymerization of perylene bisimide acrylates. A structure property relationship was gained. We demonstrated that "clicked" and directly polymerized materials are comparable in their thermotropic and structural behavior. Therefore poly(perylene bisimide)s (PPBI) from direct polymerization could be substituted with "clicked" ones in OPV applications. This solves a variety of issues in the direct nitroxide mediated radical polymerization of perylene bisimide acrylates.

Subsequently, a series of differently substituted PPBIs with narrow PDIs of 1.09 was synthesized to elucidate the influence of the substitution pattern of PBI on thermal and structural behavior of the polymers, which was shown here for the first time. Two types of pendant PBIs were "clicked" to poly(propargyl oxystyrene) by copper-catalyzed azide-alkyne cycloaddition; those carrying hydrophilic oligoethylene glycol (OEG) swallow-tail substituents or those carrying hydrophobic alkyl swallow-tail substituents. In each series, the length of the spacer between the nitrogen of the triazole unit and the nitrogen of the PBI is varied from $(CH_2)_6$ to $(CH_2)_8$ and to

$(CH_2)_{11}$. Thus, the polymers carrying hydrophilic OEG swallow-tails were systematically compared with PPBIs bearing alkyl swallow-tails. The study revealed that the introduction of OEG swallow-tail substituents at the imide position leads to amorphous polymers while short spacers and alkyl swallow-tail substituents allow a liquid crystalline smectic C order in the polymers. This work is to our knowledge the first report of amorphous PPBIs and smectically ordered PPBIs.

By having the possibility to attach diverse chromophores to a polymer backbone, perylene derivatives such as perylene diester benzimidazole (PDB), which exhibits an extended absorption up to 700 nm, and perylene diester imide (PDI) with blue-shifted absorption, were synthesized as azides. These building blocks were then "clicked" to the poly(propargyl oxystyrene) backbone. The optical, electrical, structural and thermal properties were determined for these polymers, gaining insights into new classes of polymeric materials. To elucidate the suitability of perylene polymers from "click" reactions for electronic application, we studied the charge carrier mobility of four different perylene polymers in single carrier devices by fitting the space charge limited current (SCLC) according to Mott-Gurney equation. Some of the polymers exhibited excellent electron transport properties for n-type polymers with mobilities up to 5.5×10^{-3} $cm^2V^{-1}s^{-1}$ which was found for amorphous PPBI, followed by liquid crystalline PPBI with 6.9×10^{-4} $cm^2V^{-1}s^{-1}$ and liquid crystalline poly(perylene benzimidazole diester) with 1.0×10^{-4} $cm^2V^{-1}s^{-1}$.

In a next step, the gained experience in the synthesis of n-type polymers was transferred to the synthesis of a p-type semiconductor side-chain polymer. An azide carrying tetraphenyl benzedine derivative was synthesized and could be "clicked" to poly(propargyl oxystyrene) successfully by copper-catalyzed azide–alkyne cycloaddition, using the principles developed before.

Another way to gain complex polymer architecture through the application of "click" chemistry was the synthesis of donor-acceptor block copolymers which are comprised of a hydrophobic triphenylamine block and a PPBI block which was synthesized by "click" chemistry with either hydrophobic or hydrophilic PBI substituents. The focus lay on the phase separation of the block copolymers. It could be shown by AFM measurements that short block copolymers, where one block carries hydrophilic PBIs, show distinct phase separation, while short block copolymers substituted with hydrophobic PBIs do not show phase separation. This could be attributed to the higher χ parameter in the hydrophilic-hydrophobic block copolymer. Further supplementary studies are required here to elucidate the bulk and film morphology.

In a second part of the thesis, novel donor-acceptor block copolymer architectures were investigated. As a completely new structural concept for donor-acceptor block copolymers, a donor-acceptor dibrush block copolymer was synthesized successfully. This was accomplished by innovatively combining a "grafting from" RAFT-polymerization of a triphenylamine-donor monomer, with a "grafting to" approach of a PPBI acceptor polymer for which "click" chemistry was utilized. Nanoparticles of 60 nm in diameter could be obtained from this dibrush block copolymer.

Finally, another new structural concept was presented with a donor-acceptor dendritic-linear hybrid block copolymer. Here a linear PPBI acceptor block was polymerized from a second

generation dendron macroinitiator, carrying triphenylamine, by nitroxide mediated radical polymerization.

To sum up, this work demonstrates the vast applicability of “click” chemistry and controlled radical polymerization techniques such as NMRP and RAFT for the synthesis of highly complex semiconductor polymer architectures and builds the foundation for a simplified and upscalable synthetic procedure for semiconductor polymers and block copolymers.

Chapter 2

Zusammenfassung

Diese Dissertation beschäftigt sich mit der Synthese und Charakterisierung von halbleitenden Seitenkettenpolymeren und –blockcopolymeren für die Anwendung in organischen Photovoltaik-Bauelementen. Besonderer Augenmerk liegt dabei auf der Entwicklung und der Anwendung von modernen Synthesetechniken für die einfache und reproduzierbare Synthese solcher Polymere, auch im größeren Maßstab. Methoden zur kontrollierten radikalischen Polymerisation wie NMRP und RAFT, die zu wohldefinierten Polymeren mit enger Molekulargewichtsverteilung führen können, und ihre Kombination mit polymeranalogen Reaktionen, wie der Kupfer-katalysierten Azid-Alkin Zykloaddition („Klick“ Chemie), wurden erfolgreich dazu verwendet komplexe Polymerarchitekturen zu synthetisieren. Mit dieser Methode sollte ein genereller Ansatz für die Synthese von halbleitenden Seitenkettenpolymeren entwickelt werden. Zwei Arten von Gerüstpolymeren, Poly(Propargylacrylat) und Poly(Propargyloxystyrol), wurden dabei verwendet. „Klick“ Chemie sollte es ermöglichen die thermischen, strukturellen, elektronischen und optischen Eigenschaften des Polymers durch eine modulare Substitution mit unterschiedlichen Halbleiterresten einzustellen. Das thermotrope Phasenverhalten der synthetisierten Polymere analysierten wir umfassend mittels Differentieller Wärmeflusskalorimetrie (DSC), temperaturabhängiger Polarisationsmikroskopie (POM), sowie temperaturabhängiger Röntgendiffraktometrie (XRD). Nanostrukturierte Aggregate wurden mittels Transmissions-Elektronen-Spektroskopie (TEM) und Rasterkraftmikroskopie (AFM) untersucht.

In einem ersten Teil der Arbeit wurde generell untersucht, wie Perylendiimid (PBI) mittels Azid-Alkin „Klick“ Chemie an eine Polymerhauptkette angebracht werden kann. Dazu wurde ein Azid-funktionalisiertes PBI an Poly(Propargylacrylat) „geklickt“. Es gelang uns die fundamentale Frage der Vergleichbarkeit der resultierenden „geklickten“ Polymere mit Polymeren, die eine ähnliche Struktur besitzen, aber durch kontrollierte radikalische Polymerisation hergestellt wurden, zu klären. Erste Ergebnisse einer Struktur-Eigenschafts-Beziehung wurden gewonnen. Es wurde gezeigt, dass diese Polymere in ihrem thermotropen und strukturellen Verhalten durchaus vergleichbar sind. Es sollte also möglich sein Poly(Perylendiimid)e (PPBI), die durch direkte Polymerisation hergestellt wurden, in organischen Photovoltaikanwendungen durch „geklickte“ Polymere zu ersetzen. Dies löst eine Vielzahl an Problemen, die in der direkten Nitroxid-vermittelten radikalischen Polymerisation von Perylendiimidacrylat auftreten.

Anschließend wurde eine Reihe von unterschiedlich substituierten PPBIs mit niedrigen Molekulargewichtsverteilungen von 1.09 synthetisiert, um herauszufinden wie unterschiedliche Substitutionsmuster des PBIs das thermische und strukturelle Verhalten der Polymere beeinflussen. Dies wurde hier zum ersten Mal gezeigt. Dazu wurden zwei unterschiedliche Arten

von PBIs durch „Klick“-Chemie an die Poly(Propargyloxystyrol) Hauptkette angebracht. Die einen tragen hydrophile Oligoethylenglykol Schwalbenschwanz-Substituenten, die anderen hydrophobe Alkyl-Schwalbenschwanz-Substituenten. In beiden Reihen wurde die Länge der Alkylkette zwischen dem Stickstoff des gebildeten Triazolrings und dem Stickstoff des PBIs von $(CH_2)_6$ über $(CH_2)_8$ zu $(CH_2)_{11}$ variiert. Auf diese Weise konnten die Polymere, die hydrophile Oligoethylenglykol-Substituenten tragen, systematisch mit den Polymeren, die hydrophobe Alkyl-Substituenten tragen, verglichen werden. Die Studie ergab, dass die Substitution mit Oligoethylenglykol-Schwalbenschwänzen an der Perylen Imid-Position zu amorphen Polymeren führt, während Alkyl-Schwalbenschwanz-Substituenten zu flüssigkristallinem smektisch C Verhalten führten. Diese Arbeit ist nach unserem Wissen der erste Bericht eines amorphen PPBIs und eines PPBIs das eine smektisch C Phase aufweist.

Da nun die Möglichkeit bestand verschiedenste Farbstoffe an einer Polymerhauptkette zu befestigen wurden neue Perylenderivate wie beispielsweise Perylendiesterbenzimidazol, das eine erweiterte Absorption bis zu 700 nm aufweist, und Perylendiesterimid, mit einer blauverschobenen Absorption, als Azid synthetisiert. Diese Bausteine wurden dann an das Poly(Propargyloxystyrol) Rückgrat „geklickt“. Die optischen, elektronischen, strukturellen und thermischen Eigenschaften dieser Polymere wurden ermittelt, was den Einblick in neue Klassen an Polymermaterialien ermöglichte. Um die Eignung der „geklickten“ Perylen-Polymere für elektronische Anwendungen aufzuklären, wurde die Ladungsträgermobilität von vier unterschiedlichen Polymeren in *Single Carrier Devices* gemessen und durch Auswertung mit der *Space Charge Limited Current* Methode bestimmt. Für n-Typ Polymere zeigten einige der Verbindungen ausgezeichnete Elektronentransport-Fähigkeiten mit Mobilitäten bis zu 5.5×10^{-3} $cm^2V^{-1}s^{-1}$ für amorphes PPBI, 6.9×10^{-4} $cm^2V^{-1}s^{-1}$ für flüssigkristallines PPBI und 1.0×10^{-4} $cm^2V^{-1}s^{-1}$ für flüssig-kristallines Poly(Perylendiesterbenzimidazol).

In einem nächsten Schritt wurde die gewonnene Erfahrung mit der Synthese von n–Typ Polymeren auf die Synthese von p-Typ Polymere übertragen. Dazu wurde ein Azid-funktionalisiertes Tetraphenylbenzedin synthetisiert und erfolgreich an Poly(Propargyloxystyrol) „geklickt“.

Ein anderer Weg, komplexe Polymerarchitekturen durch die Anwendung von „Klick“-Chemie zu erlangen ist die Synthese von Donor-Akzeptor Blockcopolymeren, die aus einem hydrophoben Triphenylaminblock und einem PPBI Block bestehen, welcher durch „Klick“ Chemie entweder aus hydrophilen oder aus hydrophoben PBIs synthetisiert wurde. Der Fokus der Arbeit lag dabei auf der Phasenseparation der Blockcopolymere. Es konnte gezeigt werden, dass kurze Blockcopolymere, die mit hydrophilen Perylendiimiden substituiert waren, eine ausgeprägtere Phasenseparation zeigten. Die entsprechenden Polymere, die mit hydrophoben Perylendiimidderivaten substituiert waren, zeigten keine Phasenseparation. Dies konnte dem höheren χ Parameter der hydrophilen-hydrophoben Blockcopolymere zugerechnet werden. Weiterführende Studien sind notwendig, um die genauen Feststoff- und Dünnfilmmorphologien der Proben aufzuklären.

In einem zweiten Teil dieser Dissertation wurden neuartige Donor-Akzeptor Blockcopolymer-Architekturen erforscht. Als komplett neues Strukturkonzept für Donor-Akzeptor

Blockcopolymere wurde ein Doppelbürsten-Blockcopolymer erfolgreich synthetisiert, indem, ausgehend von einem funktionellen Blockcopolymer, auf innovative Art und Weise die RAFT Polymerisation eines Triphenylamin-Donor-Monomers und die „Klick“ Reaktion mit einem PPBI Akzeptorpolymer kombiniert wurden. Aus dem erhaltenen Doppelbürsten-Blockcopolymer konnten 60 nm große Partikel erhalten werden.

Des Weiteren konnte als neues Strukturkonzept auch ein Donor-Akzeptor dendritisch-lineares Hybrid-Blockcopolymer gezeigt werden, dass durch Anpolymerisieren von PBI an ein Triphenylamin-tragendes Dendron zweiter Generation erhalten werden konnte.

Zusammenfassend präsentiert diese Arbeit die umfassende Anwendbarkeit von „Klick“ Chemie und Techniken der kontrollierten radikalischen Polymerisation, wie NMRP und RAFT, für die Synthese von hochkomplexen Halbleiter-Polymerarchitekturen und bildet die Grundlage für eine vereinfachte und hochskalierbare Vorgehensweise für die Synthese von Halbleiterpolymeren und Blockcopolymeren.

Chapter 3

Introduction

3.1 Motivation

Since the beginning of the 20th century, the development and application of synthetic polymers has become a valuable supplementation of materials such as metal, wood, glass, ceramic, wool and cotton. In the course of technological progress, the requirements to polymeric materials continuously grew larger with every new area of application. Today's production of polymers spans mass products as polyethylene, functional polymers as polycarbonate and high performance polymers as aramids as well as very specialized polymers for niche applications. The diversity of specific properties of the polymers arises from the vast range of usable monomers, variation of processing parameters and the possible modification and blending with additives and other materials. Through this, polymers can, for example, exhibit high mechanical toughness, optical clarity, biodegradability, biocompatibility, electrical conductivity or semiconductor behavior. The knowledge about structure-property-relationships and polymerization techniques, which guaranty a controlled composition and molecular architecture of the polymers, are of crucial importance to be able to prepare such tailor-made materials. Especially semiconductor polymers and block copolymers demand a high degree of perfection in their synthesis and are probably the most complex functional polymers synthesized up to now. Starting from the demonstration of electrical conductivity in doped conjugated polymers by Heeger, Diarmid and Shirakawa in the late 70s (Nobel Prize in chemistry in 2000), a bunch of applications such as organic light emitting devices (OLED),[1] organic field effect transistors (OFET)[2, 3] and organic photovoltaics (OPVs)[4] has emerged by now. Semiconductor polymers are either based on conjugated polymers, e.g. poly(3-hexylthiophene) or carry their semiconductor moieties as side-chains attached to the polymer backbone. In general, one can differentiate between electron acceptor (n-type) and electron donor (p-type) semiconductors, depending on the position of the HOMO and LUMO levels of the respective compounds and their charge carrier mobility. The synthesis of such polymers, which possess exactly defined electronic, optical, structural and thermal properties, requires an enormous synthetic effort and a combination of various techniques.

This thesis is concerned with the development and application of modern synthetic techniques for the easy and reproducible synthesis of such semiconductor polymers, which will allow their production in higher quantities in the future. Controlled radical polymerization, which leads to well-defined polymers with narrow molecular weight distributions, and its combination with polymer analogous reactions, such as copper-catalyzed azide-alkyne cycloaddition (CuAAC, "click"

chemistry), is applied successfully to develop new complex semiconductor polymer architectures. Thereby, a general approach for the synthesis of side-chain semiconductor polymers could be generated, which allowed the tuning of the thermal, structural, electronic and optical properties by modular substitution with different semiconductor units. In the following parts, the key features of the synthetic concepts "*controlled radical polymerization*" and "*click chemistry*" are discussed in detail and a short review of relevant literature is given.

3.2 Controlled Radical Polymerization (CRP)

Among different polymerization techniques, radical polymerization methods stand out due to their low experimental effort, enhanced functional group tolerance and broad application area.[5] Nevertheless, conventional free radical polymerization has the drawback of producing only broadly distributed polymers with no ideal control over molecular weight. This is due to side reactions such as the recombination of two growing radicals, disproportionation of two radicals into an unsaturated and a saturated chain-end and transfer reactions of a radical to monomer, solvent or another polymer chain. Also, the initiator does not start all chains at the same time. The initiating radicals are generated over a fragmentation process from a compound which has a longer half-life and thus initiation takes place over a longer period. In contrast, in an ideal "living" polymerization, all chains are initiated at the beginning of the process, grow at a similar rate and survive the polymerization without any irreversible chain transfer or termination. The termination problems of free radical polymerization can be partly avoided by using the so called controlled radical polymerization (CRP) methods.[6] These techniques minimize the rate of termination R_t by reducing the concentration of radicals in the solution. As can be seen from Equation 1, the rate of termination R_t is dependent on the square of the radical concentration [P·]. This is because two radicals have to react with each other for termination. Equation 2 gives the linear dependency of the rate of propagation, R_p on the radical concentration. When the two equations are set into relation with each other, as in Equation 3, it is clear that the ratio R_t/R_p should be small, if a controlled polymerization with a minimal amount of dead chains is desired.[7] A lower ratio of R_t/R_p can be obtained by reducing the concentration of free radicals in the reaction. To accomplish this, different strategies can be pursued.

$$R_t = k_t[P\cdot]^2 \qquad (1)$$

$$R_p = k_p[P\cdot][M] \qquad (2)$$

$$R_t / R_p = k_t[P\cdot] / k_p[M] \qquad (3)$$

All strategies share the fact that they are based on an equilibrium between a dormant species and an active radical species. Here, the radical species is active for a very short time and is terminated reversibly to the dormant species. The equilibrium lies on the side of the dormant species. Some important common aspects in all these polymerization techniques are that a quantitative initiation takes place, that the reversible deactivation of propagating radicals is rapid and that all chains begin to grow at the same time (in contrast to free radical polymerization,

where chains are initiated over a longer period of time). Under these conditions, molecular weights can increase linearly with conversion and molecular weight distributions can be very narrow. After the polymerization the major part of the polymers will comprise of dormant chains, still carrying their active end group. These macroinitiators can be easily reinitiated to form block copolymers even without storing them under inert gas or at low temperatures.

The three main types of CRP are nitroxide mediated radical polymerization (NMRP), reversible addition-fragmentation chain transfer polymerization (RAFT) and atom transfer radical polymerization (ATRP). In the following, the three methods shall be discussed in more detail.

Nitroxide Mediated Radical Polymerization (NMRP)

Nitroxide Mediated Radical Polymerization (NMRP)[8, 9] is based on a thermal equilibrium between an alkoxyamine as end capped dormant species and its active radical species, which is able to initiate/grow the polymer.[10] The equilibrium lies on the side of the dormant species. Thus, the concentration of active growing radicals is reduced and therefore termination by coupling reactions between two radicals and disproportionation are less likely to occur. The used initiating systems can be basically separated into bimolecular and unimolecular initiators. Bimolecular initiators were used in the early days of NMRP. Here, the polymerization is started by a conventional radical initiator such as azo-bis-(isobutyronitril) (AIBN) in the presence of a stable nitroxide radical which does not react with another nitroxide but only with a propagating radical. The produced free radicals are reversibly terminated by the nitroxide and form the controlled growing species *in situ*. The limitation of this system is the poorly defined structure and concentration of the initiating species. In contrast, thermolysis of well-defined unimolecular alkoxyamine initiators releases initiating radical and nitroxide in a ratio of 1:1 and leads to better control than bimolecular initiation. These initiators are formally coupling products of a radical species and a nitroxide radical and are more convenient to use. The mechanism of NMRP is shown in Scheme 1.[9] At higher temperature, the carbon-oxygen bond of the alkoxyamine fragments into the stable nitroxide radical and a propagating radical. The radical chain-end can now either grow, be reversibly terminated by the nitroxide radical or be terminated by chain-chain coupling or disproportionation. While the reversible termination of the radical with the nitroxide is the desired way of termination, the second way of termination is still inevitably occurring during the polymerization, producing dead chains. The concentration of propagating radicals and stable nitroxide radicals are equal at the beginning of the polymerization. At this point, the so called *persistent radical effect*[11-13] has to be taken into account. This effect describes the following thought: At the start of the polymerization the concentration of free radicals is

Scheme 1: *Mechanism of nitroxide mediated radical polymerization.*[9]

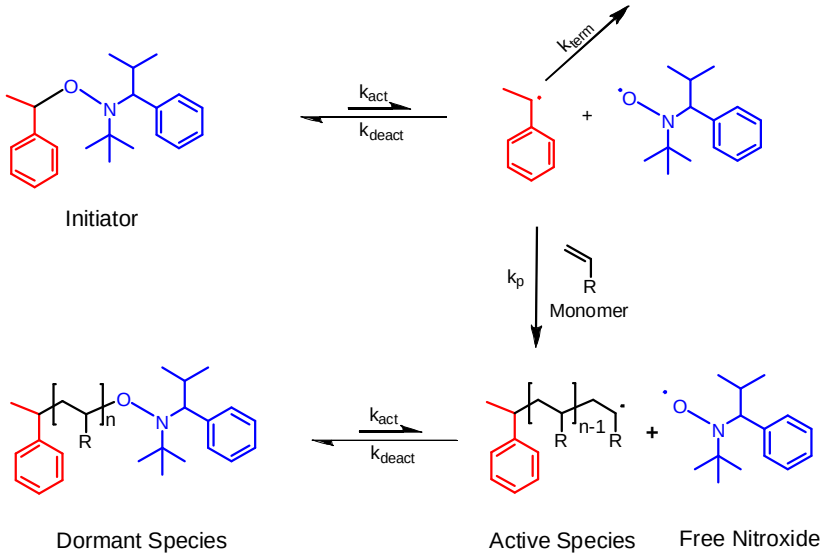

relatively high. Here, the probability of two active chain-ends meeting is about as high as one active chain-end meeting a nitroxide radical. Now, if two chain-ends meet and are irreversibly terminated by recombination, not only a dead chain is produced but also two free nitroxides are left without their former radicals to recombine. So, free nitroxides begin to accumulate in the reaction and thereby shift the equilibrium between active and dormant species more to the side of the dormant species, according to the principle of Le Chatelier. This shift in the equilibrium leads to a lower concentration of radicals in the polymerization and eventually to a point of equilibrium where the rate of activation is so low that only a negligible rate of termination is occurring. This equilibrium can be reached faster when an excess of nitroxide is added to the alkoxyamine prior to the start of the polymerization, leading to a better control of the polymerization.

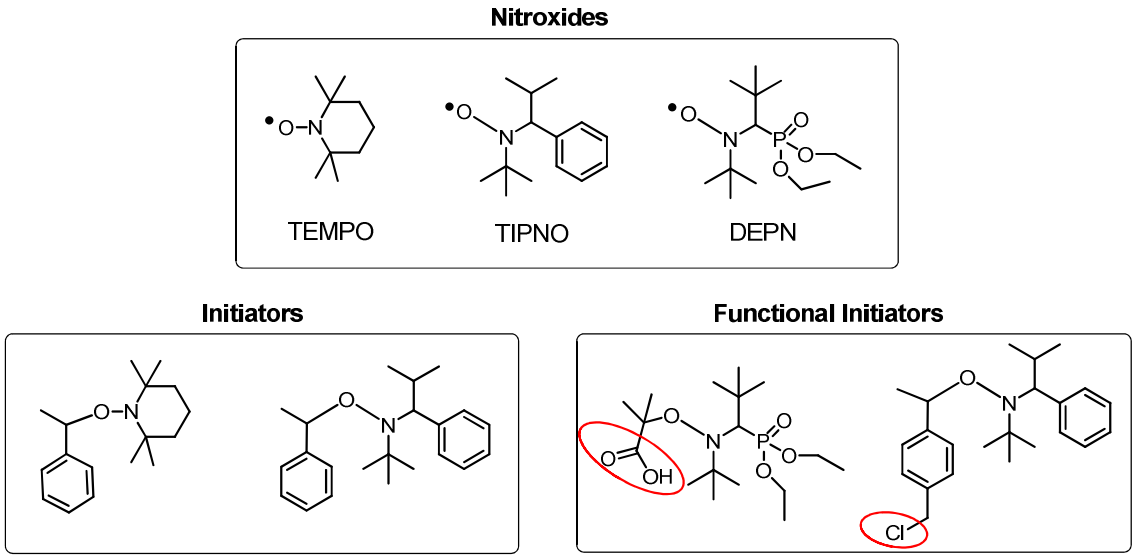

Figure 1: *Chemical structures of free nitroxides and unimolecular initiators for NMRP. Some initiators carry functional groups like COOH or Cl (highlighted by red circles), which can be converted easily before or after the polymerization.*[9]

An overview of common nitroxides and initiators is given in Figure 1. Commonly used nitroxides are 2,2,6,6-tetramethylpiperidinyloxyl (TEMPO),[14] *N*-*tert*-butyl-*N*-(1-diethylphosphono-2,2-dimethylpropyl)-*N*-oxyl (DEPN)[15] and 2,2,5,5-tetramethyl-4-phenyl-3-azahexane-3-oxyl (TIPNO).[8] NMRP mediated by TEMPO is limited by slow polymerization and a limited range of suitable monomers, mainly styrene and its derivatives. Nitroxides such as DEPN and TIPNO which were developed later and the use of their corresponding unimolecular alkoxyamines broadened the applicability of NMRP towards acrylates, acrylamides and acrylonitriles. Unimolecular alkoxyamines can be synthesized with functional groups as chloromethyl or a carbonic acid group, which allows further derivatization of the polymers, e.g. for labeling or coupling reactions.

Reversible Addition-Fragmentation Chain Transfer (RAFT)

RAFT stands for *Reversible Addition Fragmentation Chain Transfer*.[16-18] In this CRP method, an equilibrium between active growing polymer chains and dormant chains (macro-RAFT agents) ensures that all chains grow at a similar rate. RAFT polymerization uses thiocarbonylthio compounds, such as dithioesters, dithiocarbamates, trithiocarbonates, and xanthates in order to mediate the polymerization via a reversible chain-transfer process. Scheme 2 depicts the mechanism of RAFT.[19] Initiation is very similar to the one in free radical polymerization. The reaction is started by a common radical source like AIBN, which is thermally activated. These radicals are able to start a growing polymer chain. In a second step, the growing radical is terminated, for example by a thiocarbonyl thio compound (the so called RAFT- or chain transfer agent).

Scheme 2: *Mechanism of Reversible Addition Fragmentation Chain Transfer (RAFT).*[19]

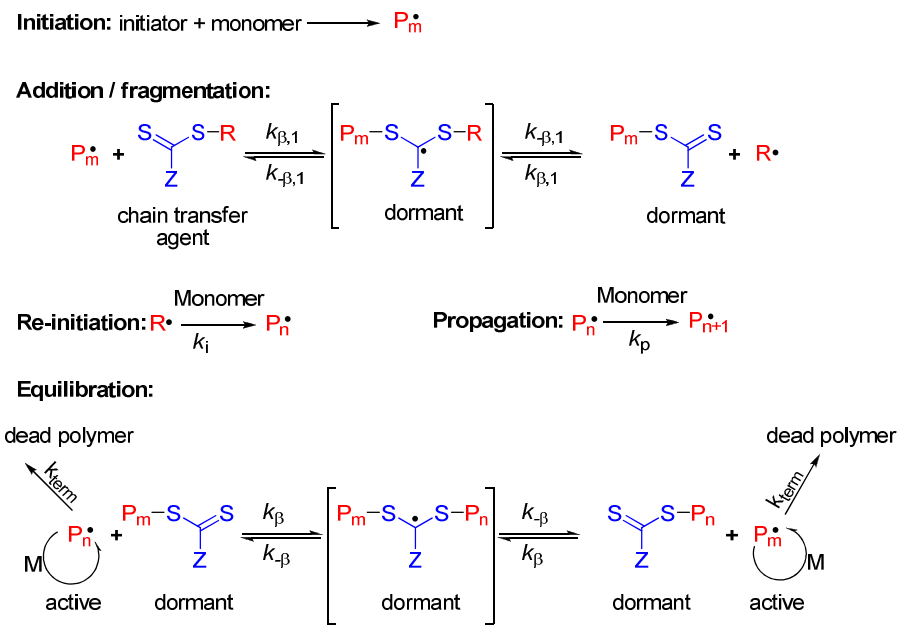

The following transition state is not stable and the R group leaves as a radical R·, which reinitiates a new chain. In the final stage, the macro-RAFT agents and the propagating chains exist in equilibrium. By this way, very few radicals can be shared between many growing chains. This results in similar polymerization rates for all chains by simultaneously lowering the radical concentration.

Because of the similarities between free radical polymerization and RAFT, the conditions for RAFT polymerization are similar to the conditions in free radical polymerization, regarding temperature, solvent and accessible monomers.

RAFT agents have to be selected according to the respective monomer being polymerized.[18, 20] They are composed of a thiocarbonyl compound which bears a leaving group R and a group Z. R-S has to be a weak single bond and R· should be a good initiating species. The Z group modifies the

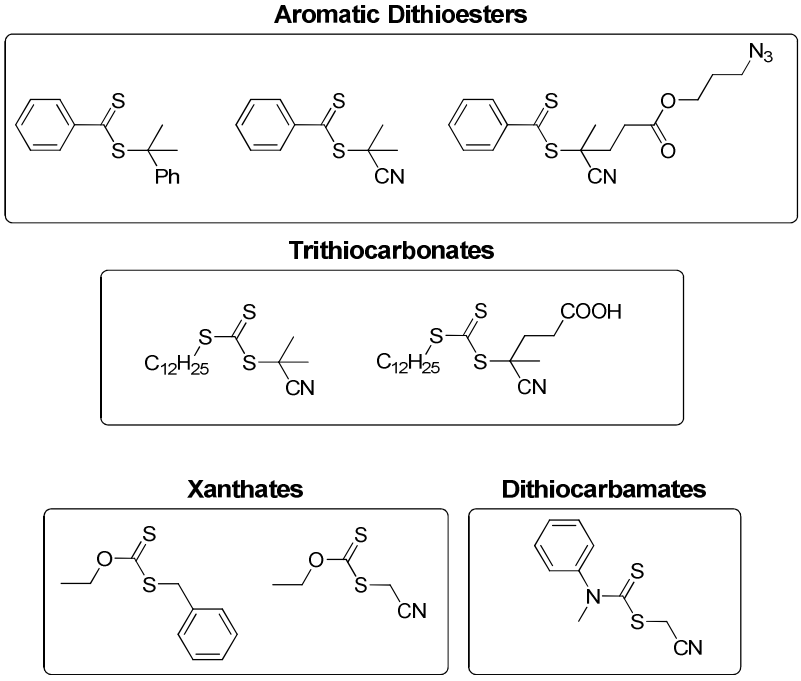

Figure 2: *Different classes of common RAFT agents like aromatic dithioesters, trithiocarbonates, xanthates and dithiocarbamates.*[20]

addition and fragmentation rates. Figure 2 gives an overview of common RAFT agents.[19] In general they can be distinguished between RAFT agents for more activated monomers and for less activated monomers. For activated monomers such as methyl methacrylate, methyl acrylate acrylic acid, acrylamide, acrylonitrile and styrene usually aromatic dithioesters or trithiocarbonates are used. Less activated monomers such as vinyl acetate, *N*-vinylpyrrolidone and *N*-vinylcarbazole can be polymerized controlled using xanthates.[20]

Atom Transfer Radical Polymerization (ATRP)

In *Atom Transfer Radical Polymerization* (ATRP)[21, 22] the concentration of radicals is lowered by an equilibrium between a dormant halide species (usually a bromide) and an active radical species. The transformation of these species into one another is governed by the Cu(I)/(II) redox process with a complexed copper halide. Scheme 3 shows the mechanism of ATRP.[21] The initiating step shown here involves an activated organic bromide R-Br, which reacts with the CuBr metal center undergoing an electron transfer with simultaneous halogen atom abstraction and expansion of its coordination sphere to $CuBr_2(L)$. The resulting R· is the reactive radical that initiates the polymerization.

Scheme 3: *Mechanism of atom transfer radical polymerization (ATRP).*[21]

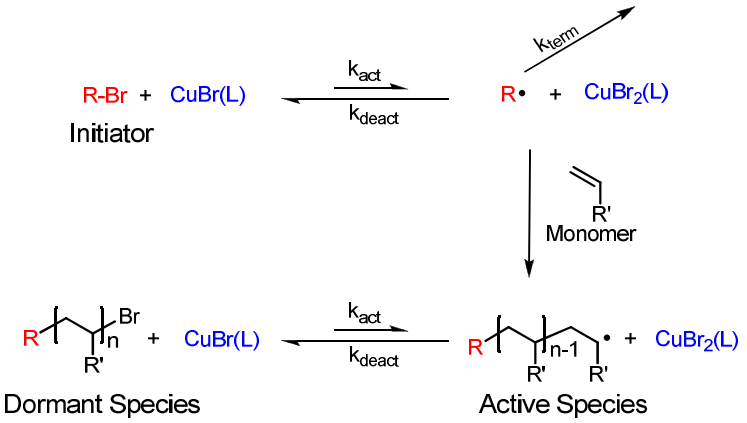

The $CuBr_2(L)$ species reduces the concentration of propagating radicals by the reversible reaction to R-Br, minimizing termination of living polymers. The successful ATRP of a specific monomer requires well matched components. The catalyst system is the key aspect of ATRP since it determines the position of the equilibrium and the rate of exchange between propagating and dormant species. Proper functioning of the metal catalyst requires suitable ligands that solubilize the transition metal salt in organic solvents and adjust the redox potential of the metal center for appropriate activity. It was shown that bidentate and multidentate nitrogen ligands usually work best. Typical initiators and some common ligands are shown in Figure 3.[23] Bromides are more reactive than chlorides while iodides are highly reactive, but undergo light induced side reactions and are therefore not used. The reactivity of the initiator should be matched to the monomer's reactivity. This is accomplished by using halides with organic groups similar to the structure of the propagating radical. Polymerization temperatures lie between 60 °C and 120 °C, depending on the reactivity of the monomer and the used catalyst system.

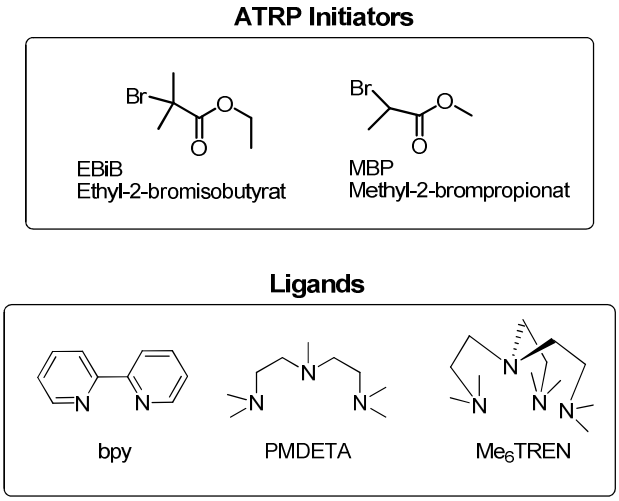

Figure 3: *Overview of commonly used nitrogen ligands and standard activated bromide initiators for atom transfer radical polymerization (ATRP).*[23]

3.3 Click Chemistry

Without a doubt, the vast number of reactions summarized under the term „click" chemistry constitutes a widely used trend in modern synthesis.[24] It describes nearly perfect "spring-loaded" reactions for the rapid synthesis of compounds. These reactions should fulfill the following criteria. They should

- be modular and wide in scope
- give very high yields
- generate only inoffensive byproducts
- be stereo-specific
- be conducted under simple reaction conditions
- have readily available starting materials and reagents
- be conducted in no solvent or in a solvent that is benign (such as water) or can be easily removed
- allow easy product isolation.

These criteria were established by Sharpless in 2001 in a paper with the title "Click Chemistry: Diverse Chemical Function from a Few Good Reactions".[25] To clarify the simplicity of this chemistry, he coined the term „*Click Chemistry*" for it. Though the reactions, which were collected here, were not new, the concept of pure and easy chemistry, combined with the catchy term „click" chemistry stayed in the minds of many who read the article. The popularity of the „click" chemistry concept is rising strongly since its introduction and the number of publications dealing with it is growing strongly each year. Figure 4 represents a literature search of the term "*click chemistry*" with SciFinder Scholar™ 2007 performed in March 2011, clarifying its popularity.

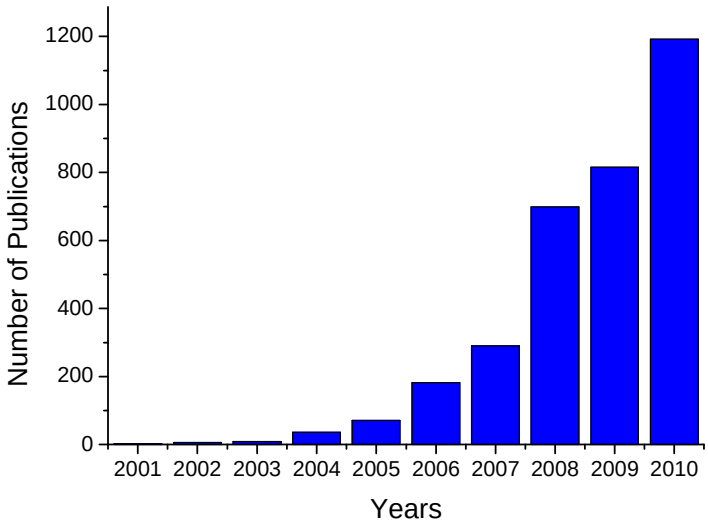

Figure 4: *Number of scientific publications concerning the term "click chemistry" (Search result of SciFinder Scholar™ 2007, performed in March 2011).*

Especially polymer chemists and material chemists like the idea of creating complex molecular architectures with a synthetic system which is comparable to a LEGO toolbox, from which arbitrary building bricks can be taken and "clicked" together in an easy, fast and reliable way. A schematic representation of different examples of how "click" chemistry can be applied in different synthetic situations is shown in Figure 5. "Click" chemistry does not only allow to couple small molecules with other small molecules, but to compose highly complex architectures. It is possible to functionalize end groups of polymers,[26] use it to introduce markers in biomolecules,[27] functionalize nanoparticles,[28] microspheres[29] or surfaces,[30, 31] build up complex dendritic architectures,[32] couple two polymers with each other to form block copolymers[33] or produce side chain functionalized polymers.[34, 35]

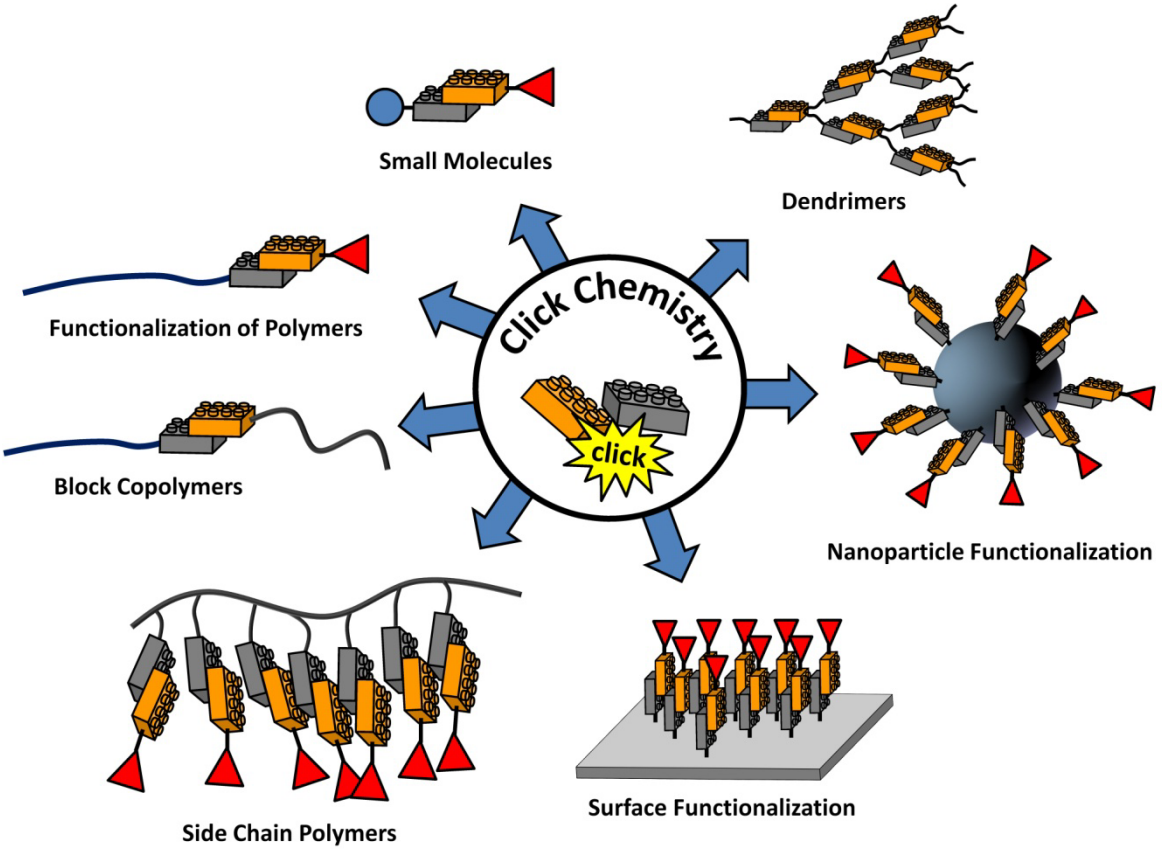

Figure 5: *Schematic illustration of different possibilities to use "click" chemistry as a synthetic tool. The modularity of the concept reminds of a LEGO toolbox where arbitrary "building bricks" can be "clicked" together to form complex structures.*

Meanwhile, "click" type coupling reactions can be seen as standard reactions in organic synthesis and especially in the design of new functional materials. The range of "click" chemistry methods is constantly developing. Figure 6 gives an overview of the most popular "click" strategies. Upcoming metal-free "click"-methods[36] as thiol/ene "click"-chemistry,[37, 38] strain promoted azide-alkyne reactions,[39, 40] thiol-para fluoro phenyl "click" chemistry[41] or the reversible addition-fragmentation chain transfer-hetero Diels-Alder (RAFT-HDA) "click"-reaction

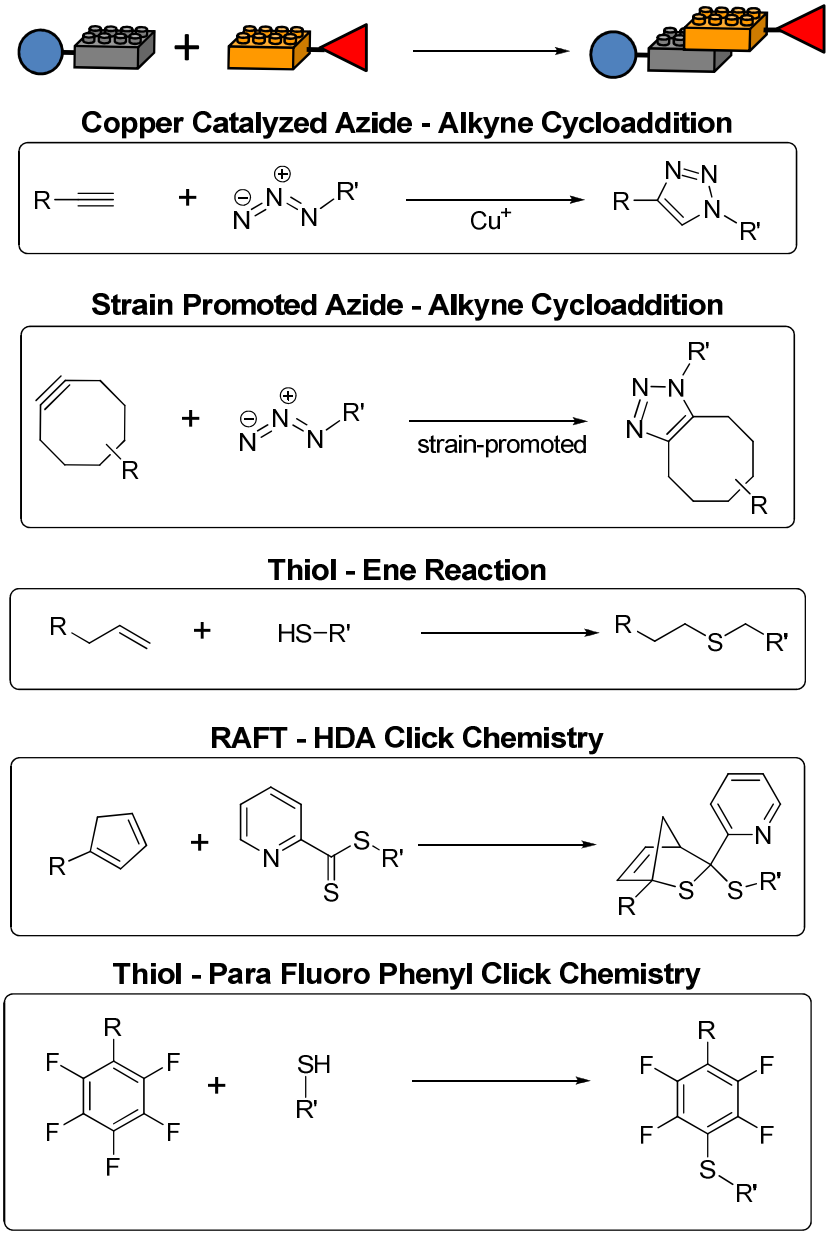

Figure 6: *Overview of the most used „click" chemistry strategies.*

of cyclopentadienes and dithioesters[42, 43] are promising approaches to replenish established techniques such as the Cu(I)-catalyzed 1,3-dipolar cycloaddition of azides and alkynes (CuAAC).[25, 44, 45] Nevertheless, CuAAC is currently the most commonly used "click"-reaction, outstanding for its versatility and easy to introduce clickable groups. In the following paragraph, the mechanism and properties of CuAAC are explained in more detail.

Copper-catalyzed Azide-Alkyne Cycloaddition (CuAAC)

As mentioned before, copper catalyzed cycloaddition reactions between azides and alkynes are the most reliable and versatile type of "click" chemistry and are therefore highly popular. Basically, this reaction can be described as a 1,3-dipolar cycloaddition. The principles of 1,3-dipolar cycloadditions of 1,3-dipoles and dipolarophiles were described by Huisgen.[46, 47] The uncatalyzed reaction between an azide and an alkyne has to be conducted at higher temperatures and requires a long reaction time due to the relatively inert educts. Also, the resulting products are not regiospecific, but give a mixture of the 1,4- and 1,5-disubstituted triazole regioisomeres (Figure 7a). It was not until 2002, that Sharpless et al.[48] and Meldal et al.[49] published independently from each other that this reaction can be catalyzed by Cu(I) species to form regiospecific 1,4-disubstituted 1,2,3-triazoles at ambient temperature with complete conversion in a short time (Figure 7b). Later on, the formation of pure 1,5-disubstituted regioisomeres was achieved with Ruthenium catalysis which catalyzes not only the coupling reaction between an azide and a terminal alkyne but also between internal alkynes and azides to give 1,5-disubstituted or 1,4,5-trisubstituted 1,2,3-triazoles (Figure 7c).[50]

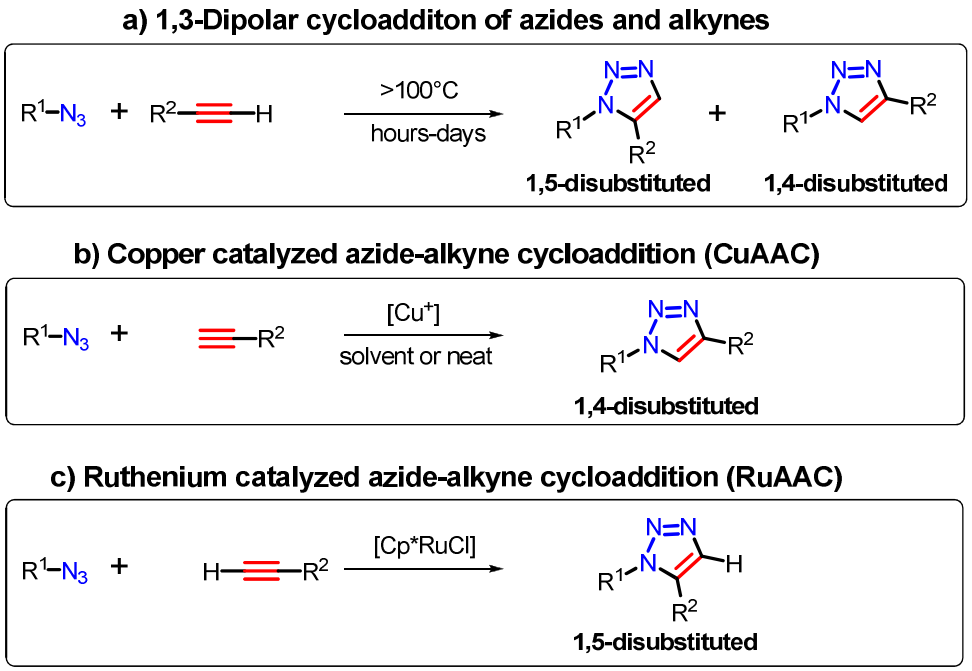

Figure 7: *a) Uncatalyzed 1,3 dipolar cycloaddition of azides and alkynes which yields 1,4- and 1,5-disubstituted triazole products; b) Copper catalyzed azide-alkyne cycloaddition (CUAAC), forming only 1,4-disubstituted triazoles; c) Ruthenium catalyzed azide-alkyne cycloaddition (RuAAC), leading exclusively to 1,5-disubstituted or 1,4,5-trisubstituted triazoles.*

The relatively high stability of azide and alkyne groups, that was a disadvantage in the uncatalyzed Huisgen cycloaddition, is also one of the biggest advantages of CuAAC. Without catalyst, the functional groups are stable and inert under a wide range of conditions and tolerate most chemical functionalities. This also makes these groups easy to introduce in molecules. An

early proposed catalytic cycle of copper-catalyzed azide-alkyne cycloaddition is shown in Figure 8a). Here, only one copper is participating in the catalysis. Figure 8b) shows a variation of the catalytic cycle where two copper complexes are involved. According to DFT calculations the latter would be energetically more favorable.[51]

The formation of copper acetylide starts the catalytic cycle. This step probably occurs through a π-alkyne copper complex intermediate which significantly acidifies the terminal hydrogen of the alkyne, making it easier to be deprotonated. The alkyne is then activated by coordination to copper. In the next step, the azide is coordinated. Then the C-N bond is formed, resulting in a stained copper metallacycle. This is followed by the formation of Cu-triazole complex. In a final step, the catalyst dissociates and is regenerated via protonation of the triazole-copper complex.

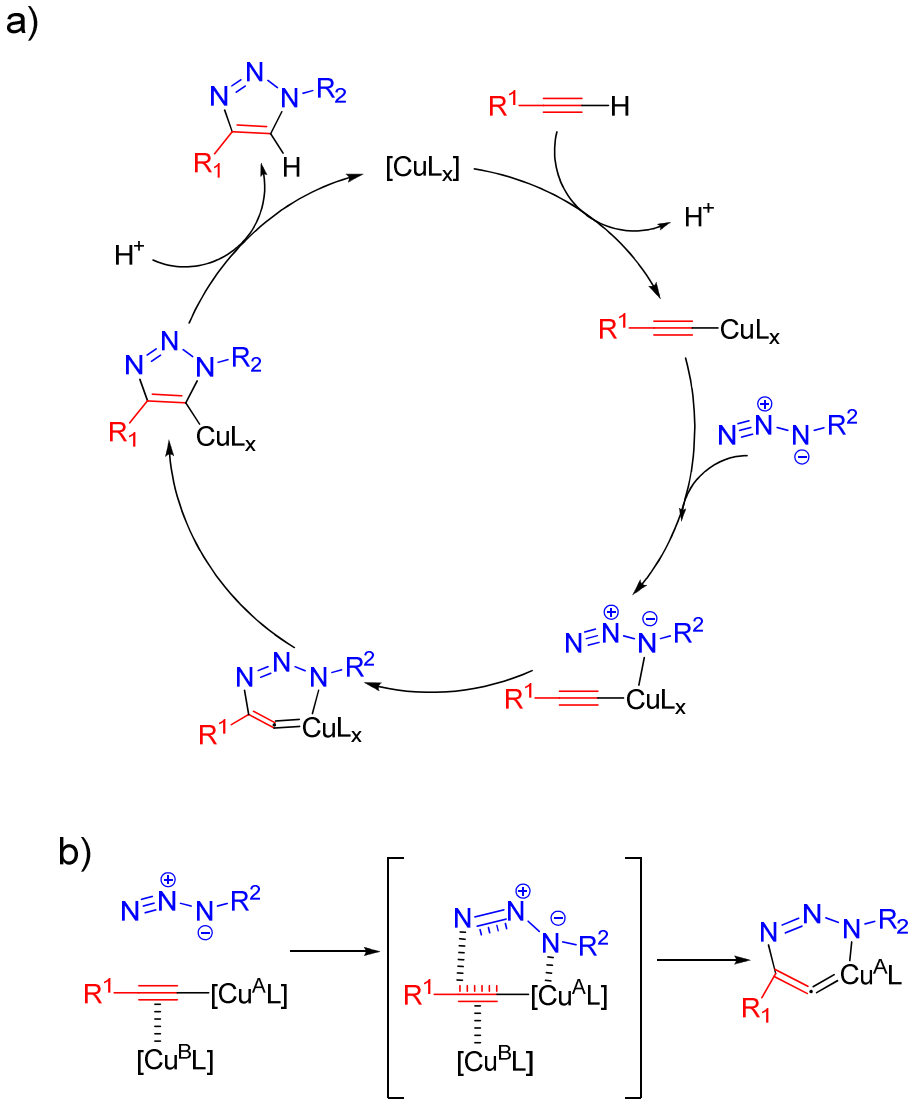

Figure 8: *a) Early proposed catalytic cycle for the CuAAC. b) Introduction of a second copper(I) atom favorably influences the energetic profile of the reaction.*[51]

Catalyst/Ligand Systems for CuAAC

A wide range of experimental conditions for the CuAAC can be employed. The choice of the catalyst is dictated by the particular requirements of the experiment. Usually many different combinations will produce the desired results. A summary was shown by Meldal and Tornøe.[52] The most commonly used protocols and their advantages and limitations are discussed below.

Of course, in all cases, a copper source has to be utilized. In aqueous media, cuprous bromide and acetate are favored, as is the sulfate from *in situ* reduction of $CuSO_4$ by ascorbate. These reagents are readily soluble in water without additional ligands.

In organic solvents, however, Cu(I) salts are either poorly or not soluble at all. In this case, an additional ligand is needed to dissolve the copper ion in the organic medium. “Soft” ligands as in $Cu(PPh_3)_3Br$ are often used in reactions in organic solvents such as $CHCl_3$, in which cuprous salts have limited solubility. Furthermore, this catalyst/ligand system has the advantage that it is air-stable in its solid form, ready to use and can be purchased. Amines are usually used as “hard” donor ligands. Such ligands can be monodentate (e.g. diisopropyl ethylamine, DIPEA) or multidentate (e.g. pentamethyldiethylenetriamine, PMDETA). Also, these ligands have the additional function to deprotonate the terminal alkynes due to their basicity. The copper salt and the ligand are usually added separately to the reaction, so that the ligated species is formed *in situ*. In some cases it can be beneficial to let the complex be built prior to use as a stock solution in deoxygenized solvents.

Especially in organic solvents, oxygen and the following presence of Cu(II) species promote side reactions such as the oxidative Glaser coupling of acetylenes.[53] For this reason, exclusion of oxygen, which oxidizes Cu(I) to Cu(II) easily and the use of pure Cu(I) salts are required to obtain pure products with high yields. A possibility to work under normal atmosphere is the addition of ascorbate, which is a mild reduction agent and reduces Cu(II) to Cu(I).

Another possibility to conduct CuAAC is the catalysis by minor amounts of Cu(I) supplied by elemental copper which is added as wire or turnings to the reaction.[54] Usually, these reactions have to be stirred for longer time due to the minimal amount of catalyzing Cu(I), but they also have the benefit of less residual copper in the reaction, which is interesting for biological applications.

Combination of Copper-Catalyzed Azide-Alkyne Cycloaddition (CuAAC) and Controlled Radical Polymerizations (CRP)

Due to the extreme modularity of the “click” concept, arbitrary organic “building bricks” can be “clicked” together. This makes it possible to form polymers which would not be accessible by normal polymerization, or only with very tedious effort. Table 1 shows an overview of polymers synthesized by “click” chemistry. For polymer chemistry, especially the possibility to form block copolymers by the coupling of two polymers,[55] the concept of side chain modification[34, 35, 56, 57] and a combination of both[58, 59] is interesting. By this, it is for example possible to compare the influence of small structural changes in pendant groups of a polymer on its properties. Thus, the degree of polymerization and PDI of the compared polymers can be kept exactly constant. Zhang

et al. for example synthesized side-chain liquid crystalline polymers by “clicking” mesogenes with different spacer-lengths to poly(propargyl acrylate) obtained by radical polymerization.[57] While the concept of “click” chemistry was applied successfully here, the polymers exhibited higher polydispersities due to the non-controlled nature of the free radical polymerization of the scaffold block. However, narrow polydispersities are important in material science to elucidate the properties of polymers correctly. Therefore, a combination of “click” chemistry and controlled and/or living polymerization methods should be applied. The combination of CuAAC with the three most commonly used controlled radical polymerization methods (CRP), atom transfer radical polymerization (ATRP),[56, 60-62] reversible addition-fragmentation chain transfer polymerization (RAFT)[63, 64] and nitroxide mediated radical polymerization (NMRP)[65-68] has proven to be a powerful tool. Haddleton et al. built up libraries of glycopolymers by “clicking” sugar azides to poly(propargyl methacrylate), obtained by ATRP.[56] The reaction of an azide carrying polymer with alkynes from ATRP was shown by Matyjaszewski **e**t al.[60] Block copolymers from protected poly(oxystyrene) and poly(propargyl oxystyrene) were prepared with NMRP by Voit et al. and “clicked” with azide functionalized adamantyl[35] and also dendronized with azide carrying dendrons.[65] The synthesis of graft-polymers by “click” chemistry was shown by Hennink et al.[69] and Stenzel et al.[63], who grafted azide carrying polymers to an alkyne bearing polymer to form polymer brushes. The preparation of block copolymers from an alkyne and an azide carrying polymer by “click” chemistry was shown by van Hest et al. with high conversion.[55] A combination of side chain functionalization and polymer-polymer coupling by “click” chemistry was shown by Segalman et al.[58] and Matyjaszewski et al.[59] where block copolymers with pendant units were synthesized by two subsequent “click” reactions.

The combinations of ionic polymerization and “click” chemistry is found rather seldom.[70, 71] Despite the fact that ionic polymerization techniques can give very narrow molecular weight distributions, they have the drawback that they demand very high purity of solvent, educts and reagents and need a complex set up which stands in contrast to the convenient “click” chemistry concept.

Table 1: *Overview of polymers synthesized with the help of "click" chemistry.*

Entry	Polymer	Polymerization method	Catalyst/ conditions	Ref.
1	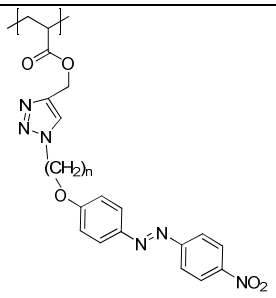	Free Radical	CuBr/NHPMI	57
2	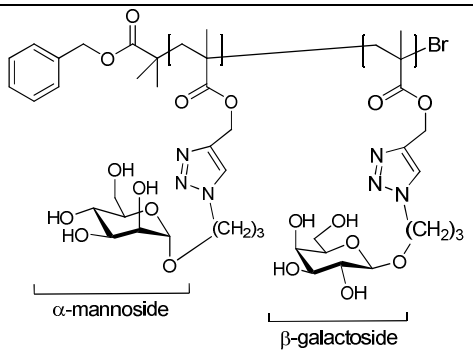	ATRP	$Cu(PPh_3)_3Br$/ DIPEA	56
3	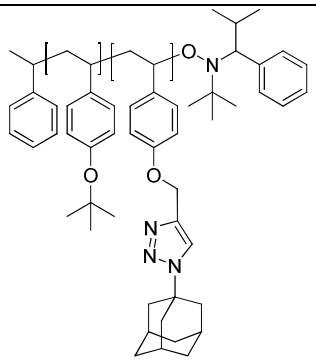	NMRP	$Cu(PPh_3)_3Br$/ DIPEA	35
4	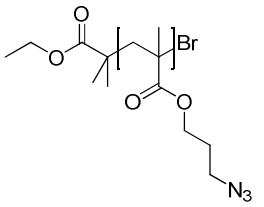	ATRP	CuBr/DMF	*60*
5	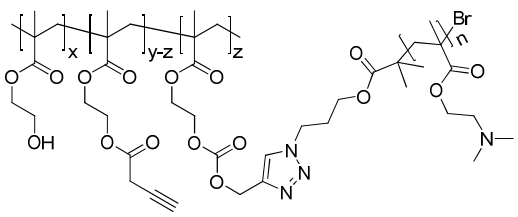	ATRP	CuBr/DMF	*69*

Entry	Polymer	Polymerization method	Catalyst/ conditions	Ref.
6	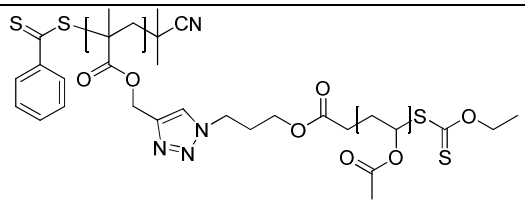	RAFT/MADIX	CuI/DBU	63
7	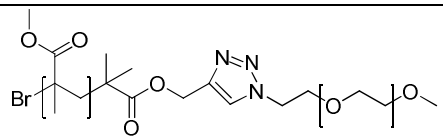 PMMA-b-PEG	ATRP	CuI/DBU	55
8	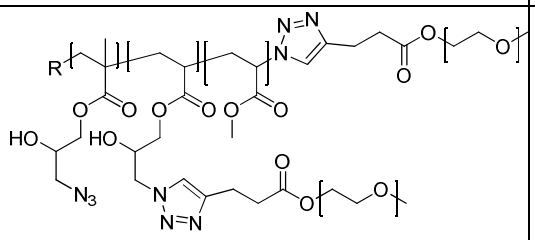	ATRP	CuBr/PMDETA	*59*

DIPEA = N,N-diisopropylethylamine, NHPMI = N-(n-hexyl)-2-pyridylmethanimine, DMF = dimethylformamide, DBU = 1,8-diazabicyclo[5.4.0]undec-7-ene, PMDETA = N,N,N',N'',N''-pentamethyldiethylenetriamine.

Semiconductor Polymers and Block Copolymers by “Click” Chemistry

Electro-optic active polymers and block copolymers are gaining higher interest in the last years.[72] Such polymers can be synthesized either by direct polymerization or by a combination of direct polymerization and “click” chemistry. Kumar et al. for example synthesized polyimides with side-chain oligothiophene by this.[73] Park et al. synthesized polymers by a “click” polymerization.[74] A series of P3HT and PPV derivatives which were side-chain functionalized with phthalocyanine by “click” chemistry was shown by Campo et al.[75] Further side-chain functionalization of P3HT[77] or PEDOT[76] was shown by Miyanishi et al. and Bu et al. Kito et al. functionalized helical polymers with perylene bisimide.[78] Block copolymers of P3HT and poly(perylene bisimide) were synthesized by Segalman et al. through a double-“click” approach. Polystyrene and P3HT was coupled by “click” chemistry by Urien.[79]

Table 2: *Overview of electro-active polymers synthesized with the help of „click“ chemistry.*

Entry	Polymer	Catalyst/ conditions	Ref.
1	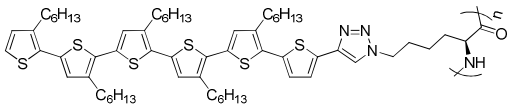	$CuSO_4$/NaAscorbat	73
2	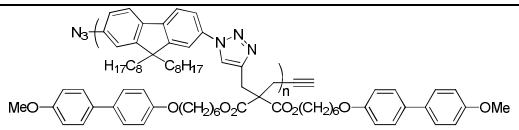	$CuSO_4$/NaAscorbat	74
3	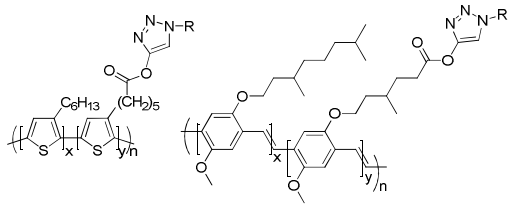 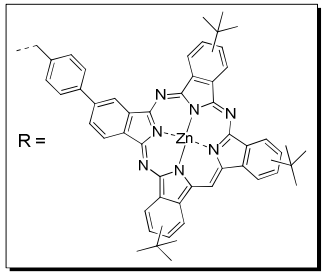	CuBr/PMDETA	75

Entry	Polymer	Catalyst/ Conditions	Ref.
4	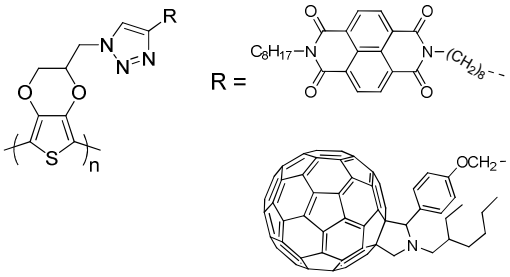	$Cu/Cu(CH_3CN)_4PF_6$	*76*
5	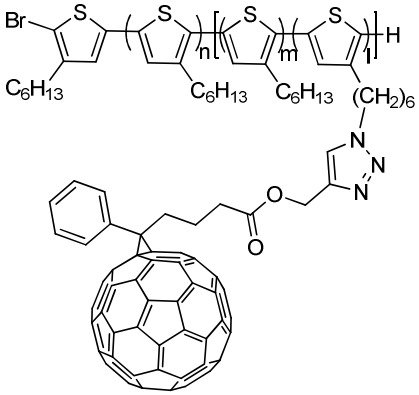	CuBr/PMDETA	77
6	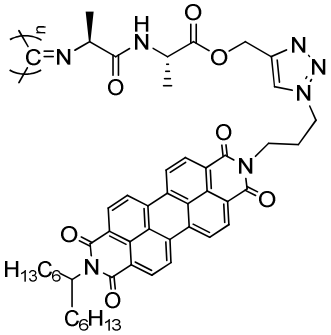	CuBr/PMDETA	78
7	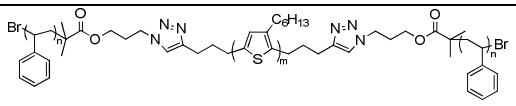	CuI/DBU	79
8	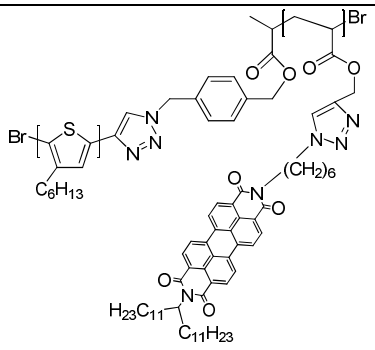	CuBr/PMDETA	58

Bibliography

1. Burroughes, J. H.; Bradley, D. D. C.; Brown, A. R.; Marks, R. N.; Mackay, K.; Friend, R. H.; Burns, P. L.; Holmes, A. B. *Nature* **1990,** 347, (6293), 539-541.
2. Sirringhaus, H.; Tessler, N.; Friend, R. H. *Science* **1998,** 280, (5370), 1741-1744.
3. Drury, C. J.; Mutsaers, C. M. J.; Hart, C. M.; Matters, M.; Leeuw, D. M. d., *Low-cost all-polymer integrated circuits*. AIP: **1998**; Vol. 73, p 108-110.
4. Yu, G.; Gao, J.; Hummelen, J. C.; Wudl, F.; Heeger, A. J. *Science* **1995,** 270, (5243), 1789-1791.
5. Braunecker, W. A.; Matyjaszewski, K. *Progress in Polymer Science* **2007,** 32, (1), 93-146.
6. Matyjaszewski, K.; Davis, T. P., In *Handbook of Radical Polymerization*, John Wiley & Sons, Inc.: **2003**.
7. Fukuda, T. *Journal of Polymer Science Part A: Polymer Chemistry* **2004,** 42, (19), 4743-4755.
8. Benoit, D.; Chaplinski, V.; Braslau, R.; Hawker, C. J. *Journal of the American Chemical Society* **1999,** 121, (16), 3904-3920.
9. Hawker, C. J.; Bosman, A. W.; Harth, E. *Chemical Reviews* **2001,** 101, (12), 3661-3688.
10. Fukuda, T.; Terauchi, T.; Goto, A.; Ohno, K.; Tsujii, Y.; Miyamoto, T.; Kobatake, S.; Yamada, B. *Macromolecules* **1996,** 29, (20), 6393-6398.
11. Fischer, H. *Macromolecules* **1997,** 30, (19), 5666-5672.
12. Fischer, H. *Chemical Reviews* **2001,** 101, (12), 3581-3610.
13. Tang, W.; Fukuda, T.; Matyjaszewski, K. *Macromolecules* **2006,** 39, (13), 4332-4337.
14. Rizzardo, E. *Chem. Austr.* **1987,** 54, 32.
15. Chong, Y. K.; Ercole, F.; Moad, G.; Rizzardo, E.; Thang, S. H.; Anderson, A. G. *Macromolecules* **1999,** 32, (21), 6895-6903.
16. Chiefari, J.; Chong, Y. K.; Ercole, F.; Krstina, J.; Jeffery, J.; Le, T. P. T.; Mayadunne, R. T. A.; Meijs, G. F.; Moad, C. L.; Moad, G.; Rizzardo, E.; Thang, S. H. *Macromolecules* **1998,** 31, (16), 5559-5562.
17. Moad, G.; Rizzardo, E.; Thang, S. H. *Accounts of Chemical Research* **2008,** 41, (9), 1133-1142.
18. Moad, G.; Rizzardo, E.; Thang, S. H. *Australian Journal of Chemistry* **2005,** 58, (6), 379-410.
19. Barner-Kowollik, C., In *Handbook of RAFT Polymerization*, Wiley-VCH Verlag GmbH & Co. KGaA: **2008**.
20. Moad, G.; Rizzardo, E.; Thang, S. H. *Polymer* **2008,** 49, (5), 1079-1131.

21. Wang, J.-S.; Matyjaszewski, K. *Journal of the American Chemical Society* **1995,** 117, (20), 5614-5615.

22. Wang, J.-S.; Matyjaszewski, K. *Macromolecules* **1995,** 28, (22), 7572-7573.

23. Tang, W.; Matyjaszewski, K. *Macromolecules* **2007,** 40, (6), 1858-1863.

24. Lahann, J., In *Click Chemistry for Biotechnology and Materials Science*, John Wiley & Sons, Ltd: 2009.

25. Kolb, H. C.; Finn, M. G.; Sharpless, K. B. *Angewandte Chemie International Edition* **2001,** 40, (11), 2004-2021.

26. Mantovani, G.; Ladmiral, V.; Tao, L.; Haddleton, D. M. *Chemical Communications* **2005**, (16), 2089-2091.

27. Paredes, E.; Das, S. R. *ChemBioChem* **2010,** 12, (1), 125-131.

28. Meinhardt, T.; Lang, D.; Dill, H.; Krueger, A. *Advanced Functional Materials* **2010,** 21, (3), 494-500.

29. Goldmann, A. S.; Walther, A.; Nebhani, L.; Joso, R.; Ernst, D.; Loos, K.; Barner-Kowollik, C.; Barner, L.; Müller, A. H. E. *Macromolecules* **2009,** 42, (11), 3707-3714.

30. Chen, R. T.; Muir, B. W.; Such, G. K.; Postma, A.; Evans, R. A.; Pereira, S. M.; McLean, K. M.; Caruso, F. *Langmuir* **2009,** 26, (5), 3388-3393.

31. Li, Y.; Wang, J.; Cai, C. *Langmuir* **2011**, 27, (6), 2437-2445.

32. Killops, K. L.; Campos, L. M.; Hawker, C. J. *Journal of the American Chemical Society* **2008,** 130, (15), 5062-5064.

33. Nasrullah, M. J.; Vora, A.; Webster, D. C. *Macromolecular Chemistry and Physics* **2010,** 212, (6), 539-549.

34. Lang, A. S.; Neubig, A.; Sommer, M.; Thelakkat, M. *Macromolecules* **2010,** 43, (17), 7001-7010.

35. Fleischmann, S.; Komber, H.; Voit, B. *Macromolecules* **2008,** 41, (14), 5255-5264.

36. Becer, C. R.; Hoogenboom, R.; Schubert, U. S. *Angewandte Chemie International Edition* **2009,** 48, (27), 4900-4908.

37. Gress, A.; Volkel, A.; Schlaad, H. *Macromolecules* **2007,** 40, (22), 7928-7933.

38. Lowe, A. B.; Hoyle, C. E.; Bowman, C. N. *Journal of Materials Chemistry* **2010,** 20, (23), 4745-4750.

39. Agard, N. J.; Prescher, J. A.; Bertozzi, C. R. *Journal of the American Chemical Society* **2004,** 126, (46), 15046-15047.

40. Baskin, J. M.; Prescher, J. A.; Laughlin, S. T.; Agard, N. J.; Chang, P. V.; Miller, I. A.; Lo, A.; Codelli, J. A.; Bertozzi, C. R. *Proceedings of the National Academy of Sciences* **2007,** 104, (43), 16793-16797.

41. Becer, C. R.; Babiuch, K.; Pilz, D.; Hornig, S.; Heinze, T.; Gottschaldt, M.; Schubert, U. S. *Macromolecules* **2009,** 42, (7), 2387-2394.

42. Inglis, A. J.; Stenzel, M. H.; Barner-Kowollik, C. *Macromolecular Rapid Communications* **2009,** 30, (21), 1792-1798.

43. Inglis, A. J.; Sinnwell, S.; Stenzel, M. H.; Barner-Kowollik, C. *Angewandte Chemie International Edition* **2009,** 48, (13), 2411-2414.

44. Binder, W. H.; Sachsenhofer, R. *Macromolecular Rapid Communications* **2007,** 28, (1), 15-54.

45. Binder, W. H.; Sachsenhofer, R. *Macromolecular Rapid Communications* **2008,** 29, (12-13), 952-981.

46. Huisgen, R. *Angewandte Chemie International Edition in English* **1963,** 2, (10), 565-598.

47. Huisgen, R. *Angewandte Chemie International Edition in English* **1963,** 2, (11), 633-645.

48. Vsevolod, V. R.; Green, L. G.; Fokin, V. V.; Sharpless, K. B. *Angewandte Chemie International Edition* **2002,** 41, (14), 2596-2599.

49. Tornøe, C. W.; Christensen, C.; Meldal, M. *The Journal of Organic Chemistry* **2002,** 67, (9), 3057-3064.

50. Zhang, L.; Chen, X.; Xue, P.; Sun, H. H. Y.; Williams, I. D.; Sharpless, K. B.; Fokin, V. V.; Jia, G. *Journal of the American Chemical Society* **2005,** 127, (46), 15998-15999.

51. Hein, J. E.; Fokin, V. V. *Chemical Society Reviews* **2010,** 39, (4), 1302-1315.

52. Meldal, M.; TornÃ¸e, C. W. *Chemical Reviews* **2008,** 108, (8), 2952-3015.

53. Christopher, J. D.; David, C.; Andreas, H. *Journal of Polymer Science Part A: Polymer Chemistry* **2009,** 47, (15), 3795-3802.

54. Himo, F.; Lovell, T.; Hilgraf, R.; Rostovtsev, V. V.; Noodleman, L.; Sharpless, K. B.; Fokin, V. V. *Journal of the American Chemical Society* **2005,** 127, (1), 210-216.

55. Opsteen, J. A.; Hest, J. C. M. v. *Chemical Communications* **2005**, (1), 57-59.

56. Ladmiral, V.; Mantovani, G.; Clarkson, G. J.; Cauet, S.; Irwin, J. L.; Haddleton, D. M. *Journal of the American Chemical Society* **2006,** 128, (14), 4823-4830.

57. Li, Z.; Zhang, Y.; Zhu, L.; Shen, T.; Zhang, H. *Polymer Chemistry* **2010,** 1, (9), 1501-1511.

58. Tao, Y.; McCulloch, B.; Kim, S.; Segalman, R. A. *Soft Matter* **2009,** 5, (21), 4219-4230.

59. Tsarevsky, N. V.; Bencherif, S. A.; Matyjaszewski, K. *Macromolecules* **2007,** 40, (13), 4439-4445.

60. Sumerlin, B. S.; Tsarevsky, N. V.; Louche, G.; Lee, R. Y.; Matyjaszewski, K. *Macromolecules* **2005,** 38, (18), 7540-7545.

61. Gao, H.; Matyjaszewski, K. *Journal of the American Chemical Society* **2007,** 129, (20), 6633-6639.

62. Geng, J.; Lindqvist, J.; Mantovani, G.; Haddleton, D. M. *Angewandte Chemie International Edition* **2008,** 47, (22), 4180-4183.

63. Quémener, D.; Hellaye, M. L.; Bissett, C.; Davis, T. P.; Barner-Kowollik, C.; Stenzel, M. H. *Journal of Polymer Science Part A: Polymer Chemistry* **2008,** 46, (1), 155-173.

64. Zhang, X.; Lian, X.; Liu, L.; Zhang, J.; Zhao, H. *Macromolecules* **2008,** 41, (21), 7863-7869.

65. Fleischmann, S.; Kiriy, A.; Bocharova, V.; Tock, C.; Komber, H.; Voit, B. *Macromolecular Rapid Communications* **2009,** 30, (17), 1457-1462.

66. Malkoch, M.; Thibault, R. J.; Drockenmuller, E.; Messerschmidt, M.; Voit, B.; Russell, T. P.; Hawker, C. J. *Journal of the American Chemical Society* **2005,** 127, (42), 14942-14949.

67. Sieczkowska, B.; Millaruelo, M.; Messerschmidt, M.; Voit, B. *Macromolecules* **2007,** 40, (7), 2361-2370.

68. Fleischmann, S.; Hinrichs, K.; Oertel, U.; Reichelt, S.; Eichhorn, K.-J.; Voit, B. *Macromolecular Rapid Communications* **2008,** 29, (12-13), 1177-1185.

69. Jiang, X.; Lok, M. C.; Hennink, W. E. *Bioconjugate Chemistry* **2007,** 18, (6), 2077-2084.

70. Reinicke, S.; Schmalz, H. *Colloid & Polymer Science* **2011**, 1-16.

71. Touris, A.; Hadjichristidis, N. *Macromolecules* **2011,** 44, (7), 1969–1976.

72. Michinobu, T. *Chemical Society Reviews* **2011,** 40, (5), 2306-2316.

73. Kumar, R. J.; MacDonald, J. M.; Singh, T. B.; Waddington, L. J.; Holmes, A. B. *Journal of the American Chemical Society* **2011,** 133, (22), 8564-8573.

74. Park, J. S.; Kim, Y. H.; Song, M.; Kim, C.-H.; Karim, M. A.; Lee, J. W.; Gal, Y.-S.; Kumar, P.; Kang, S.-W.; Jin, S.-H. *Macromolecular Chemistry and Physics* **2010**, 211, (23), 2464-2473.

75. Campo, B. J.; Duchateau, J.; Ganivet, C. R.; Ballesteros, B.; Gilot, J.; Wienk, M. M.; Oosterbaan, W. D.; Lutsen, L.; Cleij, T. J.; de la Torre, G.; Janssen, R. A. J.; Vanderzande, D.; Torres, T. *Dalton Transactions* **2011,** 40, (15), 3979-3988.

76. Bu, H.-B.; Götz, G.; Reinold, E.; Vogt, A.; Schmid, S.; Segura, J. L.; Blanco, R.; Gómez, R.; Bäuerle, P. *Tetrahedron* **2011,** 67, (6), 1114-1125.

77. Miyanishi, S.; Zhang, Y.; Tajima, K.; Hashimoto, K. *Chemical Communications* **2010,** 46, (36), 6723-6725.

78. Kitto, H. J.; Schwartz, E.; Nijemeisland, M.; Koepf, M.; Cornelissen, J. J. L. M.; Rowan, A. E.; Nolte, R. J. M. *Journal of Materials Chemistry* **2008,** 18, (46), 5615-5624.

79. Urien, M.; Erothu, H.; Cloutet, E.; Hiorns, R. C.; Vignau, L.; Cramail, H. *Macromolecules* **2008,** 41, (19), 7033-7040.

Chapter 4

4. Overview

This thesis contains seven manuscripts out of which three are already published, one is submitted, one is prepared for publication and two appear in the form of a manuscript. In my work, I was interested in the synthesis and characterization of novel semiconductor polymers and new complex block copolymer architectures by controlled radical polymerization methods and polymer analogous reactions. All polymers were expected to be synthesized with a high degree of control over molecular weight and with narrow molecular weight distributions.

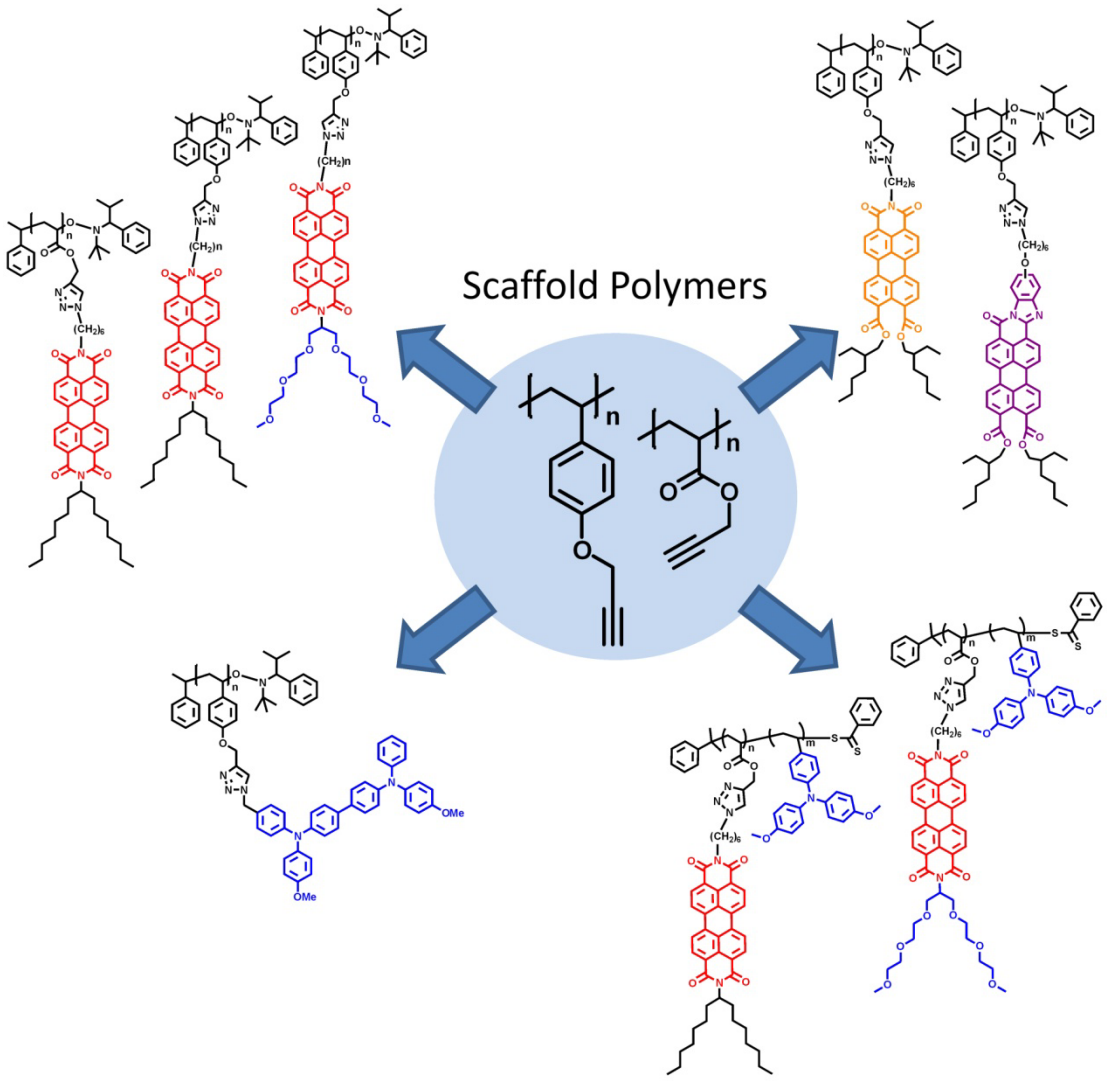

Figure 1: *Diverse functionalization from scaffold polymers such as poly(propargyl oxystyrene) and poly(propargyl acrylate) towards semiconductor homopolymers and block copolymers.*

The focus of the work lies on the development of a general method for the synthesis of narrow distributed side-chain semiconductor polymers (Chapter 5, 6, 7, 10, 11). This comprises of the synthesis of different n-type and p-type semiconductor polymers by a modular synthetic strategy, where a few well controlled polymers can be taken as starting point for the conversion to many different semiconductor polymers (Figure 1). This was accomplished by a combination of controlled radical polymerization techniques and polymer analogous functionalization by the so called “click” chemistry with the respective semiconductor units (see Chapter 3 for details).

First, a scaffold polymer with alkyne units, either poly(propargyl acrylate) or poly(propargyl oxystyrene) was synthesized by nitroxide mediated radical polymerization, with narrow molecular weight distributions. Second, the respective semiconductor moiety, which carries an azide group, is attached as side-chain by copper-catalyzed azide-alkyne cycloaddition “click” reaction in a suitable solvent. Thus, different organic semiconductor units can be attached in order to enhance light absorption or tune the electronic properties or polarity of such a side-chain polymer. This general method helps to avoid problems in the direct polymerization of semiconductor monomers. The latter is often tedious because ideal polymerization conditions have to be found anew for each new monomer. The approach circumvents problems of solubility, transfer and termination reactions during the direct polymerization, the resulting broad molecular weight distributions and lack of control of the polymerization. It also has the advantage that different polymers and block copolymers synthesized from the same scaffold polymer can be compared with each other very reliably because they intrinsically exhibit the same degree of polymerization and molecular weight distribution and would only differ in their chemical substitution pattern. The modularity of the concept is only limited by the solubility of the educts, the formed product and the catalyst in the used solvent (high dilutions can be realized here) and that no sterical hindrance is blocking the access to the active sites. The method presented here is also suitable for scaling up of the synthesis of semiconductor homopolymers since the starting monomers are commercially available or can be easily synthesized in large quantities. This thesis spans a wide range of these possible strategies.

n-Type perylene bisimides were “clicked” to poly(propargyl acrylate) to form poly(perylene bisimides) and were compared with poly(perylene bisimide acrylate)s, synthesized by direct controlled radical polymerization (Chapter 5). Perylene bisimide derivatives, differing in their polarity, were “clicked” to poly(propargyl oxystyrene) and compared with each other to elucidate structure-property relationships (Chapter 6). The range of available perylene polymers was extended in Chapter 7 by “clicking” perylene diester benzimidazole and perylene diester imide. One of these new polymers exhibits broad absorption up to 700 nm. These polymers were also compared with two poly(perylene bisimides) described in Chapter 6, regarding their charge carrier mobility. Two manuscripts complete the study about side-chain polymers. Chapter 10 describes the synthesis of a side-chain p-type polymer by “click” chemistry while Chapter 11 deals with the synthesis of hydrophilic-hydrophobic and hydrophobic-hydrophobic donor-acceptor (D-A) semiconductor block copolymers by “click” chemistry and RAFT. These polymers were compared regarding their phase separation properties.

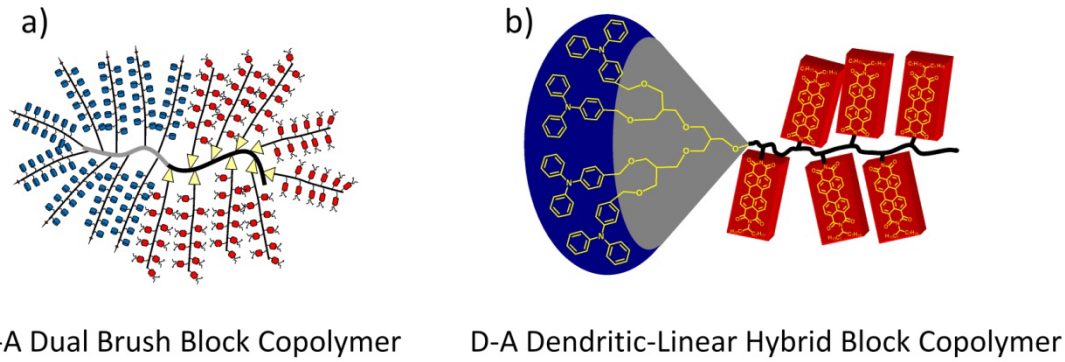

Figure 2: *Schematic representation of a) a donor-acceptor dual brush block copolymer and b) a donor-acceptor dendritic-linear hybrid block copolymer.*

A second key aspect of this thesis is the development of new concepts for complex semiconductor block copolymer architectures (Figure 2). Linear-linear semiconductor block copolymers have been described in the literature to obtain microphase separation in the range of the exciton diffusion length and thus a high D-A interface.

Here, we went one step further and developed novel block copolymer architectures and studied the properties of the resulting new compounds. The highly complex synthesis of a D-A dibrush block copolymer was realized which lead to D-A nano objects (Chapter 8). This was accomplished by a combination of “grafting to” and “grafting from” approaches from a block copolymer with one alkyne carrying block.

Besides the study of dual brush block copolymers, D-A dendritic-linear hybrid block copolymers were synthesized to extend the possibilities of polymer architecture for D-A block copolymers. The starting point of the synthesis was a second generation dendron carrying donor units. This was functionalized with an alkoxyamine initiator suitable for nitroxide mediated radical polymerization and the acceptor carrying monomer could be polymerized from it as a linear block (Chapter 9).

In the following, a brief summary of the main results of each manuscript is presented. A more detailed description of the synthesis, characterization and interpretation of the data can be found in the respective chapters (Chapters 5-11).

NMRP versus "Click" Chemistry for the Synthesis of Semiconductor Polymers Carrying Pendant Perylene Bisimides (Chapter 5)

The nitroxide mediated radical polymerization (NMRP) of perylene bisimide acrylate (PerAcr) (Figure 3a) lacks good control over molecular weight and molecular weight distribution. Here, we elucidate the cause of this by a kinetic study of the polymerization of perylene bisimide acrylate with a $(CH_2)_{11}$ spacer between imide and acrylate group. The result of the study is that transfer reactions occur permanently during this polymerization. This can be seen in the kinetic plot. The addition of 5 mol% of styrene as comonomer along with 0.1 equivalents of free nitroxide improves the kinetics to a linear progression but the PDI increases continuously with conversion. Also, the constantly initiated new chains lead to a very strong tailing of the polymer to low molecular weights.

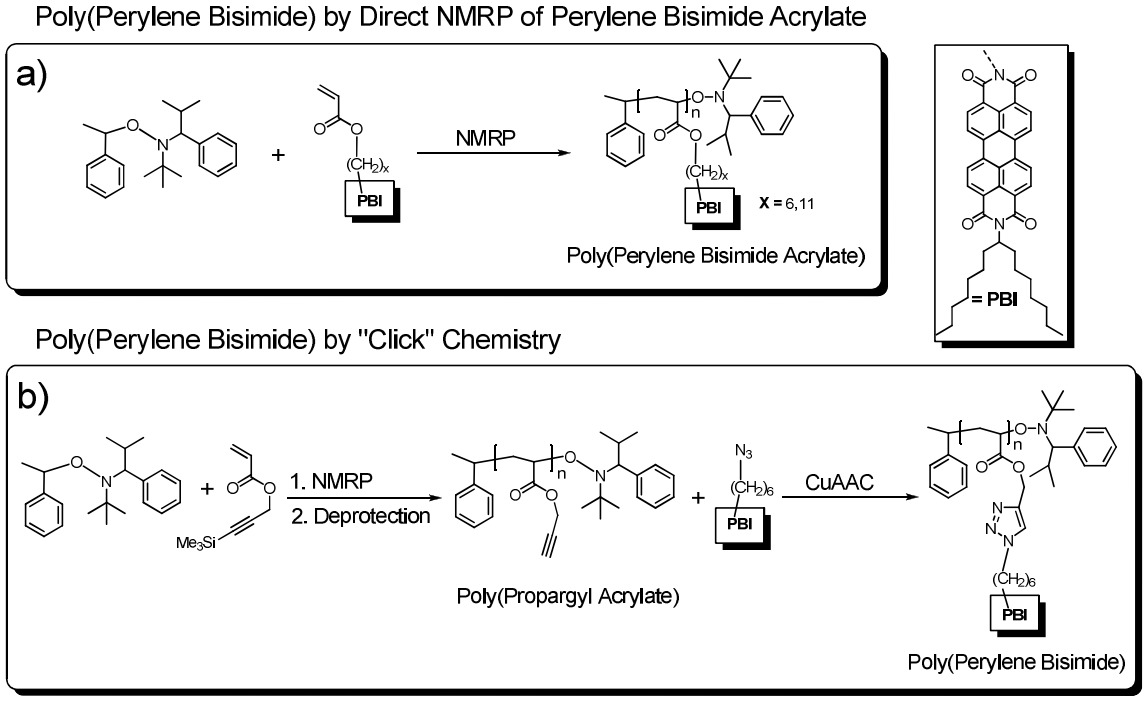

Figure 3: *Synthetic routes to poly(perylene bisimide)s. a) shows the direct polymerization of a perylene bisimide acrylate. b) shows the synthesis of poly(perylene bisimide)s via a combination of nitroxide mediated radical polymerization of a scaffold polymer and a subsequent polymer analogues copper-catalyzed azide-alkyne cycloaddition (CuAAC, "click" chemistry).*

The challenge is to circumvent this problem in synthesis and to find an alternative route to poly(perylene bisimides) (PPBI) with narrow molecular weight distribution. This is accomplished by the controlled synthesis of an alkyne carrying polymer, poly(propargyl acrylate) by NMRP and a subsequent polymer analogous reaction with a perylene bisimide azide with a $(CH_2)_6$ spacer between imide and azide (Figure 3b). The synthesis of poly(TMS-propargyl acrylate), which is the precursor for poly(propargyl acrylate), is also analyzed by a kinetic study. The kinetics of the polymerization in *o*-DCB shows linear dependencies of $\ln([M]_0/[M]_t)$ versus time up to 65 %

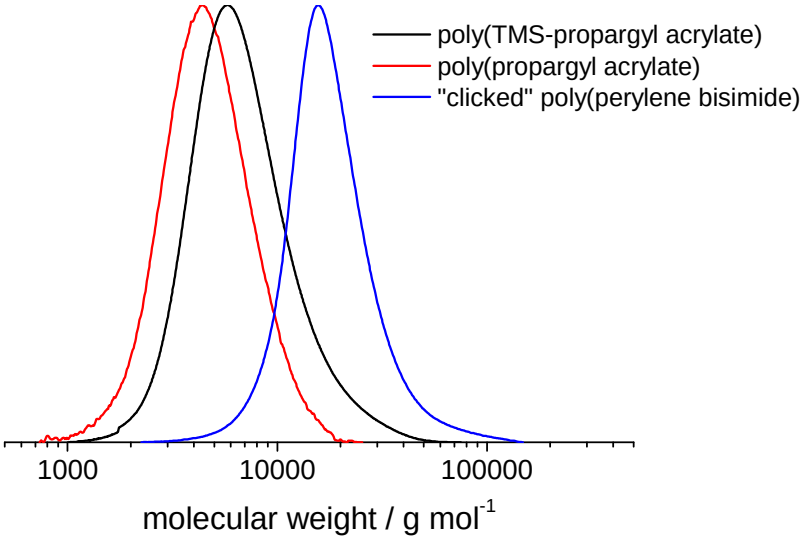

Figure 4: *SEC traces of protected poly(TMS-propargyl acrylate) (black line), deprotected poly(propargyl acrylate) (red line) and "clicked" poly(perylene bisimide) (blue line).*

conversion, indicating a constant number of radicals. Polymers with molecular weights up to 5 800 g/mol and PDIs below 1.20 are obtained by the polymerization. The protected polymer is deprotected with tetrabutylammoniumfluoride. The copper-catalyzed azide-alkyne cycloaddition (CuAAC, "click" reaction) between this polymer and the perylene bisimide azide is monitored by FTIR spectroscopy and ^{1}H NMR which indicates a quantitative conversion within the margins of the experimental error in ^{1}H NMR. A significant rise in molecular weight from 4 200 g/mol to 15 800 g/mol and a PDI of 1.17 are observed in SEC measurements (Figure 4). The "clicked" polymer, having a $(CH_2)_6$ spacer, is compared with a directly synthesized poly(perylene bisimide acrylate), also having a $(CH_2)_6$ spacer. Additionally, a directly synthesized poly(perylene bisimide acrylate), carrying a $(CH_2)_{11}$ spacer, was also compared. The result of this study is that both polymers with $(CH_2)_6$ spacer have similar thermal and structural properties and that the behavior of the polymer with $(CH_2)_{11}$ spacer differs. The "clicked" polymer has a T_g at 175 °C and a T_m at 288 °C while the polymer from direct polymerization with $(CH_2)_6$ spacer has a T_g at 193 °C and a T_m at 311 °C and has thereby a quite similar thermal behavior. Both polymers exhibit a liquid crystalline lamellar structure in powder diffraction with similar d spacing. The polymer from direct polymerization with $(CH_2)_{11}$ spacer exhibits only a T_m at 189 °C and exhibits a different liquid crystalline lamellar ordering than the other two polymers. Here, also a 110 reflection can be observed in XRD. All polymers show similar absorption spectra in $CHCl_3$ solution ($c = 10^{-5}$ mol·L^{-1}) with the characteristic absorption maxima of poly(perylene bisimide) at 527 nm, 491 nm and 464 nm.

These results let us conclude that it is possible to synthesize PPBIs with narrow molecular weight distributions by the modular approach of "click" chemistry, and these polymers have similar properties as poly(perylene bisimide acrylate)s obtained from direct polymerization.

Modular Synthesis of Poly(perylene bisimides) using "Click" Chemistry: A Comparative Study (Chapter 6)

In Chapter 5, the comparability of "clicked" poly(perylene bisimide)s (PPBI) and PPBIs synthesized by direct nitroxide mediated radical polymerization (NMRP) of perylene bisimide (PBI) monomers is discussed. The result of that study is that the properties of such polymers are quite comparable. Here, differently substituted "clicked" PPBIs are compared with one another. The modular approach of "click" chemistry enables such comparative studies, where many different polymers can be synthesized from one alkyne polymer, keeping the degree of polymerization and the PDI constant. Such an alkyne polymer is synthesized by NMRP of trimethylsilyl-protected propargyl oxystyrene and subsequent deprotection to poly(propargyl oxystyrene) with $M_{n,SEC}$ = 7 400 g/mol and a PDI of 1.11. By utilizing the techniques developed above, two types of pendant PBIs are attached to the poly(propargyl oxystyrene) backbone by "click" chemistry; those carrying hydrophilic oligoethylene glycol (OEG) swallow-tail substituents or those carrying hydrophobic alkyl swallow-tail substituents (Figure 5). In each series, the length of the spacer between the nitrogen of the triazole unit and the nitrogen of the PBI is varied from $(CH_2)_6$ to $(CH_2)_8$ and to $(CH_2)_{11}$. Finally, the polymers carrying hydrophilic OEG swallow-tails are systematically compared with polymers bearing alkyl swallow-tails. All synthesized PPBIs exhibit monomodal distributions, similar molecular weights around 60 000 g/mol and PDIs around 1.09 in SEC (Figure 6).

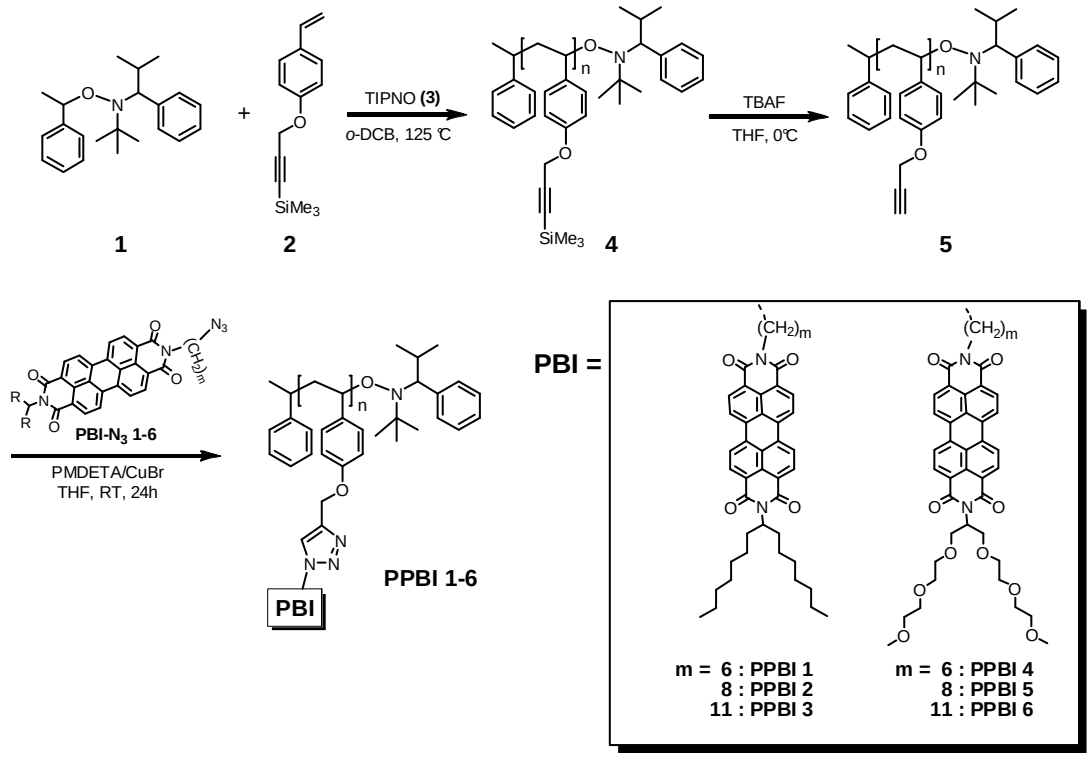

Figure 5: *Synthetic scheme of the synthesis of the six poly(perylene bisimide)s by "click" chemistry. Three of the polymers carry perylene bisimides with hydrophilic oligoethylene glycol swallow-tail substituents (**PPBI 4-6**) and three carry perylene bisimides with hydrophobic alkyl swallow-tail substituents (**PPBI 1-3**). The two different types of polymers were each synthesized with three different spacer lengths of $(CH_2)_6$, $(CH_2)_8$ and $(CH_2)_{11}$.*

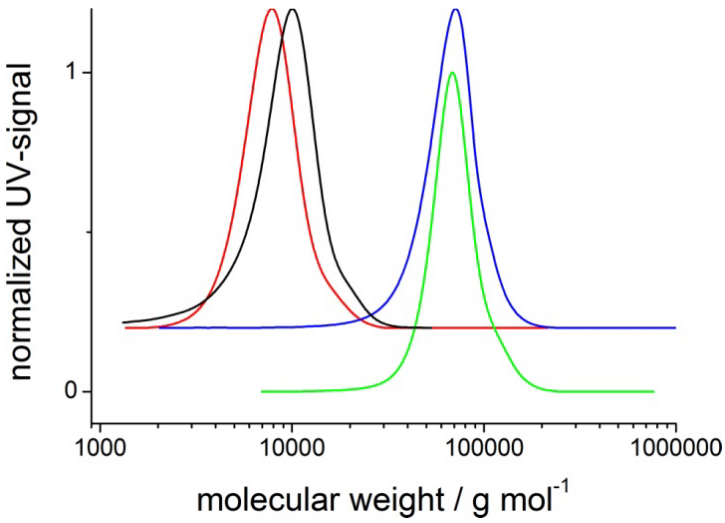

Figure 6: *Normalized UV-signal of SEC traces (detection at 254 nm) of poly(TMS-propargyl oxystyrene) (black line), deprotected poly(propargyl oxystyrene) (red line) and exemplarily one hydrophobic* ***PPBI 1*** *(green line) and one hydrophilic* ***PPBI 4*** *(blue line) polymer (both with $(CH_2)_6$ spacer). A clear increase in molecular weight for* ***PPBI 1*** *and* ***PPBI 4*** *after the "click" reaction and monomodal narrow distributions of molecular weight can be observed. The upper curves are vertically displaced for clarity.*

It is found that longer spacers shift the T_g of the polymers to lower temperatures due to the higher plasticization of the backbone. This occurs in PPBIs either with alkyl swallow-tail (**PPBI 1-3**) or with OEG swallow-tail substituents (**PPBI 4-6**). The phase behaviour of the compounds is strongly influenced by the length of spacer and nature of substituents. Only the PPBIs with alkyl swallow-tail and a spacer length of $(CH_2)_6$ and $(CH_2)_8$ show a melting peak in DSC. This melting peak is shifted to lower temperatures with increasing spacer length. The observed phase of the polymers is studied by powder diffraction experiments and can be determined to be a lamellar liquid crystalline (LC) smectic C phase where the side-chain mesogen is tilted. XRD shows a lamellar structure with reflections in a ratio of 1:2:3 in the low q regime for both polymers. The PPBI with the long $(CH_2)_{11}$ spacer exhibits no melting transition. Due to the long $(CH_2)_{11}$ spacer, the flexibility and softness is so large, that it results in a completely amorphous behaviour and only a T_g is observed. Also XRD measurements show no reflections in the low q region and thereby confirm an amorphous state of the polymer at RT (Figure 7).

Unlike in **PPBIs 1-3** with alkyl swallow-tail substituents, no liquid crystalline order can be observed in **PPBIs 4-6** with OEG swallow-tail groups. It seems that the introduction of OEG swallow-tails at the PPBI leads automatically to amorphous polymers for any used spacer length.

To elucidate the origin of the LC behaviour of the hydrophobic polymers with $(CH_2)_6$ and $(CH_2)_8$ spacer further, a model compound (**PBI-Sty**) of the hydrophobic polymer with $(CH_2)_6$ spacer is synthesized by a "click" reaction of propargyl oxystyrene and **PBI-N_3** with $(CH_2)_6$ spacer. Model compound **PBI-Sty** exhibits a clear lamellar structure with reflections in a ratio of 1:2:3:4 in the low q regime in XRD but no higher reflections, indicating also a liquid crystalline structure. The reflections can be attributed to a smectic A phase because the lamellar spacing equals the estimated length of one molecule. **PBI-Sty** shows birefringence in polarized light microscopy, the observed textures could best be described as focal conic.

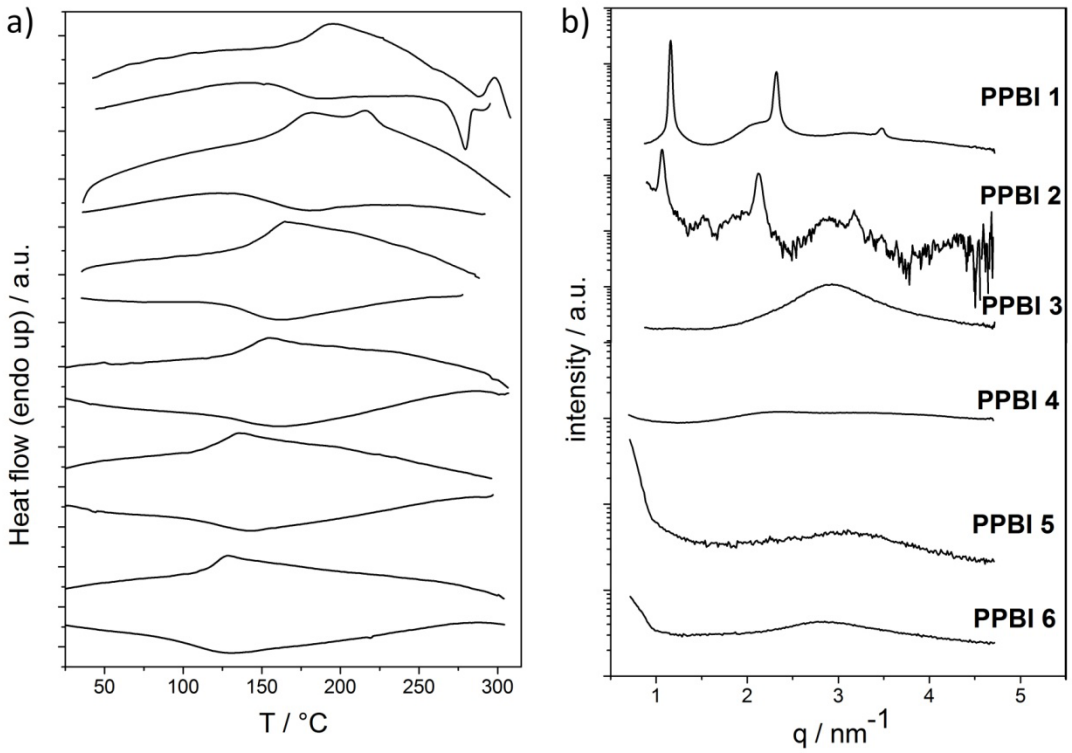

Figure 7: *a) DSC traces (second heating and cooling cycle) of hydrophobic* ***PPBI 1****,* ***2*** *and* ***3*** *and hydrophilic* ***PPBI 4****,* ***5*** *and* ***6*** *(from top to bottom) recorded at 40K/min. b) Diffraction patterns of* ***PPBI 1-6*** *at RT.*

All polymers show similar absorption spectra in $CHCl_3$ solution (c = 10^{-5} mol·L^{-1}) with the characteristic absorption maxima of PPBI at 527 nm, 491 nm and 464 nm. While hydrophilic and hydrophobic polymers behave quite similar in their absorption, the fluorescence measurements reveal a red shift of the fluorescence peak at 611 nm in hydrophobic polymers to 624 nm in hydrophilic polymers. This could be attributed to a smaller delocalization length in the excited state for the hydrophobic polymers.

Especially the presence of a glassy state with LC order at RT in these polymers allows tailoring the required film properties for applications. Polar groups in perylene bisimide containing polymers are suitable for the phase separation in block copolymers due to an additional hydrophilic-hydrophobic driving force and thereby an increased χ parameter. Amorphous PPBIs are also interesting compounds for further studies because it is quite exceptional that perylene bisimide derivatives have no higher molecular ordering, even though the basic π-π-stacking signal is observed in XRD. The applicability of these polymers as acceptor materials in suitable devices is under study.

Highly Efficient Electron-Transport Side-Chain Perylene Polymers (Chapter 7)

Since the above study proves the versatility of "click" chemistry for the synthesis of perylene containing polymers, an expansion of the available "clickable" perylene derivatives is worthwhile. Such new derivatives can exhibit altered electronic properties such as different HOMO and LUMO levels and thereby new band-gap energies. The result is a changed absorption which can be either shifted to higher or lower wavelengths, or more importantly, broadened, which allows harvesting more light. While a broad absorption is beneficial in photovoltaic application, this is not the only parameter which a compound has to fulfill. Besides absorption, the charge carrier mobility plays a major role for the successful application of a compound in devices. For this reason, we studied the charge carrier mobility of two poly(perylene bisimides) **(PPBI)**, whose synthesis is described in Chapter 6, and of newly synthesized poly(perylene diester benzimidazole) **(PPDB)**, with broad absorption up to 700 nm, and poly(perylene diester imide) **(PPDI)**, with a blue shifted absorption, compared to **PPBI** (Figure 8). All polymers were synthesized by "click" chemistry from the same scaffold polymer, poly(propargyl oxystyrene) ($M_{n,SEC}$ = 7 400 g/mol, PDI = 1.11). The poly(propargyl oxystyrene) was obtained via nitroxide mediated radical polymerization. The **PPBIs** differ in their swallow-tail substitution. **PPBI 1** is substituted with an alkyl swallow-tail and exhibits a liquid crystalline smectic C phase between 298 °C and RT (T_g at 182 °C). **PPBI 2** is substituted with an oligoethylene glycol swallow-tail and does not exhibit any crystallinity or liquid crystallinity but only a T_g at 142 °C.

The newly synthesized polymers **PPDB** and **PPDI** are analyzed by FTIR and ^{1}H NMR spectroscopy which indicates a quantitative conversion in "click" reaction within the margins of the experimental error in ^{1}H NMR. The "clicked" polymers exhibit monomodal distribution and very similar PDIs (1.09) as the scaffold polymer, poly(propargyl oxystyrene). Their molecular weight is determined by SEC to be 26 000 g/mol for **PPDB** and 15 000 g/mol for **PPDI**. It is evident that the molecular weights of **PPDB** and **PPDI** determined by SEC are underestimated, compared to the theoretical molecular weights of 44 000 g/mol and 40 000 g/mol, respectively. These values can be calculated assuming 100% conversion because the scaffold polymer resembles the polystyrene standard of the SEC and thereby its molecular weight of 7 400 g/mol corresponds to 44 repeating units.

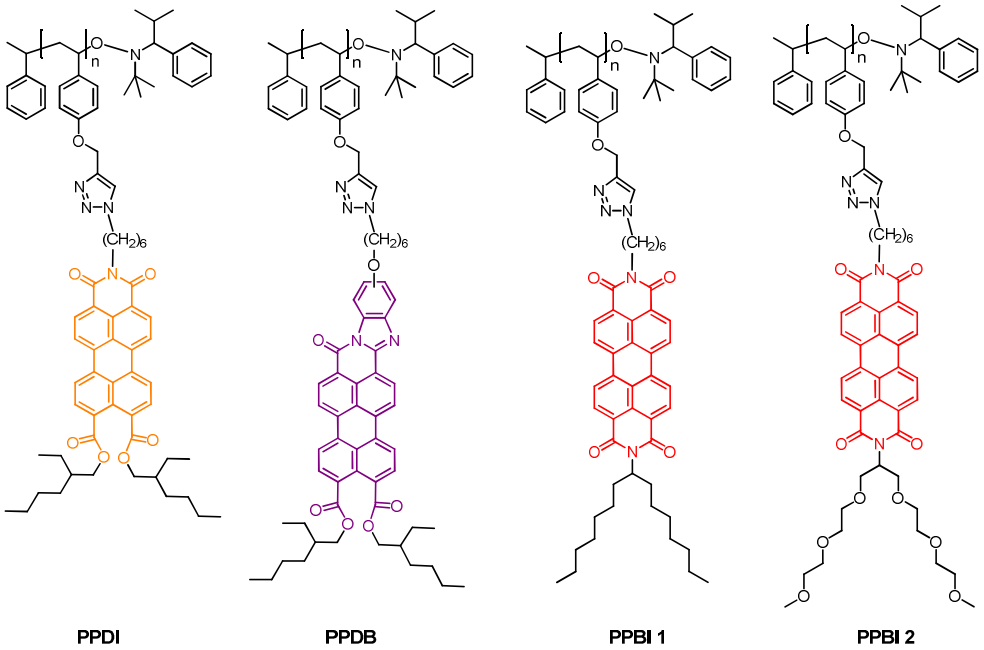

Figure 8: *Chemical structures of the four different studied poly perylenes, poly(perylene diester imide)* ***(PPDI)****, poly(perylene diester benzimidazole)* ***(PPDB)*** *and poly(perylene bisimide)s with alkyl swallow-tail* ***(PPBI 1)*** *or with oligoethylene glycol swallow-tail* ***(PPBI 2)****.*

In DSC, **PPDB** exhibits no T_g but only a melting peak at 285 °C. The x-ray diffraction pattern of **PPDB** shows three clear reflections in the low q regime at 1.05 nm^{-1}, 2.05 nm^{-1} and 2.84 nm^{-1}. No reflections at higher q values can be observed except the π-π stacking distance of the perylene core at 18.13 nm^{-1}, what resembles 3.5 Å. This shows that the observed phase in **PPDB** is a liquid crystalline ordering which is "frozen in" at RT. **PPDI** shows a T_g at 124 °C and a very weak melting peak at 192 °C. The x-ray diffraction pattern of **PPDI** shows also three reflections in the low q regime at 1.31 nm^{-1}, 2.48 nm^{-1} and 3.51 nm^{-1}. No reflections at higher q values can be observed except the π-π stacking distance of the perylene core at 17.93 nm^{-1} which is much weaker compared to **PPDB**. This shows that the observed phase in **PPDI** has also a liquid crystalline ordering which is "frozen in" below the T_g at 124 °C.

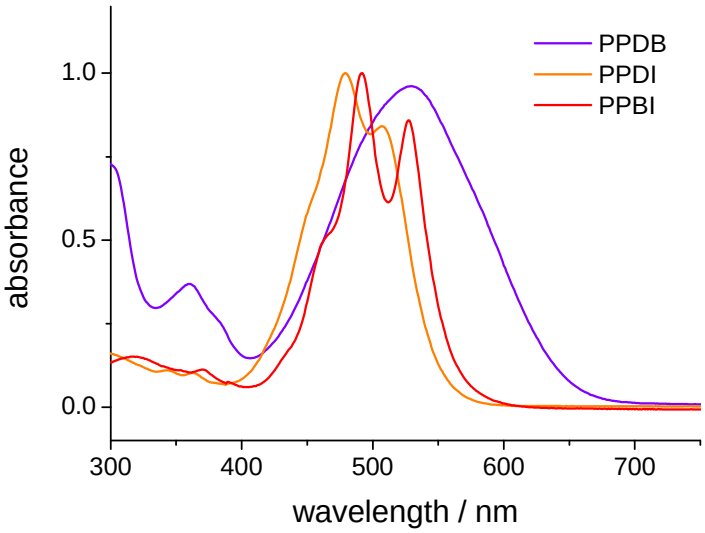

Figure 9: *Absorption spectrum of poly(perylene diester benzimidazole),* ***PPDB*** *(purple line), poly(perylene diester imide),* ***PPDI*** *(orange line) and poly(perylene bisimide),* ***PPBI*** *(red line).*

PPDI shows a fine structured absorption similar to the one of **PPBI** with absorption maxima at 507 nm, 478 nm and 453 nm. The spectrum is blue shifted compared to **PPBI** due to the smaller aromatic system. **PPDB** shows no fine structure but a featureless broad absorption up to 700 nm and with a maximum at 528 nm (Figure 9). These enhanced absorption properties will be beneficial for the application in photovoltaic devices due to the broader light harvesting.

The bulk charge carrier mobility of **PPDB**, **PPDI**, **PPBI 1** and **PPBI 2** is studied in single carrier devices by fitting the space charge limited currents (SCLC) according to Mott-Gurney equation. For determination of the electron mobility, each material is tested in electron-only devices. The hole mobility is determined from hole-only devices. A scheme of both single carrier devices is shown in Figure 10. **PPDI** has an electron mobility of 2.0×10^{-6} $cm^2V^{-1}s^{-1}$ which is almost two orders of magnitude below the electron mobility of **PPDB** with 1.0×10^{-4} $cm^2V^{-1}s^{-1}$. **PPBI 1** however shows a significantly higher electron mobility of 6.9×10^{-4} $cm^2V^{-1}s^{-1}$ compared to **PPDB**. Although optical properties were improved through the incorporation of a benzimidazole unit to the perylene core, the charge transport of **PPDB** suffers compared to the perylene bisimide derivative **PPBI 1**.

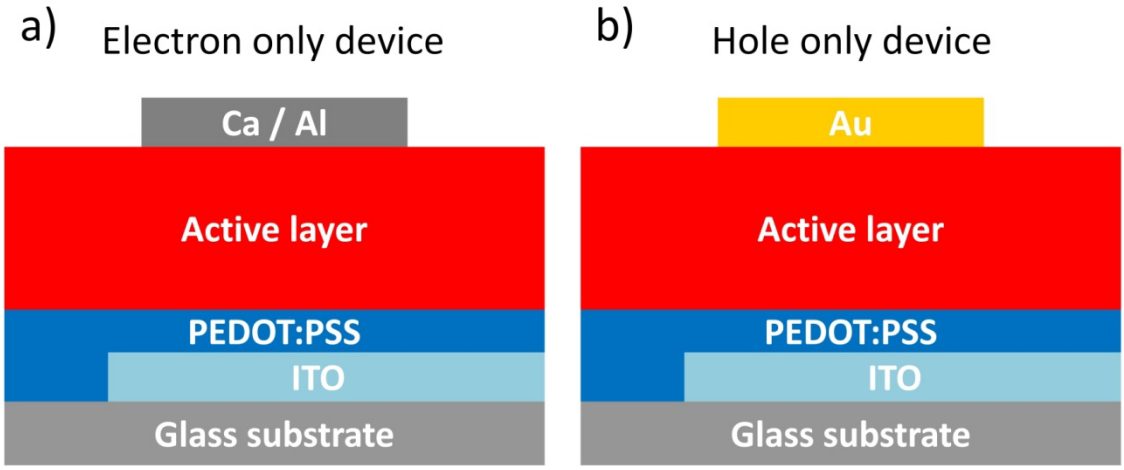

Figure 10: *a) Scheme of an electron-only device with a calcium top electrode, capped with aluminum; b) scheme of a hole-only device with gold top electrode.*

A comparison between **PPBI 1** and **PPBI 2** shows that not only the structure of the π-conjugation system hast an impact on the material's semiconductor properties. Altering the solubilizing side-chains at the imide position of the perylene from a branched alkyl to a branched oligoethylene glycol leads to a major increase of almost one order of magnitude in electron mobility from 6.9×10^{-4} $cm^2V^{-1}s^{-1}$ to 5.5×10^{-3} $cm^2V^{-1}s^{-1}$. The coupling of the perylene bisimide unit and the imide substituents are negligible because of the nodes in the HOMO and LUMO at the imide nitrogen. Thus, the improved charge transport properties of the amorphous **PPBI 2** can be rather explained by a potentially more favorable packing of the PBIs in the polymer thin film compared to films of the liquid crystalline **PPBI 1**.

Evaluation of hole-only devices and the corresponding Mott-Gurney fits of **PPDI** result that its hole mobilities of 3.0×10^{-6} $cm^2V^{-1}s^{-1}$ is higher than its electron mobility. Hence, a perylene core modified by a diester and an imide unit leads to a more pronounced p-type behavior of this material. For compounds **PPDI**, **PPBI 1** and **PPBI 2** the hole mobilities are all 1-2 orders of magnitude below their electron mobilities. This demonstrates that electron transport through the LUMO is more favorable than the hole transport via the HOMO, which is expected for n-type semiconductors.

Click Chemistry for p-type Semiconductor Materials (Chapter 10)

All manuscripts described above deal with the synthesis of n-type semiconductor polymers by "click" chemistry. As the concept is very modular, basically everything with an azide can be attached to an alkyne carrying backbone, as long as all educts, reagents and products are soluble in the reaction medium and no sterical hindrance is existent. It is obvious that not only the synthesis of n-type materials by "click" chemistry is feasible, but also the synthesis of p-type materials, as for example, polymers carrying tetraphenyl benzedine derivatives. The synthesis of such polymers by direct controlled radical polymerization of vinyl tetraphenyl benzedine, as described in literature, is tedious. We wanted to show that such polymers can be synthesize by "click" chemistry with narrow PDI very easily.

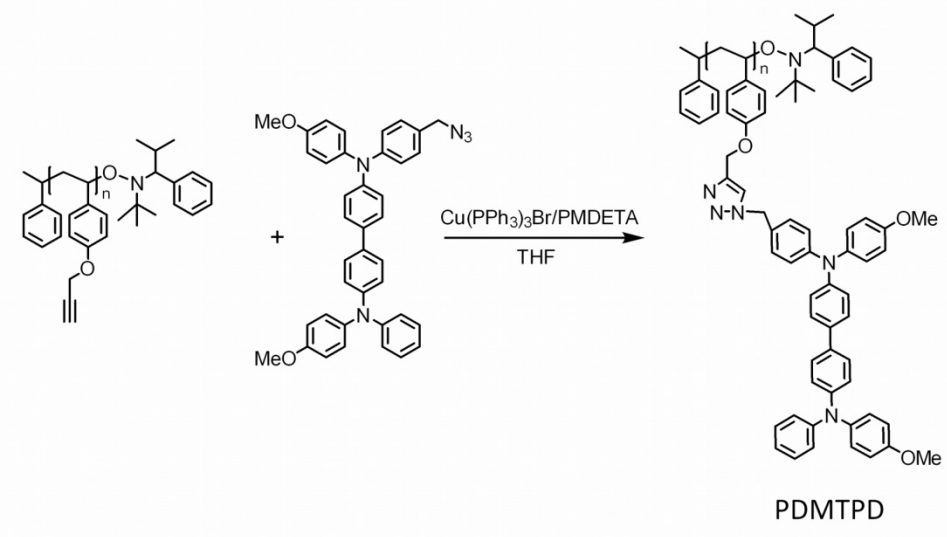

Figure 11: *Synthetic scheme of the synthesis of poly(N,N'-bis(4-methoxyphenyl)-N-phenyl-N'-4-triazolylphenyl-(1,1'-biphenyl)-4,4'-diamine),* ***PDMTPD****, by "click" chemistry.*

Thus, a *N*,*N*'-bis(4-methoxyphenyl)-*N*-phenyl-*N*'-4-azidomethylphenyl-(1,1'-biphenyl)-4,4'-diamine with an azide function (**DMTPD-N_3**) (see Figure 11) is synthesized. This azide is then "clicked" to the poly(propargyl oxystyrene) homopolymer ($M_{n,SEC}$ = 7 400 g/mol, PDI = 1.11) from nitroxide mediated radical polymerization, which is described in Chapter 6. The conversion of the reaction was again monitored by ^{1}H NMR spectroscopy which indicates a quantitative conversion within the margins of the experimental error in ^{1}H NMR. The "clicked" polymer poly(*N*,*N*'-bis(4-methoxyphenyl)-*N*-phenyl-*N*'-4-triazolylphenyl-(1,1'-biphenyl)-4,4'-diamine) (**PDMTPD**) (Figure 11) exhibits monomodal distribution and a very similar PDI of 1.09 as the scaffold polymer poly(propargyl oxystyrene) (Figure 12). The molecular weight was determined by SEC to be 17 000 g/mol. It is evident that the molecular weight determined by SEC is underestimated compared to the theoretical molecular weight of 34 000 g/mol, which can be calculated from 44 repeating units assuming 100% conversion in the "click" reaction.

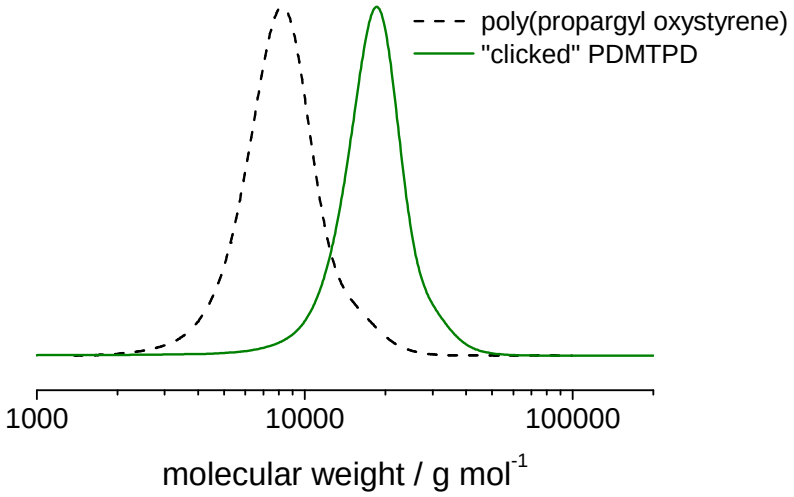

Figure 12: *SEC traces of scaffold polymer poly(propargyl oxystyrene) (dashed line) and "clicked" semiconductor polymer PDMTPD (green solid line). It can be seen that the molecular weight of the "clicked" polymer is significantly increased after the "click" reaction, while the shape of the curve is preserved.*

The thermal properties of the polymer are determined by DSC measurements. No melting peak can be observed in both polymers. While the scaffold polymer exhibits a T_g around 59 °C, **PDMTPD** shows a much higher T_g at 144 °C. Absorption at 354 nm can be observed in UV/Vis measurements in THF (c = 10^{-5} mol/L) and a strong fluorescence at 410 nm when excited at 354 nm.

Polymers synthesized by this approach can be introduced as one block in fully functionalized block copolymers for organic photovoltaics or as homopolymer in blend systems or bilayer architectures. Also, this work opens the general field of polymer analogous functionalization of alkyne carrying polymers with p-type semiconductor moieties.

Semiconductor Block Copolymers: The Influence of Polar Substitution on Microphase Separation (Chapter 11)

The synthesis of semiconductor homopolymers by "click" chemistry was shown in four detailed manuscripts above. As block copolymers have the intrinsic benefit to microphase separate into nanometer sized domains, donor-acceptor block copolymers are promising materials for photovoltaic applications. Such block copolymers were already synthesized by direct nitroxide mediated radical polymerization. The requirement for order-disorder (ODT) phase separation is that the χN parameter is high enough. This can be accomplished by synthesizing longer block copolymers and thereby to increase N, or to enhance the Flory Huggins parameter χ by, for example, using polymers that are chemically more distinct, or combining both properties. The main idea here is that hydrophilic-hydrophobic block copolymers should phase separate in a more pronounced way, compared to hydrophobic-hydrophobic polymers.

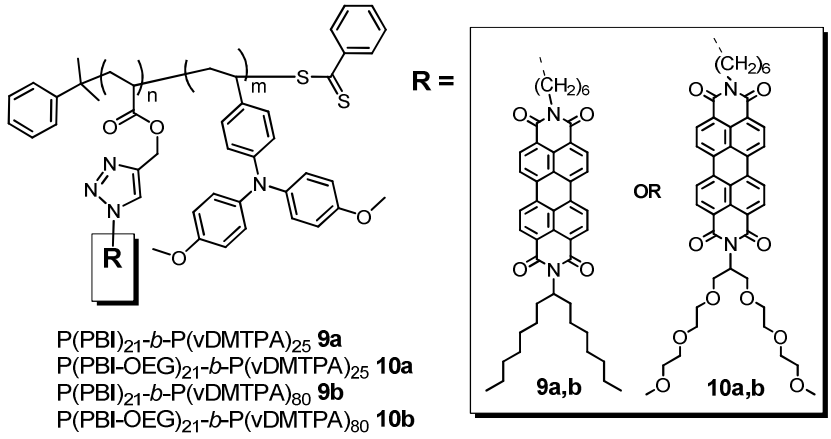

Figure 13: *Chemical structure of the synthesized block copolymers with either hydrophobic-hydrophobic (**9a, 9b**) or hydrophilic-hydrophobic (**10a, 10b**) blocks.*

To elucidate this, two hole transport block copolymers with an alkyne carrying propargyl acrylate block and a hydrophobic p-type poly(vinyl dimethoxy triphenylamine) block are synthesized by reversible addition-fragmentation chain transfer polymerization (RAFT) with molecular weights of 9 800 g/mol (PDI = 1.11) and 30 000 g/mol (PDI = 1.20), respectively. Both block copolymers are synthesized from the same poly(TMS-propargyl acrylate) with 4 200 g/mol and a PDI of 1.09. Finally, hydrophilic perylene bisimide with an oligoethylene glycol swallow-tail or hydrophobic perylene bisimide with an alkyl swallow-tail is "clicked" to the deprotected block copolymers (Figure 13). The conversion is monitored by ^{1}H NMR spectroscopy which indicates a quantitative conversion within the margins of the experimental error in ^{1}H NMR. The resulting hydrophilic-hydrophobic and hydrophobic-hydrophobic block copolymers are studied by AFM to investigate the phase separation of films of the block copolymers (Figure 14). Indeed, in the block copolymers with smaller molecular weights (**9a**, **10a**), only the hydrophilic-hydrophobic block copolymer **10a** shows lamellar phase separation while the hydrophobic-hydrophobic block

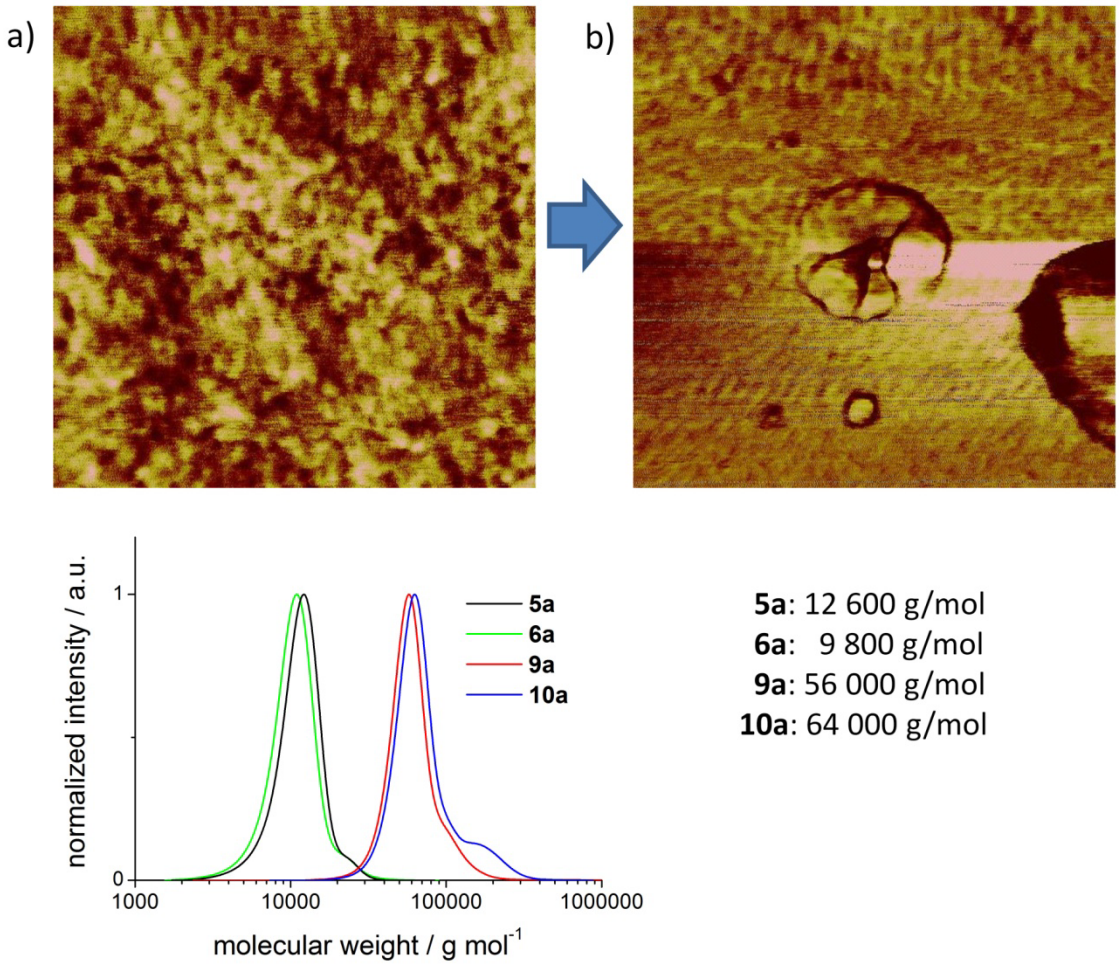

Figure 14: *AFM image of a) hydrophobic-hydrophobic block copolymer **9a** and b) hydrophilic-hydrophobic block copolymer **10a**. c) shows the SEC traces of precursor polymers **5a** and **6a**, the hydrophobic-hydrophobic block copolymer **9a** and the hydrophilic-hydrophobic block copolymer **10a**.*

copolymer **9a** does not show an ordered structure. This may be attributed to the higher χ parameter in the hydrophilic-hydrophobic block copolymer. In the higher molecular weight block copolymers, a worm like phase separation can be observed in both block copolymers. In this case, N is high enough for phase separation and the additional rise in χ may not have a deciding effect on the phase separation. Further TEM and SAXS studies are required to understand phase separation in bulk and thin films. This preliminary study proves that in semiconductor block copolymers, the introduction of polar groups in one block can lead to improved phase separation, which may be attributed to hydrophilic-hydrophobic interactions of the blocks.

Semiconductor Nanoparticles from Donor-Acceptor Dual Brush Block Copolymers (Chapter 8)

Nanoscale phase separation of donor/acceptor domains can be achieved by the self-assembly of block copolymers as shown in the previous section. Another strategy to obtain ordered interfacial morphology utilizes dual brush block copolymers, which can form distinct nano-objects. If dual brush block copolymers from D-A materials can be realized, distinct D-A phase separation could be obtained in such nano-objects.

We tackle the synthetic challenge to obtain D-A nanoparticles with controlled size and composition for the first time by the realization of a dual brush block copolymer via a combination of reversible addition-fragmentation chain transfer polymerization (RAFT) and "click" chemistry. The particles obtained from toluene solution exhibit a well-defined size of about 50-60 nm and globular structure. The synthesis is accomplished by an elegant and feasible synthetic approach which innovatively combines a "grafting from" polymerization of a donor monomer based on RAFT, with a "grafting to" approach of an acceptor polymer for which a copper-catalyzed azide-alkyne cycloaddition (CuAAC, "click" chemistry) is utilized. First poly(trimethylsilyl propargyl acrylate) with 29 repeating units is synthesized by RAFT

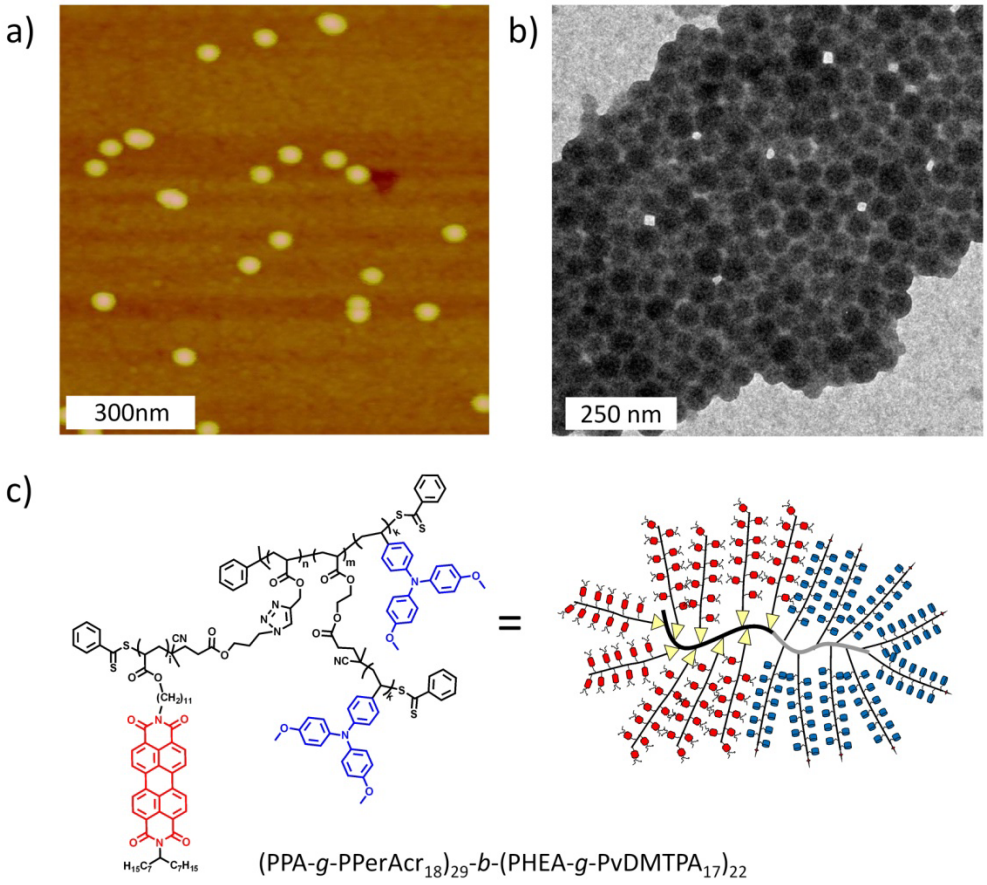

Figure 15: *a) AFM image, b) TEM image and c) chemical structure and schematic representation of donor-acceptor dual brush block copolymer* (PPA-*g*-PPerAcr$_{18}$)$_{29}$-*b*-(PHEA-*g*-PvDMTPA$_{17}$)$_{22}$.

polymerization (PDI = 1.09). This macro-RAFT agent is then used to prepare the block copolymer $PTMSPA_{29}$-*b*-$PHEA_{22}$ with a PDI of 1.16 by the subsequent polymerization of hydroxyethyl acrylate (HEA). The subsequent esterification of the hydroxyl groups of PHEA with the chain-transfer-agent (CTA) 4-cyanopentanoic acid-4-dithiobenzoate immobilizes the CTA on the polymer backbone. The complete functionalization can be proven by FTIR and ^{1}H NMR. The "grafting from" polymerization of the monomer *bis*(4-methoxyphenyl)-4'-vinylphenylamine) (= vinyldimethoxytriphenylamine, vDMTPA) using RAFT gives rise to the donor-brush block copolymer $PTMSPA_{29}$-*b*-(PHEA-*g*-$PvDMTPA_{17})_{22}$ with a PDI of 1.16. This is followed by the deprotection of the trimethylsilyl propargyl groups, resulting in donor polymer PPA_{29}-*b*-(PHEA-*g*-$PvDMTPA_{17})_{22}$, carrying free alkyne groups. Finally, the dual brush block copolymer (PPA-*g*-$PPerAcr_{18})_{29}$-*b*-(PHEA-*g*-$PvDMTPA_{17})_{22}$ is prepared by CuAAC of the alkyne carrying polymer and the azide functionalized poly(perylene bisimide acrylate) (PPerAcr) with 18 repeating units (PDI = 1.2). The PPerAcr was synthesized by RAFT with a CTA carrying an azide-group. The efficiency of the "click" reaction is determined by the analysis and comparison of ^{1}H NMR signals of the polymers and is estimated to be around 60%.

Because the molecular weight of the dual brush block copolymer cannot be detected by SEC, dynamic light scatting (DLS) measurements are carried out to compare the brush block copolymers before and after the "click" reaction. DLS results show that the hydrodynamic radius increases dramatically from about 7 nm to 29 nm. Atomic force microscopy (AFM) and transmission electron microscopy (TEM) are performed to visualize the nano particle morphology. Figure 15 shows in a) an AFM height image and in b) a TEM image of (PPA-*g*-$PPerAcr_{18})_{29}$-*b*-(PHEA-*g*-$PvDMTPA_{17})_{22}$, spin-coated from diluted toluene solution on a silicon wafer or drop-cast on a TEM grid, respectively. Very uniform globular structures can be observed in both cases. The typical particle has a height of 12 nm and a diameter of 53 nm in AFM and 60.3±6.8 nm in TEM, which is consistent with the DLS results (radius = 29 nm).

UV/Vis absorption measurements of the dual brush block copolymer (PPA-*g*-$PPerAcr_{18})_{29}$-*b*-(PHEA-*g*-$PvDMTPA_{17})_{22}$ clearly show the superposition of the TPA absorption at 300 nm and the characteristic fingerprint bands of perylene bisimide homopolymer at 472 nm, 493 nm and 535 nm. The emission of TPA, which is usually observed at 390 nm (excitation at 300 nm) is almost completely quenched in the dual brush block copolymer. The quenching of fluorescence indicates either energy or charge transfer between TPA and PerAcr. Excitation of the dual brush block copolymer at 493 nm (absorption max. of PerAcr) reveals a relatively weak fluorescence at 624 nm which attributes to the perylene bisimide polymer emission.

Further analyses are under way to determine the structural order, phase separation and also to identify the mechanism of build-up of these D-A nano particles from dual brush block copolymers.

Semiconductor Dendritic-Linear Block Copolymers by Nitroxide Mediated Radical Polymerization (Chapter 9)

In addition to the already discussed linear-linear block copolymers and dual brush block copolymer, other novel polymer architectures can be interesting to study. Dendrons, for example, feature the attribute of being monodisperse macromolecules. Hybrid block copolymers from such monodisperse dendritic architectures and a linear block could exhibit narrower PDIs compared to similar linear-linear block copolymers. Also the use of a dendritic block helps to introduce one of the blocks in amorphous state, so that a crystallization of the second block can be well tuned in an amorphous matrix. For this reason, we realize the first synthesis of a donor-acceptor dendritic-linear hybrid block copolymer comprised of a p-type dendritic and an n-type linear block, which is synthesized by nitroxide mediated radical polymerization. For this, a triphenylamine (TPA) bearing second generation polyether dendron [G2]-OH as donor is functionalized with an alkoxyamine initiator and subsequently perylene bisimide acrylate (PerAcr) (electron acceptor) is polymerized as a linear block to obtain a hybrid block copolymer named [G2]-*b*-PPerAcr (Figure 16a)).

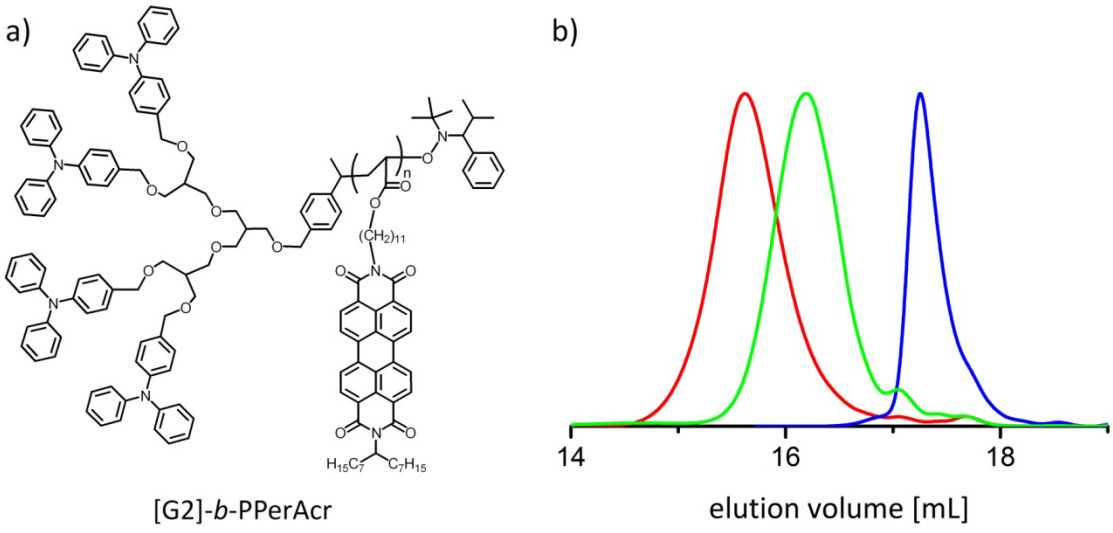

Figure 16: *a) Molecular structure of hybrid block copolymer [G2]-b-PPerAcr; b) SEC trace of macroinitiator [G2]-TIPNO (blue line) and two hybrid block copolymers [G2]-b-PPerAcr with different molecular weights (green and red line).*

We demonstrate the synthesis of two such hybrid block copolymers with different volume fractions of perylene bisimide and with molecular weights of 4 400 g/mol and 7 200 g/mol and PDIs around 1.12 (Figure 16 b)). While the amorphous dendron exhibits a glass transition temperature of 36 °C in DSC, no T_g can be detected in the hybrid block copolymers, which only exhibit melting points around 120°C, due to the side-chain liquid crystalline PPerAcr. The absorption spectra of films of the hybrid block copolymers clearly show the superposition of the

single absorption band of the TPA units in [G2]-OH at 303 nm and the characteristic fingerprint bands of PPerAcr at 472 nm, 493 nm and 535 nm in film. Photoluminescence measurements of the films of the hybrid block copolymers show a complete quenching of fluorescence when excited at 493 nm, indicating possible hole transfer from perylene bisimide to the TPA of the dendron. In comparison, a reference homopolymer PPerAcr shows an intense red fluorescence at 632 nm.

This novel architecture of semiconductor block copolymers has potential applications in organic photovoltaics, as well as organic field effect transistors, if the desired microphase separation can be achieved.

Individual contributions to joint publications

This thesis consists of seven individual manuscripts. Three are already published (Chapters 5, 6 and 9), one is submitted (Chapter 8), one is prepared for submission (Chapter 7) and two appear in the form of a manuscript (Chapter 10 and 11). In the following, the contributions of the individual authors to the papers are specified.

Chapter 5

This work is published in *Macromolecules* **2010**, 43, 7001–7010 under the title:

"NMRP versus "Click" Chemistry for the Synthesis of Semiconductor Polymers Carrying Pendant Perylene Bisimides"

By **Andreas S. Lang**, Anne Neubig, Michael Sommer and Mukundan Thelakkat.

I synthesized the "click" polymers and their precursors, did all the measurements and wrote the paper.

Anne Neubig helped me as practical student with the synthesis of the monomers and was involved in scientific discussion of the project.

Michael Sommer synthesized the PPBI $(CH_2)_6$ by direct NMRP.

Mukundan Thelakkat supervised the project and corrected the manuscript.

Chapter 6

This work is published in *Polymer Chemistry* **2011**, DOI: 10.1039/C1PY00191D under the title:

"Modular Synthesis of Poly(perylene bisimides) using Click Chemistry: A Comparative Study"

By **Andreas S. Lang** and Mukundan Thelakkat.

I did all of the synthesis and measurements and wrote the paper.

Mukundan Thelakkat supervised the project and corrected the manuscript.

Chapter 7

This work is prepared for submission under the title:

"Highly Efficient Electron-Transport Side-Chain Perylene Polymers"

By **Andreas S. Lang**, Mathis Muth and Mukundan Thelakkat.

I synthesized the PBI polymers and measured the basic properties of the polymers. I wrote the paper.

Mathis Muth did the SCLC measurements, was involved in scientific discussion and wrote the SCLC part of the paper.

Mukundan Thelakkat supervised the project and corrected the manuscript.

Chapter 8

This work is submitted to *Angewandte Chemie Int. Ed.,* **2011** under the title:

"Semiconductor Nanoparticles from Donor-Acceptor Dual Brush Block Copolymers"

By Guo-Dong Fu, **Andreas S. Lang**, Zhicheng Zheng, Fang Yao, Weian Zhang, Axel H. E. Müller and Mukundan Thelakkat.

Guo-Dong Fu synthesized the dual brush block copolymer and wrote the paper.

I synthesized the PBI monomer, helped with the synthesis of the polymers, was involved in scientific discussion and interpretation of the data and corrected and wrote parts of the manuscript.

Zhicheng Zheng did the AFM and TEM measurements.

Fang Yao synthesized the RAFT-agent with azide functionality.

Weian Zhang synthesized a RAFT-agent.

Axel H. E. Müller was involved in scientific discussion and corrected the manuscript.

Mukundan Thelakkat supervised the project and corrected the manuscript.

Chapter 9

This work is published in *Macromolecular Rapid Communication* **2009**, 30, (14), 1243-1248 under the title:

"Semiconductor Dendritic-Linear Block Copolymers by Nitroxide Mediated Radical Polymerization"

By **Andreas S. Lang**, Franz René Kogler, Michael Sommer, Ulrich Wiesner and Mukundan Thelakkat.

I synthesized the dendritic-linear block copolymer, did all of the measurements and wrote the paper.

Franz René Kogler synthesized the precursor dendron.

Michael Sommer synthesized the chlorinated initiator and was involved in scientific discussion.

Ulrich Wiesner supervised the work of Franz René Kogler.

Mukundan Thelakkat supervised the project and corrected the manuscript.

Chapter 10

This work is prepared as a basis for further investigations towards:

„Click" Chemistry for p-Type Semiconductor Materials

By **Andreas S. Lang** and Mukundan Thelakkat.

I synthesized the polymers and wrote the paper.

Mukundan Thelakkat supervised the project and corrected the manuscript.

Chapter 11

This work is prepared as a basis for further investigations towards:

"Semiconductor Block Copolymers: The Influence of Polar Substitution on Microphase Separation"

By **Andreas S. Lang**, Guo-Dong Fu and Mukundan Thelakkat.

I synthesized the "click" block copolymers and wrote the paper.

Guo-Dong Fu did the RAFT polymerization of donor carrying diblock copolymers.

Mukundan Thelakkat supervised the project and corrected the manuscript.

Chapter 5

NMRP versus "Click"-Chemistry for the Synthesis of Semiconductor Polymers Carrying Pendant Perylene Bisimides

*Andreas S. Lang, Anne Neubig, Michael Sommer and Mukundan Thelakkat**

Applied Functional Polymers, Department of Macromolecular Chemistry I, University of Bayreuth, Universitätsstr. 30, 95440 Bayreuth, Germany

Published in *Macromolecules* **2010**, *43*, 7001–7010

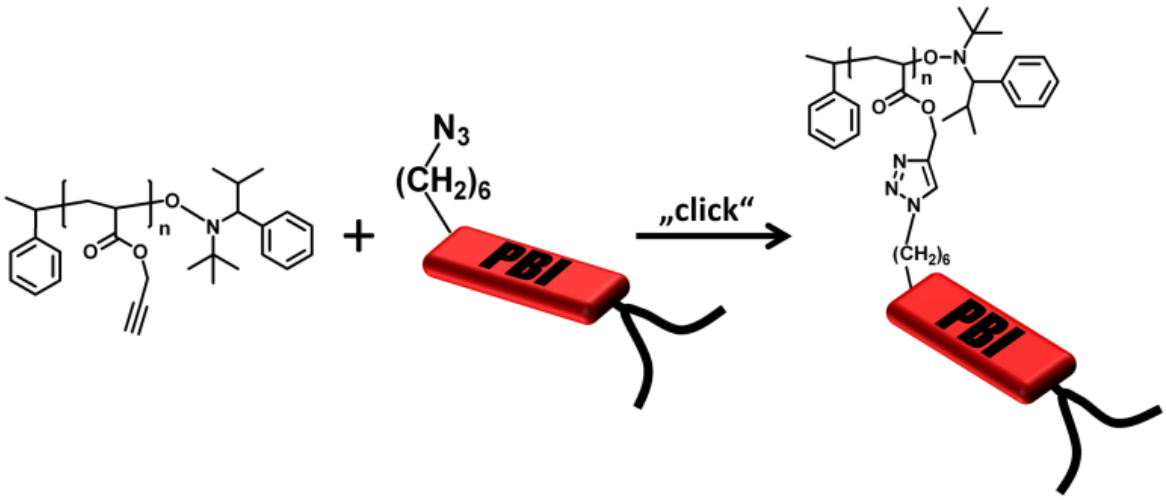

Abstract

The synthesis of well defined polymers with pendant perylene bisimide (PBI) groups by a combination of nitroxide mediated radical polymerization (NMRP) of trimethylsilyl propargyl acrylate followed by copper catalyzed azide-alkyne cycloaddition (CuAAC, “click”-chemistry) is described. The kinetics of NMRP of trimethylsilyl propargyl acrylate polymerization was monitored by ^{1}H NMR and size exclusion chromatography (SEC). Almost quantitative conversion in “click”-reaction with an azide functionalized PBI derivative was proven by FTIR and ^{1}H NMR analysis. Thus semiconductor polymers carrying PBI pendant groups with M_n up to 15 800 g·mol^{-1} and polydispersity indices as good as 1.16 were obtained by this route. These polymers were compared with poly(perylene bisimide acrylate)s, PPerAcr$(CH_2)_{11}$ and PPerAcr$(CH_2)_6$, which were synthesized by direct NMRP of PBI-acrylates. These samples do not carry any triazol unit and they differ in their spacer length connecting the PBI unit to the main chain. All polymers were comparatively studied by SEC, thermogravimetry, differential scanning calorimetry, polarization microscopy, UV/Vis spectroscopy and photoluminescence measurements. The crystalline structure of the polymers was analyzed by X-ray diffraction. Inductively coupled plasma mass spectrometry analysis confirmed that copper content in the “click”-polymer could be reduced down to 126 ppm (wt/wt).

Introduction

Controlled radical polymerization (CRP) techniques are convenient alternatives to living ionic polymerization.[1] They feature the advantage of enhanced functional group tolerance and overcome the rigorous conditions of ionic polymerization, still providing good control over molecular weight and narrow polydispersity indices (PDI = M_w/M_n). Nevertheless, control of molecular weight and PDI in CRP can be limited when it comes to the application of high molecular weight monomers, monomers with sterical hindrance or monomers whose analogue polymers are not soluble in suitable organic solvents. The intention of bypassing such challenging issues in polymerizations by attaching the side groups at an easy to polymerize scaffold polymer block by polymer analogous reactions is often limited by incomplete conversion. However, coupling reactions that lead to quantitative conversions at moderate reaction conditions and in reasonable time, without side products and in a simple manner were summarized by Sharpless et al. in 2001 under the term “click”-chemistry.[2] Meanwhile, these types of coupling reactions can be seen as standard reactions in organic synthesis and especially in the design of new functional materials. Upcoming metal-free “click”-methods[3] as thiol/ene “click”-chemistry[4] or the reversible addition fragmentation chain transfer - hetero Diels-Alder (RAFT-HDA) “click”-reaction of cyclopentadienes and dithioesters[5, 6] are promising approaches to replenish established techniques such as the Cu(I)-catalyzed 1,3-dipolar cycloaddition of azides and alkynes (CuAAC).[2, 7, 8] Nevertheless, CuAAC is currently the most commonly used “click”-reaction, outstanding for its versatility and easy to introduce clickable groups. Especially the combination of CuAAC with the three most commonly used CRP methods, atom transfer radical polymerization (ATRP)[9-12], reversible addition-fragmentation chain transfer polymerization

(RAFT)[13, 14] and nitroxide mediated radical polymerization (NMRP)[15-18] has proven to be a powerful tool for material synthesis. The modularity of these concepts allows studying an endless variety of different functional or nonfunctional polymers, all deriving from one synthesized alkyne or azide bearing polymer. By this approach it is possible to compare the influence of small structural changes in the pendant groups on the properties of the final polymer, keeping the degree of polymerization and PDI of the compared polymers exactly constant.

Perylene bisimide[19, 20] (PBI = perylene tetracarboxylic acid bisimide) derivatives represent an important class of light absorbing n-type semiconductor materials, exhibiting a relatively high electron affinity among large-bandgap materials.[21] PBIs combine high quantum yields of photoluminescence with excellent photochemical and thermal stability and are promising compounds for application in organic electronic devices.[22-24] Also, suitable substituted PBIs exhibit long range order via supramolecular self-assembly[25] or liquid crystalline behavior.[26-28]

Polymers with PBI as pendant groups feature high electron mobility combined with good film forming properties.[29] Such polymers were already incorporated as one block in semiconductor donor-acceptor block copolymers for photovoltaic application.[22, 23, 30-34] Nevertheless, the homopolymerization of PBI containing acrylates remains problematic because it results in polymers with broad molecular weight distributions. Also limited solubility of resulting PBI polymers, combined with the need to work in highly concentrated solutions, restricts the nature of the substituents of PBI monomers. Considering that narrow molecular weight distributions are important to understand structure-property relationships in polymers and block copolymers, a synthetic route to PBI-containing polymers with narrow PDIs and a higher independence of the chemical nature of the PBI derivative is desirable. With this in mind, a combination of NMRP and “click”-chemistry seems to be a very promising approach. PBI was employed successfully in “click”-chemistry by Langhals et al. as fluorescence label.[35] Nolte et al. already showed that the clicking of PBI to polyisocyanopeptides is possible quantitatively. [36] However, these polymerizations were not controlled and showed broad polydispersities. Very recently, Segalman et al. obtained PBI-containing block copolymers by a double “click”-approach, first coupling P3HT with poly(trimethylsilyl propargyl acrylate) obtained by ATRP, followed by a second CuAAC with an azide containing PBI.[33]

Motivated by these successful examples of the combination of PBI with “click”-chemistry, we investigated the suitability of this synthetic concept in detail to establish a general method towards narrow distributed polymers with pendant PBI units. First, we give a detailed study of the synthesis of a “clicked” PBI-polymer with a $(CH_2)_6$ spacer by combination of CuAAC and NMRP. Secondly, we examine how the triazol unit of “clicked” polymers changes the polymer properties. For this purpose, we synthesized two reference PBI polymers directly by NMRP that do not carry any triazol unit and which differ in their spacer lengths, e.g. $(CH_2)_6$ and $(CH_2)_{11}$ spacers. The three PBI polymers depicted in Figure 1 are compared with respect to their structural, optical and thermal properties.

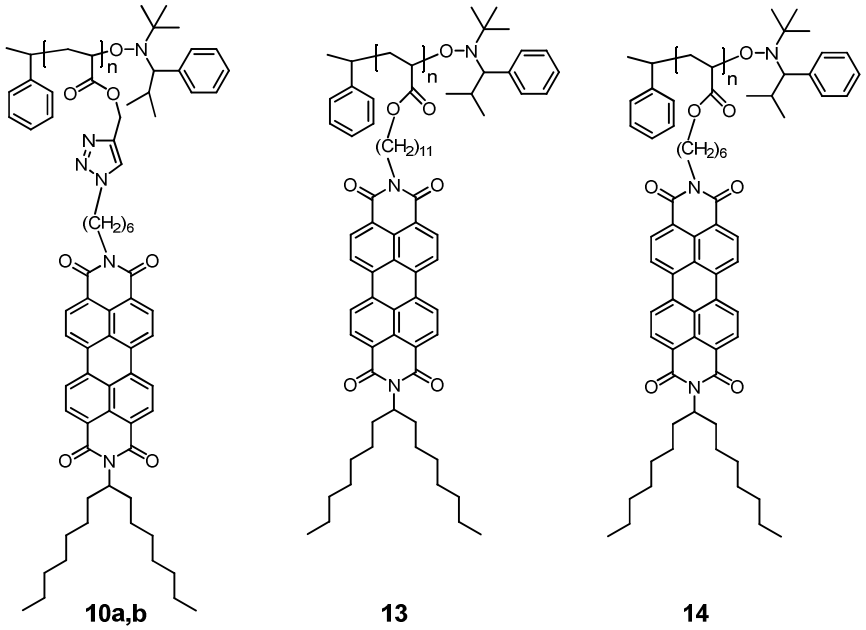

Figure 1: *“Clicked” PBI-polymers **10a,b** with a spacer length of $(CH_2)_6$ and the two reference perylene bisimide polymers PPerAcr $(CH_2)_{11}$ **13** and PPerAcr$(CH_2)_6$ **14** with spacer length of $(CH_2)_{11}$ and $(CH_2)_6$ respectively, synthesized directly by nitroxide mediated polymerization.*

Results and Discussion

Polymer Synthesis

The polymers **10a,b** with different molecular weights were obtained by a combination of NMRP and “click”-chemistry whereas the polymers PPerAcr$(CH_2)_{11}$ **13** and PPerAcr$(CH_2)_6$ **14** were obtained by the direct NMRP of acrylate monomers carrying the respective PBI pendant groups with $(CH_2)_{11}$ or $(CH_2)_6$ spacers respectively. As a typical example, the kinetics of the polymerization of **13** is given in Figure 2. The polymerization was conducted with 0.1 equivalents of additional free nitroxide to shift the equilibrium to the dormant species and enhance control of the polymerization. The kinetic plots for the polymerization are given in Figure 2a. As can be evidently seen, the polymerization kinetics do not follow a perfect linear first order and the PDI increases continuously with conversion. Further increase of free nitroxide to 0.2 and 0.5 equivalents also did not improve the PDI (Figure 10-12). On the other hand, even though the addition of 5 mol% of styrene[34, 37] as comonomer along with 0.1 equivalents of free nitroxide improves the kinetics to a linear progression, the PDI still rises strongly with conversion. This behavior can be ascribed to transfer reactions occurring permanently during the polymerization. Because of these reasons, a new synthetic route for PBI carrying polymers by “click”-chemistry is investigated by avoiding the transfer reactions in direct NMRP. The poly(perylene bisimide acrylate) polymers **13** and **14** reported in this work were polymerized without the addition of styrene because it has no beneficial effect on the quality of the polymers at higher conversions and enhances the reaction time. The SEC and thermal data of the polymers are summarized in Table 1.

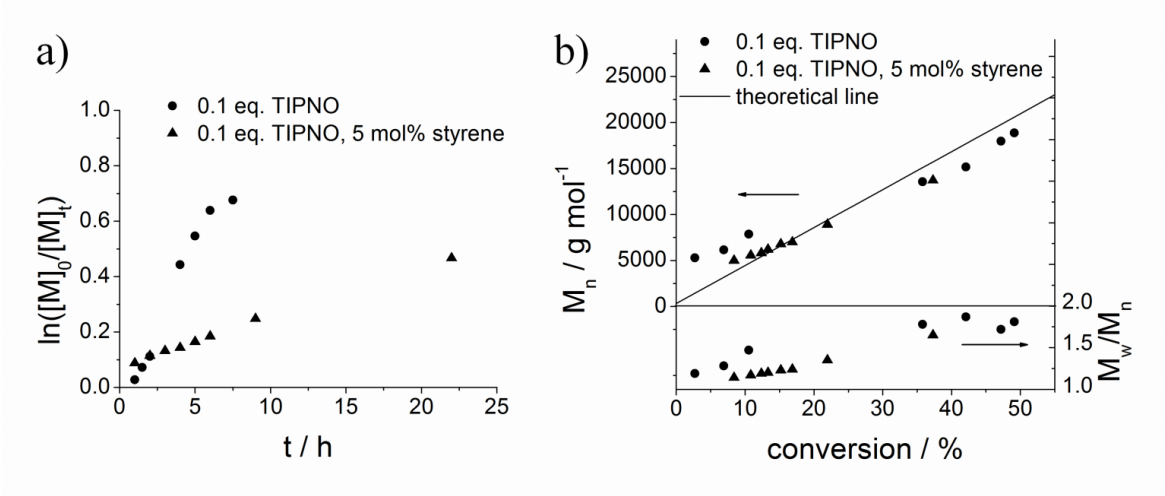

Figure 2: *Homopolymerization to poly(perylene bisimide acrylate) PPerAcr(CH_2)$_{11}$ using **11** as initiator in o-dichlorobenzene solution at 125 °C and a ratio of $[M]_0$:$[I]_0$ of 50:1. ● Experiment with additional 0.1 equivalents of free nitroxide 2,2,5-tri-methyl-4-phenyl-3-azahexane-3-nitroxide (TIPNO); ▲ experiment with 0.1 equivalents of TIPNO and additional 5 mol% of styrene. (a) First-order kinetic plots. (b) Dependence of M_n and M_w/M_n on the monomer conversion.*

An overview of the synthetic route to obtain the alkyne polymers **4a,b** from propargyl acrylate **1** is given in Scheme 1 and their conversion to “clicked” PBI-polymers **10a,b** is given in Scheme 2. For the sake of comparison with PBI-polymers directly synthesized via NMRP, we used an acrylate monomer to build up the alkyne carrying precursor polymer. Thus propargyl acrylate **1** was prepared by the reaction of acrylic acid chloride with propargyl alcohol.[38] Because the polymerization of the unprotected propargyl acrylate **1** by NMRP is complicated by coupling reactions of the alkyne, which leads to cross-linking,[9, 16] the alkyne function was protected with trimethylsilyl chloride under catalysis of $AgNO_3$ and 1,8-diazabicyclo[5.4.0]undec-7-ene.[16] To avoid deprotection, monomer **2** was stored at -14 °C under inert gas atmosphere and was freshly distilled each time before use. The polymerization of **2** was conducted at 125 °C using alkoxyamine **11** as initiator and with a ratio of monomer to initiator [M]:[I] = 50:1. Additional 0.1 equivalents of free nitroxide 2,2,5-tri-methyl-4-phenyl-3-azahexane-3-nitroxide (TIPNO) were added to shift the equilibrium of the NMRP more towards the dormant species and thereby to increase the control over the polymerization. The low molecular weight polymer **3a** was obtained by quenching the reaction at a lower conversion. Our first attempts to polymerize **2** in bulk showed only very low conversions below 5%, even after 24 hours. After dilution with *o*-dichlorobenzene (*o*-DCB), reasonable conversions above 60% were observed in this time span. For further investigation of this effect, we studied kinetics of the polymerization at monomer concentrations of 9 mol·L^{-1} and 27 mol·L^{-1} in *o*-DCB by determining the conversion by ^{1}H NMR at different intervals during the polymerization. All other reaction conditions were kept constant. The recorded kinetic plots for polymerizations at both concentrations showed linear dependencies of $\ln([M]_0/[M]_t)$ versus time up to 65 % conversion (Figure 3), indicating a constant number of radicals. Interestingly, the apparent rate constant k_{app} ($k_{app} = \ln([M]_0[M]_t/t)$ observed

Scheme 1: *Synthesis of alkyne polymers* ***4a,b*** *by nitroxide mediated radical polymerization and subsequent deprotection of* ***3a,b****; DBU = 1,8-Diazabicyclo[5.4.0]undec-7-ene, TIPNO = 2,2,5-tri-methyl-4-phenyl-3-azahexane-3-nitroxide, TBAF = tetra-n-butylammonium fluoride, THF = tetrahydrofuran, o-DCB = ortho-dichlorobenzene.*

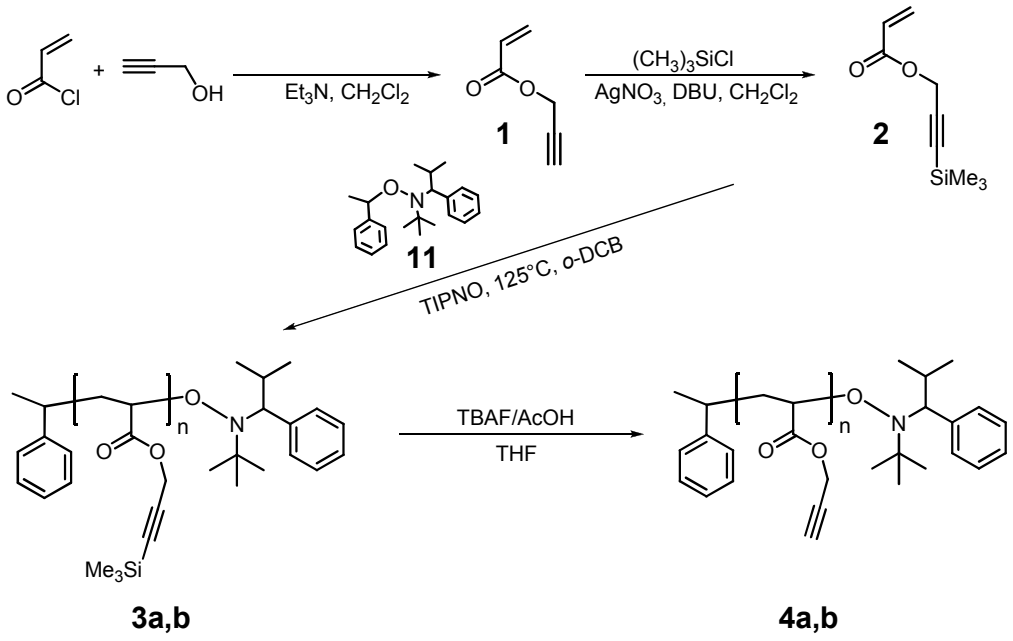

4a: M_n = 1300 g/mol; PDI = 1.1
4b: M_n = 4200 g/mol; PDI = 1.2

for the higher concentration ($[M]_0$ = 27 mol·L^{-1}, k_{app} = 2.0·10^{-2} h^{-1}) was lower than for the polymerization with the lower monomer concentration ($[M]_0$ = 9 mol·L^{-1}, k_{app} = 3.6·10^{-2} h^{-1}). This rise of k_{app} upon dilution stands in contrast to usual rate laws of radical polymerizations, where a deceleration of the polymerization would be expected upon dilution. At further dilution of the monomer, we observed a decline in k_{app} according to usual polymerization rate laws for diluted systems.[39] Considering the still low rate of polymerization of 3-(trimethylsilyl)prop-2-ynyl acrylate in NMRP, this technique is applicable for the synthesis of lower molecular weight polymers, but not ideal for polymers with very high molecular weights. In both polymerizations the plot of molecular weight ($M_{n,SEC}$) against conversion initially correlates with the theoretical molecular weight, calculated from conversion. Above a conversion of 20%, a low molecular shoulder around 2 500 g·mol^{-1} emerges in size exclusion chromatography (SEC) curves (Figure 13) and the plotted M_n declines under the theoretical calculated line. Simultaneously the PDI rises. It is noted, that after cleaning the polymers from monomer and solvent by dialysis against THF for 5 days, the SEC curves were monomodal and did not show the low molecular weight shoulder anymore. Dialysis was used here because the precipitation of poly(3-(trimethylsilyl)prop-2-ynyl acrylate) from THF in MeOH/H_2O leads to a turbid dispersion and a high loss of polymer. After dialysis, the observed PDIs were narrow and the M_n were closer to the theoretical values, calculated from conversion. This was also observed for polymers cleaned by reprecipitation. The deprotected polymers **4a,b** were obtained by removing the trimethylsilyl group using tetra-*n*-butylammonium fluoride, buffered with acetic acid according to a published procedure of Haddleton et al.[10] SEC

Table 1: *Overview of the analysis data of the polymers, with respect to molecular weight and polydispersity determined by SEC, thermal stability determined by thermogravimetric analysis and observed phase transitions and enthalpies from differential scanning calorimetry.*

polymer	M_n [g/mol] (SEC)[a]	M_w/M_n (SEC)[a]	T_{onset} [°C][b]	$T_{m,1}$ [°C][c]	ΔH [J/g][c]	$T_{m,2}$ [°C][c]	ΔH [J/g][c]	notes
3a	2 100	1.17	-	-	-	-	-	protected alkyne polymer from **2**
4a	1 300	1.17	-	-	-	-	-	deprotected alkyne polymer from **3a**
10a	5 200	1.16	-	-	-	-	-	“clicked” PBI-polymer from **4a**
3b	5 800	1.20	-	-	-	-	-	protected alkyne polymer from **2**
4b	4 200	1.20	-	-	-	-	-	deprotected alkyne polymer from **3b**
10b	15 800	1.17	310	175	1.2	288	0.5	“clicked” PBI-polymer from **4b**
13	18 400	1.68	359	189	7.6	n.o.	-	reference polymer PPerAcr(C_{11})
14	12 500	1.80	356	193	4.6	311	0.5	reference polymer PPerAcr(C_6)

Note: [a] Measured with size exclusion chromatography in tetrahydrofuran and calibrated with polystyrene standards; [b] Measured by thermogravimetric analysis under N_2 atmosphere; [c] Measured by differential scanning calorimetry under N_2 atmosphere.

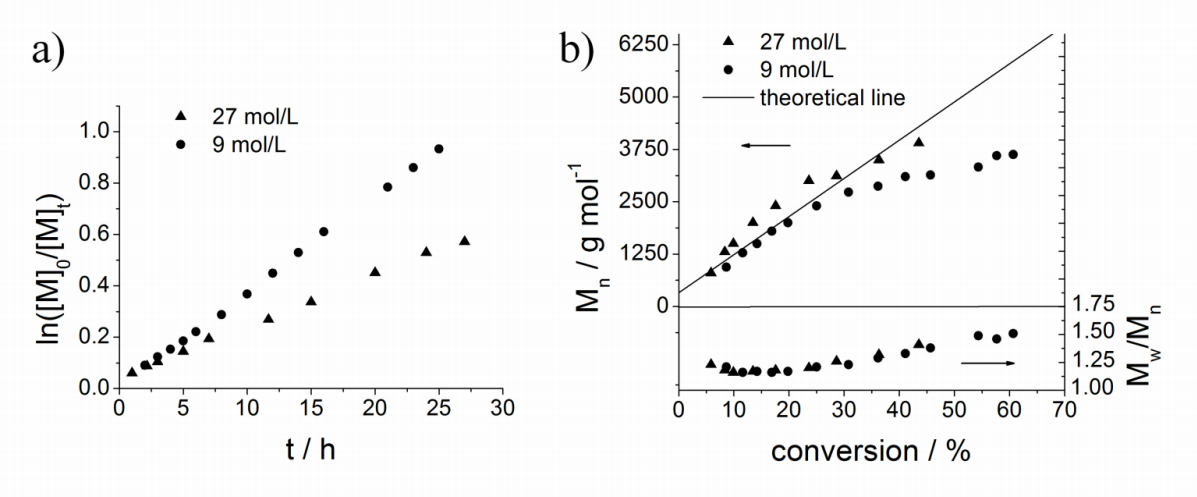

Figure 3: *Kinetics and evolution of molecular weight and PDI for the homopolymerization of protected propargyl acrylate **2** using **11** as initiator in o-dichlorobenzene solution at 125 °C at a ratio of $[M]_0:[I]_0$ of 50:1 and with additional 0.1 equivalents of free nitroxide 2,2,5-tri-methyl-4-phenyl-3-azahexane-3-nitroxide to improve the control of the polymerization. The two experiments only differ in the concentration of the monomer in o-dichlorobenzene. It can be observed that the polymerization with the lower monomer concentration has a higher apparent rate constant k_{app} than the more concentrated one: ▲ 27 mol·L^{-1} and ● 9 mol·L^{-1}. (a) First-order kinetic plots. (b) Dependence of M_n and M_w/M_n on the monomer conversion.*

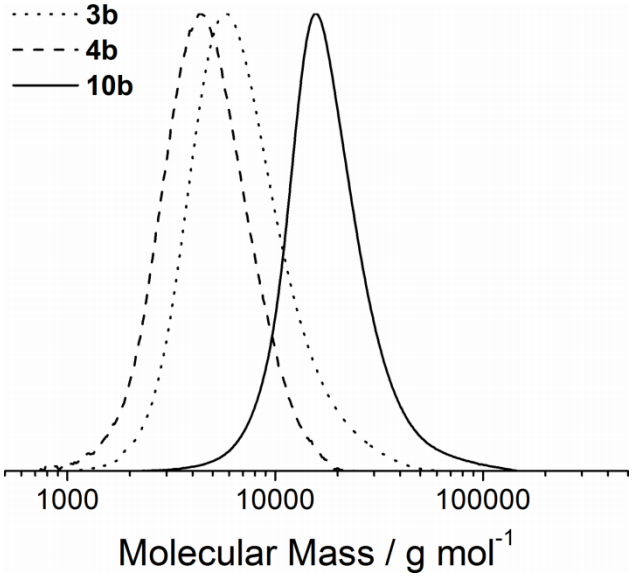

Figure 4: *Normalized UV-signal of SEC traces (detection at 254 nm) of protected polymer **3b** (dotted line), deprotected polymer **4b** (dashed line) and “clicked” PBI-polymer **10b** (straight line). A clear decrease in molecular weight after deprotection of **3b** to **4b** and a clear increase in molecular weight after the “click”-reaction from **4b** to **10b** as well as monomodal narrow distribution of molecular weight can be observed.*

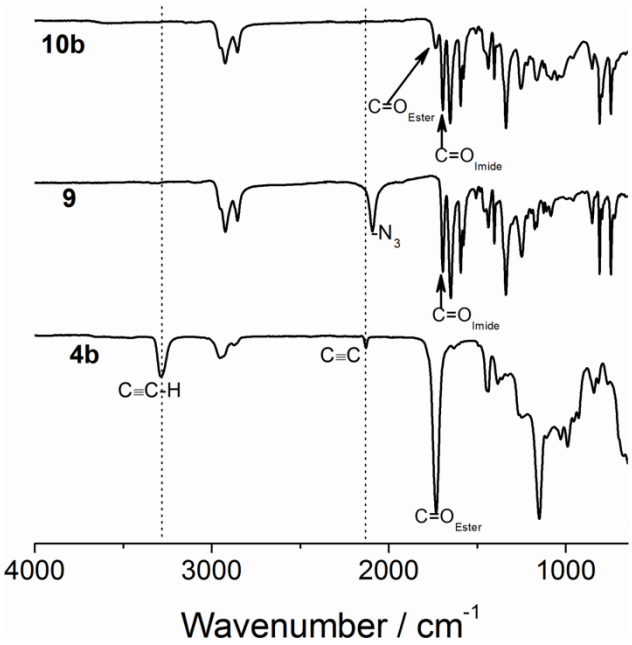

Figure 5: *FTIR spectra of “clicked” PBI-polymer **10b**, PBI azide **9** and alkyne polymer **4b**. After the “click”-reaction between alkyne polymer **4b** and PBI azide **9** the superposition of the C=O stretching vibrations of **4b** and **9** can be observed in the product **10b**. The strong azide vibration in **9** and the alkyne vibration in **4b** cannot be observed anymore in **10b**, indicating complete conversion of these groups.*

analysis indicates a decrease in hydrodynamic volume of the polymers after deprotection, as expected. Additionally, FTIR analysis shows the expected C≡C vibration at 2129 cm^{-1} and the C≡C-*H* vibration at 3288 cm^{-1} (Figure 5). The SEC, TGA and thermal data of all polymers are given in Table 1.

The synthesis of azide functionalized PBI **9** for the cycloaddition reaction with the alkyne polymers **4a,b** is presented in Scheme 2. PBI **5** was synthesized according to literature procedures for asymmetric PBIs[28] and was coupled with 2-(6-bromo hexyloxy) tetrahydro-2*H*-pyran **6** to give PBI **7** with a protected alcohol group.[40] The subsequent deprotection with pyridinium *p*-toluenesulfonate and acetic acid yielded PBI alcohol **8,** which was converted into azide **9** elegantly by a Mitsunobu reaction with diphenyl phosphoryl azide and diethyl azodicarboxylate/PPh_3.[41] To obtain a model monomer **12** for the “clicked” PBI-polymers and for a first test of the “click”-chemistry, the azide functionalized PBI **9** was used in a “click”-reaction with 4 equivalents of propargyl acrylate **1** at RT in degassed THF with 0.1 equivalents of CuBr/N,N,N’,N’’,N’’-pentamethyldiethylenetriamine (PMDETA) as a catalyst/ligand system. After 1h, complete conversion was observed (^{1}H NMR and FTIR). The triazol carrying PBI acrylate monomer **12** was obtained in pure form after filtering through a short silica column and precipitation in MeOH/water. The ^{1}H NMR spectrum in Figure 6 clearly shows the shift of the C$H_2$$N_3$ protons of **9** from 3.28 ppm to 4.38 ppm in **12**. It also features the OCH_2 protons of **12** at 5.36 ppm, the protons of the acrylic double bond between 5.8 and 6.6 ppm, the signal of the 1,2,3-triazol proton at 7.64 ppm as a singlet and the protons of the perylene core between 8.55 and 8.74 ppm. A direct polymerization of **12** was not feasible due to its low solubility. For the CuAAC of PBI azide **9** with the deprotected polymers **4a,b**, PMDETA/CuBr was used as catalyst system. The reaction mixture was degassed before addition of CuBr and was stirred for 5 hours under inert gas atmosphere. We also monitored the “click”-reaction by online ^{1}H NMR measurements. The completion of the reaction was achieved in ~1h. To remove the catalyst, the reaction mixture was filtered over a short silica column and precipitated in MeOH/H_2O. Further purification was achieved by soxhlet extraction with methyl ethyl ketone to remove the remaining PBI **9**. The rest amount of copper, determined by inductively coupled plasma mass spectrometry was found to be 188 ppm (wt/wt) and could be further decreased by an additional precipitation step in aqueous ammonia solution to 126 ppm. SEC traces show a clear increase of the hydrodynamic volume of the polymers after the “click”-reaction. The molecular weights and PDIs determined by SEC were found to be 5 200 g·mol^{-1} and 1.16 for **10a** and 15 800 g·mol^{-1} and 1.17 for **10b** respectively. Their molecular weights are strongly underestimated by the polystyrene calibration. Because the alkyne polymers **4a** and **4b** have an average degree of polymerization of 9 and 35 respectively, the theoretical molecular weights for **10a** and **10b** are 8 000 and 29 000 g·mol^{-1} respectively. A determination of the molecular weight by analysis of end-groups by ^{1}H NMR was not possible because all reliable signals of the initiating group were superimposed by the signals of the polymer. The ^{1}H NMR spectra of **10a** and **10b** prove the quantitative conversion of the alkyne groups by the disappearance of the signals of the alkyne proton at 2.45 ppm and the complete shift of the OCH_2 protons from 4.69 ppm in **4** to 5.23 ppm in **10** (Figure 6). The C$H_2$$N_3$ protons of the azide at 3.28 ppm shift to 4.00 ppm, residual azide

Scheme 2: *Synthesis of perylene bisimide (PBI) azide **9** followed by "click"-reaction to model monomer **12** and "clicked" PBI-polymers **10a,b** with different molecular weights; DMF = dimethylformamide, PPTS = pyridinium p-toluenesulfonate, DPPA = diphenylphosphoryl azide, DEAD = diethyl azodicarboxylate, PMDETA = N,N,N',N'',N''-pentamethyldiethylenetriamine.*

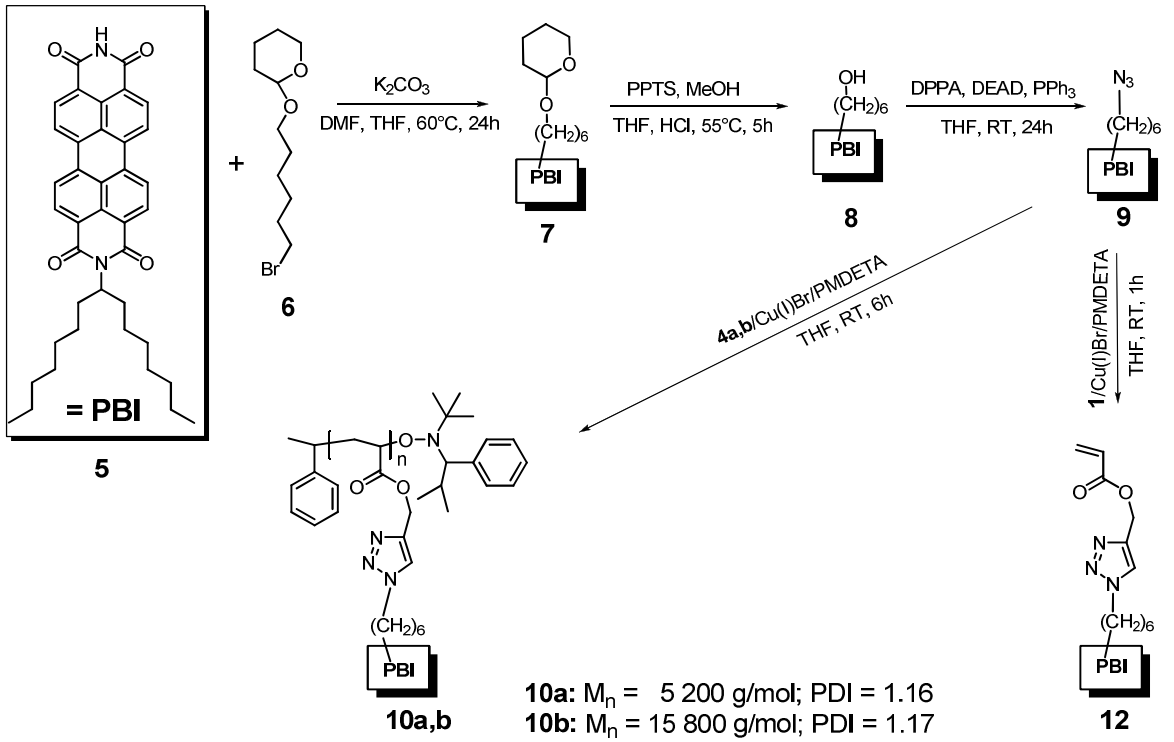

signal in the cleaned polymer was not observed. The 1,2,3-triazol proton was not observed as a single signal but can be determined by integration together with the broad signal of the perylene protons between 7.28 and 8.44 ppm. The spectrum exhibits all other expected signals of PBI **9** broadened to featureless signals. FTIR measurements also indicate complete conversion by disappearance of the C≡C vibration at 2129 cm^{-1} and of the C≡C-*H* vibration at 3288 cm^{-1} (Figure 5). Also the strong azide vibration at 2090 cm^{-1} cannot be observed any more. Further, the spectrum of **10b** shows a superposition of the imide $C=O_{Imide}$ vibration of PBI at 1695 cm^{-1} and the acrylate $C=O_{Ester}$ vibration at 1732 cm^{-1}.

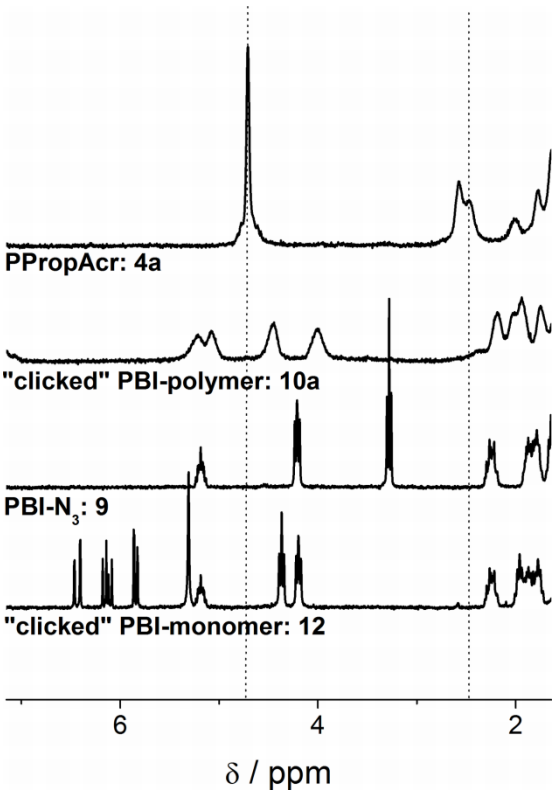

Figure 6: *^{1}H NMR spectra of alkyne polymer **4a**, “clicked” PBI-polymer **10a**, PBI azide **9** and “clicked” PBI model-monomer **12** in $CHCl_3$. It can be seen, that the signals of the “clicked” PBI-polymer **10a** match very well with the signals of the model compound **12**. Signals from residual alkyne cannot be observed in the 1 H NMR spectrum of **10a**.*

Polymer Characterization

Because it is important to know how the properties of the “clicked” PBI-polymer differ from PBI homopolymers without triazol unit, we compared the “clicked” PBI-polymer **10b** with the two reference PBI polymers PPerAcr$(CH_2)_{11}$ **13** and PPerAcr$(CH_2)_6$ **14** obtained by direct NMRP. The polymer **13** with spacer lengths of $(CH_2)_{11}$ relatively matches the length from the imide nitrogen to the ester bond in the polymer backbone of **10a,b** and polymer **14** with a $(CH_2)_6$ spacer fits the length of the $(CH_2)_6$ spacer used in the azide PBI. In the following we discuss differences and similarities of the polymer **10b** in comparison to **13** and **14**; polymer **10b** is chosen for its similarity in molecular mass compared to **13** and **14**.

All three polymers exhibit good solubility in $CHCl_3$ and a low solubility in THF. Films out of $CHCl_3$ could be cast easily and showed similar absorption spectra (Figure 20). Absorption and fluorescence of the polymers **10b**, **13** and **14** in solution are shown in Figure 7. The absorption spectra of in solution ($CHCl_3$, 10^{-5} M) show the characteristic fingerprint spectra for aggregated PBIs with vibronic bands of PBI at 464 nm, 490 nm and 527 nm. The relative intensity of the vibronic bands for S_0-S_1 transition can be compared to assess the degree of aggregation.[42] The absorption spectra of PBI polymer **13** and “clicked” PBI-polymer **10b** are almost identical and the quotients of the vibronic bands $A_{490/527}$ are 1.12 and 1.09 respectively. Polymer **14** shows

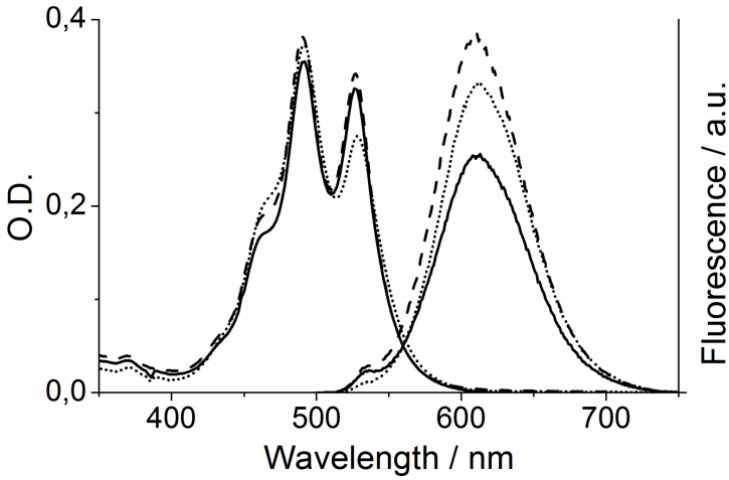

Figure 7: *Optical density of “clicked” PBI-polymer* ***10b*** *(solid line), reference polymer* ***13*** *(dashed line) and reference polymer* ***14*** *(dotted line) in chloroform solution (c = 10^{-5} mol·L^{-1}). The fluorescence spectra of* ***10b****,* ***13*** *and* ***14*** *excited at 490 nm, are also shown.*

higher quotients of the absorption with $A_{490/527}$ of 1.36. This indicates that in $CHCl_3$ solution the perylene cores in polymer **14** aggregate stronger than the perylene cores in the polymers **10b** and **13**. All three polymers exhibit a weak red, featureless fluorescence at 611 nm ($CHCl_3$, 10^{-5} M, excited at 490 nm). The small shoulder at 527 nm in the fluorescence spectra derive from minimal amounts of residual low molecular weight PBIs, which show a much stronger fluorescence, compared to the polymer.

In order to understand the influence of triazol unit and spacer length on bulk properties, the phase behavior of compounds **10b**, **13** and **14** was investigated by DSC measurements, polarized optical microscopy (POM) and X-ray diffraction experiments. The DSC thermograms and the X-ray diffractograms are shown in Figure 8 and 9 respectively.

In DSC, PPerAcr$(CH_2)_{11}$ **13** shows an endothermic phase transition at 189 °C with ΔH = 7.6 J/g on heating. The examination of the sample by polarized optical microscopy showed, that this phase transition observed at 200 °C in POM is a transition into isotropic melt from an easy to shear, birefringent liquid crystalline state. Upon cooling from isotropic melt and annealing at 194 °C a birefringent phase appears, which corresponds to the transition at 168 °C in DSC on cooling. At lower temperature and RT the polymer could not be sheared any more, but does not show a change in texture or growth of crystallites. The difference in transition temperature in DSC and POM could arise due to differences in rate of heating/cooling and possible differences in calibration in addition to supercooling effects. It is not clear if this effect could also derive from two superimposed phase transitions of a melting and a liquid crystalline–isotropic phase transition. A temperature dependent X-ray study shows a decrease of sharp reflexes beginning at 172 °C and a complete isotropization at 192 °C (Figure 16) indicating the presence of two different transitions. In X-ray diffraction at RT, distinct reflections at q = 2.09, 3.37 and 4.19 nm^{-1} can be observed as well as mixed reflections between 5 and 8 nm^{-1}. The reflexes at 2.09 and 4.19 nm^{-1} indicate a lamellar structure, following the ratio 1:2. The reflex at 3.37 nm^{-1} represents the (110) reflection. The ratios of the three observed reflections one to another proof a non-hexagonal ordering. The broad reflection at 18.09 nm^{-1} derives from the π-π stacking order of the

perylene bisimides representing a mean distance of 0.347 nm. The observed reflections cannot be observed at 210 °C, clearly indicating the isotropic phase (Figure 15).

PPerAcr$(CH_2)_6$ **14** shows an endothermic phase transition at 193 °C with ΔH = 4.6 J/g in DSC on heating. In POM studies polymer **14** exhibits an easy to shear intermediate phase showing birefringence between 193 and 325 °C, which clears at about 325 °C. The DSC measurement confirms a melting point at 311 °C (Figure 19) with a very small enthalpy of ΔH = 0.5 J/g. In X-ray diffraction at RT, distinct reflections at q = 1.31, 2.62 and 3.94 nm^{-1} can be observed as well as unresolved mixed reflections between 5 and 8 nm^{-1}. The ratios of the q values are 1:2:3 indicating a lamellar 2D structure similar to polymer **13**. But polymer **14** has a lower order compared to polymer **13**, in which the region between 5 and 8 nm^{-1} is better resolved. These observations also explain the lower ΔH of the phase transition in this polymer. The broad reflection at 17.64 nm^{-1} which is weaker in polymer **14** than in polymer **13** derives from the π-π stacking order of the perylene bisimides representing a mean distance of 0.356 nm. In temperature dependent X-ray studies, the first reflections at 1.31 and 2.92 nm^{-1} remain unaffected in the high temperature regime (up to 250 °C) (Figure 18).

It is now interesting to compare “clicked” PBI-polymer **10b** with the reference polymers **13** and **14** concerning their structural properties and phase behavior. “Clicked” PBI-polymer **10b** shows a small endothermic phase transition at 175 °C with ΔH = 1.2 J/g in DSC on heating. As in polymer **14**, no transition into isotropic phase was observed in POM after the phase transition at 175 °C but an easy to shear liquid crystalline, birefringent phase between 175 and 280 °C, which clears at about 280 °C. The DSC measurement confirms a melting point at 288 °C with a very small enthalpy of ΔH = 0.5 J/g. This shows that the thermal behavior of **10b** is quite similar to the one of polymer **14**. In X-ray diffraction distinct reflections at the same q values as in polymer **14** at q = 1.31 and 2.62 nm^{-1} can be observed, mixed reflections between 5 and 8 nm^{-1} were not observed at all. Together with the even lower ΔH of the phase transition this indicates a lower order compared to polymers **13** and **14**. The ratios of the q values are 1:2 and indicate a lamellar 2D structure as in **13** and **14**. The broad reflection at 17.74 nm^{-1}, which is even weaker than in polymer **14**, derives from the π-π stacking order of the perylene bisimides, representing a mean distance of 0.354 nm.

It is evident that in bulk, the length of the spacer is decisive for the phase behavior of the PBI-polymers. The triazol unit of “clicked” PBI-polymer **10b** seems to be quite stiff and does not enhance the flexibility of the PBI unit and main chain. The long spacer in polymer **13** enables a higher flexibility which allows better packing of the PBI pendant groups and correspondingly enthalpy of transition was higher in polymer **13** compared to **14** and **10b**. A more detailed X-ray study of PBI polymers by SAXS and WAXS is planned for the future in order to elucidate the unit cell dimensions and to obtain a clear picture of molecular packing.

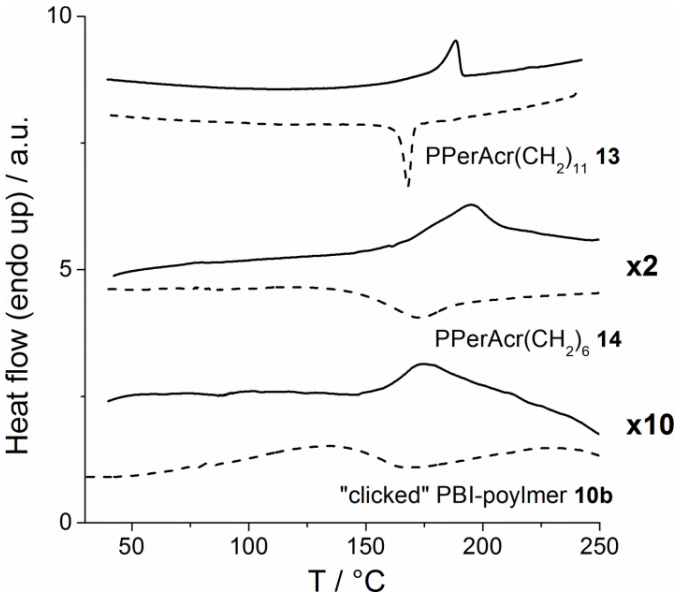

Figure 8: *Second heating (solid line) and second cooling (dashed line) of “clicked” PBI-polymer* ***10b****, PPerAcr(CH₂)₁₁* ***13*** *and PPerAcr(CH₂)₆* ***14*** *in DSC. The DSC traces of* ***14*** *and* ***10b*** *are scaled up two times and ten times respectively to enhance the visibility of the phase transitions. Enlarged temperature region between 250 and 350 °C is given in supporting information (Figure 19).*

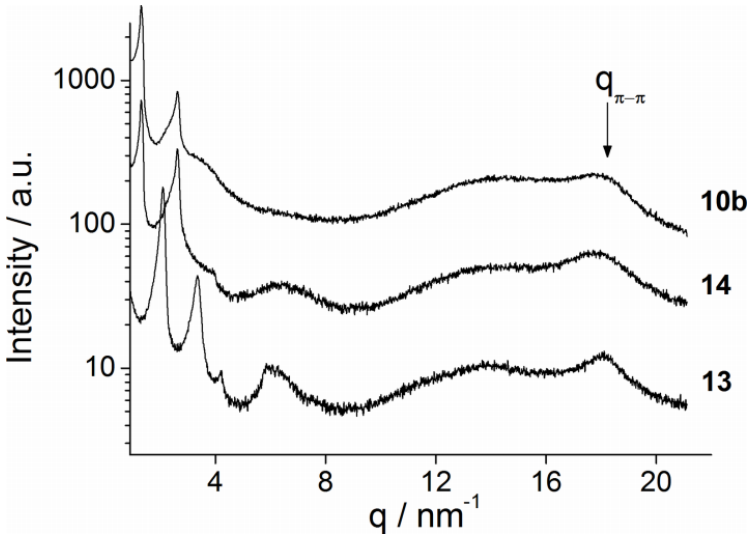

Figure 9: *X-ray diffraction of “clicked” PBI-polymer* ***10b****, PPerAcr(CH₂)₁₁* ***13*** *and PPerAcr(CH₂)₆* ***14*** *at RT. The location of the scattering vector corresponding to the π-π stacking of perylene bisimide is marked.*

Conclusion

To conclude, we studied the kinetics of nitroxide mediated radical polymerization of perylene acrylate and found evidence for permanent transfer reactions during the polymerization, leading to continuously rising PDIs. To overcome this drawback of this polymerization we studied the suitability of the NMRP of trimethylsilyl propargyl acrylate for the first time followed by a “click” reaction of PBI azide. We were able to obtain well defined precursor polymers with molar masses

up to 5 800 g·mol^{-1} and PDIs as good as 1.17, which maintained their good PDIs after deprotection of the alkyne group. The deprotected polymer could be coupled with PBI azide quantitatively, to give fully functionalized semiconductor polymers with molecular weights up to 15 800 g·mol^{-1} and PDIs as good as 1.16. Comparison of the properties of these polymers with PBI containing polymers from direct NMRP with different spacer lengths of $(CH_2)_6$ and $(CH_2)_{11}$ showed that the phase behavior of PBI containing polymers strongly depends on the alkyl spacer length between the PBI and the backbone. All three polymers showed a lamellar 2D ordering at RT and showed a liquid crystalline-like phase behavior at high temperatures. Further detailed studies on the influence of spacer length and of substitution pattern at the PBI nitrogen on the phase behavior of PBI-polymers are currently undertaken.

Experimental Section

General

PBI **5** was prepared according to a literature procedure.[43] The initiator 2,2,5-trimethyl-3-(1-phenylethoxy)-4-phenyl-3-azahexan **11** and the free nitroxide *N*-tert-butyl-*α*-isopropyl-*α*-phenylnitroxid were also synthesized according to published procedures.[44] Dialysis was carried out in THF with a dialysis tubing of regenerated cellulose with a molecular weight cut-off of 1000 purchased from Roth. Acrylic acid chloride (≥97%), *o*-dichlorobenzene (99%), tetrabutylammonium fluoride (1M solution in THF), 6-bromo-1-hexanol (97%), 2-(6-bromo hexyloxy) tetrahydro 2-H-pyran) (97%), dimethylformamide (99.8%), diethyl azodicarboxylate (40% in toluene), diphenylphosphoryl azide (97%), pyridinium p-toluenesulfonate (98%), silver nitrate (≥99.0%) and triphenylphosphine (≥95.0) were purchased from Sigma-Aldrich. 1,8-diazabicyclo[5.4.0]undec-7-ene (≥99.0%), trimethylsilyl chloride (98%) and PMDETA (≥98%) were purchased from Fluka. CuBr (98%) was bought from Acros. All reagents were used without further purification unless otherwise noted.

^{1}H NMR (300 MHz) spectra were recorded on a Brucker AC 300 spectrometer and calibrated to $CHCl_3$ (7.26 ppm for ^{1}H). UV-vis spectra of solutions in $CHCl_3$ with a concentration of 10^{-5} mol·L^{-1} were recorded on a Hitachi 3000 spectrophotometer and photoluminescence spectra were acquired on a Shimadzu RF 5301 PC spectrofluorophotometer upon excitation at 490 nm. SEC measurements were carried out in THF with two Varian MIXED-C columns (300x7.5 mm) at room temperature and at a flow rate of 0.5 mL/min using UV (Waters model 486) with 254 nm detector wavelength and refractive index (Waters model 410) detectors. Polystyrene standards and *o*-DCB as an internal standard were used for calibration. Differential scanning calorimetry experiments were conducted at heating rates of 10 K·min^{-1} or 40 K·min^{-1} under N_2 atmosphere with a Perkin Elmer Diamond DSC, calibrated with indium. The endothermic maximum was taken as T_m. Thermogravimetry measurements were conducted on a Mettler Toledo TGA/SDTA 851^e under N_2 atmosphere at a heating rate of 10K/min. Temperature of decomposition (T_{onset}) was calculated from the onset of the respective curve. ICP-MS was measured on Agilent 7500ce. X-ray diffraction experiments were performed on a Huber Guinier Diffractometer 6000 equipped with a Huber quartz monochromater 611 with Cu-$K_{\alpha1}$: 1.54051 Å.

Propargyl acrylate (1).[38]

Propargyl alcohol (37.2g, 662.9 mmol) and triethylamine (61.4 g, 607.6 mmol) were dissolved in 250 mL of dry methylene chloride. The solution was cooled to 0 °C in an ice bath and acryloyl chloride (50.0 g, 552.4 mmol) was added dropwise over 40 min. The solution was allowed to stir for 24 h at room temperature. The reaction was quenched with water, the organic phase recovered and evaporated. The pure product **(1)** was obtained after distillation under reduced pressure. The strongly smelling, colorless liquid weighed 42.5 g (69.8%): ^{1}H NMR (300 MHz, $CHCl_3$): δ (ppm) 6.43 (dd, 1H, *J* = 17.3, *J* = 1.3, CH=CH*H*), 6.12 (dd, 1H, *J* = 17.3, *J* = 10.5, C*H*=CH_2), 5.86 (dd, 1H, *J* = 10.5, *J* = 1.4, CH=C*H*H), 4.73 (d, 2H, *J* = 2.5, OCH_2), 2.48 (t, 1H, *J* = 2.5, C≡C-*H*); IR (ATR): ν (cm^{-1}) 3296 (≡C-*H*), 2950, 2131 (C≡C, 1725 (C=O), 1635, 1620, 1437, 1407, 1365, 1293, 1257, 1171, 1053, 983, 934, 888, 840, 808, 670.

3-(Trimethylsilyl)prop-2-ynyl acrylate (2).

Silver nitrate (2.45 g, 14.5 mmol) was suspended in 320 mL of dry methylene chloride. Propargyl acrylate **(1)** (32.02 g, 290.8 mmol) and 1,8-diazabicyclo[5.4.0]undec-7-ene (46.50 g, 305.3 mmol) were added to the suspension. The reaction mixture was heated to 40 °C and trimethylsilyl chloride (44.20 g, 407.1 mmol) was added dropwise. The solution was stirred for 24 h at 40 °C, cooled to RT and concentrated under reduced pressure. Protected propargyl acrylate **(2)** was obtained after distillation in high vacuum. The colorless liquid weighed 29.7 g, (56.0 %): ^{1}H NMR (300 MHz, $CHCl_3$): δ (ppm) 6.49 (dd, 1H, *J* = 17.4, *J* = 1.4, CH=CH*H*), 6.15 (dd, 1H, *J* = 17.3, *J* = 10.4, C*H*=CH_2), 5.87 (dd, 1H, *J* = 10.4, *J* = 1.4, CH=C*H*H), 4.76 (s, 2H, OCH_2), 0.18 (s, 9H, Si(CH_3)$_3$).

General Procedure for Preparation of Trimethylsilyl Protected Poly(propargyl acrylate) (3):

Freshly distilled 3-(trimethylsilyl)prop-2-ynyl acrylate **(2)** (1.00 g, 5.5 mmol), alkoxyamine 2,2,5-trimethyl-3-(1-phenylethoxy)-4-phenyl-3-azahexan **(11)** (35.74 mg, 109.8 µmol) and free nitroxide *N*-tert.-butyl-*α*-isopropyl-*α*-phenylnitroxid (2.410 mg, 10.98 µmol) were dissolved in 200 µL *o*-DCB and degassed by three freeze-pump-thaw cycles. The reaction mixture was heated to 125 °C and quenched in an ice bath after the reaction time. The solvent and monomer were removed by dialysis against THF for 5 days. The solvent was changed every second day. Poly(3-(trimethylsilyl)prop-2-ynyl acrylate) **(3)** was obtained as a slightly yellow substance. The low molecular weight polymer **3a** was obtained by quenching the reaction at a lower conversion. ^{1}H NMR (300 MHz, $CHCl_3$): δ (ppm) 4.68 (br s, 2H, OCH_2), 2.44 (br s, 1H, CH_2C*H*), 2.09-1.35 (br s, 2H, CH_2CH), 0.19 (br s, 9H, Si(CH_3)$_3$). IR (ATR): ν (cm^{-1}) 2954, 2178 (C≡C*)*, 1736 (C≡O*)*, 1444, 1355, 1249, 1147, 1029, 948, 829, 758, 698. GPC: **3a**: conv.: 22%, M_n = 2100 g/mol, PDI = 1.17; **3b**: conv.: 63%, M_n = 5800 g/mol, PDI = 1.20.

General Procedure for Deprotection of Trimethylsilyl Protected Poly(propargyl acrylate) (4):

Poly(3-(trimethylsilyl)prop-2-ynyl acrylate) **(3)** (400 mg, 2.19 mmol based on monomer units) was dissolved in 30 mL tetrahydrofuran. The solution was purged with argon for 10 minutes and cooled to -20 °C. Subsequently a likewise degassed solution of acetic acid (172 mg, 2.87 mmol)

and 1 M tetrabutylammonium fluoride in THF (2.87 mL, 2.87 mmol) was added dropwise. The reaction mixture was stirred for 30 min at -20 °C and 2 h at RT. The mixture was passed through a short silica column to remove an excess of tetrabutylammonium fluoride, concentrated under reduced pressure and dialyzed against THF for 5 days. The solvent was changed every second day. The product **(4)** was obtained after freeze drying as a slightly yellowish powder. ^{1}H NMR (300 MHz, $CHCl_3$): δ (ppm) 4.68 (br s, 2H, OCH_2), 2.56 (br s, 1H, C≡C*H*), 2.44 (br s, 1H, CH_2C*H*), 2.07-1.35 (br s, 2H, CH_2CH). IR (ATR): ν (cm^{-1}) 3288 (≡C-*H*), 2954, 2129 (C≡C*)*, 1732 (C≡O*)*, 1438, 1384, 1361, 1249, 1149, 1028, 989, 954, 927, 841, 817. GPC: **4a**: M_n = 1300 g/mol, PDI = 1.17; **4b**: M_n = 4200 g/mol, PDI = 1.20.

Perylene-THP (7).

N-(1-Heptyloctyl)-perylene-3,4,9,10-tetracaboxylic acid bisimide **(5)** (3.00 g, 5.0 mmol), 2-(6-bromo hexyloxy) tetrahydro 2-H-pyran) **(6)** (1.85 g, 7.0 mmol) and K_2CO_3 (1.00 g, 9.0 mmol) were dissolved in a mixture of 56 mL dry dimethylformamide and 19 mL of dry tetrahydrofuran. The reaction mixture was heated to 60 °C and the progress of the reaction was monitored by thin film liquid chromatography in $CHCl_3$. After 24 h the reaction mixture was cooled to RT. The product was precipitated in 300 mL of MeOH, filtered, washed with MeOH again and dried under vacuum. The product was obtained as a red powder and weighed 3.64 g (93%). ^{1}H NMR (300 MHz, $CHCl_3$): δ (ppm) 8.72-8.46 (m, 8H, Ar*H*), 5.26-5.11 (m, 1H, N-C*H*), 4.57 (t, 1H, J = 3.8 Hz, OC*H*), 4.18 (t, 2H, J = 7.7 Hz, N-CH_2), 3.90-3.81 (m, 1H, OCHH_{ring}), 3.79-3.69 (m, 1H, OCH*H*), 3.54-3.44 (m, 1H, OC*H*H$_{ring}$), 3.44-3.34 (m, 1H, OC*H*H), 2.33-2.17 (m, 2H, 2αCH*H*), 1.93-1.43 (m, 16H, 2αC*H*H, 7CH_2), 1.41-1.14 (m, 20H, 10CH_2), 0.82 (t, 6H, J = 6.8 Hz, 2CH_3).

N-(1-Heptyloctyl), N'-(hexyl-6'-hydroxy)-perylene-3,4,9,10-tetracaboxylic acid bisimide (8).

Perylene-THP **(7)** (3.64 g, 4.6 mmol) was dissolved in 60 mL of tetrahydrofuran. Pyridinium p-toluenesulfonate (0.120 g, 0.46 mmol), 20 mL of MeOH and 1 mL of concentrated HCl were added. The reaction mixture was heated to 55 °C for 5 h, cooled to RT, precipitated in 300 mL of MeOH, filtered, washed with MeOH and dried under reduced pressure. The obtained raw product was purified by column chromatography with hexane:THF 4:1 on a silica column to remove impurities. The pure product was obtained by applying a gradient of hexane:THF from 1:1 to pure THF. The fractions containing the pure product **(8)** were combined and the solvent removed under reduced pressure. The obtained red powder weighed 2.34 g (72%). ^{1}H NMR (300 MHz, $CHCl_3$): δ (ppm) 8.74-8.57 (m, 8H, Ar*H*), 5.25-5.12 (m, 1H, N-C*H*), 4.22 (t, 2H, *J* = 7.63 Hz, N-CH_2), 3.66 (dd, 2H, *J* = 12.69 Hz, *J* = 5.90 Hz, CH_2OH), 2.33-2.17 (m, 2H, 2αCH*H*), 1.94-1.73 (m, 4H, 2αC*H*H, N-CH_2CH_2), 1.66-1.44 (m, 6H, 3CH_2), 1.39-1.17 (m, 20H, 10CH_2), 0.83 (t, 6H, *J* = 6.8 Hz, 2CH_3).

N-(1-Heptyloctyl), N'-(hexyl-6'-azido)-perylene-3,4,9,10-tetracaboxylic acid bisimide (9).

Triphenylphosphine (740 mg, 2.82 mmol) was dissolved in 25 mL of dry tetrahydrofuran. N-(1-Heptyloctyl), N'-(hexyl-6'-hydroxy)-perylene-3,4,9,10-tetracaboxylic acid bisimide (8) (900 mg, 1.28 mmol) was added and dissolved. Subsequently a mixture of diethyl azodicarboxylate (1280

mg, 2.98 mmol, 40% in toluene) and diphenylphosphoryl azide (871 mg, 3.07 mmol) was added. The reaction mixture was stirred for 24 h at RT, poured into MeOH, the precipitate filtered, washed with MeOH and purified over a short silica column with CHCl3: Acetone 95:5. The fractions containing the pure product were combined and evaporated under reduced pressure. The obtained red powder weighed 753 mg (81%). ^{1}H NMR (300 MHz, $CHCl_3$): δ (ppm) 8.72-8.51 (m, 8H, Ar*H*), 5.26-5.13 (m, 1H, N-C*H*), 4.21 (t, 2H, *J* = 7.6, N-CH_2), 3.30 (t, 2H, *J* = 6.9, CH_2-N3), 2.35-2.18 (m, 2H, 2αCH*H*), 1.97-1.73 (m, 4H, 2αC*H*H, N-CH_2CH_2), 1.72-1.60 (m, 2H, C$H_2CH_2N_3$), 1.54-1.18 (m, 24H, 12CH_2), 0.84 (t, 6H, *J* = 6.8, 2CH_3). IR (ATR): ν (cm^{-1}) 2923, 2855, 2092 (-N3), 1964, 1650, 1593, 1578, 1507, 1437, 1404, 1338, 1248, 1174, 1163, 1125, 1108, 1084, 958, 851, 809, 795, 745, 724.

General Procedure for "Click"-Reaction of Azide functionalized Perylene Bisimide and Propargyl Acrylate to "Click" Monomer (12).

Propargyl acrylate **(1)** (60.8 mg, 0.55 mmol) and PMDETA (3.6 mg, 20 µmol) were added to a solution of PBI-N_3 **(9)** (100.0 mg, 0.138 mmol) in 2 mL of THF. The mixture was degassed by two freeze-pump-thaw cycles. Subsequently, CuBr (1.00 mg, 6.9 µmol) was added under argon stream. The reaction was stirred at RT for 1h to completeness, the product precipitated in MeOH/H_2O : 10:4 and filtered. The product **(12)** was obtained as a red powder. ^{1}H NMR (300 MHz, $CHCl_3$): δ (ppm) 8.75-8.58 (m, 8H, Ar*H*), 7.63 (s, 1H, triazol-*H*) 6.43 (dd, 1H, *J* = 17.3 Hz, *J* = 1.5 Hz, CH=CH*H*), 6.13 (dd, 1H, *J* = 17.4 Hz, *J* = 10.4 Hz, C*H*=CH_2), 5.83 (dd, 1H, *J* = 10.4 Hz, *J* = 1.5 Hz, CH=CH*H*), 5.30 (s, 2H, OCH_2), 5.25-5.11 (m, 1H, N-C*H*), 4.36 (t, 2H, *J* = 7.2 Hz, N-C$H_{2,perylene}$), 4.19 (t, 2H, *J* = 7.5 Hz, N-C$H_{2,triazol}$), 2.32-2.15 (m, 2H, 2αCH*H*), 2.03-1.70 (m, 6H, 2αC*H*H, N-CH_2C$H_{2,perylene}$, N-CH_2C$H_{2,triazol}$), 1.60-1.12 (m, 24H, 12CH_2), 0.82 (t, 6H, *J* = 6.20 Hz, 2CH_3). IR (ATR): ν (cm^{-1}) 3094, 2924, 2855, 1723, 1693, 1651, 1594, 1578, 1508, 1483, 1460, 1438, 1404, 1338, 1295, 1253, 1219, 1175, 1125, 1109, 1081, 1048, 983, 964, 851, 809, 795, 745, 658.

General Procedure for "Click"-Reaction of Poly(propargyl acrylate) (4) and PBI-N_3 (9):

Poly(propargyl acrylate) **(4)** (10.0 mg, 0.091 mmol based on monomer units), PBI-N_3 **(9)** (79.3 mg, 0.109 mmol) and PMDETA (1.58 mg, 9.1 µmol) were dissolved in 2.0 mL THF in a schlenk flask and degassed by three freeze-pump-thaw-cycles. Subsequently CuBr (1.30 mg, 9.1 µmol) was added under argon stream. The reaction mixture was stirred for 6 h, run over a short pad of silica to remove catalyst, precipitated into MeOH, filtered, dried and purified further by soxhlet extraction with methyl ethyl ketone. The "clicked" PBI-polymer was obtained as a red powder. ^{1}H NMR (300 MHz, $CHCl_3$): δ (ppm) 8.29-6.97 (br s, 9H, Ar*H*, triazol-*H*), 5.46-5.10 (br s, 2H, OCH_2), 5.11-4.85 (br s, 1H, N-C*H*), 4.67-4.30 (br s, 2H, N-C$H_{2,perylene}$), 4.09-3.76 (br s, 2H, N-C$H_{2,triazol}$), 2.58-1.00 (br s, 35H, 17CH_2, C$H_{backbone}$), 0.95-0.67 (br s, 6H, 2CH_3). IR (ATR): ν (cm^{-1}) 2924, 2855, 1732, 1695, 1654, 1594, 1578, 1438, 1404, 1339, 1249, 1168, 1125, 1108, 1082, 851, 810, 795, 746, 666. GPC: **10a**: M_n = 5200 g/mol, PDI = 1.16; **10b**: M_n = 15800 g/mol, PDI = 1.17.

6-Bromo-1-hexyl acrylate (15).

6-Bromo-1-hexanol (5.0 g, 28mmol) and Na_2CO_3 (4.5 g, 42 mmol) were dissolved in 30 mL of dry THF and cooled to 0 °C. Acrylic acid chloride (4.98 g, 55.0 mmol) was added to the solution dropwise and the reaction was stirred for 24 h. The mixture was extracted with diethyl ether, washed with $NaHCO_3$ solution two times, dried with Na_2SO_4 and solvent was evaporated. The pure product was obtained by column chromatography with THF:cyclohexane / 1:3 and weighed 1.5 g (22.7%). ^{1}H NMR (300 MHz, $CHCl_3$): δ (ppm) 6.36 (dd, 1H, *J* = 17.2 Hz, *J* = 1.5 Hz, CH=CH*H*), 6.07 (dd, 1H, *J* = 17.3 Hz, *J* = 10.4 Hz, C*H*=CH_2), 5.38 (dd, 1H, *J* = 10.5 Hz, *J* = 1.5 Hz, CH=C*H*H), 4.12 (t, 2H, *J* = 6.6 Hz, OCH_2), 3.37 (t, 2H, *J* = 6.8 Hz, CH_2Br), 1.89-1.77 (m, 2H, C$H_2$$CH_2$Br), 1.71-159 (m, 2H, C$H_2$$CH_2$O), 1.51-1.30 (m, 4H, 2C$H_2$). IR (ATR): ν ($cm^{-1}$) 2937, 2860, 1721, 1636, 1620, 1462, 1436, 1407, 1295, 1271, 1186, 1057, 984, 967, 810, 729, 668.

N-(1-Heptyloctyl), N'-(hexyl-6'-acrylate)-perylene-3,4,9,10-tetracaboxylic acid bisimide (16).

The asymmetric perylene bisimide **(5)** (623 mg, 1.04 mmol) was dissolved in a mixture of 7.5 mL of DMF and 2.5 mL of THF together with 6-bromo-1-hexyl acrylate **(15)** (489 mg, 2.07 mmol) and K_2CO_3 (258 mg, 1.86 mmol) and heated to 50 °C for 3d. After cooling to RT the solution was precipitated in MeOH/H_2O, filtered, washed with MeOH, dried in vacuum and cleaned by column chromatography with THF:hexanes / 1:3.5. The product was obtained after removal of the solvents as a red powder and weighed 300 mg (38.2%). NMR (300 MHz, $CHCl_3$): δ (ppm) 8.73-8.50 (m, 8H, Ar*H*), 6.38 (dd, 1H, *J* = 17.3 Hz, *J* = 1.5 Hz, CH=CH*H*), 6.11 (dd, 1H, *J* = 17.1 Hz, *J* = 10.3 Hz, C*H*=CH_2), 5.80 (dd, 1H, *J* = 10.5 Hz, *J* = 1.5 Hz, CH=C*H*H), 5.24-5.12 (m, 1H, N-C*H*), 4.19 (t, 2H, *J* = 7.4 Hz, N-CH_2), 4.16 (t, 2H, *J* = 6.6 Hz, OCH_2), 2.32-2.17 (m, 2H, 2αCH*H)*, 1.94-1.65 (m, 6H, 2αC*H*H, N-CH_2CH_2, OCH_2CH_2), 1.53-1.44 (m, 4H, CH_2), 1.40-1.14 (m, 20H, 10CH_2), 0.82 (t, 6H, *J* = 7.1 Hz, 2CH_3). IR (ATR): ν (cm^{-1}) 2923, 2855, 1712, 1694, 1652, 1594, 1578, 1507, 1461, 1437, 1404, 1338, 1251, 1194, 1125, 1059, 983, 961, 851, 809, 795, 745, 664.

Poly(perylene bisimide $(CH_2)_6$ acrylate) (14).

Perylene bisimide acrylate **(16)** (276 mg, 0.36 mmol), initiator **(11)** (0.794 mg, 2.44 µmol) and free nitroxide TIPNO (0.054 mg, 0.24 µmol) were added to 140 µL *o*-DCB degassed by three freeze-pump-thaw-cycles and stirred at 125 °C. The reaction was quenched in an ice bath and precipitated into MeOH. The rest monomer was extracted out by soxhlet extraction with methyl ethyl ketone. The polymer was obtained as a red powder. NMR (300 MHz, $CHCl_3$): δ (ppm) 8.29-7.09 (br s, 8H, Ar*H*), 5.15-4.84 (br s, 1H, C*H*), 4.42-3.76 (br s, 4H, OCH_2, NCH_2), 2.71-1.16 (br s, 35H, 17CH_2, C$H_{backbone}$), 0.94-0.79 (br s, 6H, 2CH_3). IR (ATR): ν (cm^{-1}) 2924, 2855, 1730, 1695, 1653, 1593, 1579, 1506, 1454, 1437, 1404, 1389, 1337, 1248, 1216, 1166, 1125, 1107, 1089, 999, 958, 851, 809, 795, 745, 724. GPC: **14**: M_n = 12500 g/mol, PDI = 1.80.

Acknowledgement

The financial support for this research work from German Research Council (DFG/SFB 481-Project B4) and SPP 1355 (DFG) is gratefully acknowledged.

Additional Figures

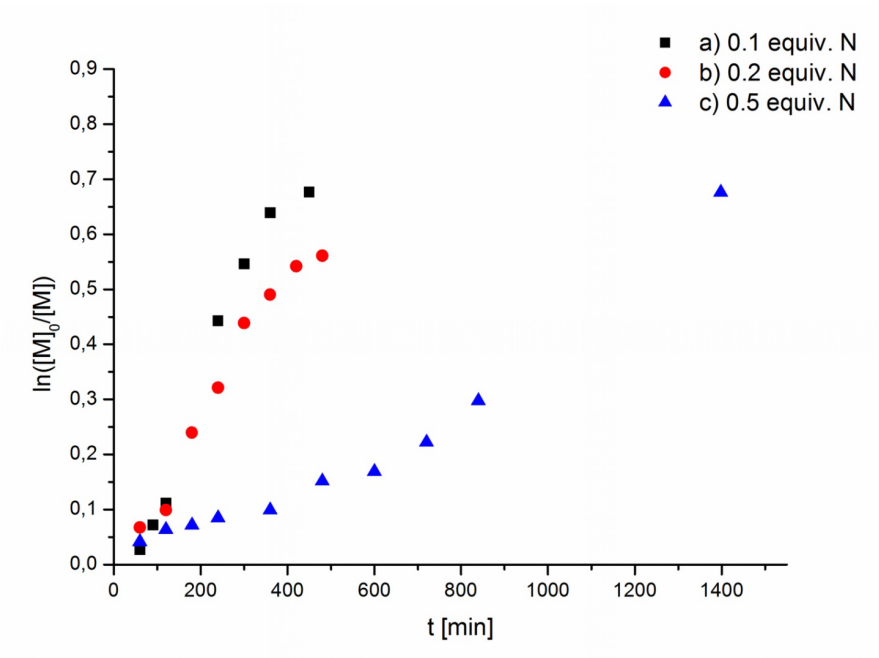

Figure 10: *Kinetic plots of the homopolymerization of perylene bisimide acrylate (PerAcr) via NMRP with different amounts of additional free nitroxide N. a: [M]:[I]:[N] = 50:1:0.1; b: [M]:[I]:[N] = 50:1:0.2; c: [M]:[I]:[N] = 50:1:0.5.*

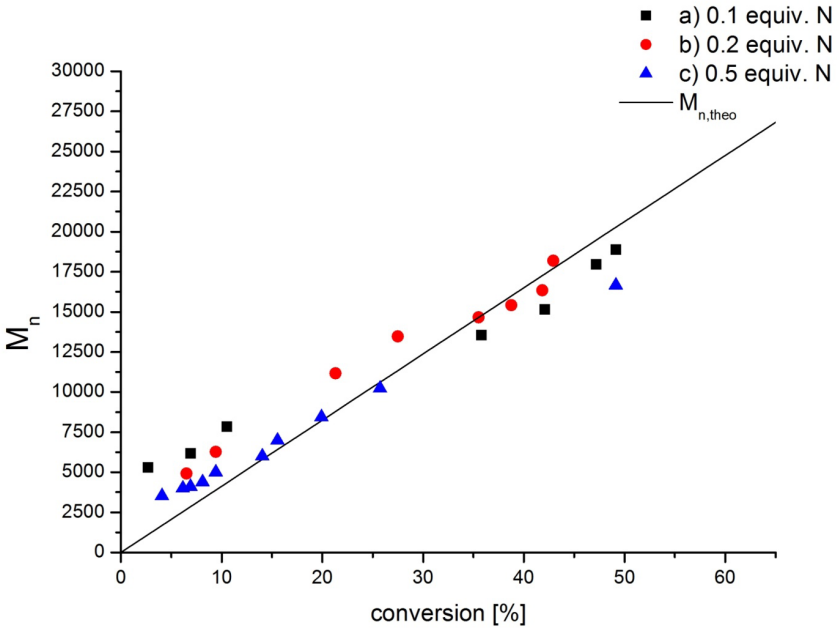

Figure 11: *Dependence of the molecular weight M_n of PPerAcr on the conversion. The straight line describes the theoretical molecular weight, calculated from $[M]_0$:$[I]_0$ in NMRP. a: [M]:[I]:[N] = 50:1:0.1; b: [M]:[I]:[N] = 50:1:0.2; c: [M]:[I]:[N] = 50:1:0.5.*

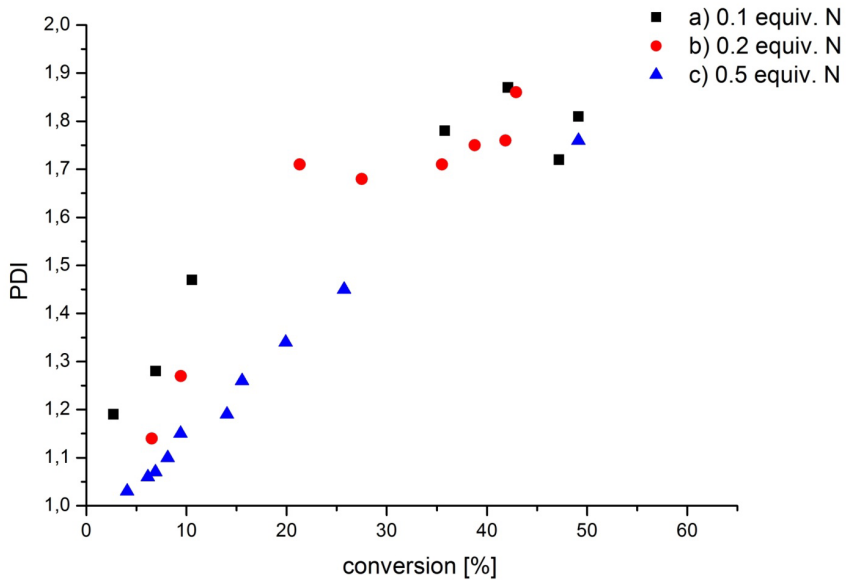

Figure 12: *Dependence of the PDI of PPerAcr on the conversion. a: [M]:[I]:[N] = 50:1:0.1; b: [M]:[I]:[N] = 50:1:0.2; c: [M]:[I]:[N] = 50:1:0.5.*

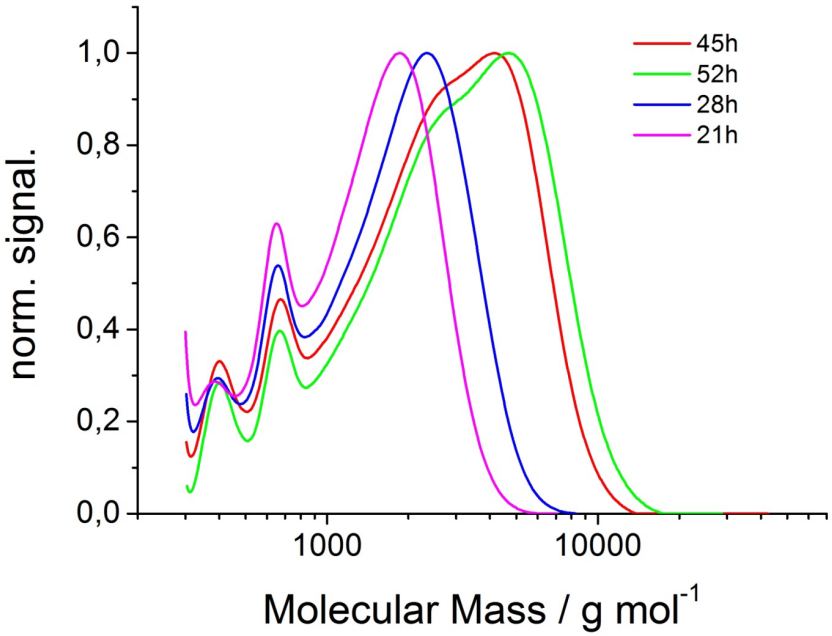

Figure 13: *SEC traces of raw samples from a polymerization of trimethylsilyl propargyl acrylate **2** via NMRP ($[M]_0$:$[I]_0$:[N] of 50:1:0.1). Clearly an emerging shoulder at 2500 g/mol can be seen at higher conversion.*

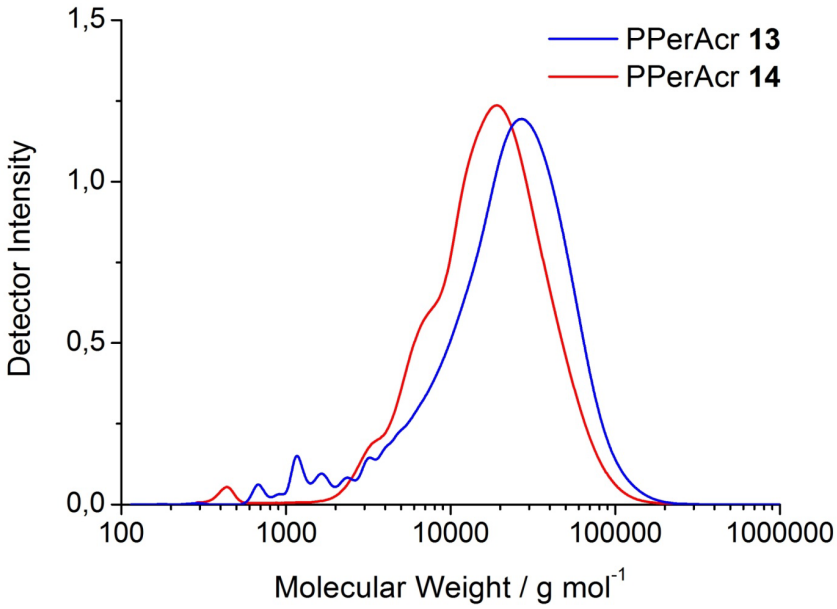

Figure 14: *Molecular weights of reference polymers PPerAcr(CH$_2$)$_{11}$* ***13*** *and PPerAcr(CH$_2$)$_6$ 14 determined by SEC with PS standard calibration and UV-detection at 254 nm.*

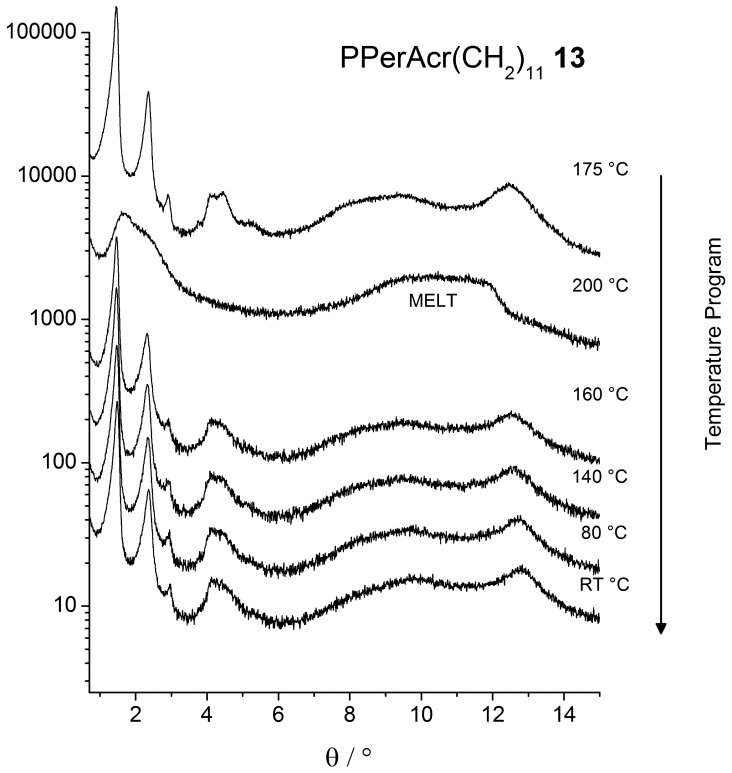

Figure 15: *X-ray diffractions of polymer PPerAcr(CH$_2$)$_{11}$* ***13*** *at different temperatures.*

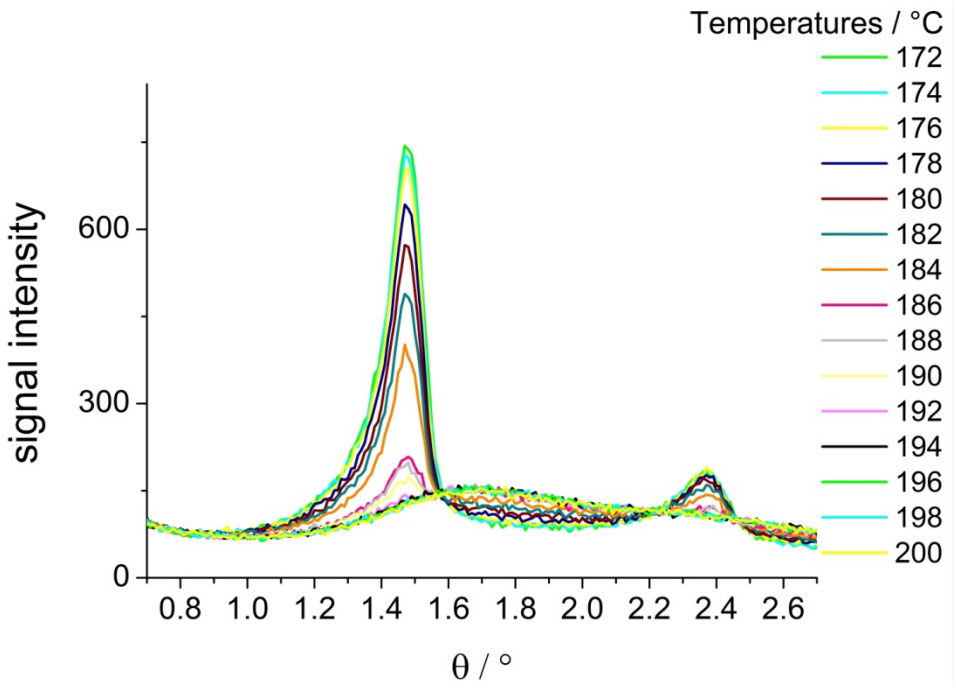

Figure 16: *Enlargement of the first two sharp reflections in X-ray diffractions of PPerAcr(CH$_2$)$_{11}$* ***13*** *at different temperatures, measured in two °C steps. Complete isotropization takes place at 192 °C.*

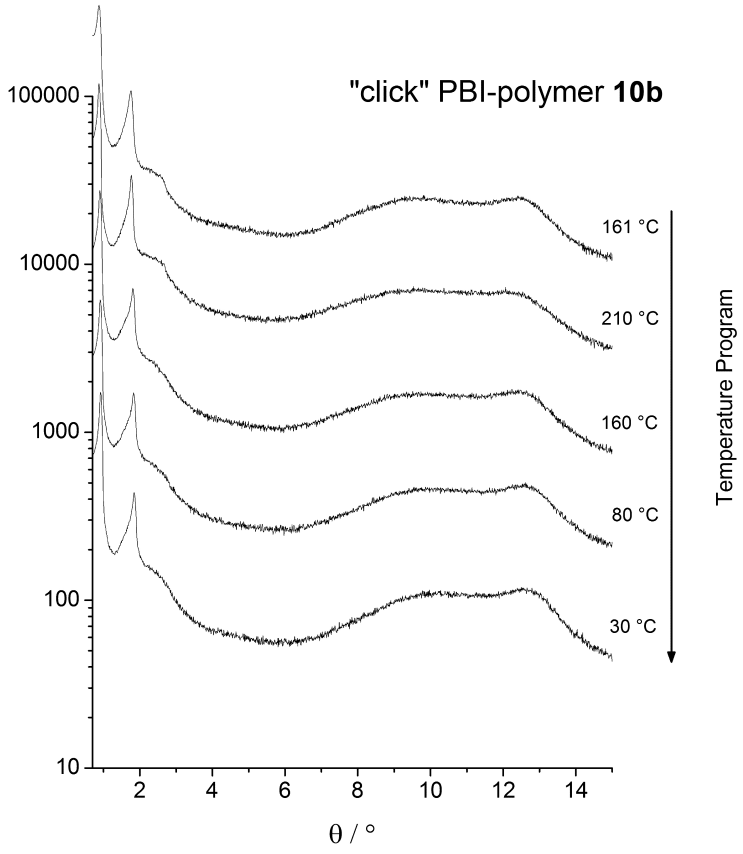

Figure 17*: X-ray diffractions of “click” PBI-polymer* ***10b*** *at different temperatures.*

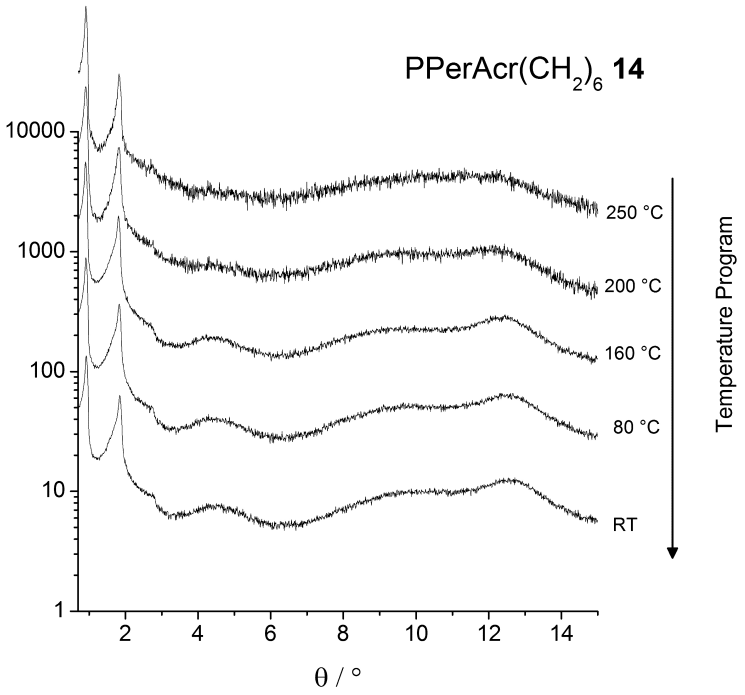

Figure 18: *X-ray diffractions of PPerAcr(CH$_2$)$_6$* ***14*** *at different temperatures.*

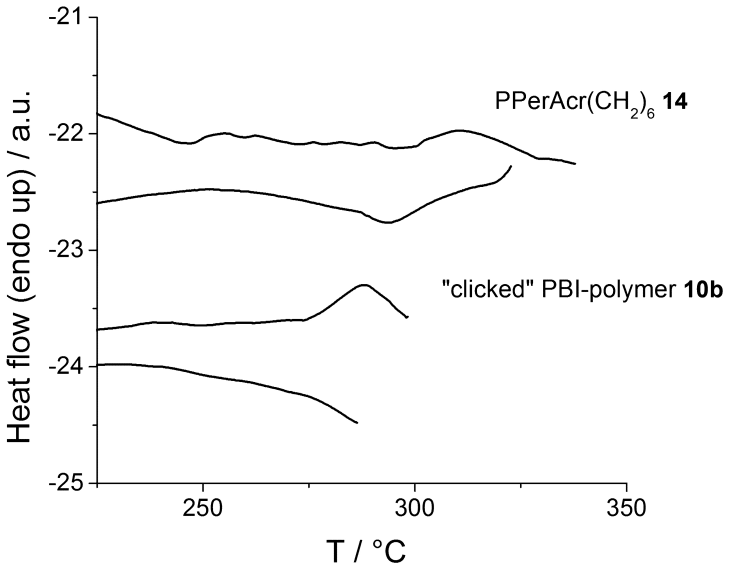

Figure 19: *Second heating and second cooling of polymers PPerAcr(CH$_2$)$_{11}$* ***13*** *and PPerAcr(CH$_2$)$_6$* ***14*** *in DSC at heating and cooling rate of 40 K /min. The measurement had to be conducted at high scanning rates because the melting points were near the temperature of decomposition of the polymers.*

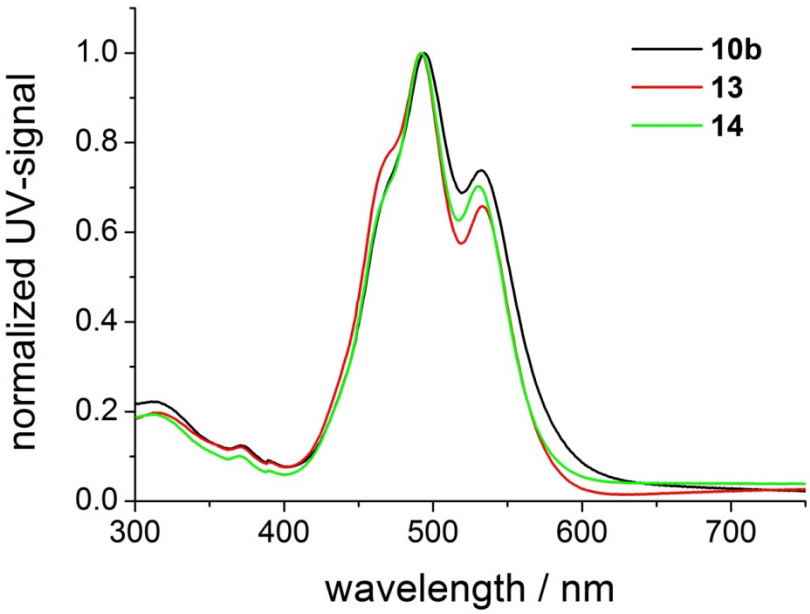

Figure 20: *UV-Vis absorption spectra of films of “clicked” PBI-polymer* ***10b****, as well as reference polymers PPerAcr(CH$_2$)$_{11}$* ***13*** *and PPerAcr(CH$_2$)$_6$* ***14*** *spin-cast from chloroform solution.*

Bibliography

1. Hadjichristidis, N.; Iatrou, H.; Pitsikalis, M.; Mays, J. *Progress in Polymer Science* **2006,** 31, (12), 1068-1132.
2. Kolb, H. C.; Finn, M. G.; Sharpless, K. B. *Angewandte Chemie International Edition* **2001,** 40, (11), 2004-2021.
3. Becer, C. R.; Hoogenboom, R.; Schubert, U. S. *Angewandte Chemie International Edition* **2009,** 48, (27), 4900-4908.
4. Gress, A.; Volkel, A.; Schlaad, H. *Macromolecules* **2007,** 40, (22), 7928-7933.
5. Inglis, A. J.; Stenzel, M. H.; Barner-Kowollik, C. *Macromolecular Rapid Communications* **2009,** 30, (21), 1792-1798.
6. Inglis, A. J.; Sinnwell, S.; Stenzel, M. H.; Barner-Kowollik, C. *Angewandte Chemie International Edition* **2009,** 48, (13), 2411-2414.
7. Binder, W. H.; Sachsenhofer, R. *Macromolecular Rapid Communications* **2007,** 28, (1), 15-54.
8. Binder, W. H.; Sachsenhofer, R. *Macromolecular Rapid Communications* **2008,** 29, (12-13), 952-981.
9. Sumerlin, B. S.; Tsarevsky, N. V.; Louche, G.; Lee, R. Y.; Matyjaszewski, K. *Macromolecules* **2005,** 38, (18), 7540-7545.

10. Ladmiral, V.; Mantovani, G.; Clarkson, G. J.; Cauet, S.; Irwin, J. L.; Haddleton, D. M. *Journal of the American Chemical Society* **2006,** 128, (14), 4823-4830.

11. Gao, H.; Matyjaszewski, K. *Journal of the American Chemical Society* **2007,** 129, (20), 6633-6639.

12. Geng, J.; Lindqvist, J.; Mantovani, G.; Haddleton, D. M. *Angewandte Chemie International Edition* **2008,** 47, (22), 4180-4183.

13. Quémener, D.; Hellaye, M. L.; Bissett, C.; Davis, T. P.; Barner-Kowollik, C.; Stenzel, M. H. *Journal of Polymer Science Part A: Polymer Chemistry* **2008,** 46, (1), 155-173.

14. Zhang, X.; Lian, X.; Liu, L.; Zhang, J.; Zhao, H. *Macromolecules* **2008,** 41, (21), 7863-7869.

15. Fleischmann, S.; Kiriy, A.; Bocharova, V.; Tock, C.; Komber, H.; Voit, B. *Macromolecular Rapid Communications* **2009,** 30, (17), 1457-1462.

16. Malkoch, M.; Thibault, R. J.; Drockenmuller, E.; Messerschmidt, M.; Voit, B.; Russell, T. P.; Hawker, C. J. *Journal of the American Chemical Society* **2005,** 127, (42), 14942-14949.

17. Sieczkowska, B.; Millaruelo, M.; Messerschmidt, M.; Voit, B. *Macromolecules* **2007,** 40, (7), 2361-2370.

18. Fleischmann, S.; Hinrichs, K.; Oertel, U.; Reichelt, S.; Eichhorn, K.-J.; Voit, B. *Macromolecular Rapid Communications* **2008,** 29, (12-13), 1177-1185.

19. Würthner, F. *Chemical Communications* **2004**, (14), 1564-1579.

20. Langhals, H. *Helvetica Chimica Acta* **2005,** 88, (6), 1309-1343.

21. Horowitz, G.; Kouki, F.; Spearman, P.; Fichou, D.; Nogues, C.; Pan, X.; Garnier, F. *Advanced Materials* **1996,** 8, (3), 242-245.

22. Lindner, S. M.; Hüttner, S.; Chiche, A.; Thelakkat, M.; Krausch, G. *Angewandte Chemie International Edition* **2006,** 45, (20), 3364-3368.

23. Sommer, M.; Lindner, S. M.; Thelakkat, M. *Advanced Functional Materials* **2007,** 17, (9), 1493-1500.

24. Sharma, G. D.; Balraju, P.; Mikroyannidis, J. A.; Stylianakis, M. M. *Solar Energy Materials and Solar Cells* **2009,** 93, (11), 2025-2028.

25. Wicklein, A.; Ghosh, S.; Sommer, M.; Würthner, F.; Thelakkat, M. *ACS Nano* **2009,** 3, (5), 1107-1114.

26. Struijk, C. W.; Sieval, A. B.; Dakhorst, J. E. J.; van Dijk, M.; Kimkes, P.; Koehorst, R. B. M.; Donker, H.; Schaafsma, T. J.; Picken, S. J.; van de Craats, A. M.; Warman, J. M.; Zuilhof, H.; Sudholter, E. J. R. *Journal of the American Chemical Society* **2000,** 122, (45), 11057-11066.

27. Xu, Y.; Leng, S.; Xue, C.; Sun, R.; Pan, J.; Ford, J.; Jin, S. *Angewandte Chemie* **2007,** 119, (21), 3970-3973.

28. Wicklein, A.; Lang, A.; Muth, M.; Thelakkat, M. *Journal of the American Chemical Society* **2009,** 131, (40), 14442-14453.

29. Hüttner, S.; Sommer, M.; Thelakkat, M. *Applied Physics Letters* **2008,** 92, (9), 093302.

30. Lindner, S. M.; Thelakkat, M. *Macromolecules* **2004,** 37, (24), 8832-8835.

31. Zhang, Q.; Cirpan, A.; Russell, T. P.; Emrick, T. *Macromolecules* **2009,** 42, (4), 1079-1082.

32. Rajaram, S.; Armstrong, P. B.; Kim, B. J.; Fréchet, J. M. J. *Chemistry of Materials* **2009,** 21, (9), 1775-1777.

33. Tao, Y.; McCulloch, B.; Kim, S.; Segalman, R. A. *Soft Matter* **2009,** 5, (21), 4219-4230.

34. Sommer, M.; Lang, A. S.; Thelakkat, M. *Angewandte Chemie International Edition* **2008,** 47, (41), 7901-7904.

35. Langhals, H.; Obermeier, A. *European Journal of Organic Chemistry* **2008,** 2008, (36), 6144-6151.

36. Kitto, H. J.; Schwartz, E.; Nijemeisland, M.; Koepf, M.; Cornelissen, J. J. L. M.; Rowan, A. E.; Nolte, R. J. M. *Journal of Materials Chemistry* **2008,** 18, (46), 5615-5624.

37. Charleux, B.; Nicolas, J.; Guerret, O. *Macromolecules* **2005,** 38, (13), 5485-5492.

38. Li, J.; He, W.-D.; Han, S.-c.; Sun, X.-l.; Li, L.-y.; Zhang, B.-y. *Journal of Polymer Science Part A: Polymer Chemistry* **2009,** 47, (3), 786-796.

39. Fischer, H. *Chemical Reviews* **2001,** 101, (12), 3581-3610.

40. Hofmann, C. C.; Lindner, S. M.; Ruppert, M.; Hirsch, A.; Haque, S. A.; Thelakkat, M.; Köhler, J. *The Journal of Physical Chemistry B* **2010**, *114, (28),* 9148-9156.

41. Ustinov, A. V.; Dubnyakova, V. V.; Korshun, V. A. *Tetrahedron* **2008,** 64, (7), 1467-1473.

42. Lindner, S. M.; Kaufmann, N.; Thelakkat, M. *Organic Electronics* **2007,** 8, (1), 69-75.

43. Langhals, H.; Saulich, S. *Chemistry - A European Journal* **2002,** 8, (24), 5630-5643.

44. Benoit, D.; Chaplinski, V.; Braslau, R.; Hawker, C. J. *Journal of the American Chemical Society* **1999,** 121, (16), 3904-3920.

Chapter 6

Modular Synthesis of Poly(perylene bisimides) using Click Chemistry: A Comparative Study

*Andreas S. Lang and Mukundan Thelakkat**

Applied Functional Polymers, Department of Macromolecular Chemistry I, University of Bayreuth, Universitätsstr. 30, 95440 Bayreuth, Germany

Published In *Polymer Chemistry*, **2011**, 10.1039/c1py00191d

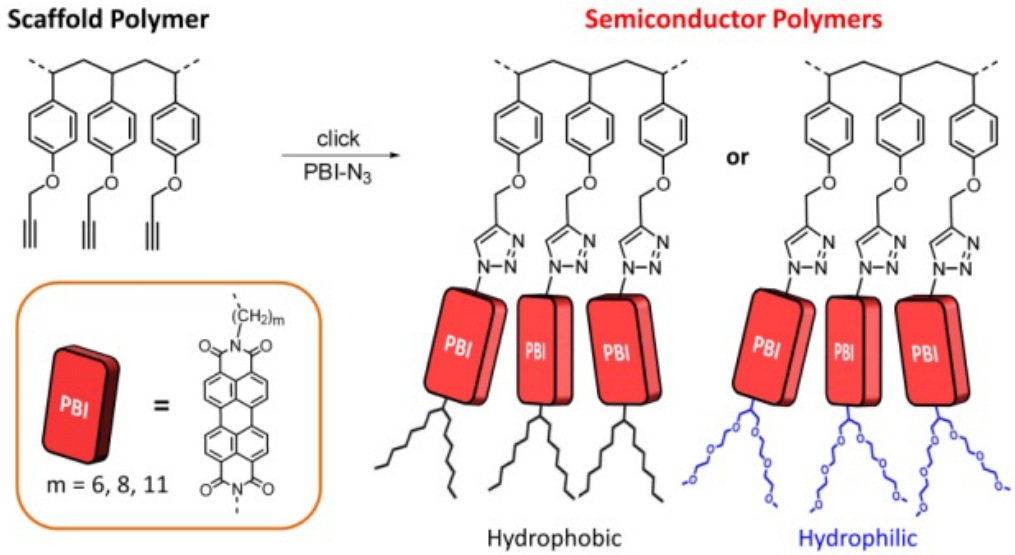

Abstract

A systematic study of the influence of the chemical substitution pattern of side chain polymers carrying perylene bisimide (PBI) pendants is presented. To achieve a high comparability, the modular approach of copper-catalyzed azide-alkyne cycloaddition (CuAAC, "click" chemistry) was chosen to attach six differently substituted PBI azide moieties to a poly(propargyloxystyrene) backbone to obtain poly(perylene bisimides), PPBIs. The *N*, *N'* substituted PPBIs differ structurally in two ways. On the one hand, the *N*-swallow-tail substituent was varied between hydrophilic oligoethylenglycol and hydrophobic alkyl groups. On the other hand, the length of the *N'*-alkyl spacer, connecting PBI moiety and polymer backbone, was varied from $(CH_2)_6$ to $(CH_2)_8$ and to $(CH_2)_{11}$. The polymer analogous reactions between PBI-azides and poly propargyl oxystyrene were monitored by ^{1}H NMR and were found to be nearly quantitative in all cases. The resulting PPBIs exhibit M_n around 60 000 g/mol and narrow PDIs of 1.1. Structure-property relationships of all polymers were elucidated by studying their thermal behaviour using DSC and their structural properties with XRD measurements.

Introduction

Recent synthetic developments in polymer science such as the combination of controlled radical polymerization (CRP) and copper-catalyzed azide-alkyne cycloaddition (CuAAC, "click" chemistry)[1] have given scientists an elegant tool to create polymers in a diversity never known before. Generally, in this concept, an alkyne or azide functionalized monomer is polymerized using CRP followed by a subsequent polymer analogous copper-catalyzed "click" reaction with a respective azide or alkyne derivative. This allows the synthesis of manifold complex polymers out of functional "building bricks" and a single easy-to-obtain scaffold polymer. By this modular approach, the influence of the substitution pattern in a series of "click" polymers can be studied, without causing any differences in polymer length and molecular weight distribution. Thus, structure-property relationships can be determined more reliably. Narrow molecular weight distributions for such scaffold polymers can be accomplished by choosing one of the three CRP methods, atom transfer radical polymerization (ATRP),[2, 3] reversible addition-fragmentation chain transfer polymerization (RAFT)[4, 5] or nitroxide mediated radical polymerization (NMRP).[6-8] For example, Haddleton et al. used these principles to build up libraries of glycopolymers by the combination of "click" chemistry and ATRP.[3] Zhang et al. determined the influence of different spacer lengths of azobenzene-containing side–chain liquid crystalline polymers which were synthesized by "click" chemistry and free radical polymerization.[9] In a previous work, we comparatively studied poly(perylene bisimides) (PPBI) prepared from direct NMRP of perylene bisimide acrylates and those synthesized by "click" chemistry between an azide functionalized PBI and poly(propargyl acrylate).[6]

PBI derivatives represent an important class of light absorbing n-type semiconductor materials,[10, 11] exhibiting a relatively high electron affinity among large-bandgap materials.[12] Thus, PBIs are promising materials for the application in organic electronic devices.[13-15] Polymers with

Scheme 1: *Synthetic scheme for alkyne functionalized scaffold polymer* ***5*** *and "clicked"* ***PPBIs 1-6.***

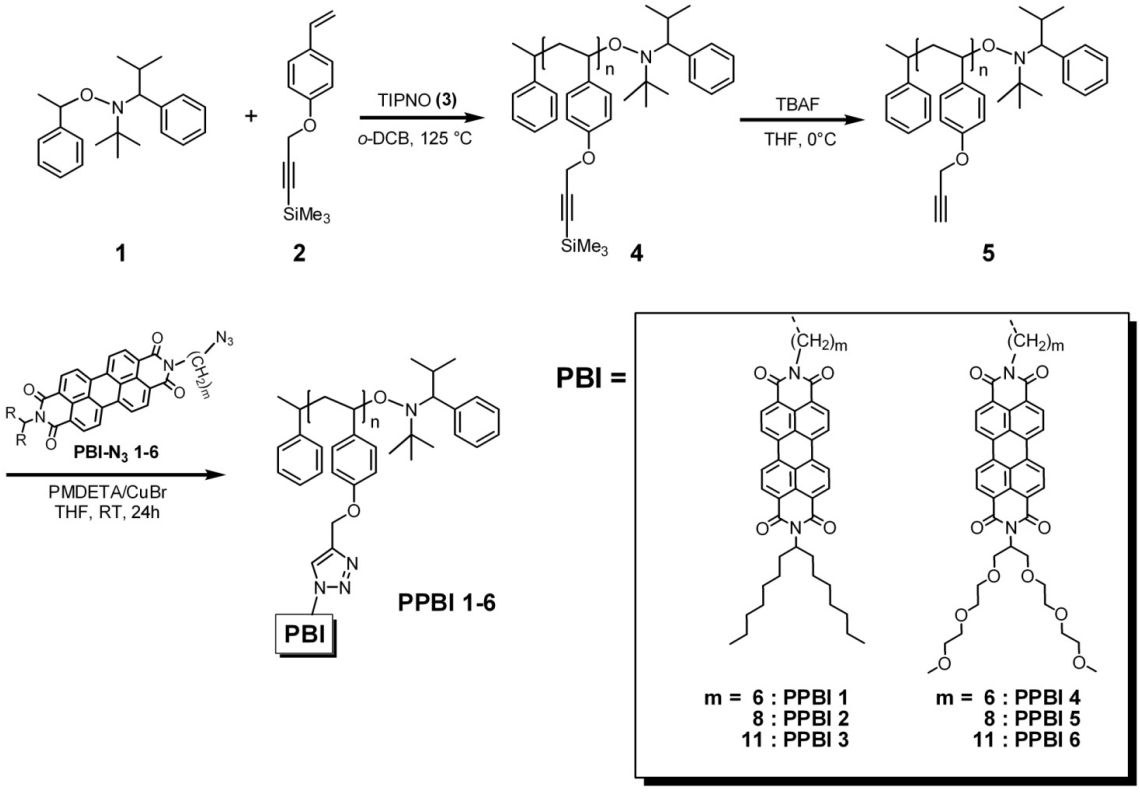

PBI as pendant groups feature additional advantages of good film forming properties.[16] Such polymers were already incorporated as one block in semiconductor donor-acceptor block copolymers for photovoltaic application.[13, 14, 17-21] Nevertheless, the polymerization of PBI monomers by direct NMRP is not ideal and is limited to certain substituted monomers because this polymerization works only in very concentrated solution.[6] The choice of chemical substitution of the pendant PBIs is thereby limited by the solubility of the monomers and the corresponding polymers under polymerization conditions. Also, transfer reactions were observed in the NMRP of PBI acrylates which lead to broad molecular weight distribution in the homopolymerization and to the formation of homopolymer in the synthesis of block copolymers. These problems can be overcome by a combination of "click" chemistry and NMRP in which case differently substituted PBIs can be attached to a scaffold polymer very easily. Here, we report the synthesis of six differently substituted PBI polymers, utilizing "click" chemistry as synthetic route. Two types of pendant PBIs were attached; those carrying oligoethylene glycol (OEG) and alkyl swallow-tail substituents. Each type of PPBI was synthesized with three different alkyl spacers of $(CH_2)_6$, $(CH_2)_8$ and $(CH_2)_{11}$. We studied the polymers regarding thermal, structural and optical properties. Thus, the polymers carrying hydrophilic OEG swallow-tails were systematically compared with polymers with PBIs bearing alkyl swallow-tails.

Results and Discussion

The chemical structures and the synthetic route for the "clicked" polymers **PPBI 1-6** are shown in Scheme 1. Poly(propargyl oxystyrene) **5** was chosen as an alkyne carrying scaffold polymer because it is easy to synthesize and provides polymers with narrow PDIs. The polymerization of the protected monomer **2** by nitroxide mediated radical polymerization (NMRP) and the accessibility of poly(propargyl oxystyrene) for "click" reactions was demonstrated by Voit et al. previously.[8, 22, 23] The alkyne group of the monomer has to be protected with a trimethylsilyl group because otherwise crosslinking would occur during the polymerization. We conducted the polymerization of **2** in *o*-dichlorobenzene at 125 °C in presence of 0.1 equivalents of free nitroxide **3** to shift the NMRP equilibrium more to the dormant species and thereby to control the polymerization in a better way. The protected polymer **4** could be obtained with $M_{n,SEC}$ = 9 300 g/mol and a PDI of 1.11 corresponding to 44 repeating units. After deprotection of **4** with tetrabutylammonium fluoride, the expected scaffold alkyne polymer **5** with $M_{n,SEC}$ = 7 400 g/mol and a PDI of 1.11 was obtained.

The "click" reaction of the azides **PBI-N_3 1**-**6** (1.2 molar eq) with the alkyne carrying polymer **5** was conducted in anisole at RT. A stock solution of PMDETA/CuBr in anisole was prepared and used as a ligand/catalyst system. The approach of using a stock solution, which can be stored under inert gas atmosphere for long time, is more exact and convenient than adding ligand and copper species separately. Anisole is preferable as solvent, because it dissolves both PBI-azides and PPBIs, in contrast to THF, which is only a moderate solvent for PPBIs. After the "click"-reaction, the polymers were cleaned by removing the excess of PBI azides by soxhlet extraction with methyl ethyl ketone or acetone (see experimental part).

All PPBIs exhibited monomodal distribution and very similar PDIs (1.09) as the scaffold polymer **5**. Figure 1 shows exemplarily the size exclusion chromatography (SEC) traces of **PPBI 1** (hydrophobic) and **PPBI 4** (hydrophilic) in comparison to protected polymer **4** and deprotected scaffold polymer **5**. The detailed SEC data of the polymers are presented in Table 1. Slightly smaller molecular weights were obtained for polymers with longer spacers than for those with shorter ones. We ascribe this to a difference in solution behaviour of the PPBIs in THF (SEC solvent), which is only a moderate solvent for PPBIs as aforementioned. Since the protected polymer **4** resembles the PS-standard used for SEC calibration, we could calculate the number of repeating units in **4** and **5** as 44. Thus, theoretical molecular weights of all PPBIs for 100% conversion in "click" reaction were calculated from this value (Table 1). It is evident that the molecular weights of PPBIs, determined by SEC are overestimated compared to the theoretical molecular weights. This is well known in main chain and side chain rigid rod polymers.[24] All polymers were analyzed by FTIR spectroscopy. The alkyne C≡C vibration at 2120 cm^{-1} and the C≡C-H vibration at 3286 cm^{-1} present in polymer **5** cannot be observed in the **PPBIs 1-6** anymore. Also the strong azide vibration which is present in all PBI azides at around 2090 cm^{-1} cannot be observed in any of the **PPBIs 1-6**, proving that no unreacted azide is left in the polymer after purification. The polymers were also analyzed by ^{1}H NMR to estimate the conversion in "click" reaction. Figure 2 shows the ^{1}H NMR spectrum of alkyne polymer **5** and exemplarily the spectra of hydrophobic **PPBI 1** and of hydrophilic **PPBI 4**. After the "click" reaction, the signals of the

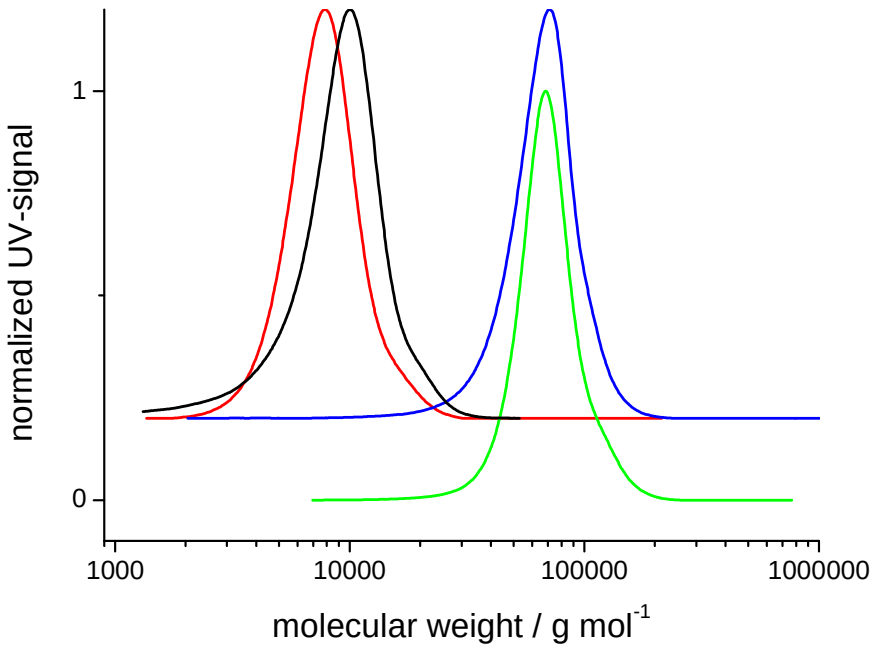

Figure 1: *Normalized UV-signal of SEC traces (detection at 254 nm) of protected polymer* ***4*** *(black line), deprotected polymer* ***5*** *(red line) and exemplarily one hydrophobic* ***PPBI 1*** *(green line) and one hydrophilic* ***PPBI 4*** *(blue line) polymer (both with $(CH_2)_6$ spacer). A clear increase in molecular weight for* ***PPBI 1*** *and* ***PPBI 4*** *after the "click" reaction and monomodal narrow distributions of molecular weight can be observed. The upper curves are vertically displaced for clarity.*

prominent alkyne proton at 2.5 ppm, as well as that of the OCH_2 group at 4.6 ppm of polymer **5** disappear. In the "clicked" polymers, the OCH_2 signals are shifted to 5.1 ppm. The signal of the newly formed triazole proton, usually occurring around 7.6 ppm, cannot be seen in the spectra because it is superimposed by the broad signals of the aromatic protons of perylene, but can be determined by integration between 8.4 and 7.4 ppm. The CH_2N_3 protons of the PBI azides at 3.3 ppm cannot be observed any more in the PPBIs, proving the absence of remaining PBI-N_3 in the polymer. The corresponding protons in the "clicked" polymers are now located adjacent to the newly-built triazole unit and occur at 4.0 ppm. The fact that a) no acetylene protons are present and b) all OCH_2(C≡C) protons are converted to OCH_2(triazole) indicates a quantitative conversion within the margins of the experimental error in ^{1}H NMR. The optical properties of the PPBIs were investigated by UV/Vis and photoluminescence measurements (Figures 8-11). All polymers show similar absorption spectra in $CHCl_3$ solution (c = 10^{-5} mol·L^{-1}) with the characteristic absorption maxima of PBI at 527 nm, 491 nm and 464 nm. These peaks correspond to the finger-print vibration transitions (0-0, 0-1, 0-2) for the S_0-S_1 electronic transition in PBI. Both hydrophobic and hydrophilic polymers show a featureless red emission which is typical for strongly π-π-stacked PBIs. A very weak peak at 534 nm can be attributed to a very small amount of non aggregated chromophores in the polymer. While hydrophilic and hydrophobic polymers behave quite similar in their absorption, the fluorescence measurements reveal a red shift of the fluorescence peak at 611 nm in hydrophobic polymers to 624 nm in hydrophilic polymers. This could be attributed to a smaller delocalization length in the excited state for the hydrophobic

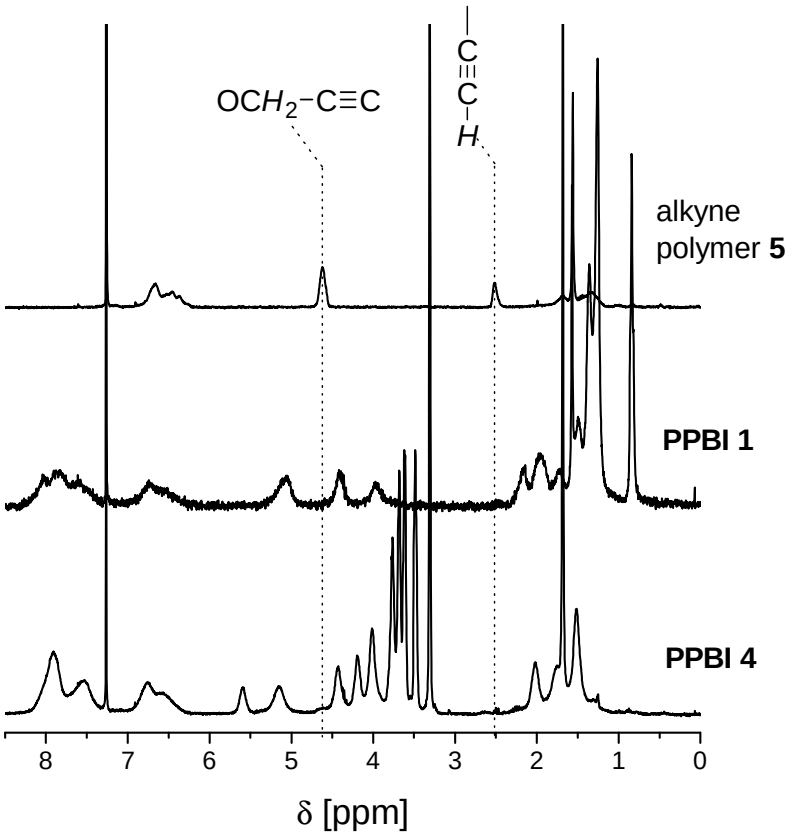

Figure 2: *^{1}H NMR spectra ($CDCl_3$) of alkyne polymer **5** and exemplarily of a PPBI with hydrophobic alkyl swallow-tail (**PPBI 1**) and one with hydrophilic OEG swallow-tail (**PPBI 4**). Signals from residual alkyne groups cannot be observed in the ^{1}H NMR spectrum of the PPBIs.*

Table 1: *SEC data such as molecular weight, PDI and thermal data of scaffold polymers **4** and **5** and "clicked" polymers **PPBIs 1-6***

polymer	M_n [g/mol] (SEC)[a]	M_w/M_n (SEC)[a]	M_n [g/mol] (theor.)[b]	T_{onset} [°C][c]	T_g [°C][d]	T_m [°C][d]	ΔH [J/g][d]	spacer	notes
4	9 300	1.11				n.o.			P(TMS-Propargyloxystyrene)
5	7 400	1.11		386	59	n.o.			P(Propargyloxystyrene)
PPBI 1	59 700	1.09	39 200	330	182	298	1.8	$(CH_2)_6$	Hydrophobic PPBI
PPBI 2	59 200	1.09	40 500	330	166	216	0.4	$(CH_2)_8$	Hydrophobic PPBI
PPBI 3	58 300	1.09	42 300	330	153	n.o.		$(CH_2)_{11}$	Hydrophobic PPBI
PPBI 4	59 600	1.09	42 200	330	142	n.o.		$(CH_2)_6$	Hydrophilic PPBI
PPBI 5	58 700	1.09	43 500	330	123	n.o.		$(CH_2)_8$	Hydrophilic PPBI
PPBI 6	55 600	1.09	45 300	330	120	n.o.		$(CH_2)_{11}$	Hydrophilic PPBI

[a] Measured with size exclusion chromatography in tetrahydrofuran and calibrated to polystyrene standards; [b]Theoretical molecular weight calculated from 100% converted 44 repeating units of **5**; [c]Measured by thermogravimetric analysis under N_2 atmosphere; [d]Measured by differential scanning calorimetry under N_2 atmosphere.

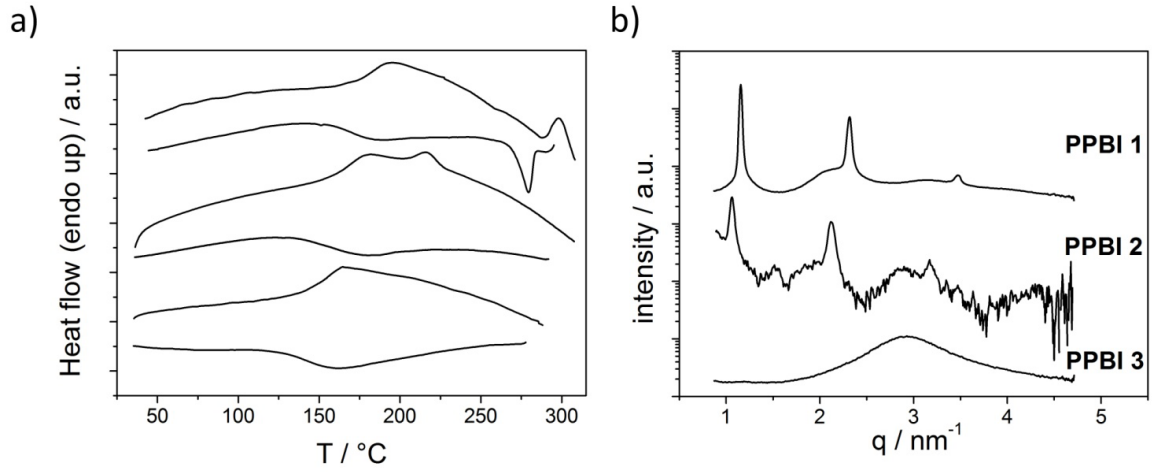

***Figure 3**: a) DSC traces (second heating and cooling cycle) of hydrophobic polymers **PPBI 1**, **2** and **3** (from top to bottom) recorded at 40K/min. b) Diffraction pattern of **PPBI 1**, **2** and **3** at RT for the SAXS regime.*

polymers.[25]To determine the influence of the different substituents on the thermal and structural properties, the phase transitions of polymers **PPBI 1-6** were investigated by DSC measurements and the structural features using X-ray diffraction experiments. The DSC thermograms and the X-ray diffractograms in SAXS regime of the hydrophobic polymers **PPBI 1-3** and hydrophilic polymers **PPBI 4-6** are shown in Figures 3 and 5 respectively.

First, the results of the hydrophobic polymers **PPBI 1-3** with alkyl swallow-tail and $(CH_2)_6$, $(CH_2)_8$ and $(CH_2)_{11}$ spacers, respectively, are discussed below.

PPBI 1 with $(CH_2)_6$ spacer exhibits a T_g at 182 °C and an endothermic transition at 298 °C (ΔH= 1.8 J/g). As observed in temperature-dependent XRD measurements (Figure 17), the transition at 298 °C is a melting point. The XRD diffraction at RT shows a liquid crystalline lamellar ordering with reflections at 1.15 nm^{-1}, 2.31 nm^{-1} and 3.47 nm^{-1} which is stable between RT and 298 °C. This corresponds to a lamellar distance of 5.46 nm. Since the length of the fully stretched PBI pendant groups is estimated to be 4.28 nm, we suggest a SmC bilayer structure for **PPBI 1** where the PBI moieties are tilted. The tilt angle depends on the degree of interdigitation/mixing up of the swallow tail substituents. The broad halos below the assigned reflections are attributed to amorphous parts of the polymer.

PPBI 2 with $(CH_2)_8$ spacer shows a T_g at 166 °C and an endothermic transitions at 216 °C. As observed in temperature dependent XRD measurements, the polymer melts into isotropic state at 216 °C (Figure 18). XRD diffraction at RT shows a lamellar ordering with reflections at 1.06 nm^{-1}, 2.12 nm^{-1} and 3.18 nm^{-1} which is stable between RT and 216 °C. This corresponds to a lamellar distance of 5.93 nm. The PBI pendants are estimated to have a length of 4.51 nm, assuming fully stretched conformation. Therefore we also suggest a SmC bilayer structure as in **PPBI 1**. The broad halos below the assigned reflections are attributed to amorphous parts of the polymer. Contrary to **PPBI 1** and **PPBI 2**, **PPBI 3** with $(CH_2)_{11}$ spacer shows only a T_g at 153 °C and no melting peak in DSC. Also, XRD measurements show no reflections in the low q region and thereby confirm an amorphous state at RT. A comparison of the three polymers **PPBI 1-3** shows a clear dependence of the melting points on the spacer length of the PBI moiety, with which it is

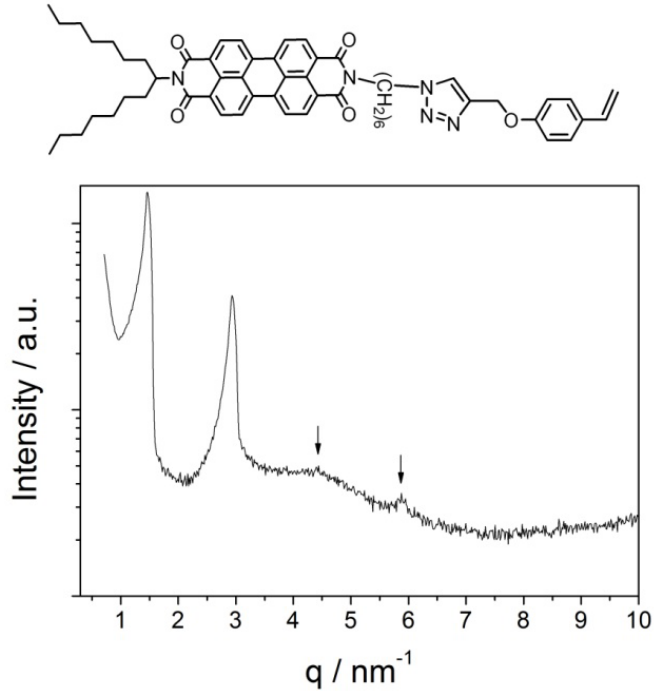

Figure 4: *Chemical structure and diffraction pattern of model monomer* ***PBI-Sty 6****.*

attached at the backbone. In the case of polymer **PPBI 3** with $(CH_2)_{11}$ spacer the flexibility and softness is so large that it results in a completely amorphous behaviour. Among the polymers **PPBI 1** and **PPBI 2**, an increase of the spacer length shifts the melting point to lower temperatures. The T_g of the three polymers also decreases with increasing length of the alkyl spacer. This effect is well known in side chain liquid crystalline polymers and is attributed to an increased plasticization of the backbone by longer alkyl spacers.[26] Comparison of the XRD data of polymers **PPBI 1** and **PPBI 2** shows an increase of the lamellar distance (from 5.46 to 5.93 nm) which fits very well to the increase of the spacer length by two methylene units. For **PPBI 1**, birefringence could be observed in polarized light microscopy (Figure 6). The observed textures were very small and could not be unequivocally attributed to typical fan shaped or focal conic smectic textures. **PPBI 2** did not show any birefringence or characteristic textures also after thermal annealing shortly under the T_c or on slow cooling at 1K/min. This can be explained by the high viscosity of the polymer in this state and taking into consideration the very low ΔH of 0.4J/g for this polymer. As expected, the amorphous polymer **PPBI 3** does not show any birefringence. To elucidate the origin of the LC behavior of the polymers **PPBI 1** and **PPBI 2**, a model compound (**PBI-Sty 6**) of **PPBI 1** was synthesized by "click" reaction of propargyloxystyrene and **PBI-N_3 1** under the same conditions as for the synthesis of the PPBIs. The compound was studied in XRD at RT (Figure 4). Interestingly, model compound **PBI-Sty 6** showed also lamellar behavior, indicated by reflections at q values of 1.46 nm^{-1}, 2.93 nm^{-1}, 4.46 nm^{-1} and 5.88 nm^{-1} which are in a ratio of 1:2:3:4. This corresponds to a lamellar distance of 4.29 nm, which correlates very well with the estimated length of the fully stretched model monomer **PBI-Sty 6** (4.28 nm). While the polymers

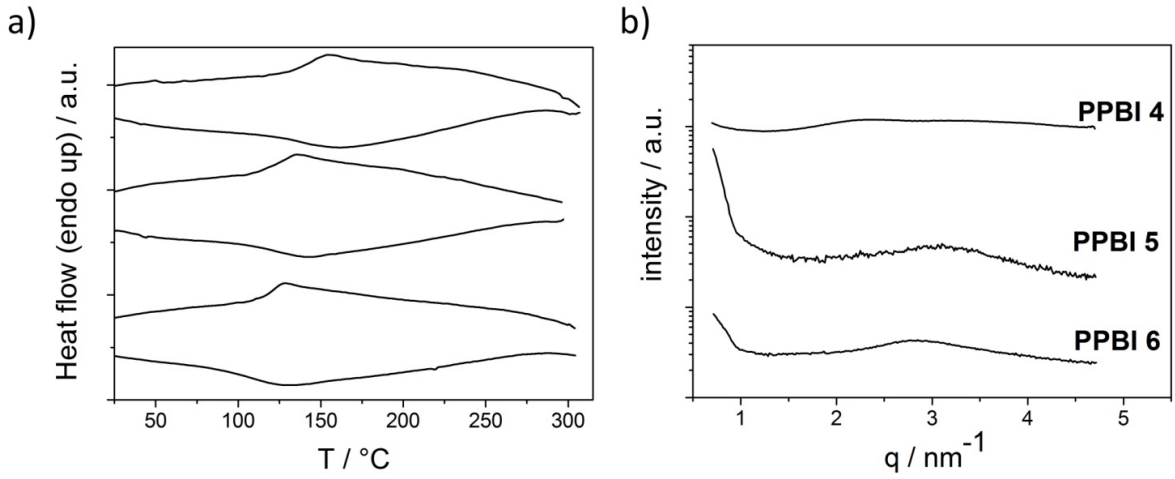

***Figure 5**: a) DSC traces (second heating cycle) of hydrophilic **PPBI 4, 5** and **6** (from top to bottom) recorded at 40K/min. b) Diffraction pattern of **PPBI 4, 5** and **6** at RT.*

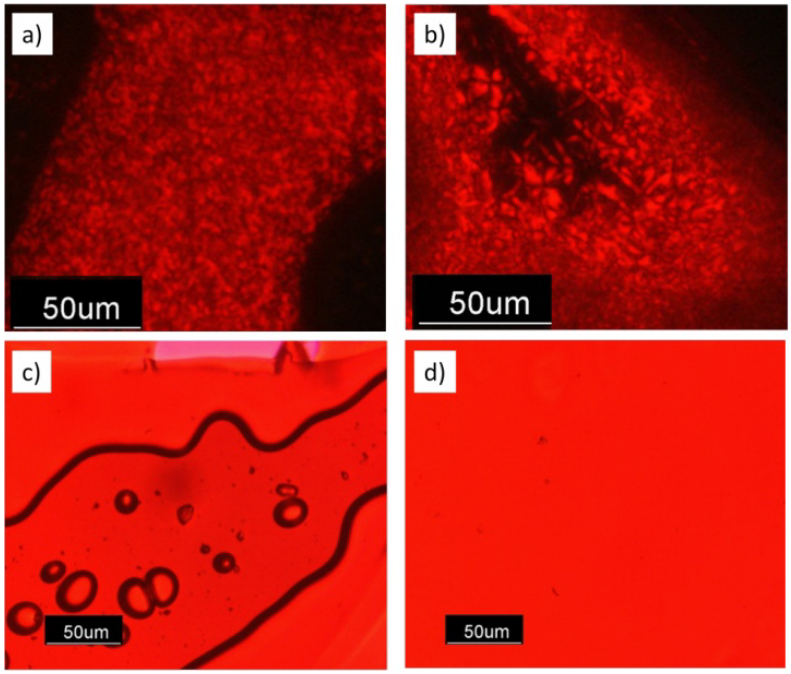

Figure 6: Optical microscopic images of a**) PPBI 1** and b) **PBI-Sty 6** at RT under crossed polarizers exhibiting birefringence. c) and d) show optical microscopic images of **PPBI 2** and **PPBI 4** respectively with a λ/4 plate. No texture could be observed for **PPBI 2** even at prolonged annealing or on slow cooling at 1K/min.

PPBI 1 and **PPBI 2** showed SmC behavior, model monomer **PBI-Sty 6** clearly exhibits a SmA phase. Low molecular, symmetrically swallow-tail-substituted PBIs often exhibit columnar hexagonal ordering due to their space-filling nature of substituents.[27] As the PBI **PBI-Sty 6** and the PBIs in the polymers are unsymmetrically substituted with a linear spacer and one swallow-tail-substituent, smectic behavior is not unexpected for these molecules. For **PBI-Sty 6**, birefringence could be observed in polarized light microscopy (Figure 6). The observed textures could best be described as focal conic.

In contrast to the hydrophobic substituted PPBIs, the hydrophilic polymers **PPBI 4-6** show no melting peaks in DSC. Also, XRD measurements at RT show no sharp reflections at small q values but only a broad halo, confirming the amorphous nature of these polymers. **PPBI 4** exhibits a T_g at 142 °C, **PPBI 5** a T_g at 123 °C and **PPBI 6** a T_g at 120 °C. There was no birefringence or texture observed in polarized light microscopy for the amorphous polymers **PPBI 4-6**, as expected. It seems that the flexible OEG swallow-tail hinders the formation of ordered liquid crystalline or crystalline structures. The tendency of OEG swallow-tail substituted PBIs to form lower molecular order compared to their alkyl swallow-tail substituted analogues can be attributed to the higher flexibility and space-filling properties of OEG and is known for low molecular PBIs.[27] The T_g of the three polymers decreases with increasing length of the alkyl spacer. As in the hydrophobic substituted PPBIs, this effect is attributed to an increased plasticization of the backbone by longer alkyl spacers.[26]

The T_gs observed in the side chain polymers (between 120 °C and 180 °C) are comparable to those observed in poly perylene acrylates with $(CH_2)_6$ spacers or polymers from PBI-N_3 clicked to an alkyne bearing polyacrylate.[6] The presence of a glassy state with LC order at RT, especially for polymer **PPBI 1** and **PPBI 2** offers possibilities of achieving order in thin films by tempering methods.

Conclusion

We showed that by the modular “click” chemistry approach in combination with nitroxide mediated radical polymerization, a variation in the substitution of side chain polymers is easily possible. “Click” chemistry has been used to synthesize three hydrophilic and three hydrophobic PPBIs with OEG- and alkyl swallow-tails, respectively. In each series, the length of the spacer between the nitrogen of the triazole unit and the nitrogen of the PBI was varied from $(CH_2)_6$ to $(CH_2)_8$ and to $(CH_2)_{11}$. Longer spacers shift the T_g to lower temperatures due to the higher plasticization of the backbone. The structural analysis revealed that the shorter spacers with six and eight methyl units (**PPBI 1** and **2**) with alkyl swallow-tail substituents lead to liquid crystalline behaviour. Based on the first XRD results, a lamellar SmC structure is suggested. When the alkyl spacer is too long, as in **PPBI 3**, no melting transition could be observed and the polymer becomes amorphous in nature. The introduction of OEG swallow-tails at the PPBI leads to amorphous polymers for any spacer length (**PPBI 4-6**). Especially the presence of a glassy state with LC order at RT allows tailoring the required film properties in these polymers. Polar groups in perylene bisimide containing polymers are suitable for the phase separation in block copolymers due to an additional polar-apolar driving force and thereby an increased χ parameter. The applicability of these polymers as acceptor materials in suitable devices is under study.

Experimental section

General

The free nitroxide *N*-tert-butyl-*α*-isopropyl-*α*-phenylnitroxid **3** was synthesized according to published procedures.[28] *N*-(1-Heptyloctyl)-perylene-3,4,9,10-tetracaboxylic acid bisimide **10** and *N*-(1,3-bis(2-(2-(2-methoxyl)ethoxyl)ethoxyl)propyl) perylene-3,4,9,10-tetracaboxylic acid bisimide **11** were prepared according to a published procedure.[27] Propargyl bromide (80% in toluene), 4-acetoxy styrene (96%), anisole (99%), 1,6-dibromo hexane (97%), 1,8-dibromo octane (97%), dimethylformamide (99.8%), silver nitrate (≥99.0%) and triphenylphosphine (≥95.0) were purchased from Sigma-Aldrich. Tetrabutylammonium fluoride (>98%), 1,8-diazabicyclo[5.4.0]undec-7-ene (≥99.0%), trimethylsilyl chloride (98%) and PMDETA (≥98%) were purchased from Fluka. CuBr (98%) was bought from Acros. All reagents were used without further purification unless otherwise noted. ^{1}H NMR (300 MHz) spectra were recorded on a Brucker AC 300 spectrometer in $CDCl_3$ and calibrated to $CHCl_3$ signal (7.26 ppm for ^{1}H). UV-vis spectra of solutions in $CHCl_3$ with a concentration of 10^{-5} mol·L^{-1} were recorded on a Hitachi 3000 spectrophotometer and photoluminescence spectra were acquired on a Shimadzu RF 5301 PC spectrofluorophotometer upon excitation at 490 nm. SEC measurements were carried out in THF with 0.25% tetrabutylammoniumbromide with two Varian MIXED-C columns (300x7.5 mm) at room temperature and at a flow rate of 0.5 mL/min using UV (Waters model 486) with 254 nm detector wavelength and refractive index (Waters model 410) detectors. Polystyrene in combination with *o*-DCB as an internal standard was used for calibration. Differential scanning calorimetry experiments were conducted at heating rates of 40 K·min^{-1} under N_2 atmosphere with a Perkin Elmer Diamond DSC, calibrated with indium. The endothermic maximum was taken as T_m. Thermogravimetry measurements were conducted on a Mettler Toledo TGA/SDTA 851^e under N_2 atmosphere at a heating rate of 10K/min. Temperature of decomposition (T_{onset}) was calculated from the onset of the respective curve. X-ray diffraction experiments for **PPBI 2**, **PPBI 5**, **PPBI 6** and **PBI-Sty** were performed on a Huber GuinierDiffractometer 6000 equipped with a Huber quartz monochromater 611 with Cu-$K_{\alpha1}$: 1.54051 Å. The samples **PPBI 1**, **PPBI 3** and **PPBI 4** were measured at the beamline ID2 at the European Synchrotron Radiation Facility in Grenoble. The energy of the photons was 12.540 keV (λ∼0.1 nm).

Synthesis

TIPNO-Sty (1)

The synthesis was conducted after the principles described in literature.[29] 2,2,5-Trimethyl-4-phenyl-3-azahexane-3-nitroxide **3** (4.29 g, 19.5 mmol), (1-bromoethyl)benzene (4.68 g, 25.3 mmol) and PMDETA (4.39 g, 25.3 mmol) were dissolved in 100 mL of toluene and degassed by purging with nitrogen for 10 min. After addition of CuBr (3.63 g, 25.3 mmol) under inert gas atmosphere, the reaction mixture was heated to 60 °C for 1 h, cooled to RT and filtered over a short column of neutral alumina which was washed with toluene. For further purification, the raw product was cleaned by column chromatography on silica with hexanes : ethyl acetate 50 : 1 as eluent, to give the two isomers of the product. The product comprises of a mixture of

colourless crystals and colourless oil and weighs 4.20 g (66.2 %).

Propargyloxystyrene[8]

Acetoxystyrene (50.00 g, 308.3 mmol) was dispersed in 250 mL of deionized water, KOH (51.84 g, 923.9 mmol) was added and the mixture was stirred for 2h. The mixture was then diluted with 600 mL of acetone and propargyl bromide (80% in toluene) (68.72 g, 46.2 mmol) was added portionwise. After 48 h the volatiles were evaporated and the H_2O phase was extracted with $CHCl_3$ three times. The combined organic phases were dried over Na_2SO_4, filtered and evaporated. For further purification, the raw product was cleaned by column chromatography over silica with hexanes/ethyl acetate : 100/1 as eluent. The product was obtained as a colourless liquid and weighed 45.71 g (93.8%). ^{1}H NMR (300 MHz, $CHCl_3$): δ (ppm) 7.40-7.32 (m, 2H, Ar*H*), 6.97-6.90 (m, 2H, Ar*H*), 6.66 (dd, 1H, J = 11.1 Hz, J = 17.7 Hz, C*H*CH_2), 5.62 (dd, 1H, J = 0.8 Hz, J = 17.6 Hz, CHC*H*H), 5.15 (dd, 1H, J = 0.8 Hz, 10.9 Hz, CHCH*H*), 4.69 (d, 2H, J = 2.4 Hz, OCH_2), 2.52 (t, 1H, J = 2.4 Hz, C≡C*H*).

TMS-Propargyloxystyrene[8] (2)

AgCl (4.14 g, 28.9 mmol) and DBU (45.75g, 300.5 mmol) were dissolved in 250 mL of DCM. Propargyloxystyrene (45.71 g, 288.9 mmol) was added and the reaction mixture was brought to reflux. After addition of $SiMe_3Cl$ (43.95 g, 404.5 mmol) the reaction was stirred for 24h and then cooled to RT. After washing with 1M HCl, $NaHCO_3$ solution and deionized H_2O, the organic phase was dried over Na_2SO_4, filtered and evaporated. For further purification, the raw product was cleaned by column chromatography over silica with hexanes/ethyl acetate : 100/1 as eluent. The fractions containing pure product were collected and evaporated and gave the product as a colourless liquid which weighed 49.22 g (73.9 %). ^{1}H NMR (300 MHz, $CHCl_3$): δ (ppm) 7.40-7.32 (m, 2H, Ar*H*), 6.98-6.90 (m, 2H, Ar*H*), 6.67 (dd, 1H, J = 11.1 Hz, J = 17.7 Hz, C*H*CH_2), 5.62 (dd, 1H, J = 0.6 Hz, J = 17.6 Hz, CHC*H*H), 5.15 (dd, 1H, J = 0.6 Hz, 10.8 Hz, CHCH*H*), 4.68 (s, 2H, OCH_2), 0.19 (s, 9H, $SiMe_3$).

General Procedure for Polymerization of TMS-propargyl oxystyrene (4)

TMS-Propargyloxystyrene **2** (4.00 g, 17.4 mmol), Initiator **1** (75.3 mg, 230µmol) and free nitroxide **3** (5.1 mg, 23 µmol) were dissolved in 2.4 mL *o*-DCB, degassed by three freeze-pump-thaw cycles and then heated at 125 °C. The reaction was quenched by cooling in an ice-bath, precipitated into methanol twice from 2 mL of THF and dried in vacuum. ^{1}H NMR (300 MHz, $CHCl_3$): δ (ppm) 6.9-6.18 (4H, br S, Ar*H*), 4.63 (s, 2H, -OCH_2), 1.79-0.92 (br s, 3H, C*H*, CH_2), 0.23 (s, 9H, $SiMe_3$). M_n = 9300 g/mol; PDI = 1.11.

General Procedure for Deprotection of (4) to (5)

Poly(TMS-propargyloxystyrene) **4** was dissolved in THF, cooled to 0°C and degassed by purging with nitrogen. 2 eq of tetrabutylammoniumfluoride and 2 eq of acetic acid were added by syringe. The mixture was stirred over night, precipitated in methanol and filtered. The

deprotected poly(propargyloxystyrene) was obtained as a white powder which was freeze-dried in benzene. ^{1}H NMR (300 MHz, $CHCl_3$): δ (ppm) 6.9-6.18 (4H, br S, Ar*H*), 4.63 (s, 2H, -OCH_2), 2.52 (br s, 1H, C≡C*H*), 1.79-0.92 (br s, 3H, C*H*, CH_2). M_n = 7400 g/mol; PDI = 1.11. IR (ATR): ν (cm^{-1}) 3286 (C≡C-H), 2919, 2120 (C≡C), 1607, 1507.

Model compound PBI-Sty (6)

Propargyloxystyrene (53 mg, 0.34 mmol) was dissolved in 20 mL of anisole together with **PBI-N3 1** (100 mg, 0.14 mmol) of the respective perylene azide. After degassing by purging with nitrogen for 10 minutes, 3 drops of stock solution of PMDETA/CuBr in anisole were added by syringe through a septum. The reaction mixture was stirred for 3h, precipitated in MeOH and dried in vacuum. The pure product **6** was obtained as a red powder and weighed 113 mg (93%).^{1}H NMR (300 MHz, $CHCl_3$): δ (ppm) 8.74-8.54 (m, 8H, 8Ar$H_{perylene}$), 7.62 (s, 1H, triazole-*H*), 7.32 (d, 2H, J = 8.8 Hz, Ar$H_{styrene}$), 6.93 (d, 2H, J = 8.8 Hz, Ar$H_{styrene}$), 6.63 (dd, 1H, J = 17.6 Hz, J = 10.7 Hz, C*H*CH_2), 5.59 (d, 1H, J = 17.4 Hz, CHC*H*H), 5.10 (d, 1H, J = 11.8 Hz, CHCH*H*), 5.23-5.14 (m, 1H, N-C*H*), 5.20 (s, 2H,OCH_2), 4.37 (t, 2H, J = 7.9 Hz, N-CH_2), 4.17 (t, 2H, J = 7.1 Hz, N-C$H_{2,triazole}$), 2.31-2.15 (m, 2H, 2αCH*H*), 2.00-1.67 (m, 4H, 2αC*H*H, N-CH_2CH_2), 1.53-1.12 (m, 24H, 12CH_2), 0.81 (t, 6H, J = 6.3 Hz, 2CH_3). IR (ATR): ν (cm^{-1}) 2923, 2854, 1692, 1649, 1594.

1-Azido-6-bromohexane[30] (7)

NaN_3 (3.95 g, 60.8 mmol) was added to a solution of 1,6-dibromohexane (38.70 g, 152.1 mmol) in 80 mL of DMSO. The solution was stirred for 1 h, poured into 250 mL of H_2O and extracted 3 times with Et_2O. The organic phase was dried with $MgSO_4$, filtered and evaporated. The crude product was purified by column chromatography over silica with a gradient of hexane : THF from 1 : 0 to 0 : 1 as eluent. The fractions containing pure **7** were evaporated and the pure product was obtained as a slightly yellowish liquid and weighed 11.0 g (87.7%).^{1}H NMR (300 MHz, $CHCl_3$): δ (ppm) 3.40 (t, 2H, *J* = 6.8 Hz), 3.27 (t, 2H, *J* = 6.5 Hz), 1.92-1.80 (2H, m), 1.66-1.55 (m, 2H), 1.51-1.35 (m, 4H). IR (ATR): ν (cm-1) 2092 (-N_3).

1-Azido-8-bromooctane[31] (8)

NaN_3 (1.43 g, 22.1 mmol) was added to a solution of 1,8-dibromooctane (15.00 g, 55.1 mmol) in 30 mL of DMSO. The solution was stirred for 1 h, poured into 150 mL of H_2O and extracted 3 times with Et_2O. The organic phase was dried over $MgSO_4$, filtered and evaporated. The crude product was purified by column chromatography over silica with a gradient of hexane : ethyl acetate from 1 : 0 to 5 : 1. The fractions containing pure **8** were evaporated and the product was obtained as a slightly yellowish liquid and weighed 3.7 g (72.5%).^{1}H NMR (300 MHz, $CHCl_3$): δ (ppm) ^{1}H NMR (300 MHz, $CHCl_3$): δ (ppm) 3.40 (t, 2H, *J* = 6.8 Hz), 3.25 (t, 2H, *J* = 6.5 Hz), 1.92-1.80 (m, 2H), 1.66-1.55 (m, 2H), 1.51-1.24 (m, 8H). IR (ATR): ν (cm-1) 2092 (-N_3).

1-Azido-11-undecane (9)

PPh_3 (11.49 g, 43.8 mmol) was dissolved in 150 mL of THF. 11-Bromo-1-undecanol (10.00 g, 39.8 mmol) was added to the solution. A mixture of diethyl azodicarboxylate (20.19 g, 46.4 mmol) and diphenylphosphoryl azide (13.55 g, 47.8 mmol) was added slowly and the reaction was stirred for 24 h at RT. After evaporation of the volatiles the pure product was obtained after column chromatography over silica with a gradient of hexane : ethyl acetate from 1 : 0 to 8 : 1. The pure product weighed 1.4 g (12.7 %). NMR (300 MHz, $CHCl_3$): δ (ppm) 3.40 (t, 2H, *J* = 6.8 Hz), 3.25 (t, 2H, *J* = 6.5 Hz), 1.92-1.80 (m, 2H), 1.66-1.55 (m, 2H), 1.48-1.21 (m, 12H). IR (ATR): ν (cm-1) 2092 (-N_3).

***N*-(1-Heptyloctyl), *N'*-(hexyl-6'-azido)-perylene-3,4,9,10-tetracaboxylic acid bisimide (PBI-N_3 1).**

N-(1-Heptyloctyl)-perylene-3,4,9,10-tetracaboxylic acid bisimide **10** (2.00 g, 3.3 mmol) was dissolved in 30 mL of DMF. NaH (60% oil-dispersion) (240 mg, 6.00 mmol) was added slowly and the mixture was allowed to stir for 1 h. Subsequently, **7** (1.03 g, 5.0 mmol) was added and the reaction was heated to 130 °C for 48 h. After cooling to RT and precipitation in MeOH the raw product was cleaned by column chromatography over silica with $CHCl_3$: acetone of 95 : 5. The fractions containing pure **PBI-N_3 1** were evaporated and gave the product as a red solid weighing 2.00 g (82.6 %). ^{1}H NMR (300 MHz, $CHCl_3$): δ (ppm) 8.72-8.51 (m, 8H, Ar*H*), 5.26-5.13 (m, 1H, N-C*H*), 4.21 (t, 2H, *J* = 7.6, N-CH_2), 3.30 (t, 2H, *J* = 6.9, CH_2-N_3), 2.35-2.18 (m, 2H, 2αCH*H*), 1.97-1.73 (m, 4H, 2αC*H*H, N-CH_2CH_2), 1.72-1.60 (m, 2H, C$H_2$$CH_2$-$N_3$), 1.54-1.18 (m, 24H, 12CH_2), 0.84 (t, 6H, *J* = 6.8, 2CH_3). IR (ATR): ν (cm-1) 2923, 2855, 2092 (-N_3), 1964, 1650.

***N*-(1-Heptyloctyl), *N'*-(octyl-8'-azido)-perylene-3,4,9,10-tetracaboxylic acid bisimide (PBI-N_3 2).**

N-(1-Heptyloctyl)-perylene-3,4,9,10-tetracaboxylic acid bisimide **10** (1000 mg, 1.66 mmol) was dissolved in 13 mL of DMF. K_2CO_3 (413 mg, 2.99 mmol) and **8** (544 mg, 2.32 mmol) were added and the reaction was heated to 100 °C. The mixture was stirred for 72h at 100 °C, cooled to RT and precipitated into 150 mL of MeOH : H_2O of 3 : 1 and filtered. The pure product was obtained as a red powder and weighed 1.20 g (96.0%).^{1}H NMR (300 MHz, $CHCl_3$): δ (ppm) 8.76-8.34 (m, 8H, Ar*H*), 5.27-5.08 (m, 1H, N-C*H*), 4.17 (t, 2H, J = 7.5 Hz, N-CH_2), 3.25 (t, 2H, J = 6.9 Hz, CH_2-N_3), 2.33-2.15 (m, 2H, 2αCH*H*), 1.96-1.80 (m, 2H, 2αC*H*H), 1.80-1.67 (m, 1H, C$H_2$$CH_2$-$N_3$), 1.50-1.07 (m, 28H, 14CH_2), 0.82 (t, 6H, J = 6.6 Hz, CH_3). IR (ATR): ν (cm-1) 2924, 2857, 2092 (-N_3), 1960, 1652.

N-(1-Heptyloctyl), N'-(undecyl-11'-azido)-perylene-3,4,9,10-tetracaboxylic acid bisimide (PBI-N_3 3).

N-(1-Heptyloctyl)-perylene-3,4,9,10-tetracaboxylic acid bisimide **10** (1000 mg, 1.66 mmol) was dissolved in 13 mL of DMF. NaH (60% in oil dispersion) (120 mg, 3.0 mmol) was added. After 30 minutes, the reaction mixture was heated to 120 °C and **9** (642 mg, 2.32 mmol) was added. The mixture was stirred for 24h at 120 °C, precipitated into 150 mL of MeOH, filtered and purified by column chromatography with $CHCl_3$ as eluent over a silica column. The product was obtained as a red powder and weighed 770 mg (57%). ^{1}H NMR (300 MHz, $CHCl_3$): δ (ppm) 8.77-8.54 (m, 8H,

Ar*H*), 5.27-5.10 (m, 1H, N-C*H*), 4.20 (t, 2H, J = 7.7 Hz, N-CH_2), 3.25 (t, 2H, J = 7.0 Hz, CH_2-N_3), 2.33-2.15 (m, 2H, 2αCH*H*), 1.94-1.52 (m, 3H, 2αC*H*H, 1H, CH_2CH$_2$-N_3), 1.49-1.14 (m, 34H, 17CH_2), 0.82 (t, J = 6.97 Hz, CH_3). IR (ATR): ν (cm-1) 2924, 2854, 2091 (-N_3), 1964, 1651.

N-(1,3-bis(2-(2-(2-methoxyl)ethoxyl)ethoxyl)propyl), N'-(hexyl-6'-azido)-perylene-3,4,9,10-tetracaboxylic acid bisimide (PBI-N_3 4).

N-(1,3-bis(2-(2-(2-methoxyl)ethoxyl)ethoxyl)propyl) perylene-3,4,9,10-tetracaboxylic acid bisimide **11** (1000 mg, 1.50 mmol) was dissolved in 10 mL of DMF and 4 mL THF. K_2CO_3 (302 mg, 2.69 mmol) and **7** (616 mg, 3.00 mmol) were added and the mixture was heated to 60 °C for 48 h. After cooling to RT and evaporation of all solvents, the product was precipitated from THF into 150 mL of cyclohexane, filtered off and purified by column chromatography with THF as eluent over a short silica column (10 cm). The product was obtained as a red powder and weighed 890 mg (74.9%). ^{1}H NMR (300 MHz, $CHCl_3$): δ (ppm) 8.68-8.51 (8H, m, Ar*H*), 5.76-5.65 (1H, m, N-C*H*), 4.25-4.14 (4H, m, 2αCH*H*, N-CH_2), 4.01-3.93 (2H, m, 2αC*H*H), 3.77-3.52 (12H, m, 2OCH_2CH_2OCH_2), 3.44-3.38 (4H, m, 2CH_2OCH$_3$), 3.32-3.24 (8H, m, CH_2-N_3, 2OCH_3) 1.86-1.72 (2H, m, CH_2CH$_2$-N_3), 1.70-1.42 (6H, m, 3CH$_2$). IR (ATR): ν (cm-1) 2911, 2864, 2093 (-N_3), 1963, 1650, 1592.

N-(1,3-bis(2-(2-(2-methoxyl)ethoxyl)ethoxyl)propyl), N'-(octyl-8'-azido)-perylene-3,4,9,10-tetracaboxylic acid bisimide (PBI-N_3 5)

N-(1,3-bis(2-(2-(2-methoxyl)ethoxyl)ethoxyl)propyl) perylene-3,4,9,10-tetracaboxylic acid bisimide **11** (600 mg, 0.90 mmol) was dissolved in 10 mL of DMF. K_2CO_3 (223 mg, 1.61 mmol) and **8** (294 mg, 1.26 mmol) were added and the mixture was heated to 100 °C for 48 h. After cooling to RT and evaporation of all solvents the product was precipitated from THF into 100 mL of cyclohexane, filtered off and purified by column chromatography with THF : $CHCl_3$ of 1 : 1 as eluent over a short silica column. The product was obtained as a red powder and weighed 457 mg (62.0 %). ^{1}H NMR (300 MHz, $CHCl_3$): δ (ppm) 8.65-8.50 (8H, m, Ar*H*), 5.75-5.65 (1H, m, N-C*H*), 4.24-4.14 (4H, m, 2αCH*H*, N-CH_2), 4.00-3.90 (2H, m, 2αC*H*H), 3.75-3.50 (12H, m, 2OCH_2CH_2OCH_2), 3.44-3.38 (4H, m, 2CH_2OCH$_3$), 3.32-3.24 (8H, m, CH_2-N_3, 2OCH_3) 1.86-1.72 (2H, m, CH_2CH$_2$-N_3), 1.70-1.42 (10H, m, 5CH$_2$). IR (ATR): ν (cm-1) 2923, 2845, 2095 (-N_3), 1964, 1650, 1594.

N-(1,3-bis(2-(2-(2-methoxyl)ethoxyl)ethoxyl)propyl), N'-(undecyl-11'-azido)-perylene-3,4,9,10-tetracaboxylic acid bisimide (PBI-N_3 6).

N-(1,3-bis(2-(2-(2-methoxyl)ethoxyl)ethoxyl)propyl) perylene-3,4,9,10-tetracaboxylic acid bisimide **11** (344 mg, 0.51 mmol) was dissolved in 10 mL of DMF. K_2CO_3 (103 mg, 0.92 mmol) and **9** (200 mg, 0.72 mmol) was added. The mixture was heated to 100 °C for 24 h. After cooling to RT all solvents were evaporated and the product was precipitated from THF into 150 mL of hexanes, filtered and purified by column chromatography over silica with THF : $CHCl_3$ 1 : 1 as eluent. The product was obtained as a red powder and weighed 161 mg (36.5 %). ^{1}H NMR (300 MHz, $CHCl_3$): δ (ppm) 8.66-8.44 (m, 8H, Ar*H*), 5.76-5.64 (m, 1H, N-C*H*), 4.25-4.14 (m, 4H, 2αCH*H*, N-CH_2), 4.03-3.90 (m, 2H, 2αC*H*H), 3.78-3.52 (m, 12H, 2OCH_2CH_2OCH_2), 3.46-3.38 (m, 4H, 2CH_2OCH$_3$), 3.24 (m, 8H, 2OCH_3, CH_2-N_3), 2.10-1.18 (m, 18H, 9CH_2). IR (ATR): ν (cm-1) 2921, 2858, 2093 (-N_3), 1963,

1650, 1593.

Stock solution of CuBr/PMDETA in anisole

CuBr (50 mg, 0.35 mmol) was added to 5 mL anisole in a schlenk tube. The solvent was degassed by purging with nitrogen for 20 minutes. Subsequently, degassed (by purging with nitrogen for 20 minutes) PMDETA (60 mg, 0.35 mmol) was added under inert gas atmosphere and the mixture was stirred for an hour. The solution was stored at RT and was taken out by syringe through a septum, when needed.

General procedure for "click"-reaction to PPBI 1-6:

Poly(propargyloxystyrene) (30 mg, 0.19 mmol) was dissolved in 20 mL of anisole together with 1.2 equivalents of the respective perylene azide. After degassing by purging with nitrogen for 10 minutes, 3 drops of stock solution of PMDETA/CuBr in anisole were added by syringe through a septum. The reaction mixture was stirred over night, filtered over silica and precipitated in MeOH. To remove the excess of perylene azide, the red polymers were extracted in a soxhlet apparatus with methyl ethyl ketone or acetone. Special remarks for the single compounds and data can be found in the following entries.

PPBI 1

The polymer was synthesized according to the general method above and extracted with methyl ethyl ketone. ^{1}H NMR (300 MHz, $CHCl_3$): δ (ppm) 8.30-7.32 (br s, 9H, 8Ar$H_{perylene}$, triazole-*H*), 7.06-6.15 (br s, 4H, Ar$H_{styrene}$), 5.38-4.86 (br s, 3H, OCH_2, N-C*H*), 4.63-4.28 (br s, 2H, N-C$H_{2,perylene}$), 4.13-3.75 (br s, 2H, N-C$H_{2,triazole}$), 2.34-0.97 (m, 35H, 17CH_2, C$H_{backbone}$), 0.85 (br s, 6H, 2CH_3).IR (ATR): ν (cm^{-1}) 2923, 2854, 1694, 1652, 1594, 1578. M_n = 59700 g/mol; PDI = 1.09; T_{onset} = 330 °C, T_g = 182 °C, T_m = 298 °C.

PPBI 2

The polymer was synthesized according to the general method above and extracted with methyl ethyl ketone. ^{1}H NMR (300 MHz, $CHCl_3$): δ (ppm) 8.40-7.40 (br s, 9H, 8Ar$H_{perylene}$, triazole-*H*), 6.97-6.18 (br s, 4H, Ar$H_{styrene}$), 5.35-4.86 (br s, 3H, OCH_2, N-C*H*), 4.53-4.24 (br s, 2H, N-C$H_{2,perylene}$), 4.15-3.83 (br s, 2H, N-C$H_{2,triazole}$), 2.34-1.00 (m, 39H, 19CH_2, C$H_{backbone}$), 0.82 (br s, 6H, 2CH_3). IR (ATR): ν (cm^{-1}) 2924, 2855, 1694, 1654, 1595, 1579, 1508, 1438, 1404, 1338, 1243, 1212, 1172, 1084, 1051, 851, 829, 809, 745, 724.M_n = 59200 g/mol; PDI = 1.09; T_{onset} = 330 °C, T_g = 166 °C, T_m = 216 °C.

PPBI 3

The polymer was synthesized according to the general method above and extracted with methyl ethyl ketone. ^{1}H NMR (300 MHz, $CHCl_3$): δ (ppm) 8.53-7.38 (br s, 9H, 8Ar$H_{perylene}$, triazole-*H*), 7.05-6.05 (br s, 4H, Ar$H_{styrene}$), 5.32-4.84 (br s, 3H, OCH_2, N-C*H*), 4.54-4.19 (br s, 2H, N-C$H_{2,perylene}$), 4.14-3.66 (br s, 2H, N-C$H_{2,triazole}$), 2.39-0.93 (m, 45H, 22CH_2, C$H_{backbone}$), 0.90-0.73 (br s, 6H, 2CH_3).IR

(ATR): ν (cm^{-1}) 2922, 2853, 1695, 1654, 1594, 1579. M_n = 58300 g/mol; PDI = 1.09; T_{onset} = 330 °C, T_g = 153 °C.

PPBI 4

The polymer was synthesized according to the general method above and extracted with methyl ethyl ketone. ^{1}H NMR (300 MHz, $CHCl_3$): δ (ppm) 8.30-7.32 (br s, 9H, 8Ar$H_{perylene}$, triazole-*H*), 7.05-6.20 (br s, 4H, Ar$H_{styrene}$), 5.72-5.40 (br s, 1H, N-C*H*), 5.30-4.95 (br s, 2H, OCH_2), 4.54-4.25 (br s, 2H, N-C$H_{2,perylene}$), 4.25-4.10 (br s, 2H, 2αC*H*H), 4.10-3.85 (br s, 4H, N-C$H_{2,triazole}$, 2αCH*H*), 3.85-3.40 (16H, m, 2OCH_2CH_2OCH_2), 3.30 (m, 6H, 2OCH_3) 2.39-1.40 (m, 11H, 4CH_2, C$H_{backbone}$). IR (ATR): ν (cm^{-1}) 2919, 2865, 1692, 1652, 1593, 1577. M_n = 59600 g/mol; PDI = 1.09; T_{onset} = 330 °C, T_g = 142 °C.

PPBI 5

The polymer was synthesized according to the general method above. The polymer was precipitated in hexane and extracted with acetone. ^{1}H NMR (300 MHz, $CHCl_3$): δ (ppm) 8.30-7.40 (br s, 9H, 8Ar$H_{perylene}$, triazole-*H*), 6.95-6.20 (br s, 4H, Ar$H_{styrene}$), 5.70-5.55 (br s, 1H, N-C*H*), 5.30-4.90 (br s, 2H, OCH_2), 4.54-4.30 (br s, 2H, N-C$H_{2,perylene}$), 4.30-4.15 (br s, 2H, 2αC*H*H), 4.15-3.85 (br s, 4H, N-C$H_{2,triazole}$, 2αCH*H*), 3.85-3.40 (16H, m, 2OCH_2CH_2OCH_2), 3.30 (m, 6H, 2OCH_3) 2.20-1.30 (m, 15H, 6CH_2, C$H_{backbone}$). IR (ATR): ν (cm^{-1}) 2921, 2860, 1693, 1652, 1593, 1577. M_n = 58700 g/mol; PDI = 1.09; T_{onset} = 330 °C, T_g = 123 °C.

PPBI 6

The polymer was synthesized according to the general method above. The polymer was precipitated in hexane and extracted with methyl ethyl ketone. ^{1}H NMR (300 MHz, $CHCl_3$): δ (ppm) 8.30-7.40 (br s, 9H, 8Ar$H_{perylene}$, triazole-*H*), 6.90-6.20 (br s, 4H, Ar$H_{styrene}$), 5.72-5.55 (br s, 1H, N-C*H*), 5.30-4.90 (br s, 2H, OCH_2), 4.54-4.25 (br s, 2H, N-C$H_{2,perylene}$), 4.25-4.10 (br s, 2H, 2αC*H*H), 4.10-3.80 (br s, 4H, N-C$H_{2,triazole}$, 2αCH*H*), 3.80-3.40 (16H, m, 2OCH_2CH_2OCH_2), 3.30 (m, 6H, 2OCH_3) 2.39-1.40 (m, 21H, 7CH_2, C$H_{backbone}$). IR (ATR): ν (cm^{-1}) 2920, 2865, 1692, 1652, 1593, 1577. M_n = 55600 g/mol; PDI = 1.09; T_{onset} = 330 °C, T_g = 120 °C.

Acknowledgement

Financial support from DFG (GRK 1640 and SPP 1355) are kindly acknowledged.

Additional Figures

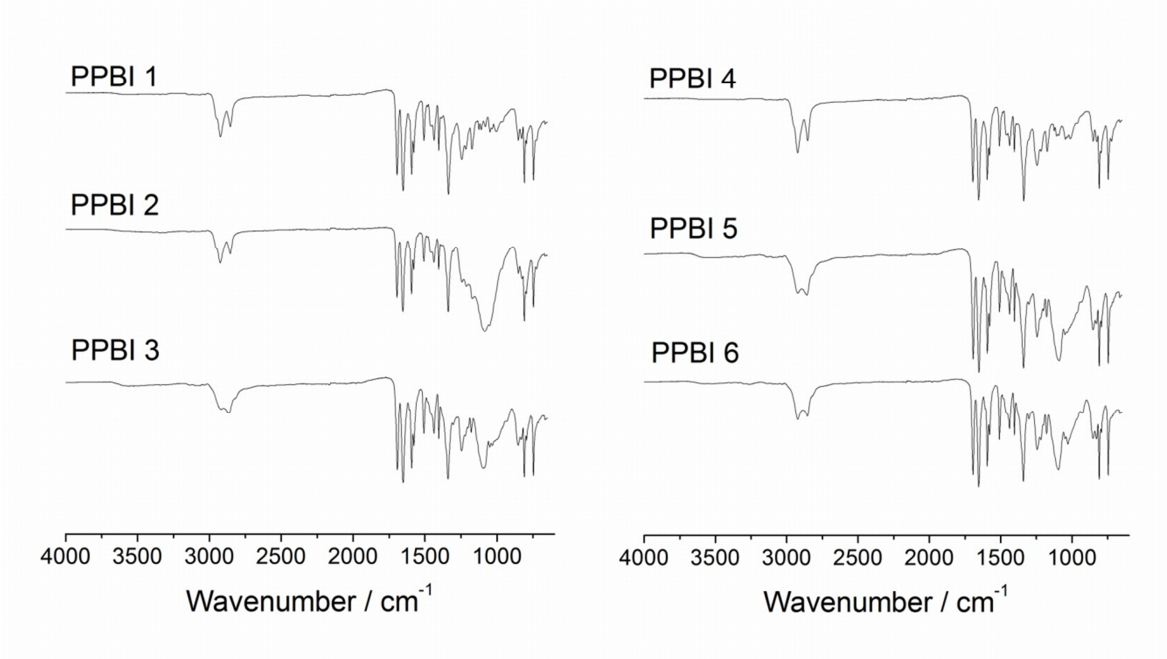

Figure 7: *FTIR spectra of hydrophobic* ***PPBIs 1-3*** *and hydrophilic* ***PPBIs 4-6****.*

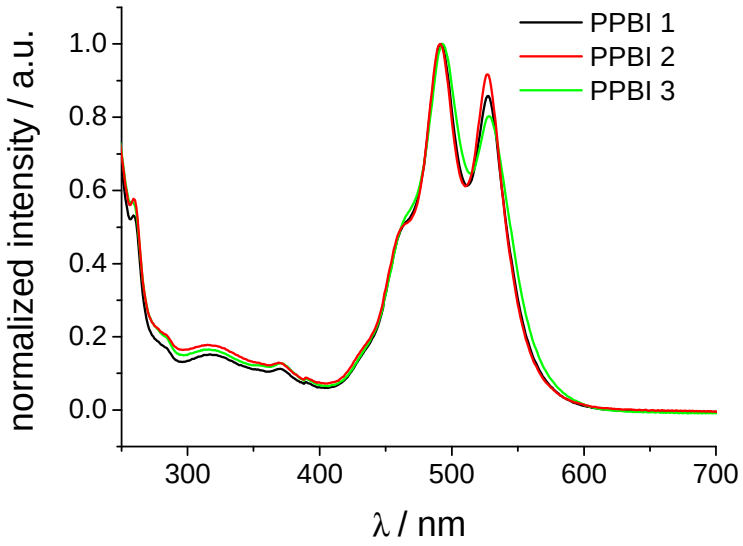

Figure 8: *Absorption spectrum of hydrophobic* ***PPBIs 1-3*** *in chloroform solution (10^{-5} M) normalized at 490 nm peak.*

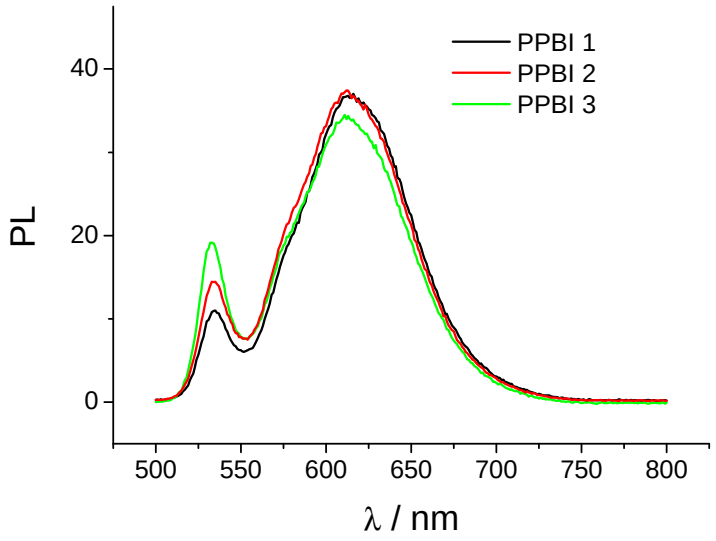

Figure 9: *Photoluminescence spectra of hydrophobic* ***PPBIs 1-3*** *in chloroform solution (10^{-5} M).*

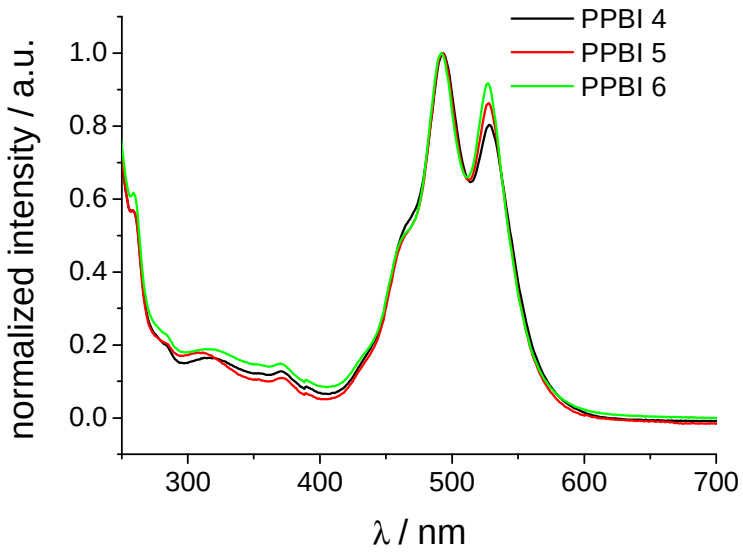

Figure 10: *Absorption spectra of hydrophilic* ***PPBIs 4-6*** *in chloroform solution (10^{-5} M) normalized at 490 nm peak.*

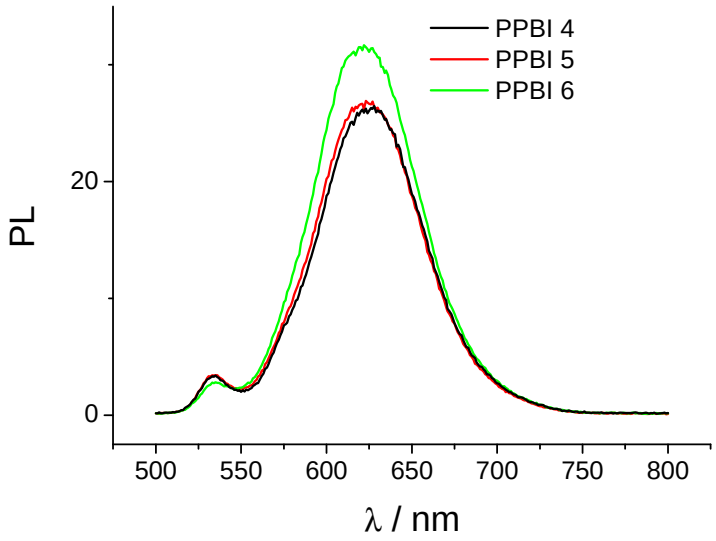

Figure 11: *Photoluminescence spectra of hydrophobic* ***PPBIs 4-6*** *in chloroform solution (10^{-5} M).*

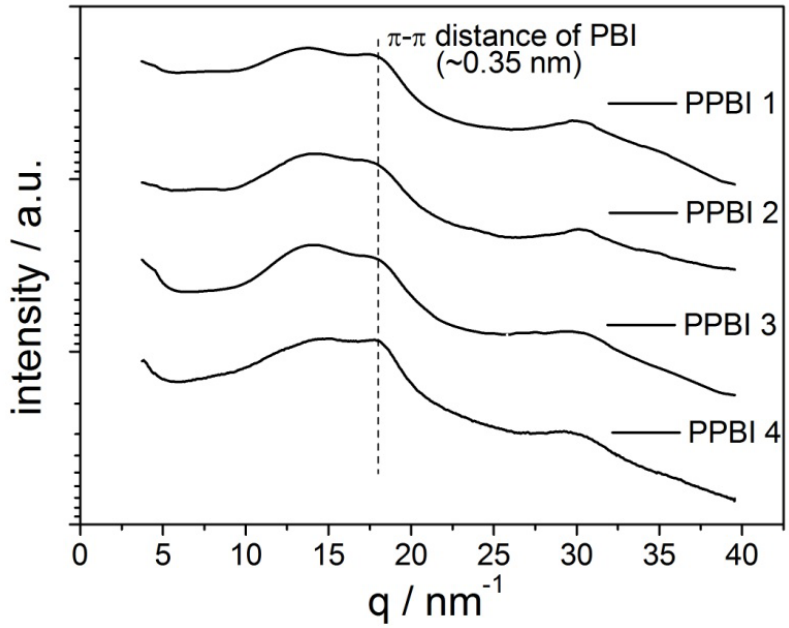

Figure 12: *WAXS data of* ***PPBI 1-4****. The dashed line indicates the π-π distance the PBIs.*

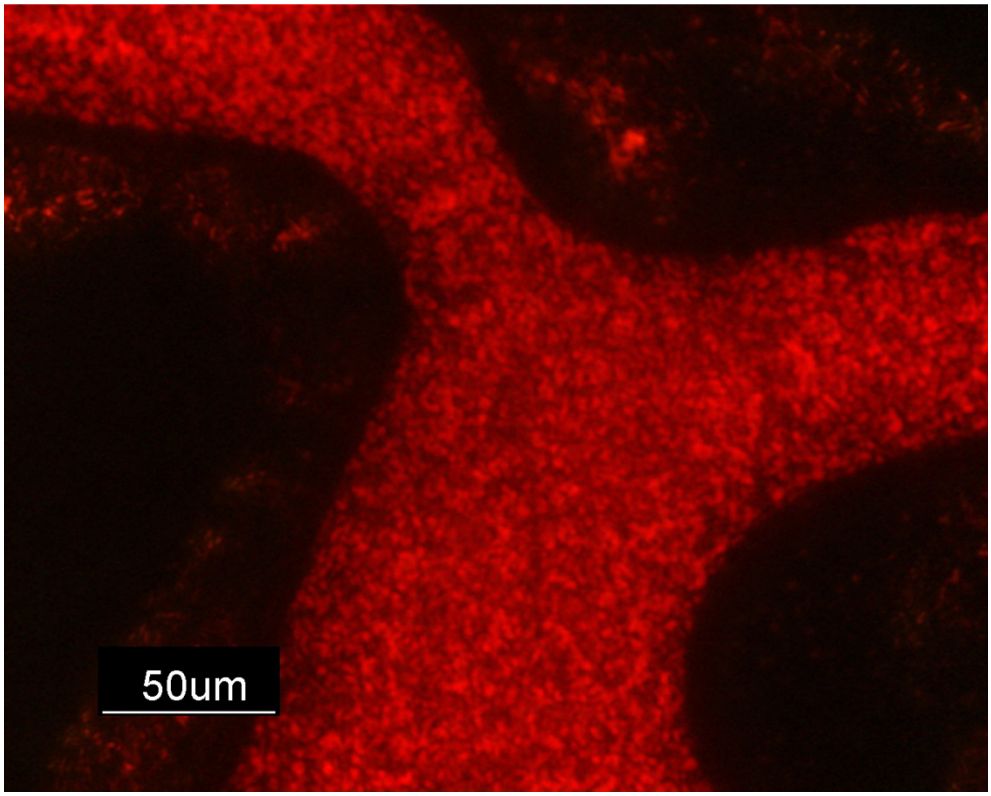

Figure 13: *Optical microscopic image of* ***PPBI 1*** *at RT (under crossed polarizers) exhibiting LC texture, which does not change in the temperature range between 290 °C and RT. Due to a very high viscosity of side chain liquid crystalline polymers, the characteristic SmC textures could not be assigned. The film was cooled down from isotropic melt with 10K/min.*

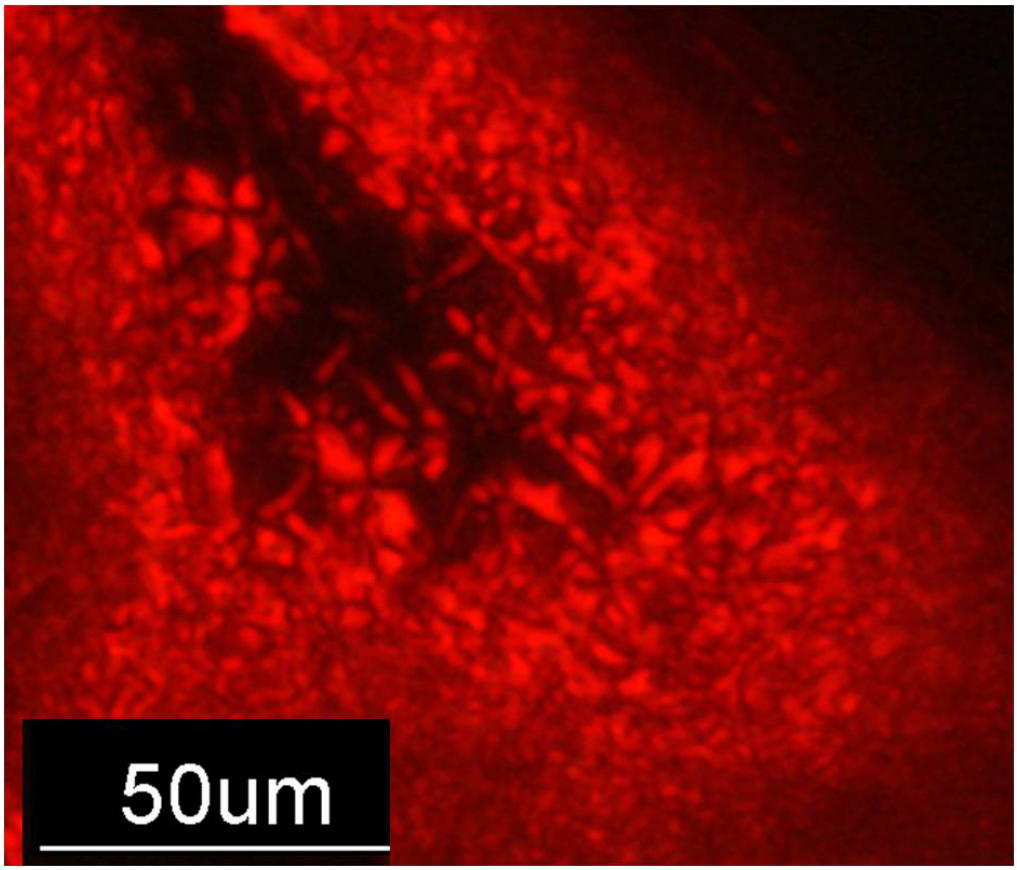

Figure 14: *Optical microscopic image of model compound* ***PBI-Sty 6*** *at RT (under crossed polarizers). The observed texture can best be described as focal conic and did not change in the temperature range between 150 °C and RT. The film was cooled down from isotropic melt with 10K/min.*

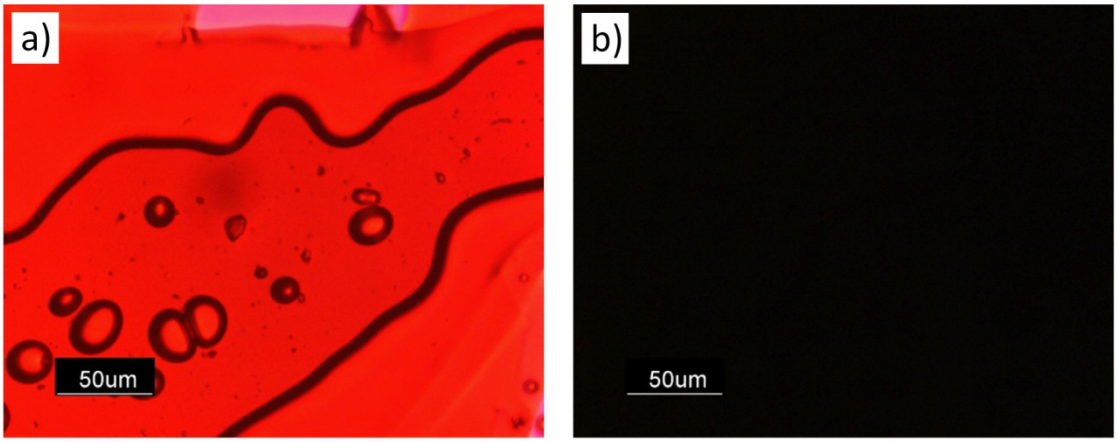

Figure 15: *Optical microscopic images of polymer* ***PPBI 2*** *at RT under crossed polarizers a) with and b) without a λ/4 plate. No birefringence or LC texture could be observed. The film was cooled down from 280 °C with 10K/min. Also long annealing just below the* T_c *and cool rates of 1K/min gave no birefringence of texture.*

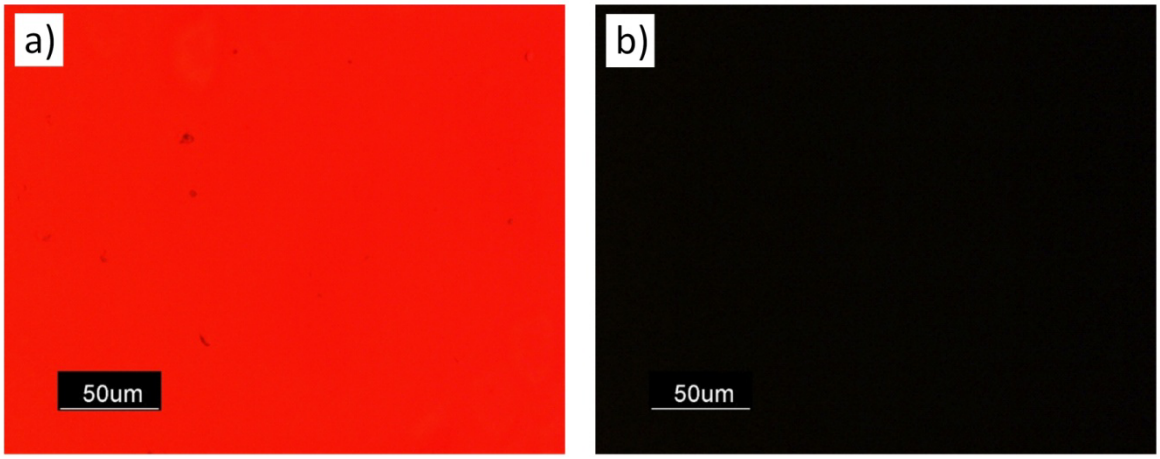

Figure 16: *Optical microscopic images of amorphous polymer* ***PPBI 4*** *at RT under crossed polarizers a) with and b) without a λ/4 plate. As expected no birefringence or LC texture is observed. The film was cooled down from 250 °C with 10K/min. Also long annealing just below the* T_c *and cool rates of 1K/min gave no birefringence of texture.*

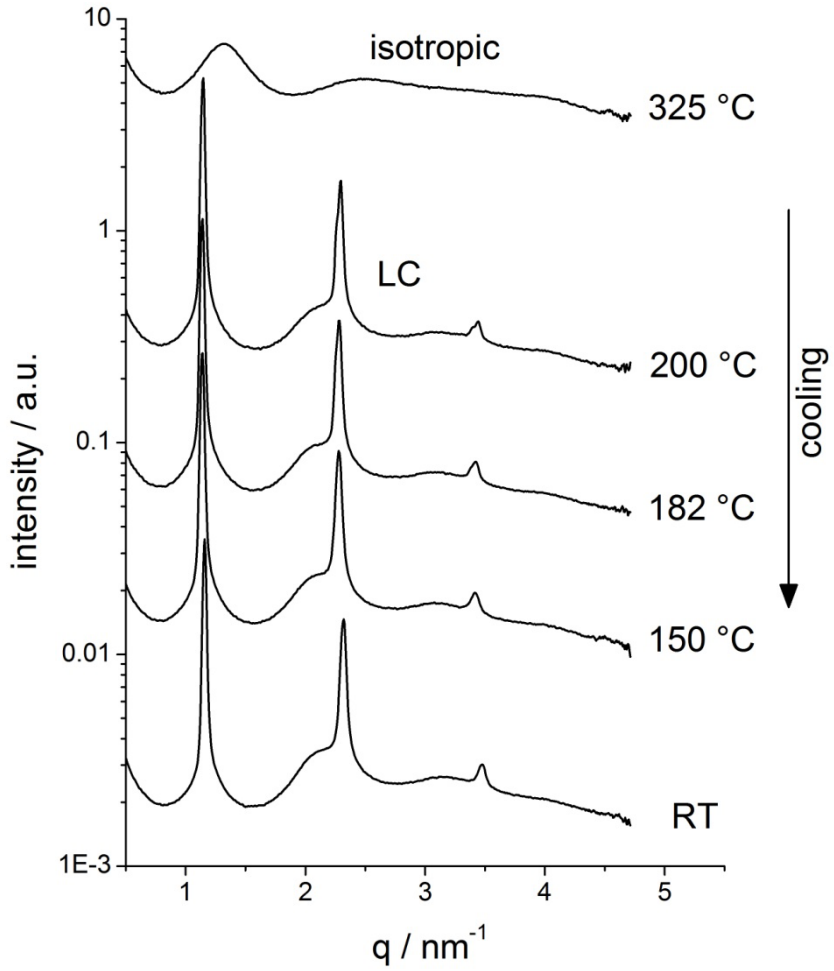

Figure 17: *Temperature dependent SAXS data of* ***PPBI 1*** *upon cooling from 325 °C.*

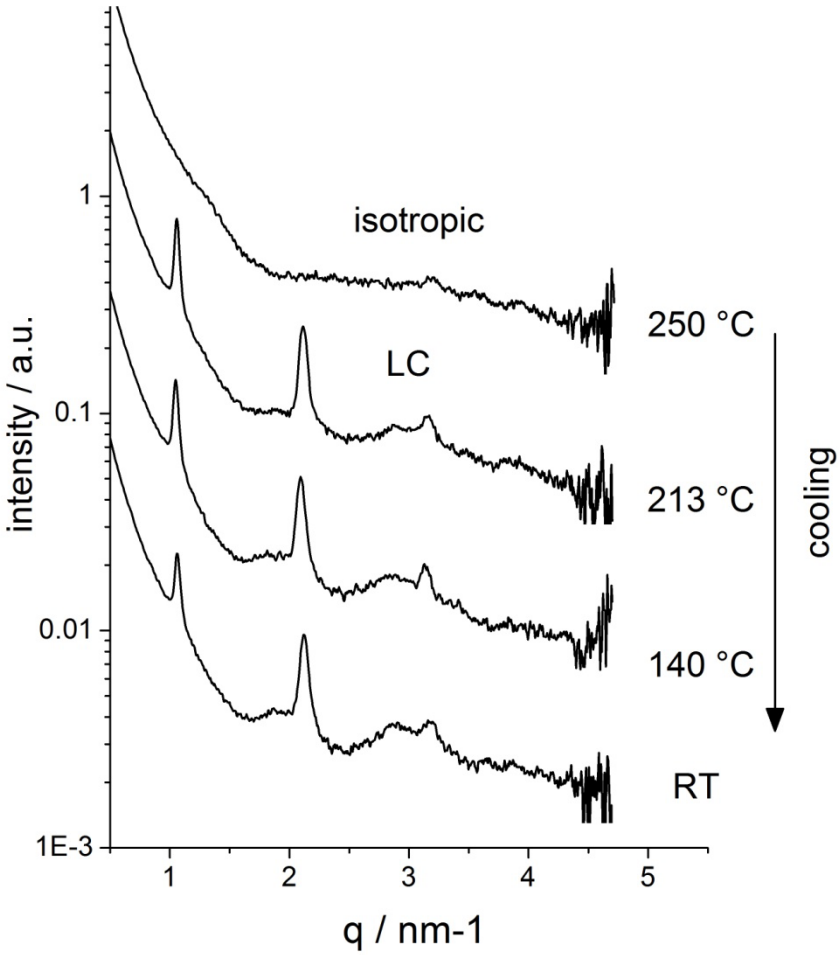

Figure 18: *Temperature dependent SAXS data of* ***PPBI 2*** *upon cooling from 250 °C.*

Bibliography

1. Binder, W. H.; Sachsenhofer, R. *Macromolecular Rapid Communications* **2008,** 29, (12-13), 952-981.

2. Gao, H.; Matyjaszewski, K. *Journal of the American Chemical Society* **2007,** 129, (20), 6633-6639.

3. Ladmiral, V.; Mantovani, G.; Clarkson, G. J.; Cauet, S.; Irwin, J. L.; Haddleton, D. M. *Journal of the American Chemical Society* **2006,** 128, (14), 4823-4830.

4. Quémener, D.; Hellaye, M. L.; Bissett, C.; Davis, T. P.; Barner-Kowollik, C.; Stenzel, M. H. *Journal of Polymer Science Part A: Polymer Chemistry* **2008,** 46, (1), 155-173.

5. Zhang, X.; Lian, X.; Liu, L.; Zhang, J.; Zhao, H. *Macromolecules* **2008,** 41, (21), 7863-7869.

6. Lang, A. S.; Neubig, A.; Sommer, M.; Thelakkat, M. *Macromolecules* **2010,** 43, (17), 7001-7010.

7. Malkoch, M.; Thibault, R. J.; Drockenmuller, E.; Messerschmidt, M.; Voit, B.; Russell, T. P.; Hawker, C. J. *Journal of the American Chemical Society* **2005,** 127, (42), 14942-14949.
8. Fleischmann, S.; Komber, H.; Voit, B. *Macromolecules* **2008,** 41, (14), 5255-5264.
9. Li, Z.; Zhang, Y.; Zhu, L.; Shen, T.; Zhang, H. *Polymer Chemistry* 1, (9), 1501-1511.
10. Würthner, F. *Chemical Communications* **2004**, (14), 1564-1579.
11. Langhals, H. *Helvetica Chimica Acta* **2005,** 88, (6), 1309-1343.
12. Horowitz, G.; Kouki, F.; Spearman, P.; Fichou, D.; Nogues, C.; Pan, X.; Garnier, F. *Advanced Materials* **1996,** 8, (3), 242-245.
13. Lindner, S. M.; Hüttner, S.; Chiche, A.; Thelakkat, M.; Krausch, G. *Angewandte Chemie International Edition* **2006,** 45, (20), 3364-3368.
14. Sommer, M.; Lindner, S. M.; Thelakkat, M. *Advanced Functional Materials* **2007,** 17, (9), 1493-1500.
15. Sharma, G. D.; Balraju, P.; Mikroyannidis, J. A.; Stylianakis, M. M. *Solar Energy Materials and Solar Cells* **2009,** 93, (11), 2025-2028.
16. Hüttner, S.; Sommer, M.; Thelakkat, M. *Applied Physics Letters* **2008,** 92, (9), 093302.
17. Lindner, S. M.; Thelakkat, M. *Macromolecules* **2004,** 37, (24), 8832-8835.
18. Zhang, Q.; Cirpan, A.; Russell, T. P.; Emrick, T. *Macromolecules* **2009,** 42, (4), 1079-1082.
19. Rajaram, S.; Armstrong, P. B.; Kim, B. J.; Fréchet, J. M. J. *Chemistry of Materials* **2009,** 21, (9), 1775-1777.
20. Tao, Y.; McCulloch, B.; Kim, S.; Segalman, R. A. *Soft Matter* **2009,** 5, (21), 4219-4230.
21. Sommer, M.; Lang, A. S.; Thelakkat, M. *Angewandte Chemie International Edition* **2008,** 47, (41), 7901-7904.
22. Fleischmann, S.; Komber, H.; Appelhans, D.; Voit, B. I. *Macromolecular Chemistry and Physics* **2007,** 208, (10), 1050-1060.
23. Fleischmann, S.; Kiriy, A.; Bocharova, V.; Tock, C.; Komber, H.; Voit, B. *Macromolecular Rapid Communications* **2009,** 30, (17), 1457-1462.
24. Liu, J.; Loewe, R. S.; McCullough, R. D. *Macromolecules* **1999,** 32, (18), 5777-5785.
25. Han, J. J.; Shaller, A. D.; Wang, W.; Li, A. D. Q. *Journal of the American Chemical Society* **2008,** 130, (22), 6974-6982.
26. Craig, A. A.; Imrie, C. T. *Macromolecules* **1999,** 32, (19), 6215-6220.
27. Wicklein, A.; Lang, A.; Muth, M.; Thelakkat, M. *Journal of the American Chemical Society* **2009,** 131, (40), 14442-14453.
28. Benoit, D.; Chaplinski, V.; Braslau, R.; Hawker, C. J. *Journal of the American Chemical Society* **1999,** 121, (16), 3904-3920.

29. Kaul, E.; Senkovskyy, V.; Tkachov, R.; Bocharova, V.; Komber, H.; Stamm, M.; Kiriy, A. *Macromolecules* **2009,** 43, (1), 77-81.

30. Jagadish, B.; Sankaranarayanan, R.; Xu, L.; Richards, R.; Vagner, J.; Hruby, V. J.; Gillies, R. J.; Mash, E. A. *Bioorganic & Medicinal Chemistry Letters* **2007,** 17, (12), 3310-3313.

31. O'Neil, E. J.; DiVittorio, K. M.; Smith, B. D. *Organic Letters* **2006,** 9, (2), 199-202.

Chapter 7

Highly Efficient Electron-Transport Side-Chain Perylene Polymers

*Andreas S. Lang, Mathis-Andreas Muth, and Mukundan Thelakkat**

[1]Applied Functional Polymers, Department of Macromolecular Chemistry I, University of Bayreuth, Universitätsstr. 30, 95440 Bayreuth, Germany

Prepared for submission

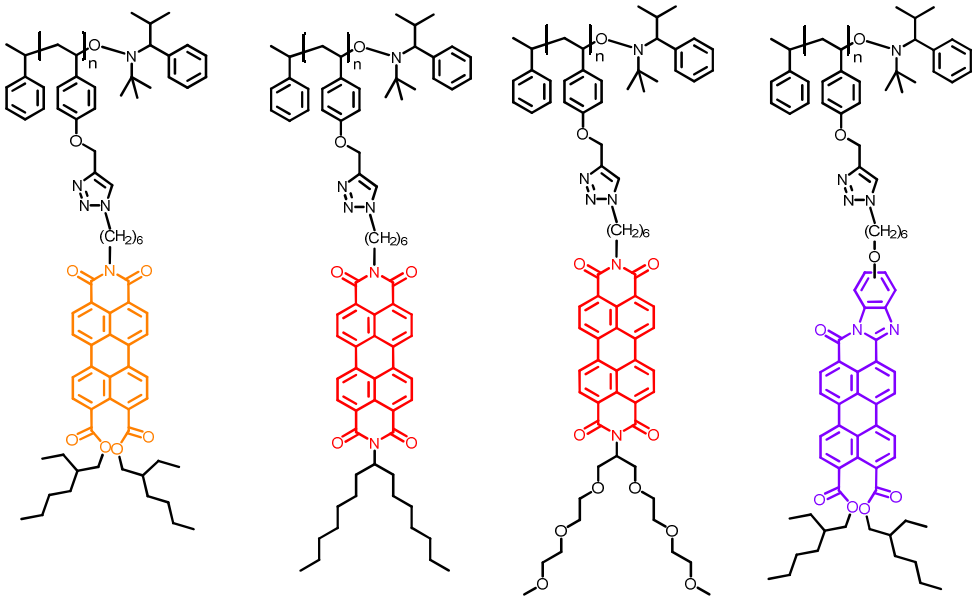

PPDI PPBI 1 PPBI 2 PPDB

Abstract

Four different semiconductor polymers, all synthesized by a combination of "click" chemistry and nitroxide mediated radical polymerization (NMRP), are compared. For the synthesis the same scaffold polymer, poly(propargyl oxystyrene) is "clicked" with different perylene chromophores. We compare here two poly(perylene bisimide)s, **PPBI 1** and **PPBI 2** with newly synthesized poly(perylene diester benzimidazole), **PPDB** and poly(perylene diester imide), **PPDI**. The new polymers exhibit narrow molecular weight distributions of 1.09 and molecular weights around $M_{n,SEC}$ = 15 000 g/mol and 26 000 g/mol in SEC. The extended π-conjugation system of **PPDB** leads to a considerably broader absorption in the visible region, compared to **PPDI and PPBIs**. Optical properties were investigated by UV/vis, thermal behavior was studied by differential scanning calorimetry (DSC) and X-ray diffraction measurements (XRD). Both new polymers exhibit a liquid crystalline (LC) mesophase over a broad temperature range. The charge carrier mobility of the different perylene containing polymers was studied in single carrier devices by fitting the space charge limited current (SCLC) according to Mott-Gurney equation. Electron mobilities as high as 5.5×10^{-3} $cm^2V^{-1}s^{-1}$ were measured.

Introduction

Solution processable organic materials for semiconductor applications such as organic light emitting diodes, organic field effect transistors[1] and organic photovoltaic devices is a field of intensive research. However, most studied semiconductor materials are good hole transporting materials (p-type), while the number of suitable electron transporting materials (n-type)[2] is still very limited. In this context perylene bisimides (**PBI**) and related molecules such as perylene diester benzimidazole (**PDB**) and perylene diester imide (**PDI**) with their favorable absorption properties in the visible wavelength regime are a promising class of dyes. Besides **PBI**,[3] **PDI** and **PDB** have already been incorporated in side chain polymers.[4] While **PDB** shows an enhanced absorption up to 700 nm,[5, 6] **PDI** shows an absorption which is red shifted compared to **PBI**. Although polymers carrying diverse perylene chromophores as pendant group can be synthesized by direct nitroxide mediated radical polymerization from their acrylate monomers,[3, 7, 8] these polymerizations have some drawbacks. They have to be conducted in highly concentrated solutions, at high temperatures, are difficult to control and usually show broad PDIs, even under controlled radical conditions. We found out, that this is due to transfer reactions occurring in the polymerization, as observed in the polymerization of **PBI** acrylates.[9] The polymer analogous functionalization of alkyne bearing polymers by "click" chemistry allows the easy and fast synthesis of quite complex polymer architectures.[10, 11] We have already shown that differently substituted poly(perylene bisimide)s can be synthesized by such methods.[9, 12] In the first part of this publication we describe the synthesis of two novel poly perylene derivatives by applying the "click" chemistry concept on **PPDB** and **PPDI**. The narrowly distributed polymers were studied according to their thermotropic behavior and molecular structure by DSC and X-ray diffraction measurements (XRD). In a second part, we compare the charge carrier mobility of the new

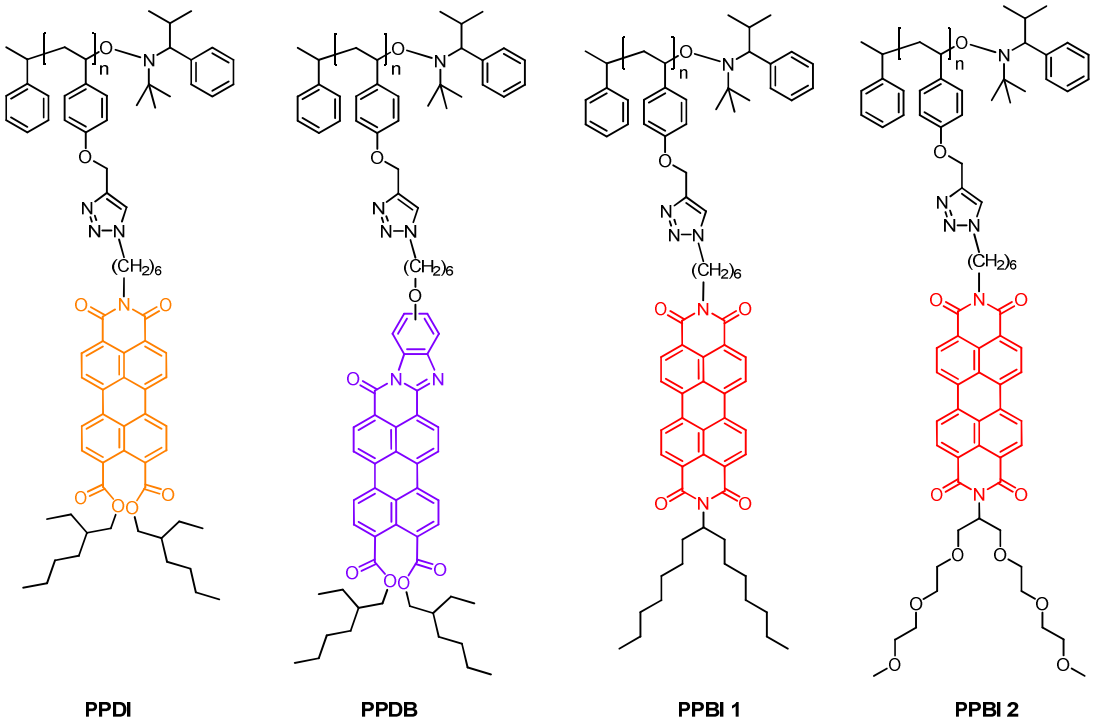

Figure 1: *Chemical structures of poly(perylene diester benzimidazole)* ***PPDB****, poly(perylene diester imide)* ***PPDI*** *and of poly(perylene bisimide) with alkyl swallow-tail,* ***PPBI 1*** *and with OEG swallow-tail,* ***PPBI 2****.*

polymers with those of two poly perylene bisimides, one with an alkyl swallow-tail and one with an oligoethylene glycol swallow-tail, by the space charge limited current (SCLC) method. The synthesis of **PPBI1** and **PPBI 2** is already reported.[12] The chemical structure of all "clicked" semiconductor polymers is shown in Figure 1.

Results and discussion

Synthesis

For the synthesis of the poly(perylene diester benzimidazole), **PPDB** and poly(perylene diester imide), **PPDI**, poly(propargyl oxystyrene) with $M_{n,SEC}$ = 7 400 g/mol and a PDI of 1.11 was synthesized as scaffold polymer carrying alkyne groups. Poly(propargyl oxystyrene) was chosen as an alkyne carrying scaffold polymer because it is easy to synthesize and polymers with narrow PDIs are accessible.[13-15] The synthesis of the azide carrying perylene derivatives **PDB-N_3** and **PDI-N_3** is shown in Scheme 1. The azides were obtained by the reaction of 1-bromo-6-azido-hexane with perylene diester benzimidazole alcohol or perylene diester imide, respectively. The "click" reaction of the azides (1.2 eq) with poly(propargyl oxystyrene) was conducted in anisole at RT, using PMDETA/CuBr as catalyst, which was added to the reaction from a stock solution (Figure 2). The approach of using a stock solution, which can be stored under inert gas atmosphere for long time, is more exact and convenient than adding ligand and copper species separately. After the "click"-reaction, the polymers were cleaned by removing the excess of perylene azides by soxhlet extraction with methyl ethyl ketone or acetone (see experimental

***Scheme 1**: Synthetic scheme for azide functionalized perylene diester benzimidazole **PDB-N$_3$** and perylene diester imide **PDI-N$_3$**.*

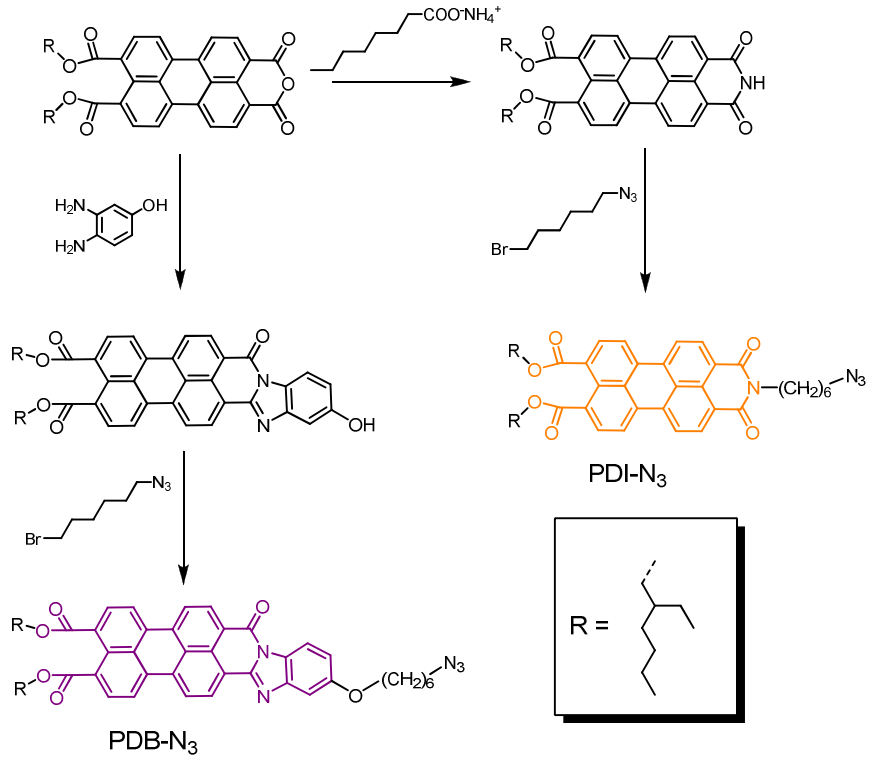

***Table 1**: Molecular weight, PDI (both determined by SEC) and theoretical molecular weight of the „clicked" polymers assuming 100% conversion.*

polymer	M_n [g/mol] (SEC)[a]	M_w/M_n (SEC)[a]	M_n [g/mol] (theor.)[b]	T_{onset} [°C][c]	T_g [°C][d]	T_m [°C][d]	ΔH [J/g][d]	notes
P(PropOSty)	7400	1.11		386	59	n.o.		P(Propargyl oxystyrene)
PPDB	26000	1.09	44000			285	8.9	P(Perylene diester benzimidazole)
PPDI	15000	1.09	40000		124	192	0.3	P(Perylene diester imide)
PPBI 1	59700	1.09	39000	330	182	298	1.8	Hydrophobic PPBI[12]
PPBI 2	59600	1.09	42000	330	142	n.o.		Hydrophilic PPBI[12]

[a] Measured with size exclusion chromatography in tetrahydrofuran and calibrated to polystyrene standards; [b]Theoretical molecular weight calculated from 100% converted 44 repeating units of **5**; [c]Measured by thermogravimetric analysis under N_2 atmosphere; [d]Measured by differential scanning calorimetry under N_2 atmosphere.

part). The "clicked" polymers exhibit monomodal distribution and very similar PDIs (1.09) as the scaffold polymer poly(propargyl oxystyrene). Figure 3 shows the size exclusion chromatography (SEC) traces of **PPDIE** and **PPDB** in comparison to poly(propargyl oxystyrene). The detailed SEC data of all polymers are presented in Table 1. Since the protected polymer **4** resembles the PS-standard used for SEC calibration, we could calculate the number of repeating units in **4** and **5** as 44. Thus, theoretical molecular weights of all PPBIs for 100% conversion in "click" reaction were calculated from this value (Table 1). It is evident that the molecular weights of **PPDB** and **PPDI** determined by SEC are underestimated compared to the theoretical molecular weights, whereas

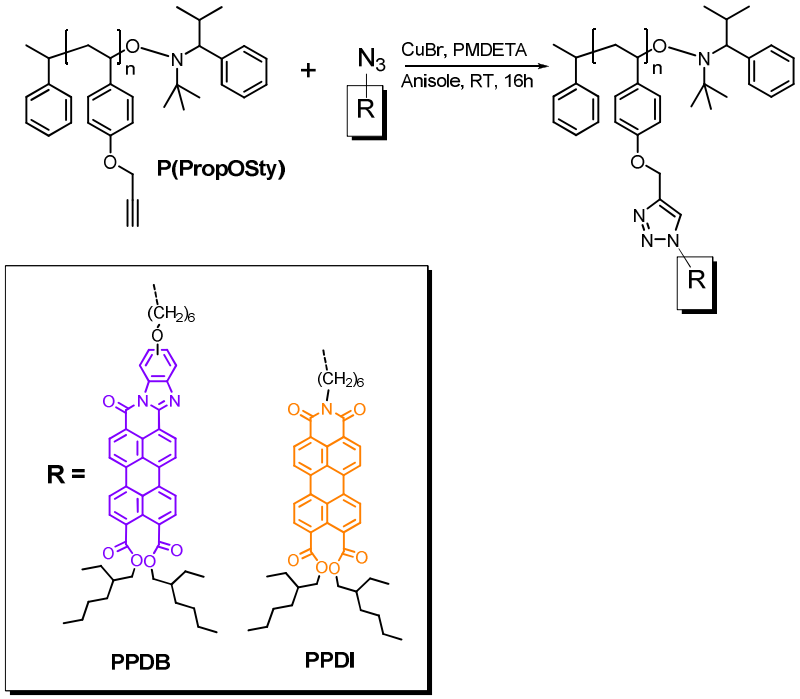

Figure 2: *Synthetic scheme of the „click" reaction of poly(propargyl oxystyrene) and perylene azides.*

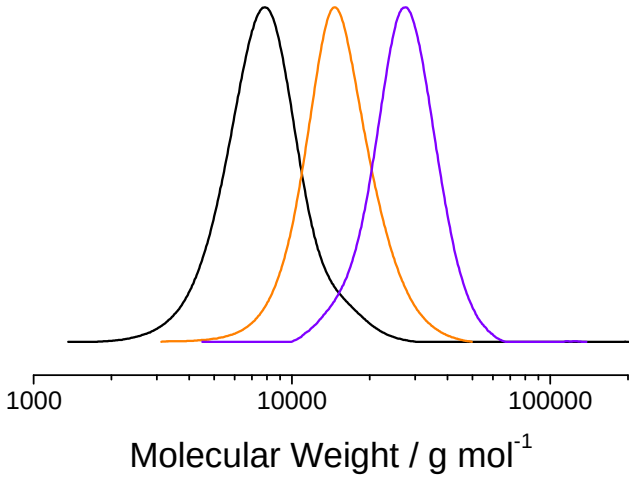

Figure 3: *SEC traces of a) poly(propargyl oxystyrene) (black line), poly(perylene diester imide)* ***PPDI*** *(orange line) and poly(perylene diester benzimidazole)* ***PPDB*** *(purple line). The curves of the "clicked" polymers are clearly shifted to higher molecular weights compared to the scaffold polymer. It is evident that the shape and molecular weight distribution of the "clicked" polymers is preserved.*

PPBI 1 and **PPBI 2** show higher values in SEC. This can be attributed by the ester groups in **PPDB** and **PPDI**, which seem to interact with the SEC column differently compared to the **PPBI** polymers. **PPDIE** and **PPDB** were analyzed by ^{1}H NMR to estimate the conversion in "click" reaction. After the "click" reaction, the signals of the prominent alkyne proton at 2.5 ppm, as well as that of the OCH_2 group at 4.6 ppm of poly(propargyl oxystyrene) disappear. In **PPDI** and **PPDB** the OCH_2 signals are shifted to 5.24 and 5.15 ppm, respectively. The signal of the newly formed

triazole proton, usually occurring around 7.6 ppm, cannot be seen in the spectra because it is superimposed by the broad signals of the aromatic protons of perylene, but can be determined by integration between 8.4 and 7.4 ppm. The CH_2N_3 protons of the perylene azides around 3.3 ppm cannot be observed any more in the "clicked" polymers, proving the absence of unreacted **PDI-N_3** and **PDB-N_3**. The corresponding protons in the "clicked" polymers are now located adjacent to the newly-built triazole unit and occur around 4.45 ppm. The fact that a) no acetylene protons are present and b) all OCH_2(CC) protons are converted to OCH_2(triazole) indicates a quantitative conversion within the margins of the experimental error in ^{1}H NMR.

The direct synthesis of acrylate monomers, carrying similar perylene chromophores were studied and reported earlier.[4] In the direct synthesis we could not achieve as high molecular weights compared to those obtained here with the "click" chemistry route and only high PDIs over 1.4.

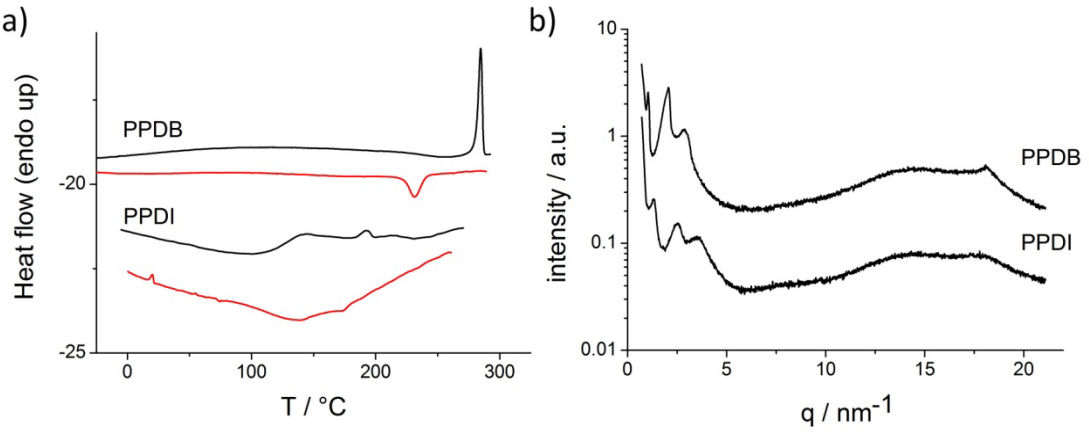

Figure 4: *a) First heating and cooling curve from DSC measurements of poly(perylene diester benzimidazole)* ***PPDB*** *and poly(perylene diester imide)* ***PPDI*** *(top to bottom).* ***PPDB*** *exhibits a clear melting peak at 285 °C while* ***PPDI*** *shows a T_g at 124 °C and a very weak melting peak at 192 °C; b) : X-Ray diffractions of* ***PPDI*** *and* ***PPDB*** *at RT.*

Thermotropic properties

The DSC thermograms and XRD patterns of **PPDB** and **PPDI** are shown in Figure 4a) and b), respectively. **PPDB** exhibits a clear melting peak with ΔH = 8.87 J/g at 285 °C into isotropic phase. There has been no observation of a T_g in this polymer. The XRD pattern of **PPDB** shows three clear reflections in the low q regime at 1.05 nm^{-1}, 2.05 nm^{-1} and 2.84 nm^{-1}. No reflections at higher q values can be observed except the π-π stacking distance of the perylene core at 18.13 nm^{-1} what resembles 3.5 Å. This shows that the observed phase in **PPDB** is a liquid crystalline ordering.

PPDI shows a T_g at 124 °C and a very weak melting peak at 192 °C with a small melting enthalpy of ΔH = 0.32 J/g. The XRD pattern of **PPDI** shows three reflections in the low q regime at 1.31 nm^{-1}, 2.48 nm^{-1} and 3.51 nm^{-1}. No reflections at higher q values can be observed except the π-π stacking distance of the perylene core at 17.93 nm^{-1} (≈ 3.5 Å) which is much weaker

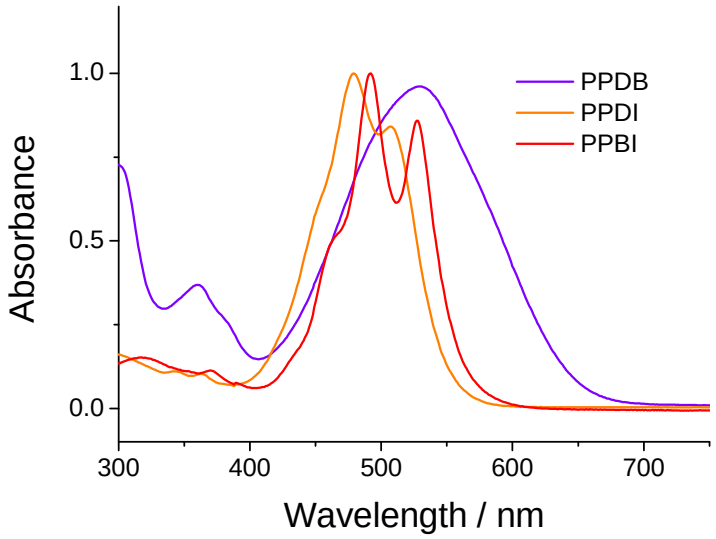

Figure 5: *Absorption spectrum of poly(perylene diester benzimidazole) PPDB (purple line), poly(perylene diester imide) PPDI (orange line) and poly(perylene bisimide) PPBI (red line) in $CHCl_3$ (c = 10^{-5} mol·L^{-1}) solution. PPDB shows a broad absorption up to 700 nm with a maximum at 528 nm. PPDI exhibits a fine vibronic structure in absorption which is blue-shifted compared to the absorption of PPBI.*

compared to **PPDB**. This all shows that the observed phase in **PPDI** is a liquid crystalline ordering which is "frozen in" below the T_g at 124 °C. Compared to directly synthesized acrylate polymers carrying similar chromophores, the here presented polymers show a different thermotropic behavior. The directly polymerized **PPDB** shows a T_m at 312°C, while the directly polymerized **PPDI** shows a T_m at 132 °C. While the "clicked" **PPDB** shows a T_m only slightly different from the one of the directly polymerized **PPDB**, the PPDI derivatives show a difference of 60 °C. It is not clear why this huge difference occurs.

The optical properties of the novel perylene polymers were investigated by UV/Vis in $CHCl_3$ solution (c = 10^{-5} mol·L^{-1}). **PPDI** shows a fine vibronic structure in absorption similar to the one of poly perylene bisimides (both **PPBI 1** and **2** show similar spectra) (also shown in Figure 5) with absorption maxima at 507 nm, 478 nm and 453 nm. The spectrum is blue shifted compared to **PPBI** due to the smaller aromatic system. **PPDB** shows no fine structure but a featureless broad absorption up to 700 nm and with a maximum at 528 nm. This can be attributed to the expanded π-system. The enhanced absorption property of **PPDB** could be very beneficial for the application in photovoltaic cells due to the broader light harvesting.

Charge Carrier Mobility

As shown above, absorption of perylene containing polymers can be varied by changing the delocalization and π-electron extension in chromophores. While a broad absorption is beneficial in photovoltaic application, this is not the only parameter which a compound has to fulfill. Besides absorption, the charge carrier mobility plays a major role in the success of a compound.

In this chapter we describe the charge carrier mobility of the four polymers. Since all compounds under investigation exhibit the same polymer scaffold, their chain length and polydispersities are identical. This allows for studying the effect of the chemical structure of the perylene groups on charge carrier mobility, independent from the molecular weight of the polymers.

For this reason we compare the electron mobility of **PPDB** and **PPDI** and two poly perylene bisimides **PPBI 1** and **PPBI 2**. **PPBI 1** is substituted with an alkyl swallow-tail and exhibits a liquid crystalline SmC phase between 298 °C and RT (T_g at 182 °C) whereas **PPBI 2** is substituted with an oligoethylene glycol swallow-tail and does not exhibit any crystallinity or liquid crystallinity but only a T_g at 142 °C.

The bulk charge carrier mobilities of **PPDB**, **PPDI**, **PPBI 1** and **PPBI 2** were determined by recording current-voltage characteristics of each material in single carrier devices; both electron-only devices and hole-only devices. A scheme of both single carrier devices is shown in Figure 6. At high voltages, the current measured is space charge limited only, and the charge carrier mobility can be extracted by fitting the *J-V* curve according to Mott-Gurney equation.[16]

$$J = \frac{9}{8} \cdot \varepsilon_r \cdot \varepsilon_0 \cdot \mu_0 \cdot e^{0.89 \cdot \gamma \cdot \sqrt{E}} \cdot \frac{V^2}{L^3} \qquad \text{Equation 1}$$

where *J* is the current density, ε_r is the dielectric constant of the polymer (assumed to be 3 in our calculations[17]), ε_0 is the permittivity of free space, μ_0 is the zero-field charge carrier mobility, γ is the field activation parameter, *E* is the electric field, *L* is the thickness of the polymer layer and *V* is the voltage drop across the device. Inserting μ_0 and γ in Equation 2 gives the field dependent charge carrier mobility μ.

$$\mu = \mu_0 \cdot e^{\gamma \cdot \sqrt{E}} \qquad \text{Equation 2}$$

Devices with different layer thicknesses *L* were prepared according to a procedure described recently.[4] All samples were thermally annealed above the material's glass transition temperatures (T_g) and allowed to cool to room temperature before measurement because higher values were obtained after this treatment for all samples. The current density-voltage characteristics of electron-only devices and hole-only devices and the corresponding Mott-Gurney fits of **PPDB**, **PPDI**, **PPBI 1** and **PPBI 2** are shown in Figure 7. The values for μ_0 and γ obtained from the best fits and the resulting electron mobilities μ at the maximum electric field are summarized in Table 2.

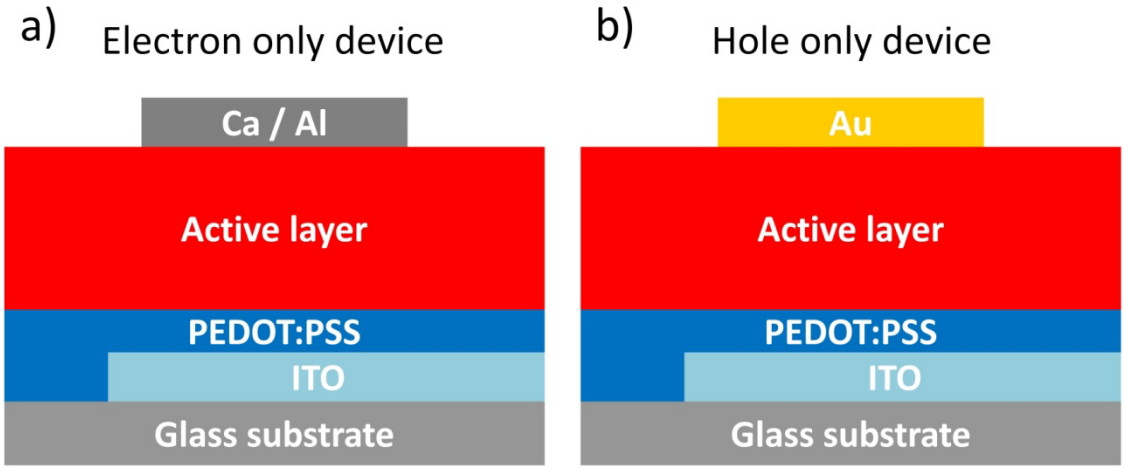

Figure 6: *a) Scheme of an electron-only device with a calcium top electrode, capped with aluminum; b) scheme of a hole-only device with gold top electrode.*

Table 2: *SCLC electron mobilities and associated field activation parameters for* ***PPDI***, ***PPDB***, ***PPBI 1*** *and* ***PPBI 2*** *from electron-only devices.*

	$\mu_{0,e}$ [$cm^2V^{-1}s^{-1}$]	γ [$cm^{0.5}V^{-0.5}$]	μ_e [$cm^2V^{-1}s^{-1}$]
PPDI	2.2×10^{-10}	2.9×10^{-3}	2.0×10^{-6}
PPDB	1.3×10^{-7}	2.0×10^{-3}	1.0×10^{-4}
PPBI 1	4.7×10^{-4}	1.3×10^{-4}	6.9×10^{-4}
PPBI 2	2.7×10^{-3}	2.2×10^{-4}	5.5×10^{-3}

As can be seen from Table 2, **PPDI** has an electron mobility of 2.0×10^{-6} $cm^2V^{-1}s^{-1}$ which is almost two orders of magnitude below the electron mobility of **PPDB** (1.0×10^{-4} $cm^2V^{-1}s^{-1}$). This is in agreement with previous observations of charge carrier mobilities of a perylene diester imide and perylene diester benzimidazole acrylate polymers.[4] Here, the less electron deficient perylene diester imide groups of **PPDI** possesses worse electron mobility compared to **PPDB** with benzimidazole functionalized perylene cores.

PPBI 1 however shows a significantly higher electron mobility of 6.9×10^{-4} $cm^2V^{-1}s^{-1}$ compared to **PPDB**. Although optical properties were improved through the implementation of a benzimidazole unit to the perylene core, the charge transport of **PPDB** suffers compared to the perylene bisimide derivative **PPBI 1**.

A comparison between **PPBI 1** and **PPBI 2** shows that not only the structure of the π-conjugation system hast an impact on the material's semiconductor properties. Altering the solubilizing side chains at the imide position of the perylene from a branched alkyl (**PPBI 1**) to a branched oligoethylene glycol (**PPBI 2**) leads to a major increase of almost one order of magnitude in electron mobility from 6.9×10^{-4} $cm^2V^{-1}s^{-1}$ to 5.5×10^{-3} $cm^2V^{-1}s^{-1}$. The coupling of the perylene bisimide unit and the imide substituents are negligible because of the nodes in the

HOMO and LUMO at the imide nitrogen.[18] Thus, the improved charge transport properties of the amorphous **PPBI 2** can be rather explained by a potentially more favorable packing of the PBIs compared to films of the liquid crystalline **PPBI 1**.

The dependency of the charge carrier mobility on the electric field is indicated by the field activation parameter γ. Both **PPDI** and **PPDB** exhibit higher γ values of 2.9×10^{-3} $cm^{0.5}V^{-0.5}$ and 2.0×10^{-3} $cm^{0.5}V^{-0.5}$ respectively, compared to **PPBI 1** (1.3×10^{-4} $cm^{0.5}V^{-0.5}$) and **PPBI 2** (2.2×10^{-4} $cm^{0.5}V^{-0.5}$). Hence the electron transport for **PPDI** and **PPDB** is more dependent on the electric field applied in a device. For applications like organic photovoltaic cells, good charge transport at comparatively low electric fields are required, which makes **PPBI 1** and **PPBI 2** potentially more favorable as n-type material.

The resultant values for μ_0, γ and μ of **PPDB**, **PPDI**, **PPBI 1** and **PPBI 2,** taken from the Mott-Gurney fits, are summarized in Table 3. For **PPDI** μ_0 and μ are 8.8×10^{-7} $cm^2V^{-1}s^{-1}$ and 3.0×10^{-6} $cm^2V^{-1}s^{-1}$ respectively and thus the hole mobility of **PPDI** is slightly higher than its electron mobility. Hence, a perylene core modified by a diester and an imide unit leads to a more pronounced p-type behavior.

For compounds **PPDI**, **PPBI 1** and **PPBI 2** the hole mobilities are 1-2 orders of magnitude below their electron mobilities. This demonstrates that electron transport through the LUMO is preferred to hole transport via the HOMO, as expected for n-type semiconductors.

Table 3: *SCLC hole mobilities and associated field activation parameters for **PPDI, PPDB, PPBI 1** and **PPBI 2** from hole-only devices.*

	$\mu_{0,h}$ [$cm^2V^{-1}s^{-1}$]	γ [$cm^{0.5}V^{-0.5}$]	μ_h [$cm^2V^{-1}s^{-1}$]
PPDI	8.8×10^{-7}	3.6×10^{-4}	3.0×10^{-6}
PPDB	1.1×10^{-6}	3.8×10^{-4}	3.7×10^{-6}
PPBI 1	4.8×10^{-6}	3.3×10^{-4}	2.7×10^{-5}
PPBI 2	4.5×10^{-5}	-4.1×10^{-5}	3.9×10^{-5}

Conclusion

We showed the elegant and feasible synthesis of diverse poly perylene derivatives through a "click" chemistry approach. The resulting poly(perylene diester benzimidazole) **PPDB** and poly(perylene diester imide) **PPDI** showed high molecular weights and narrow PDIs around 1.09. Very high conversion in the "click" reaction could be proven by ^{1}H NMR. Improved optical absorption up to 700 nm for **PPDB** was found while PPDI showed a blue shifted absorption compared to **PPBI**. The measurement of charge transport by the SCLC method resulted good electron mobilities for **PPDB** (1.0×10^{-4} $cm^2V^{-1}s^{-1}$) and the two PPBI derivatives **PPBI 1** and **PPBI 2**. Especially **PPBI 2**, which is an amorphous polymer, shows a very high electron mobility of 5.5×10^{-3} $cm^2V^{-1}s^{-1}$ which is almost one order of magnitude higher than the electron mobility for **PPBI 1** of 6.9×10^{-4} $cm^2V^{-1}s^{-1}$. PPDI results only a low electron mobility of 2.0×10^{-6} $cm^2V^{-1}s^{-1}$ but a slightly better hole mobility of 3.0×10^{-6} $cm^2V^{-1}s^{-1}$. This shows, that the nature of solubilizing side groups can influence the charge carrier mobility of perylene derivatives strongly. The orientation

and packing behavior of the material in thin films has to be verified by GISAXS and GIWAXS measurements which is the subject of current investigation.

Experimental section

General

The perylene diester benzimidazole and the perylene diester anhydride were synthesized according to a literature procedure.[4] 6-azido-1-hexanol was synthesized according to a reference.[12] Dimethylformamide (99.8%) were purchased from Sigma-Aldrich. PMDETA (≥98%) was purchased from Fluka. CuBr (98%) was bought from Acros. All reagents were used without further purification unless otherwise noted.

^{1}H NMR (300 MHz) spectra were recorded on a Brucker AC 300 spectrometer in $CDCl_3$ and calibrated to $CHCl_3$ signal (7.26 ppm for ^{1}H). UV-vis spectra of solutions in $CHCl_3$ with a concentration of 10^{-5} mol·L^{-1} were recorded on a Hitachi 3000 spectrophotometer and photoluminescence spectra were acquired on a Shimadzu RF 5301 PC spectrofluorophotometer upon excitation at 490 nm. SEC measurements were carried out in THF with 0.25% tetrabutylammoniumbromide with two Varian MIXED-C columns (300x7.5 mm) at room temperature and at a flow rate of 0.5 mL/min using UV (Waters model 486) with 254 nm detector wavelength and refractive index (Waters model 410) detectors. Polystyrene in combination with *o*-DCB as an internal standard was used for calibration. Differential scanning calorimetry experiments were conducted at heating rates of 10 K·min^{-1} or 40 K·min^{-1} under N_2 atmosphere with a Perkin Elmer Diamond DSC, calibrated with indium. The endothermic maximum was taken as T_m. X-ray diffraction experiments were performed on a Huber Guinier Diffractometer 6000 equipped with a Huber quartz monochromater 611 with Cu-$K_{\alpha1}$: 1.54051 Å.

Synthesis

Perylene diester NH-imide

Perylene diester anhydride (1800 mg, 2.84 mmol) and ammonium decanoate (1.73 g, 8.5 mmol) were added to molten imidazole (16 g) at 120 °C. The reaction was stirred for 1h. Subsequently, the reaction was cooled to 90 °C and 150 mL of H_2O were added to dissolve the imidazole. The perylene diester imide-H was filtered off and dried. The product was obtained as a orange solid and weighed 1.57 g (87%). ^{1}H NMR (300 MHz, $CHCl_3$): δ (ppm) 8.98 (s, 1H, N*H*), 8.37 (d, 2H, *J* = 7.3 Hz, Ar*H*), 8.15 (dd, 4H, *J* = 11.8 Hz, *J* = 8.5 Hz, Ar*H*), 7.95 (d, 2H, *J* = 7.4 Hz, Ar*H*), 4.38-4.24 (m, 4 H, COOCH_2), 1.94-1.18 (m, CH_2), 1.11-0.76 (m, 12H, CH_3).

Perylene diester imide azide

PDI-H (500 mg, 0.79 mmol), 1-bromo-6-azido hexane (230 mg, 1.10 mmol) and K_2CO_3 (196 mg, 1.42 mmol) were added in 8 mL of DMF. The reaction was heated to 100 °C for 2d, precipitated in MeOH/H_2O and purified by column chromatography over silica with cyclohexane : ethyl acetate / 2:1. The product was obtained as a orange waxy solid and weighed 340 mg (56 %). ^{1}H NMR (300

MHz, $CHCl_3$): δ (ppm) 8.20 (d, 2H, *J* = 7.3 Hz, Ar*H*), 7.96 (d, 2H, *J* = 7.7 Hz, Ar*H*), 7.87 (dd, 4H, *J* = 11.8, *J* = 8.11 Hz, Ar*H*), 4.38-4.24 (m, 2H, N-C$H_{2,perylene}$), 4.17-4.07 (m, 4 H, COOCH_2), 3.30 (t, 2H, J = .7.0 Hz, m, 2H, N-C$H_{2,azide}$), 1.91-1.31 (m, CH_2), 1.07-0.90 (m, 12H, CH_3).

Perylene diester benzimidazole azide

PDB-OH (1000 mg, 1.38 mmol), 1-bromo-6-azido hexane (569 mg, 2.76 mmol) and K_2CO_3 (343 mg, 2.48 mmol) were dissolved in 35 mL of DMF. The reaction was heated to 85 °C for 2 d, precipitated in H_2O and filtered. The pure purple product weighed 1123 mg (96%).^{1}H NMR (300 MHz, $CHCl_3$): δ (ppm) 8.92-6.91 (m, 8H, Ar*H*), 4.31-4.20 (m, 4 H, COOCH_2), 4.19-404 (m, 2H, OCH_2) 3.38-3.28 (m, 2H, CH_2N_3), 1.98-127 (m, 26H, CH_2), 1.07-0.85 (m, 12H, CH_3).

General procedure for the preparation of "click" polymers

Poly(perylene diester benzimidazole)

PDB-N_3 (65 mg, 0.076 mmol) and poly(propargyl oxystyrene) (10 mg, 0.063 mmol) were dissolved in 4 mL of anisole. The mixture was degassed by purging with nitrogen fir 10 minutes. Subsequently, one drop of a degassed stock solution of anisole/PMDETA/CuBr was added. The reaction was stirred over night. The substance was precipitated out in MeOH, filtered and cleaned from residual azide by soxhlet extraction with methyl ethyl ketone. The pure product was obtained as a purple powder. ^{1}H NMR (300 MHz, $CHCl_3$): δ (ppm) 8.11-7.23 (br s, 9H, Ar$H_{perylene}$, Ar$H_{triazole}$), 6.96-6.26 (br s, 4H, Ar$H_{styrene}$), 5.15 (br s, 2H, O_{Sty}CH_2), 4.43 (br s, 2H, $N_{triazole}$CH_2), 4.27 (br s, 4H, 2COOCH_2), 4.00 (br s, 2H, $N_{perylene}$CH_2), 2.03-1.10 (m, 29H, 14CH_2, C$H_{backbone}$), 1.12-0.84 (m, 12H, CH_3).

Poly(perylene diester imide)

PDI-N_3 (58 mg, 0.076 mmol) and poly(propargyl oxystyrene) (10 mg, 0.063 mmol) were dissolved in 4 mL of anisole. The mixture was degassed by purging with nitrogen fir 10 minutes. Subsequently, one drop of a degassed stock solution of anisole/PMDETA/CuBr was added. The reaction was stirred over night. The substance was precipitated out in MeOH, filtered and cleaned from residual azide by soxhlet extraction with methyl ethyl ketone. The pure product was obtained as a orange powder. ^{1}H NMR (300 MHz, $CHCl_3$): δ (ppm) 8.16-6.31 (m, 12H, Ar$H_{perylene}$, Ar$H_{triazole}$, Ar$H_{benzimidazole}$), 5.24 (br s, 2H, $O_{styrene}$CH_2), 4.47 (br s, 2H, $N_{triazole}$CH_2), 4.13 (br s, 4H, COOCH_2), 3.70 (br s, 2H, $O_{benzimidazol}$CH_2), 2.20-1.10 (m, 29H, 14CH_2, C$H_{backbone}$), 1.10-0.78 (m, 12H, CH_3).

Supporting Figures

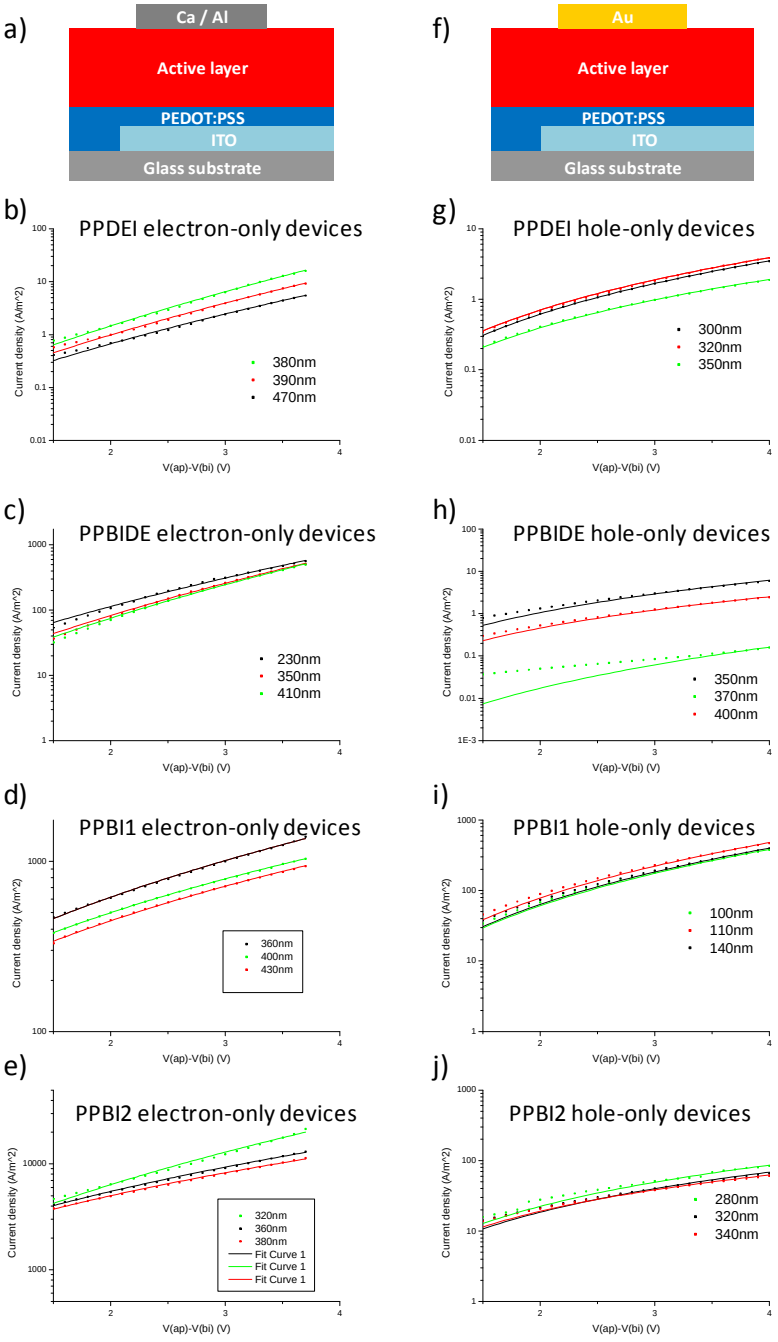

Figure 7: *Scheme of an electron-only device with a calcium top electrode, capped with aluminum (a); Current density J vs. voltage V plots (data points) and fits according to Equation 1 (straight lines) at room temperature for electron-only devices of* ***PPDI***, ***PPDB***, ***PPBI 1*** *and* ***PPBI 2*** *(b-e); Scheme of a hole-only device with gold top electrode (f); Current density J vs. voltage V plots (data points) and fits according to Equation 1 (straight lines) at room temperature for hole-only devices of* ***PPDI***, ***PPDB***, ***PPBI 1*** *and* ***PPBI 2*** *(g-j); The voltage applied (V_{ap}) was corrected for a built in potential (V_{bi}) of 2.2 eV for electron-only devices resulting from the differences in work function of calcium and ITO/PEDOT:PSS. V_{bi} in hole-only devices was estimated to be 0 eV.*

Acknowledgements

The financial support from German Research Council (DFG) under SPP 1355 and Merck, Southampton for this work is gratefully acknowledged.

Bibliography

1. Chua, L. L.; Zaumseil, J.; Chang, J. F.; Ou, E. C. W.; Ho, P. K. H.; Sirringhaus, H.; Friend, R. H. *Nature* **2005,** 434, 194.
2. Chen, Z.; Zheng, Y.; Yan, H.; Facchetti, A. *Journal of the American Chemical Society* **2008,** 131, (1), 8-9.
3. Lindner, S. M.; Thelakkat, M. *Macromolecules* **2004,** 37, (24), 8832-8835.
4. Muth, M.; Lang, A.; Carrasco, M.; Thelakkat, M. *submitted to Adv. Funct. Mater.* **2011**.
5. Wicklein, A.; Kohn, P.; Ghazaryan, L.; Thurn-Albrecht, T.; Thelakkat, M. *Chemical Communications* **2010,** 46, (13), 2328-2330.
6. Wicklein, A.; Muth, M.-A.; Thelakkat, M. *Journal of Materials Chemistry* **2010,** 20, (39), 8646-8652.
7. Lindner, S. M.; Hüttner, S.; Chiche, A.; Thelakkat, M.; Krausch, G. *Angewandte Chemie International Edition* **2006,** 45, (20), 3364-3368.
8. Sommer, M.; Lang, A. S.; Thelakkat, M. *Angewandte Chemie International Edition* **2008,** 47, (41), 7901-7904.
9. Lang, A. S.; Neubig, A.; Sommer, M.; Thelakkat, M. *Macromolecules* **2010,** 43, (17), 7001-7010.
10. Binder, W. H.; Sachsenhofer, R. *Macromolecular Rapid Communications* **2007,** 28, (1), 15-54.
11. Binder, W. H.; Sachsenhofer, R. *Macromolecular Rapid Communications* **2008,** 29, (12-13), 952-981.
12. Lang, A. S.; Thelakkat, M. *Polymer Chemistry* **2011**, 10.1039/C1PY00191D.
13. Fleischmann, S.; Komber, H.; Voit, B. *Macromolecules* **2008,** 41, (14), 5255-5264.
14. Fleischmann, S.; Komber, H.; Appelhans, D.; Voit, B. I. *Macromolecular Chemistry and Physics* **2007,** 208, (10), 1050-1060.
15. Fleischmann, S.; Kiriy, A.; Bocharova, V.; Tock, C.; Komber, H.; Voit, B. *Macromolecular Rapid Communications* **2009,** 30, (17), 1457-1462.
16. Blom, P. W. M.; Tanase, C.; Leeuw, D. M. d.; Coehoorn, R., *Thickness scaling of the space-charge-limited current in poly(p-phenylene vinylene)*. AIP: 2005; Vol. 86, p 092105.

17. Goh, C.; Kline, R. J.; McGehee, M. D.; Kadnikova, E. N.; Frechet, J. M. *J. Appl. Phys. Lett.* **2005,** 86, (null), 122110.

18. Würthner, F. *Chemical Communications* **2004**, (14), 1564-1579.

Chapter 8

Semiconductor Nanoparticles from Donor-Acceptor Dual Brush Block Copolymers

*Guo-Dong Fu,[1,2] Andreas S. Lang,[2] Zhicheng Zheng,[3] Fang Yao,[1] Weian Zhang,[3] Axel H.E. Müller[3] and Mukundan Thelakkat[2,]**

[1]School of Chemistry and Chemical Engineering, Southeast University, Nanjing, China 211189

[2]Applied Functional Polymers, Department of Macromolecular Chemistry I, University of Bayreuth, 95440-Bayreuth, Germany

[3]Macromolecular Chemistry II, University of Bayreuth, 95440-Bayreuth, Germany

Submitted to *Angewandte Chemie, International Edition* 2011

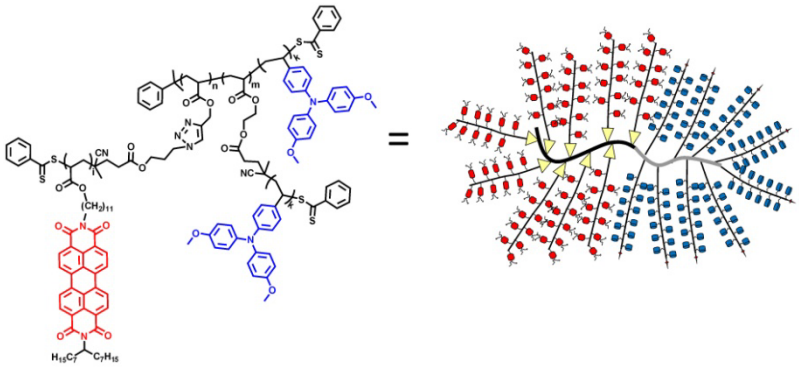

Introduction

Besides the capability of organic semiconductors to absorb light and transport charges, their performance in organic photovoltaics (OPV) is mainly dominated by the interfacial morphology arising from the phase separation of the donor/acceptor (D-A) components. This is because the dynamics of charge separation and recombination are governed by the D-A interface which in turn affects the photocurrent and the open circuit voltage.[1-3] Thus, thin films with controlled D-A morphology with domain sizes matching the exciton diffusion length (some 10s of nm) are desirable. For this reason, attempts have been made to control the D-A morphology in OPV materials by the self-assembly of D-A block copolymers.[4-6]

Another strategy to obtain ordered interfacial morphology utilizes dual brush block copolymers which can form distinct nano-objects.[7-10] For example, cylindrical polymer brushes,[11, 12] having dense side chains, show extended chain conformations and form one-dimensional nanostructures because the sterical repulsion of side chains enhances the stiffness of the backbone and hinders overlapping and entanglements with neighboring macromolecules. It is plausible that polymer brushes would present a globular structure when the length of the main chain is comparable to that of the side chains. Up to now, the chemistry for the preparation of such particles was limited to conventional monomers without any optical or electronic functions. However, there is an increasing demand for well-defined organic semiconductor systems carrying donor and acceptor domains capable of microphase separation. This is one of the ambitious tasks in the material design for organic photovoltaics (OPV). Such nano-objects with clear D-A domain separation in the range of some tens of nm would be ideal for the charge separation and transport, but their synthesis is highly challenging and was not yet accomplished.

Here, we report an elegant and feasible synthetic approach for the first time to prepare well-defined D-A nanoparticles with controlled composition and size of about 50-60 nm from a D-A dual brush block copolymer. The first TEM analysis indicates the formation of janus-type phase separated particles. This was realized by innovatively combining a “grafting from” polymerization of a donor monomer based on reversible addition fragmentation chain transfer polymerization (RAFT)[13], with a “grafting to” approach[14] of an acceptor polymer for which a copper-catalyzed azide-alkyne cycloaddition (CuAAC, click chemistry)[15] was utilized. The synthetic strategy and the detailed procedure are illustrated in Figure 1 and Figure 2 respectively. All SEC and FTIR data are shown in Figures 6 and 7.

Results and Discussion

First poly(trimethylsilyl propargyl acrylate) (PTMSPA) **1** with 29 repeating units was synthesized by RAFT polymerization (PDI = 1.09). The alkyne group was protected with a trimethylsilyl group to prevent it from participating in the polymerization and any possible crosslinking reactions. This macro-RAFT agent **1** was then used to prepare the block copolymer **2** ($PTMSPA_{29}$-*b*-$PHEA_{22}$) with a PDI of 1.16 by the subsequent polymerization of hydroxyethyl acrylate (HEA). This was followed by the esterification of the hydroxyl groups of PHEA with the chain-transfer-agent (CTA) 4-cyanopentanoic acid-4-dithiobenzoate to immobilize the RAFT-agent on the polymer backbone.

In comparison to **2** the resulting block copolymer **3** ($PTMSPA_{29}$-*b*-$(PHEA\text{-}CTA)_{22}$ does not exhibit the broad peak between 3400-3500 cm^{-1} in FTIR due to the complete conversion of the OH groups of **2** to CTA groups in **3**. Also the aromatic protons of the chain-transfer agent can be detected as signals between 7.2-8.2 ppm in ^1H NMR (see supporting information). Subsequent "grafting from" polymerization of the monomer *bis*(4-methoxyphenyl)-4'-vinylphenylamine) (= vinyldimethoxytriphenylamine, vDMTPA) from **3** using RAFT gave rise to the donor-brush block copolymer **4** ($PTMSPA_{29}$-*b*-$(PHEA$-*g*-$PvDMTPA_{17})_{22}$) with a PDI of 1.16. This was followed by the deprotection of the trimethylsilyl propargyl groups of **4** with tetrabutylammonium fluoride resulting in donor polymer **5** (PPA_{29}-*b*-$(PHEA$-*g*-$PvDMTPA_{17})_{22}$) carrying free alkyne groups. The successful deprotection was proven by the appearance of the peak at 3281 cm^{-1} in FTIR due to the C≡CH vibration and a complete disappearance of the signal at 0.20 ppm in ^1H NMR attributed to the trimethylsilyl group. Finally, the dual brush block copolymer **7** ($(PPA$-*g*-$PPerAcr_{18})_{29}$-*b*-$(PHEA$-*g*-$PvDMTPA_{17})_{22}$) was prepared by CuAAC of alkyne carrying polymer **5** and azide functionalized perylene bisimide polymer **6**.

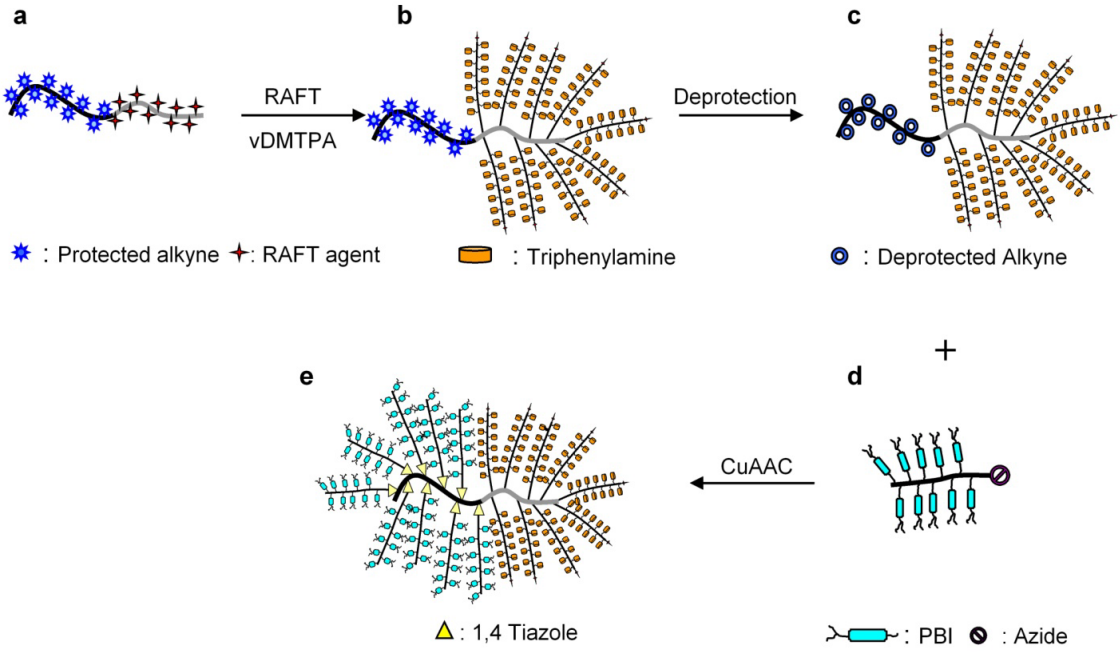

Figure 1: *Strategy for the synthesis of a D-A dual brush block copolymers (a-e). The synthesis is carried out via a combination of "grafting from" RAFT polymerization and "grafting to" by CuAAC reaction. a) PTMSPA-b-(PHEA-CTA)* ***3;*** *b) PTMSPA-b-(PEA-g-PvDMTPA)* ***4****; c) PPA-b-(PHEA-g-PvDMTPA)* ***5****; d) azide functionalized perylene bisimide polymer PPerAcr-*N_3 ***6****; e) dual brush block copolymer (PPA-g-PPerAcr)-b-(PHEA-g-PvDMTPA)* ***7****.*

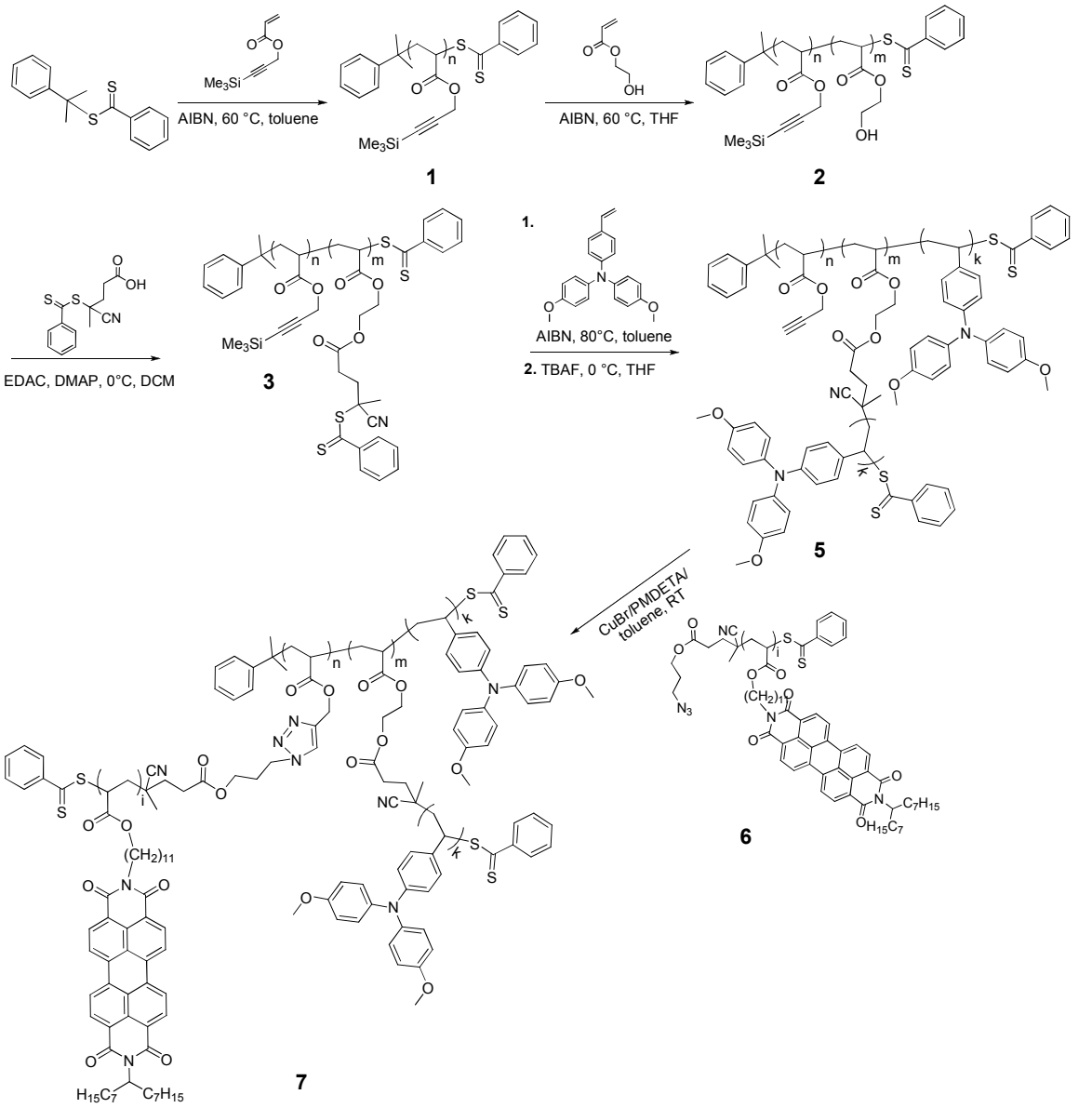

Figure 2: *Synthetic scheme of D-A dual brush block copolymer using RAFT and click chemistry.* ***1****: poly(trimethylsilyl propargyl acrylate) (PTMSPA);* ***2****: block copolymer* $PTMSPA_{29}$*-b-*$PHEA_{22}$*;* ***3****:* $PTMSPA_{29}$*-b-(PHEA-CTA)*$_{22}$*;* ***4****: mono brush block copolymer* $PTMSPA_{29}$*-b-(PEA-g-PvDMTPA*$_{17}$*)*$_{22}$*;* ***5****:* PPA_{29}*-b-(PHEA-g-PvDMTPA*$_{17}$*)*$_{22}$*;* ***6****: poly perylene acrylate* $(PPerAcr)_{18}$*;* ***7****: dual brush block copolymer* $(PPA\text{-}g\text{-}PPerAcr_{18})_{29}$*-b-(PHEA-g-PvDMTPA*$_{17}$*)*$_{22}$*.*

The perylene bisimide containing polymer **6** (poly perylene bisimide acrylate, PPerAcr-N_3) with 18 repeating units was synthesized by RAFT with a chain-transfer-agent carrying an azide-group. This terminal azide group enables the grafting of these polymer chains to the block copolymer **5** carrying alkyne groups to get an acceptor polymer brush. The molecular weight distribution of the PPerAcr-N_3 is narrow with a polydispersity index (PDI) around 1.2.

The efficiency of the "click" reaction was determined by the analysis and comparison of ^{1}H NMR signals of the polymers **2**, **4** and **7**. The conversion of the click reaction could be estimated

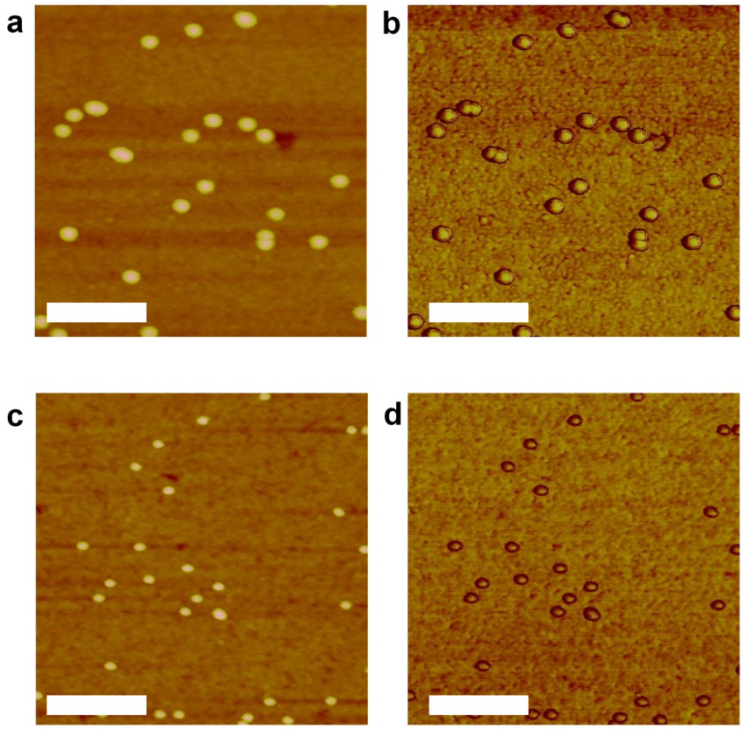

Figure 3: *AFM images from a toluene solution of **7** (0.01 g/L) drop-cast on a silicon wafer showing globular structures: a) Height image and b) phase image of dual brush block copolymer **7** ((PPA-g-PPerAcr$_{18}$)$_{29}$-b-(PHEA-g-PvDMTPA$_{17}$)$_{22}$) before thermal annealing. c) Height image and d) phase image of **7** after thermal annealing at 180 °C for 1 h. The scale bar in the images is 300 nm.*

to be around 60%. The size exclusion chromatography (SEC) analysis of **5** and **6** in *o*-DCB gave values of 47 000 g/mol and 13 600 g/mol respectively. But the final polymer **7** is so large that the molecular weight could not be detected using SEC even with *o*-DCB as eluent at elevated temperatures. Therefore, dynamic light scatting measurements (DLS) were carried out to compare the polymers **5** and **7** (Figure 8). DLS results indicate that **5** has a hydrodynamic radius of about 7 nm. After the click reaction with **6**, the radius of resulting dibrush **7** has dramatically increased to 29 nm.

Atomic force microscopy (AFM) was performed to visualize the nano particle morphology. Figure 3 a) and b) show height and phase images of **7** spin-coated from diluted toluene solution on a silicon wafer. Very uniform globular structures could be observed. The typical particle has a height of 12 nm and 53 nm in diameter. The particles were also studied after an annealing step at 180 °C for 2 h. Figure 3 c) and d) show the height and phase images of **7** after thermal treatment. The globular nanostructures are well preserved, while in comparison with the non-annealed sample, the diameter of particles decreases from 53.5±2.6 nm to 35.8±2.1 nm and the height decreases from 12 nm to 10.2 nm. The shrinkage of particles may be accounted by the crystallization of the PPerAcr brushes (T_m= 188 °C, T_{recr} = 162 °C) during the annealing, which results in a denser packing of this block.

The nanostructured particles of the D-A dual brush block copolymer were further characterized by transmission electron microscopy (TEM). Figure 4 a) and b) show TEM image of **7** obtained by drop-casting from toluene solution. The observed well-defined particles with sizes of 60.3±6.8 nm in diameter are consistent with the DLS results (radius = 29 nm) and the size

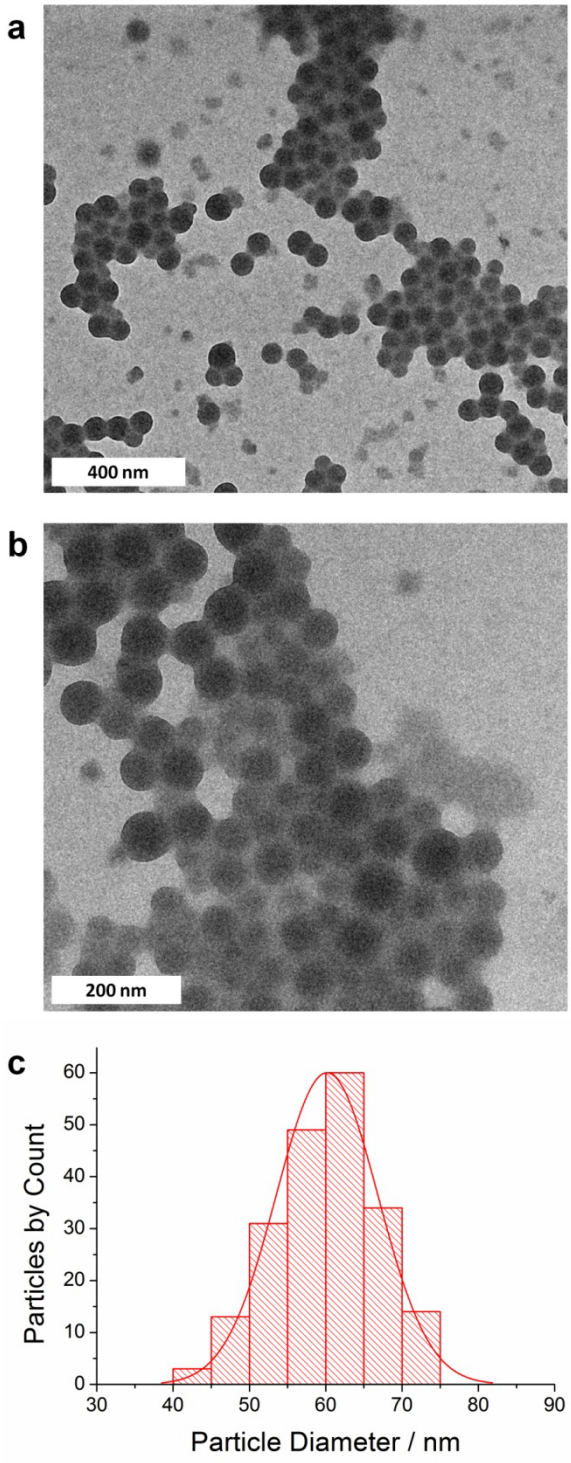

Figure 4: *TEM characterization of dual brush block copolymer* ***7*** *((PPA-g-PPerAcr$_{18}$)$_{29}$-b-(PHEA-g-PvDMTPA$_{17}$)$_{22}$). Images 4 a) and b) represent TEM images of* ***7*** *taken of a toluene solution drop-cast on a copper grid (0.01 g/L in toluene); c) shows a histogram of the distribution of 200 counted particles (d = 60.3±6.8 nm).*

obtained from AFM characterization (diameter = 53.5 nm). The very small difference in size from that observed in AFM may be explained by the different surface properties of silicon wafer and copper grid. Additionally, a close observation of the individual particles clearly indicates a dense (black) domain and an amorphous domain (grey) as expected for a phase separated janus-type

particle. A detailed analysis of these particles on different substrates is required to confirm this preliminary observation. TEM Figure 4 c) shows a histogram of the distribution of 200 counted particles clarifying the narrow distribution of the particle size.

The thermal properties of the dual brush block copolymer were investigated by thermogravimetric analysis (TGA) and differential scanning calorimetry (DSC). The polymer **7** shows high thermal stability with an onset temperature of 355 °C. In DSC (Figure 9), a melting peak at 188 °C due to PPerAcr was observed.

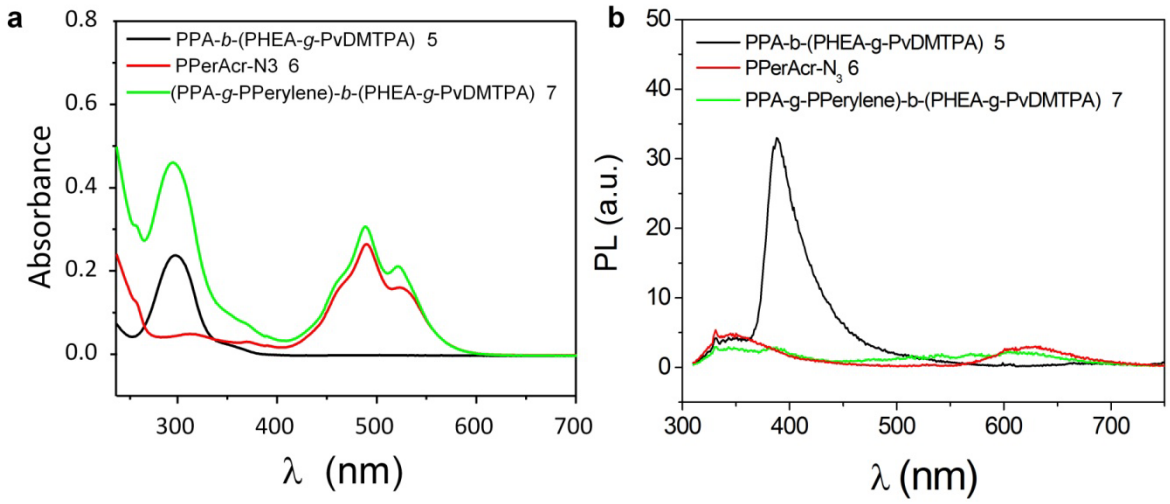

Figure 5: *Optical properties of dual brush block copolymer **7** ((PPA-g-PPerAcr)-b-(PHEA-g-PvDMTPA)). a) Absorption spectra of **5** (PPA_{29}-b-(PHEA-g-$PvDMTPA_{17})_{22}$), **6** (PPerAcr-N_3) and **7** ((PPA-g-$PPerAcr_{18})_{29}$-b-(PHEA-g-$PvDMTPA_{17})_{22}$) in solution (THF, 0.02 mg/mL), b) photoluminescence spectra of **5**, **6** and **7**, excited at 300 nm in solution (THF, 0.02 mg/mL).*

The optical properties of the D-A dual brush block copolymer were also studied. Figure 5 shows the UV-Vis absorption and photoluminescence (PL) of the PvDMTPA brush **5**, perylene bisimide homopolymer **6** and dual brush block copolymer **7**, respectively. Dual brush block copolymer **7** clearly shows the superposition of the TPA absorption of **5** at 300 nm and the characteristic fingerprint bands of perylene bisimide homopolymer **6** at 472 nm, 493 nm and 535 nm (Figure 5a)). When excited at the absorption maximum of the donor at 300 nm, **5** shows a strong TPA fluorescence at 390 nm, which is almost completely quenched in **7** (Figure 5b)). The quenching of fluorescence indicates either energy or charge transfer between TPA and PerAcr. Excitation of **7** at 493 nm (absorption max. of PerAcr) reveals a relatively weak fluorescence at 624 nm which attributes to the perylene bisimide polymer emission (not shown here). A possible explanation for the incomplete quenching of PL here may be that some of the excitons are generated at a part of the particle that is far away from the D-A interface and cannot diffuse to the PvDMTPA part due to the large size of **7** (r = 29 nm, DLS).

Conclusion

To conclude, we tackled the synthetic challenge to obtain D-A nanoparticles with controlled size and composition by the realization of a dual brush block copolymer via a combination of RAFT and click chemistry. The obtained particles from toluene solution exhibited a well-defined size and globular structure. The first TEM analysis indicates the existence of janus-type phase separated particles. Further analyses are under way to determine the structural order, phase separation and also to identify the mechanism of build-up of these D-A nano particles from dual brush block copolymers.

Experimental

General

The ^{1}H NMR (300 MHz) spectra were recorded on a Bruker AC 300 spectrometer and calibrated to $CHCl_3$ (7.26 ppm for ^{1}H). GPC measurements were carried out in dimethylacetamid with two Varian MIXED-C columns (300-7.5 mm) at room temperature and at a flow rate of 0.5 mL/min using UV (Waters model 486) with 254 nm detector wavelength and refractive index (Waters model 410) detectors. Polystyrene standards and *o*-DCB as an internal standard were used for calibration. Differential scanning calorimetry (DSC) experiments were conducted at heating rates of 20 K min^{-1} under a N_2 atmosphere with a Perkin-Elmer Diamond DSC, calibrated with indium. The endothermic maximum was taken as T_m. Thermogravimetry measurements were conducted on a Mettler Toledo TGA/SDTA 851e under a N_2 atmosphere at a heating rate of 10 K/min. Temperature of decomposition (Tonset) was calculated from the onset of the respective curve. UV-vis spectra of solutions in THF with a concentration of 0.02 mg/mL were recorded on a Hitachi 3000 spectrophotometer and photoluminescence spectra were acquired on a Shimadzu RF 5301 PC spectrofluorophotometer upon excitation at 300 nm. AFM images were recorded on a Digital Instruments Dimension 3100 microscope operated in tapping mode. The samples were prepared by dip-coating from very dilute solution of block-typed polymer brushes in toluene on clean silicon wafer. TEM images were taken on a Zeiss EM EF-TEM instrument operated at 200 kV. A 5 µl droplet of a diluted solution (0.01-0.05 mg/mL) in toluene was dropped on a copper grid coated with carbon film, followed by drying at room temperature for a short time. Statistical analysis of the size distribution of Janus nanoparticles was carried out using UTHSCSA image tool program (University of Texas). The value of each sample is the average of 200 objects.

Synthesis

3-(Trimethylsilyl)prop-2-ynyl Acrylate

Silver nitrate (2.45 g, 14.5 mmol) was suspended in 320 mL of dry methylene chloride. Propargyl acrylate (**1**; 32.02 g, 290.8 mmol) and 1,8-diazabicyclo-5.4.0]undec-7-ene (46.50 g, 305.3 mmol) were added to the suspension. The reaction mixture was heated to 40 C and trimethylsilyl chloride (44.20 g, 407.1 mmol) was added dropwise. The solution was stirred for 24 h at 40 °C,

cooled to RT, and concentrated under reduced pressure. Protected propargyl acrylate (2) was obtained after distillation in high vacuum. The colorless liquid weighed 29.7 g (56.0%): ^{1}H NMR (300MHz, $CHCl_3$): δ (ppm) 6.49 (dd, 1H, *J*=17.4, *J*=1.4, CHC*H*H), 6.15 (dd, 1H, *J*=17.3, *J*=10.4,C*H*CH_2), 5.87 (dd, 1H, *J*=10.4, *J*=1.4, CHC*H*H), 4.76 (s, 2H, OCH_2), 0.18 (s, 9H, Si(CH_3)$_3$).

2-Phenylprop-2-yl Dithiobenzonate

The synthesis followed a published method.[16] Sodium methoxide (5.40 g, 100.0 mmol) and 70 mL methanol were added into a 250 mL three-necked round bottom flask equipped with a magnetic stir bar, additional funnel and thermometer. Sulfur (3.20 g, 100.0 mmol) was added into the flask. Benzyl chloride (6.3 g, 4.48 mmol) was then added dropwise over 20 min under nitrogen. Then, the reaction was heated to 67 °C for 10 h and subsequently cooled in an ice bath. The reaction mixture was filtered to remove the salts and the solvents were evaporated under reduced pressure. The residue was then added to 50 mL of water. The solution was filtered and washed with diethyl ether. 50 mL of 1.0 N HCl was added into the aqueous solution and extracted with diethyl ether. 60 ml of 1.0 N NaOH were added to the organic phase to get sodium dithiobenzoate. Finally, 50 mL of 1.0 N HCl were added to the aqueous solution and extracted with diethyl ether. The obtained 1.06 g of dithiobenzoic acid and α-methylstyrene (1.00 g, 8.5 mmol) were added into 10 mL of carbon tetrachloride. The mixture was heated to 70 °C for 4h. The solvent and the excess of α-methylstyrene were removed under reduced pressure. The residue was purified by column chromatography on alumina (activity III) with n-hexane as eluent to give 2-phenylprop-2-yl dithiobenzoate (0.60 g, 2.2 mmol) as a dark purple oil (33.6%). ^{1}H NMR (300MHz, $CHCl_3$): δ (ppm) 7.86 (m, 2H), 7.60-7.20 (m, 8H), 2.03 (s, 6H). High resolution CI mass spectrum: found 273.0745 (M.1); C16H17S2.

Azido-dithiobenzoate RAFT Agent

(a) 3-Azido-1-propanol

3-bromo-1-propanol (5.0 g, 36 mmol) and sodium azide (3.83 g, 59.0 mmol) were dissolved in a mixture of acetone (60 mL) and water (10 mL) and the resulting solution was refluxed overnight. Acetone was removed under reduced pressure, 50 mL of water were added and the mixture was extracted with diethyl ether (3 x 50 mL). The organic layers were collected and dried over $MgSO_4$ and, after removal of the solvent under reduced pressure, 2.82 g of 3-azido-1-propanol were isolated as colorless oil (77%). ^{1}H NMR (300MHz, $CHCl_3$): δ (ppm) 3.67 (t, 2H, *J* = 6.3, CH_2-OH), 3.38 (t, 2H, *J* = 6.6, CH_2-N_3), 1.76 (quint, 2H, *J* = 6.3, CH_2-CH_2-CH_2), 1.68 (s, 1H, CH_2-O*H*).

(b) (4-Cyanopentanoic acid)-4-dithiobenzoate

The (4-cyanopentanoic acid)-4-dithiobenzoate was synthesized according to a literature procedure.[17]

(c) Azido-dithiobenzoate RAFT agent

The synthesis of the azido-dithiobenzoate RAFT agent followed a modified version of a published procedure.[18] (4-Cyanopentanoic acid)-4-dithiobenzoate (1.20 g, 4.2 mmol) and 3-azido-1-propanol (2.40 g, 24.0 mol) and 80 mL of dichloromethane were added into a round-bottom flask. The flask was put into an ice bath, then 4-dimethylaminopyridine (26 mg, 0.024 mmol) and *N*-3(-dimethylaminopropyl)-*N*′-ethylcarbodiimide hydrochloride (2.45 g, 12.5 mmol) was added to the reaction. The reaction was run overnight at room temperature. Then, the reaction mixture was washed with water three times and dried over $MgSO_4$. After removal of the solvent and purification by column chromatography over silica using hexane/ethyl acetate (4:1) as the eluent, 1 g of product was obtained. ^{1}H NMR (300MHz, $CHCl_3$): δ (ppm) 7.6-7.3 (m, 2H, C*H*$_2$-Phenyl), 4.20 (m, 2H, C*H*$_2$-O-C(=O)), 3.40 (m, 2H, C*H*$_2$-N_3), 1.94 (s, 3H, C(CN)(C*H*$_3$)), 1.95-1.85 (m, 2H, CH_2-C*H*$_2$-CH_2).

***N*,*N*-Bis(4-methoxyphenyl)-*N*-(4-vinylphenyl)amine**

(a) *N*,*N*-Bis(4-methoxyphenyl)-*N*-phenyl amine

Aniline (4.00 g, 43.0 mmol), 1-bromo-4-methoxybenzene (20.08 g, 100.7 mmol), palladium(II) acetate (0.192 g, 0.86 mol) and 30 mL of dry toluene were added into a 3-necked round-bottom flask. Sodium *tert*-butoxide (10.32 g, 107.4 mmol) and tri-*tert*-butylphosphine (696 mg, 3.4 mmol) were added into the reaction. The reaction was run for 48 h at 100 °C. After that, the reaction mixture was filtered and rinsed with acetone. After removal of the solvent by rotary evaporation, the solid was collected and washed with cold methanol. 12 g of light-yellow crystals were obtained. ^{1}H NMR (300 MHz, CH_2Cl_2): δ (ppm) 7.24-6.77 (m, 13H, Ar*H*), 3.81 (s, 6H, OC*H*$_3$).

(b) *N*,*N*-Bis(4-methoxylphenyl)-*N*-(4-carboxyphenyl)amine

A mixture of 24 mL of dimethylformamide and 3 mL of phosphorus oxychloride was cooled to 0 °C. The mixture was added dropwise into a 250 mL flask with *N*,*N*-Bis(4-methoxyphenyl)-*N*-phenyl amine (8.00 g, 26.2 mmol) in 160 mL of 1,2 dichloroethane at 0 °C. Then, the reaction was heated to 60 °C under stirring for another 4 h. The reaction mixture was slowly added into 400 mL of 10% sodium acetate. The reaction was run overnight. After that, the reaction mixture was extracted with chloroform three times. After removal of the organic solvent, the product was further purified by column chromatography over silica using dichloromethane as eluent. 8 g of solid product were obtained. ^{1}H NMR (300 MHz, CH_2Cl_2): δ (ppm) 9.77 (s, 1H, CO*H*), 7.70-6.77 (m, 12H, Ar*H*), 3.82 (s, 6H, OC*H*$_3$).

(c) *N*,*N*-Bis(4-methoxyphenyl)-*N*-(4-vinylphenyl)amine

N,*N*-Bis(4-methoxylphenyl)-*N*-(4-carboxyphenyl)amine (8.00 g, 24.0 mmol), methyl-triphenylphophoniumbromid (17.20 g, 48.1 mmol) and 100 mL of THF was added into a 250 mL of round-bottom flask. Then, potassium *t*-butoxide (7.10 g, 63.3 mmol) was added into the flask. The reaction mixture was stirred at room temperature overnight followed by addition of 34 mL of 10% of acetic acid. The aqueous solution was extracted with dichloromethane three times. The

organic phase was collected, and washed with water three times. The organic layer was then dried over Na_2SO_4. After removal of the solvent under reduced pressure the raw product was purified by column chromatography over silica using toluene as the eluent. 7 g of white crystal were obtained. ^{1}H NMR (300 MHz, CH_2Cl_2): δ (ppm) 7.23-6.80 (m, 12H, Ar*H*), 6.62 (dd, 1H, *J* = 10.9 Hz, *J* = 17.53 Hz, C*H*CH_2), 5.57 (d, 1H, *J* = 17.53 Hz, CHC*H*H), 5.07 (d, 1H, *J* = 10.9 Hz, CHCH*H*), 3.77 (s, 6H, OCH_3).

Perylene bisimide acrylate

The perylene bisimide acrylate was synthesized according to a literature reference.[19]

Polymerization:

Poly(trimethyl silyl propargyl acrylate) (PTMSPA) (1)

Trimethyl silyl propargyl acrylate (1.85 g, 10.0 mmol), 2-phenylpro-2-yl dithiobenzoate (53 mg, 0.2 mmol), AIBN (8.2 mg, 0.05mmol) and 0.5 mL of toluene were introduced into a 10 mL schlenk tube. The solution was degassed by three freeze-pump-thaw cycles. The tube was placed in a preheated oil bath with 60 °C for 20 h. Then the reaction was quenched in an ice bath. The polymer solution was added to a large amount of methanol and kept at -35 °C for 24 h. Then the top solvent was removed carefully and more methanol was added. After three cycles of freezing, removal of top solvent and addition of more methanol the product was kept under high vacuum overnight to remove the residual solvent. About 1.2 g of polymer was obtained. M_n=5.4x10^3 g/mol, DP ~ 29 , PDI = 1.09. ^{1}H NMR (300 MHz, $CHCl_3$): δ (ppm) 4.61 (s, 2H, OCH_2), 2.1-0.8 (m, 3H, backbone), 0.20 (s, 9H, Si$(CH_3)_3$).

Poly(trimethyl silyl propargyl acrylate)-*b*-poly(hydroxylethyl acrylate) (PTMSPA-b-PHEA). (2)

(0.20 g, 1.1 mmol) of PTMSPA (M_n = 5.4x10^3), 1.2 mL of HEA, (1.40 mg, 0.00853 mmol) AIBN and 0.8 mL of THF was added into a 10 mL schlenk tube. The reaction was degassed by three freeze-pump-thaw cycles. Then, the tube was put into a preheated oil bath at 60 °C for 6 h under stirring. The reaction was quenched in an ice bath. The solvent and the residual monomer were removed in high vacuum overnight. 0.3 g of red polymer was obtained. (M_n = 6.6x10^3 g/mol, PDI = 1.16). ^{1}H NMR (300 MHz, $CHCl_3$): δ (ppm) 4.70 (s, 2H, OCH_2), 4.45-4-03 (m, CH_2OH), 3.82 (CH_2OC), 2.70-1.39 (m, 6H, backbone$_{HEMA+PA}$), 0.20 (s, 9H, Si$(CH_3)_3$).

Raft Agent Immobilization. (3)

PTMSPA-*b*-PHEA (0.15 g) (M_n = 6.6x10^3 g/mol), (4-cyanopentanoic acid)-4-dithiobenzoate (0.30 g, 1.1 mmol) and 20 mL of dichloromethane was introduced into a 50 mL flask. The reaction was cooled to 0 °C, then *N*-(3-dimethylaminopropyl)-*N'*-ethylcarbodiimide hydrochloride (0.2 g, 1.0 mmol) and subsequently 4-dimethylaminopyridine (40 mg, 0.33 mmol) was added. The reaction was run at 0 °C for 2h, and at room temperature for another 24h. The polymer was precipitated with methanol. 200 mg red powder was obtained. ^{1}H NMR (300 MHz, $CHCl_3$): δ (ppm) 8.19-7.30

(m, 5H, Ar*H*), 4.70 (s, 2H, OCH_2), 4.26 (s, 4H, OCH_2CH_2O), 2.80-1.20 (m, 6H, backbone$_{HEMA+PA}$, 7H, CTA), 0.20 (s, 9H, Si(CH_3)$_3$).

PTMSPA-*b*-(PHEA-*g*-PvDMTPA) (4)

PTMSPA-*b*-PHEA immobilized raft agent (50 mg), *N*,*N*-Bis(4-methoxyphenyl)-*N*-(4-vinylphenyl)amine (0.84 g, 2.5 mmol), AIBN (2.0 mg, 0.012 mmol) and 0.9 mL of toluene were added into a 5 mL schlenk tube. The reaction was degassed by three freeze-pump-thaw cycles and the tube was put into a preheated oil bath at 80 °C for 4 h. Then, the reaction mixture was diluted with THF and precipitated in methanol. 0.6 g of yellow powder was obtained. (M_n = 4.7x10^4, PDI = 1.16). ^{1}H NMR (300 MHz, $CHCl_3$) 7.13-6.26 (m, 12H, Ar*H*), 4.71 (br s, 2H, CH_2O), 3.63 (br s, 6H, OCH_3), 2.45-088 (m, backbone), 0.20 (s, 9H, Si(CH_3)$_3$).

Deprotection of PTMSPA-*b*-(PHEA-*g*-PvDMTPA) (5)

PTMSPA-*b*-(PHEA-*g*-PvDMTPA) (0.6 g) was dissolved in 10 mL of tetrahydrofuran. The solution was purged with argon for 10 min and cooled to -20 °C. Subsequently a degassed solution of 1 M tetrabutylammonium fluoride in THF (1 mL, 1 mmol) was added dropwise. The reaction mixture was allowed to stir for 30 min at -20 °C and 2 h at RT. The mixture was passed through a silica column to remove the excess TBAF, then the polymer was precipitated in methanol. After filtering and drying under vacuum at room temperature, 0.54 g of light yellow powder was obtained. ^{1}H NMR (300 MHz, $CHCl_3$) 7.18-6.03 (m, 12H, Ar*H*), 4.71 (br s, 2H, CH_2O), 3.64 (br s, 6H, OCH_3), 2.45-088 (m, 1H, CC*H*, +backbone).

Poly(perylene bisimide acrylate) containing azide group (6)

Perylene bisimide acrylate (0.60 g, 0.7 mmol), azido-dithiobenzoate RAFT agent (5.2 mg 0.015 mmol), AIBN (1.2 mg, 0.007 mmol) and 0.6 mL of dichlorobenzene were introduced into a 5 mL schlenk tube. After 5 freeze-pump-thaw cycles, the tube was put into an oil bath with a temperature of 90 °C under stirring. After 20 h, the reaction was quenched in an ice bath. After precipitation in methanol and filtration, the polymer was further purified by soxhlet extraction with methyl ethyl ketone. 20 mg of red powder was obtained. (M_n = 5.7x10^3 g/mol, PDI = 1.24). ^{1}H NMR (300 MHz, $CHCl_3$): δ (ppm) 8.45-7.20 (br s, 8H, Ar*H*), 5.05 (br s, 1H, C*H*), 4.06 (br s, 4H, CH_2N, CH_2O), 2.50-0.91 (m, 45H, CH_2, CH_2C$H_{backbone}$), 0.85 (br s, 6H, CH_3).

D-A dual brush block copolymer by click chemistry (7)

10 mg of deprotected PTMSPA-*b*-(PHEA-*g*-PvDMTPA) (M_n = 4.7x10^4 g/mol) and 30 mg of poly(perylene bisimide acrylate) (M_n = 5.7x10^3 g/mol) (azide:akyne=1:1), 0.8 mg of CuBr and 2 mL of toluene were placed in a schlenk tube. The tube was degassed by three freeze-pump-thaw cycles. Then, 2 µL of PMDETA were added under argon flushing. The reaction was stirred at room temperature for 24 h. Then, the reaction mixture was precipitated in methanol/PMDETA (100:1 volume ratio). After filtration and rinsing with THF, 32 mg of deep red powder was obtained. ^{1}H NMR (300 MHz, $CHCl_3$): δ (ppm) 8.56-7.40 (br s, 8H, Ar$H_{perylene}$), 7.03-6.19 (br s, 12H, ArH_{TPA}), 5.08

(br s, 1H, C*H*$_{perylene}$), 4.06 (br s, 4H, C*H*$_2$N$_{perylene}$, C*H*$_2$O$_{perylene}$), 3.63 (br s, 6H, 2OC*H*$_{3,TPA}$), 2.40-1.02 (m, 42H, C*H*$_{2,perylene}$, +backbone$_{perylene+TPA}$), 0.85 (m, 6H, C*H*$_{3,perylene}$).

Acknowledgements

This work was supported by the German Research Council (SPP 1355), Alexander von Humboldt foundation and grant of NSFC 20804009. The authors also thank Eva Betthausen for DLS measurements.

Additional Figures

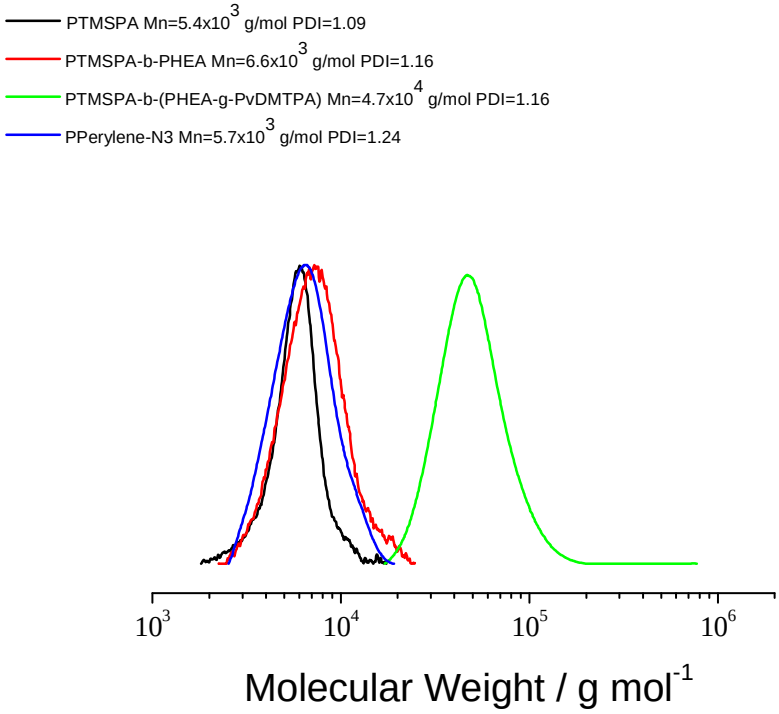

Figure 6: SEC traces of polymers.

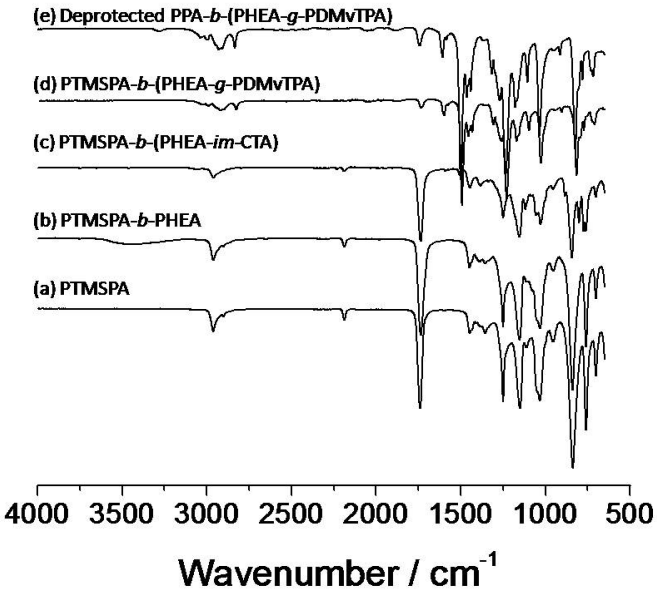

Figure 7: FTIR spectra of polymers.

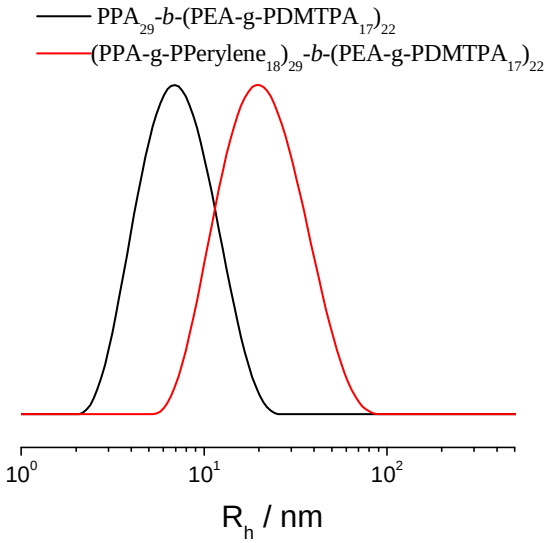

Figure 8: DLS measurement of polymers **5** and **7**.

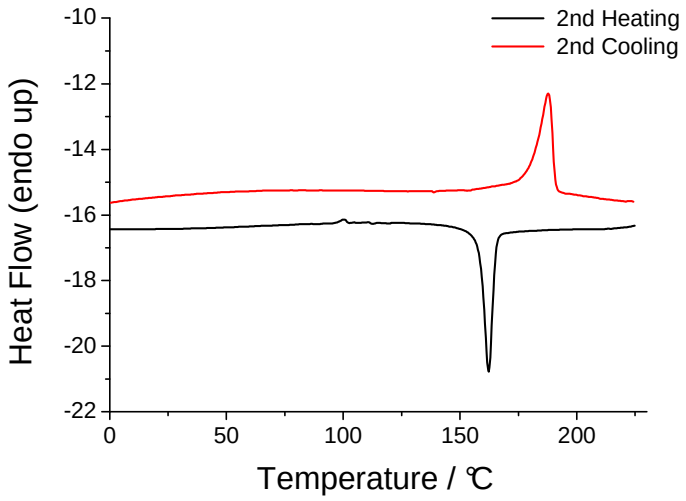

Figure 9: Second heating and second cooling curve of polymer 7 measured with heating rates of 20K/min.

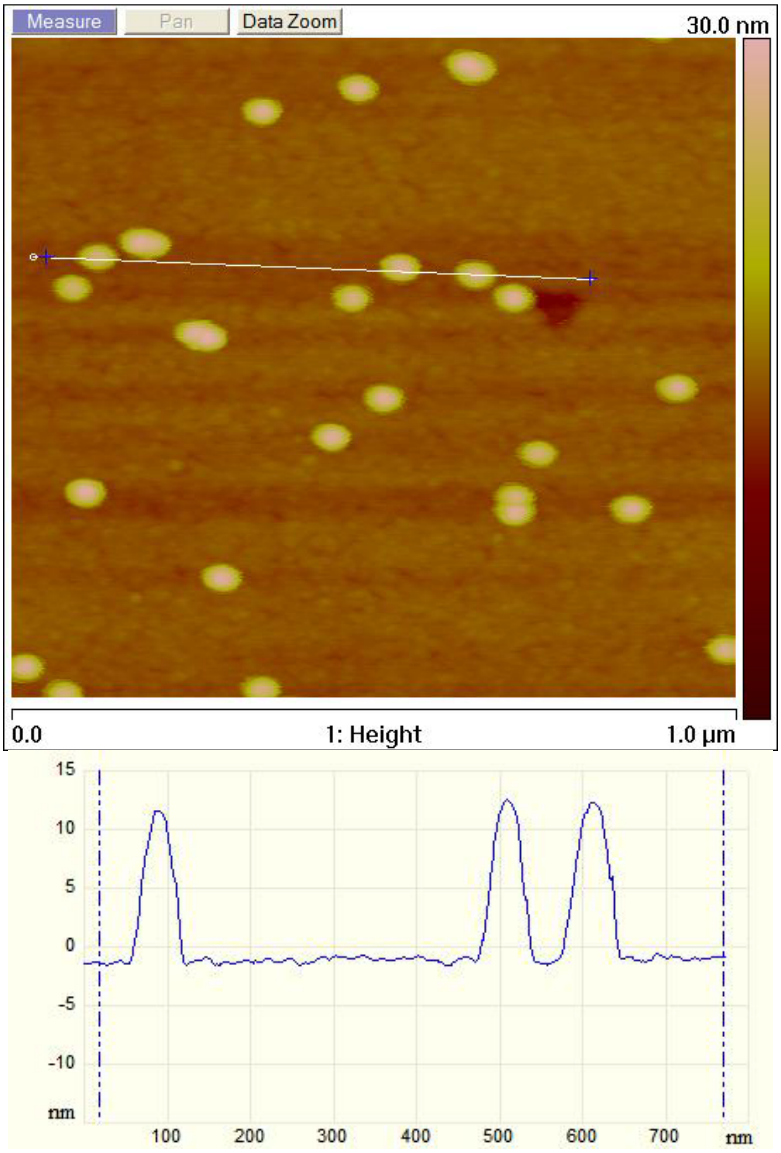

Figure 10: AFM height image of dual brush block copolymer **7** ((PPA-*g*-PPerAcr$_{18}$)$_{29}$-*b*-(PHEA-*g*-PvDMTPA$_{17}$)$_{22}$) before annealing; samples prepared by spin-coating from a toluene solution of **7** (0.01 g/L) on a silicon wafer showing globular structures with sizes of about 53.5±2.6 nm.

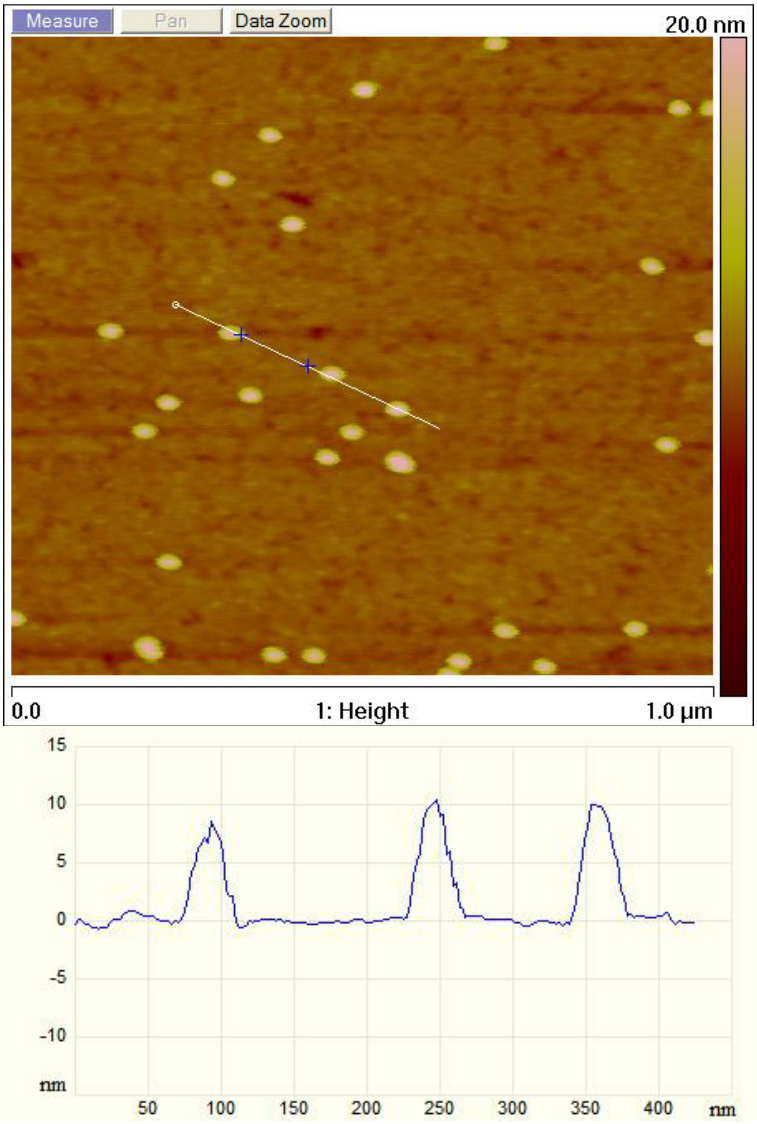

Figure 11: AFM height image of dual brush block copolymer **7** ((PPA-*g*-PPerAcr$_{18}$)$_{29}$-*b*-(PHEA-*g*-PvDMTPA$_{17}$)$_{22}$) after annealing, samples were prepared by spin-coating from a toluene solution of **7** (0.01 g/L) on a silicon wafer showing globular structures with sizes of about 35.8±2.1 nm.

Bibliography

1. Deibel, C.; Strobel, T.; Dyakonov, V. *Advanced Materials* **2010,** 22, (37), 4097-4111.

2. Kim, Y.; Cook, S.; Tuladhar, S. M.; Choulis, S. A.; Nelson, J.; Durrant, J. R.; Bradley, D. D. C.; Giles, M.; McCulloch, I.; Ha, C.-S.; Ree, M. *Nat Mater* **2006,** 5, (3), 197-203.

3. Oosterhout, S. D.; Wienk, M. M.; van Bavel, S. S.; Thiedmann, R.; Jan Anton Koster, L.; Gilot, J.; Loos, J.; Schmidt, V.; Janssen, R. A. J. *Nat Mater* **2009,** 8, (10), 818-824.

4. Lindner, S. M.; Hüttner, S.; Chiche, A.; Thelakkat, M.; Krausch, G. *Angewandte Chemie International Edition* **2006,** 45, (20), 3364-3368.

5. Sommer, M.; Lang, A. S.; Thelakkat, M. *Angewandte Chemie International Edition* **2008,** 47, (41), 7901-7904.

6. Zhang, Q.; Cirpan, A.; Russell, T. P.; Emrick, T. *Macromolecules* **2009,** 42, (4), 1079-1082.

7. Walther, A.; Muller, A. H. E. *Soft Matter* **2008,** 4, (4), 663-668.

8. Ishizu, K.; Satoh, J.; Sogabe, A. *Journal of Colloid and Interface Science* **2004,** 274, (2), 472-479.

9. Zehm, D.; Laschewsky, A.; Gradzielski, M.; Prel vost, S.; Liang, H.; Rabe, J. r. P.; Schweins, R.; Gummel, J. r. m. *Langmuir* **2009,** 26, (5), 3145-3155.

10. Cheng, Z.; Zhu, X.; Fu, G. D.; Kang, E. T.; Neoh, K. G. *Macromolecules* **2005,** 38, (16), 7187-7192.

11. Zhang, M.; Müller, A. H. E. *Journal of Polymer Science Part A: Polymer Chemistry* **2005,** 43, (16), 3461-3481.

12. Sheiko, S. S.; Sumerlin, B. S.; Matyjaszewski, K. *Progress in Polymer Science* **2008,** 33, (7), 759-785.

13. Moad, G.; Rizzardo, E.; Thang, S. H. *Australian Journal of Chemistry* **2005,** 58, (6), 379-410.

14. Zhang, B.-Y.; He, W.-D.; Li, W.-T.; Li, L.-Y.; Zhang, K.-R.; Zhang, H. *Polymer* 51, (14), 3039-3046.

15. Kolb, H. C.; Finn, M. G.; Sharpless, K. B. *Angewandte Chemie International Edition* **2001,** 40, (11), 2004-2021.

16. Moad, G.; Chiefari, J.; Chong, Y. K.; Krstina, J.; Mayadunne, R. T. A.; Postma, A.; Rizzardo, E.; Thang, S. H. *Polymer International* **2000,** 49, (9), 993-1001.

17. Mitsukami, Y.; Donovan, M. S.; Lowe, A. B.; McCormick, C. L. *Macromolecules* **2001,** 34, (7), 2248-2256.

18. Quemener, D.; Davis, T. P.; Barner-Kowollik, C.; Stenzel, M. H. *Chemical Communications* **2006**, (48), 5051-5053.

19. Sommer, M.; Lindner, S. M.; Thelakkat, M. *Advanced Functional Materials* **2007,** 17, (9), 1493-1500.

Chapter 9

Semiconductor Dendritic-Linear Block Copolymers by Nitroxide Mediated Radical Polymerization

Andreas S. Lang[†], *Franz René Kogler*[‡], *Michael Sommer*[†], *Ulrich Wiesner*[‡] *and Mukundan Thelakkat*[†,*]

[†]Applied Functional Polymers, Department of Macromolecular Chemistry I, University of Bayreuth, Universitätsstr. 30, 95440 Bayreuth, Germany

[‡]Materials Science & Engineering, Cornell University, 330 Bard Hall, Ithaca, NY 14853, USA

Published in *Macromolecular Rapid Communications*, **2009**, *30*, 1243-1248

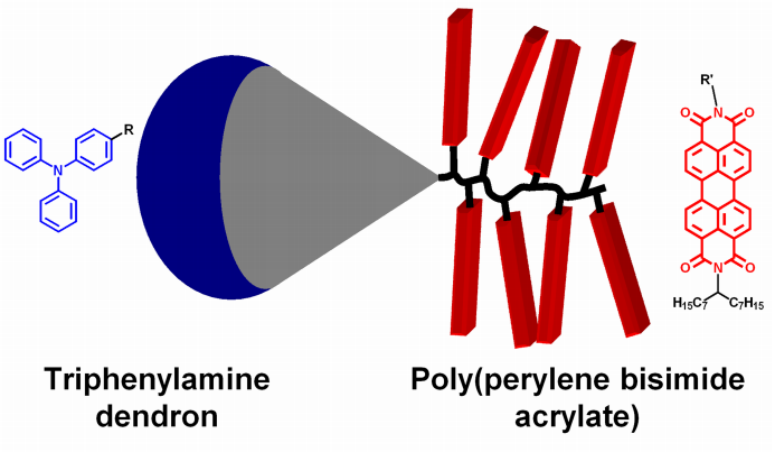

Abstract

The first synthesis of a semiconductor hybrid diblock copolymer comprised of p-type dendritic and n-type linear blocks by nitroxide mediated radical polymerization (NMRP) is reported. A triphenylamine (TPA) bearing second generation polyether dendron [G2]-OH has been functionalized with an alkoxyamine and, subsequently, perylene bisimide acrylate (PerAcr) was polymerized to obtain a hybrid block copolymer [G2]-*b*-PPerAcr. The hybrid block copolymer structure is supported by ^{1}H NMR and size exclusion chromatography. Furthermore, the novel materials were studied by UV-Vis absorption spectroscopy, photoluminescence, cyclic voltammetry, differential scanning calorimetry and thermogravimetry analysis.

Introduction

Over the past years, increased attention has been drawn to the preparation of semiconductor homopolymers[1] and block copolymers containing one[2,3] or more[4,5] functional blocks. Applications in organic electronics, such as organic field effect transistors (OFETs)[6,7] or organic solar cells (OSCs),[8,9] have been reported. In particular, the possibility to take care of absorption in visible range and providing donor and acceptor moieties all in one molecule is an interesting aspect of the block copolymer concept. Furthermore, the ability of block copolymers to microphase separate can be beneficial to the performance of electronic devices[10,11] by providing a high interface between donor and acceptor materials, being the active area for charge separation.
Recently, we reported the synthesis of a polyacrylate with pendant perylene bisimide groups (PPerAcr) by nitroxide mediated radical polymerization (NMRP).[12] This n-type semiconductor polymer has been incorporated into different fully functionalized block copolymers such as poly(vinyltriphenylamine)-*block*-poly(perylene bisimide acrylate) PvTPA-*b*-PPerAcr,[12] poly(bis(4-methoxyphenyl)-4'-vinylphenylamine)-*block*-poly(perylene bisimide acrylate) PvDMTPA-*b*-PPerAcr,[11] and, most recently poly(3-hexylthiophene)-*block*-poly(perylene bisimide acrylate) P3HT-*b*-PPerAcr[5]. All these block copolymers showed the tendency to phase separate in nanoscale regime.

In the search for novel architectures for functional materials, hybrid block copolymers, consisting of one dendritic segment and a linear polymer block[13,14] are another interesting class of block copolymers, related to linear-linear block copolymers. These polymers are interesting due to the well-defined molecular weight of the dendritic segment and their distinct phase behaviour compared to linear-linear analogs with equivalent volume fractions.[15,16] The first steps towards semiconductor hybrid block copolymers were undertaken by Fréchet et al., who reported dendronized oligo- and polythiophene block copolymers with one active block.[17,18] In this work, we expand this concept to fully functionalized semiconductor hybrid block copolymers and report the first synthesis of an amorphous triphenylamine (TPA) bearing second generation polyether dendron (electron donor) linked to poly(perylene bisimide acrylate) (PPerAcr) (electron acceptor) as a linear block, which exhibits side chain crystallinity.

Results and Discussion

A second generation dendritic alcohol was functionalized with an alkoxyamine for NMRP. It has already been shown that unimolecular alkoxyamines can be utilized to build macroinitiators involving linear polymers[19] as well as dendritic structures.[20] Moreover these macroinitiators were able to provide good control over molecular weight, maintaining low polydispersity (PDI). The TPA containing dendritic initiator [G2]-TIPNO **3** was synthesized by reaction of a chloromethyl derivative of 2,2,5-trimethyl-4-phenyl-3-azahexane-3-oxyl (TIPNO-BzCl)[21] **1**, with the dendritic alcohol **2**, carrying the hydroxyl group at the focal point. The 18-crown-6 catalyzed reaction of **2** with 8.0 equivalents of TIPNO-BzCl **1** and NaH gave the dendritic initiator [G2]-TIPNO **3**, with a degree of functionalization of more than 90% (Scheme 1). This was confirmed using ^{1}H NMR and SEC. The presence of low molecular weight impurities in the [G2]-OH educt did not affect the functionalization reaction and could be removed easily in a following purification step.

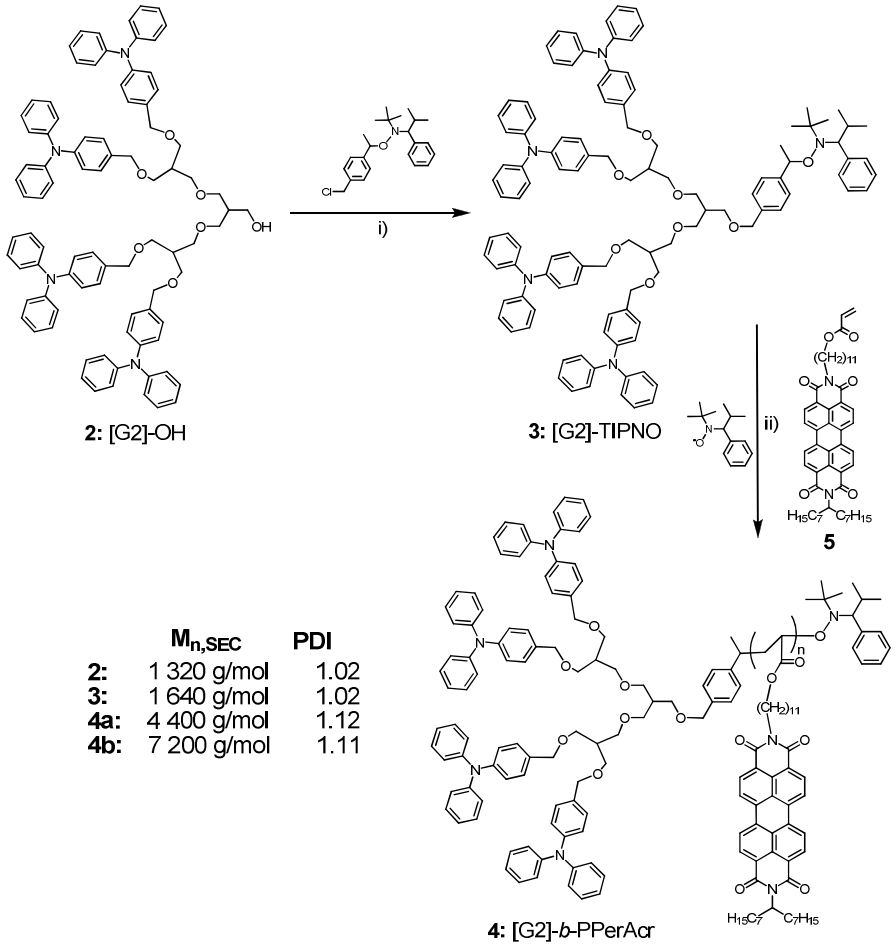

Scheme 1: *Synthesis of dendronized initiator [G2]-TIPNO **3** and hybrid block copolymers [G2]-b-PPerAcr **4a** and **b**. i) NaH, 18-crown-6, **1**, THF, RT, 24h ii) **5**, **7**, o-DCB, 125 °C.*

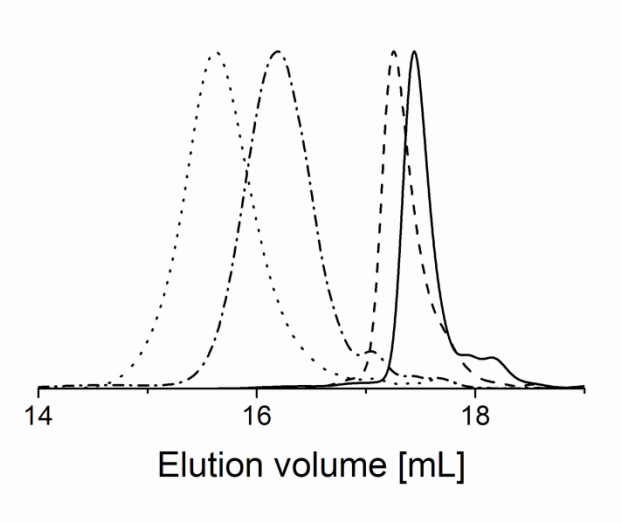

***Figure 1**: SEC elution traces (normalized UV-detector signal) of [G2]-OH 2 (straight line), [G2]-TIPNO 3 (dashed line) and [G2]-b-PPerAcr 4a (dash-dotted line) and 4b (dotted line).*

Figure 1 shows the SEC traces of **2** and **3**. The curve of **3** is clearly shifted to smaller elution volumes, indicating a rise in molecular weight. In the SEC trace of **3**, a small shoulder resulting from non-functionalized alcohol **2** can also be seen. This fraction was removed after the polymerization of PerAcr by soxhlet extraction with hexane/acetone. Comparison of the ^{1}H NMR spectra of **2** and **3** reveals the replacement of the signals of the CH_2-OH protons of **2** by new signals which can be clearly assigned to the benzyl-TIPNO group of **3** (for ^{1}H NMR data see Supporting Information). Integration of the signals of the dendritic fragment and comparison with those of the TIPNO functionality confirms the introduction of a single TIPNO group at the dendron.

The capability of dendritic macroinitiator **3** to polymerize functional acrylate monomers was then investigated under typical conditions for NMRP. The polymerizations of PerAcr **5** initiated by **3** were conducted in degassed *o*-dichlorobenzene at 125 °C for 14 h 40 min and 32 h to give the hybrid dendron-linear block copolymers **4a** and **4b**, respectively, which were purified in a soxhlet apparatus with hexane/acetone to remove non-reacted or non-functionalized dendron and monomer **5**. 0.1 equivalents of free nitroxide **7** were added to the reaction to shift the equilibrium between dormant and active species more towards the dormant species, leading to a better control of the reaction. Examination of the ^{1}H NMR spectra of **4a** and **4b** revealed signals for both the dendritic and the perylene protons (for ^{1}H NMR data, see Supporting Information). The SEC traces in Figure 1 show the two hybrid block copolymers **4a** and **4b** and the starting dendritic initiator **3** and obviously demonstrate that the purified hybrid block copolymers are free of dendritic impurities and monomer **5**. This confirms the copolymer structure in which the PPerAcr chain is attached to the focal point of the dendron. In the case of **4a,** a molecular weight ($M_{n,SEC}$) of 4 400 g/mol and a PDI of 1.12 could be determined. The $M_{n,SEC}$ of hybrid block copolymer **4b** was determined to be 7 200 g/mol with a PDI of 1.11, being also very narrow. Integration and comparison of the ^{1}H NMR signals of the dendritic fragment and PPerAcr allows to determine the relative weight percentage of the respective segments in the hybrid block

Table 1. *Molecular weight, composition, thermal and electrical properties of dendritic fragment* ***2****, dendronized initiator* ***3****, the hybrid block copolymers* ***4a*** *and* ***4b*** *and reference homopolymer* ***6****.*

#	$M_{n,SEC}$ [g/mol][a]	$M_{n,\ theo.}$ [g/mol]	wt % PerAcr[b]	M_w/M_n[a]	T_g[b] [°C]	T_m[b] [°C]	T_{onset}[c] [°C]	HOMO [eV]	LUMO [eV]
2: [G2]-OH	1 320	1 310	0	1.02	36	[f]	278	-	-
3: [G2]-TIPNO	1 640	1 650	0	1.02	36	[f]	187	5.29[d]	1.87[g]
4a: [G2]-*b*-PPerAcr$_1$	4 400	4 480[e]	63[e]	1.12	[f]	112	189	5.34[d]	3.73[d]
4b: [G2]-*b*-PPerAcr$_2$	7 200	8 200[e]	80[e]	1.11	[f]	109	330	5.34[d]	3.73[d]
6: PPerAcr	18 400	-	100	1.68	[f]	190	359	5.79[g]	3.63[d]

[a] Measured by SEC against polystyrene standards. [b] Measured by DSC, heating rate 10K/min. [c] Measured by TGA. [d] Measured by CV. [e] Calculated from ^{1}H NMR spectra. [f] T_g or T_m could not be observed from -30°C to 210°C. [g] Calculated from UV-Vis.

copolymer and calculation of the theoretical molecular weight ($M_{n,theo}$). Comparison of $M_{n,theo}$ and $M_{n,SEC}$ correlate well. Calculations yielded a $M_{n,theo}$ of 4480 g/mol for hybrid block copolymer **4a** and 8200 g/mol for **4b**. All these relevant data are summarized in Table 1.

Thermal properties of the intermediates **2** and **3**, and the final block copolymers **4a** and **4b,** were studied via differential scanning calorimetry (DSC) and thermogravimetric analysis (TGA) (Figure 2). The glass transition temperature T_g of 36 °C observed for the amorphous dendron could not be detected in the curves of the block copolymers. In **4a** the melting point of 112 °C occurred only in the first heating, with no recrystallization at cooling. For **4b** a melting point of 109 °C was observed in the second heating and respective recrystallization at cooling. The melting points can be assigned to the side chain crystalline PPerAcr. The low melting point compared to the reference homopolymer **6** (190 °C) could be due to the short chain lengths of PPerAcr in **4a** and **4b**. The TGA of **2** and **3** shows onset temperatures (T_{onset}) of 278 °C and 187 °C, respectively. The big difference in thermostability can be ascribed to the cleavage of the nitroxide group in **3**, which is also observed in **4a** showing a T_{onset} of 189 °C. The observed weight losses correlate well with the calculated theoretical molar fraction of nitroxide in the molecule. The higher T_{onset} at 330 °C observed in the bigger polymer **4b** could be ascribed to a previous cleavage of the nitroxide group during the purification process.

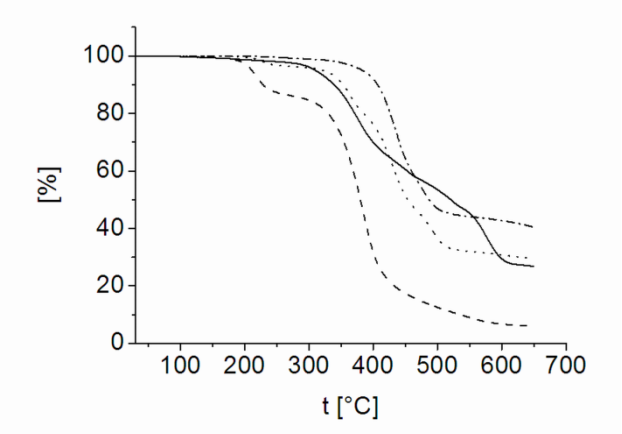

Figure 2: *TGA curves of [G2]-OH* ***2*** *(straight line), [G2]-TIPNO 3 (dashed line), [G2]-b-PPerAcr* ***4a*** *(dotted line) and* ***4b*** *(dash-dotted line). The decline around 189°C observed for* ***3*** *and* ***4a*** *is due to cleavage of the nitroxide group.*

Optical properties of **4a** and **4b** were studied by UV-Vis absorption and photoluminescence (PL) measurements of films obtained by spin coating from chloroform. The optical density for perylene bisimide absorption at 493 nm was maintained same in all samples by keeping the PerAcr content the same. The absorption spectra of **4a** and **4b** clearly show the superposition of the single absorption band of [G2]-OH **2** at 303 nm and the characteristic fingerprint bands of PPerAcr at 472 nm, 493 nm and 535 nm in film (Figure 3(a)). The absorption of TPA decreases with increasing PerAcr fraction from **4a** to **4b** as expected. The absorption spectra of PPerAcr homopolymer **6** with a M_n of 18 400 g/mol, which was measured as a reference, matches with the spectra of the hybrid block between 400 and 600 nm. Upon annealing the films for 5 h at 125°C (above melting points), a change in intensity of vibronic bands only in sample **4b** was observed. The 0-2 vibronic transition at 472 nm in polymer **4b** decreases, whereas the 0-1 and 0-0 transitions remain predominant. The quotients of the absorption $A_{472/493}$ and $A_{493/535}$ increases from 0.78 (as spun) to 0.93 (annealed) and from 1.52 (as spun) to 1.77 (annealed) respectively. A small red-shift from 535 nm to 539 nm was also observed (see supporting information). This behaviour indicates a stronger aggregation of the perylene bisimide on annealing, which was also observed in other perylene bisimide homo polymers and block copolymers.[22,23]

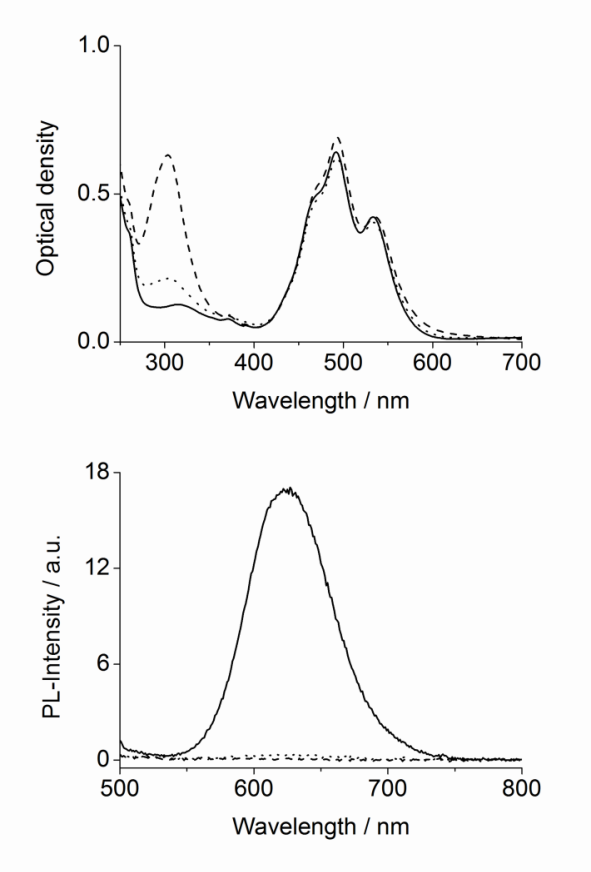

Figure 3. *a) UV-Vis absorption spectra and b) photoluminescence spectra (PL) excited at 493 nm of [G2]-b-PPerAcr **4a** (dashed line), **4b** (dotted line) and PPerAcr **6** (straight line) in thin films with the same optical density for perylene bisimide absorption at 493 nm. The PL of **4a** and **4b** is completely quenched.*

Photoluminescence measurements of the films of **4a** and **4b** show a complete quenching of fluorescence in both hybrid block copolymers when excited at 493 nm, indicating charge transfer between perylene bisimide and the TPA groups of the dendron, while the reference homopolymer PPerAcr **6** shows an intense red fluorescence at 632 nm (Figure 3(b)). The HOMO/LUMO levels were determined by cyclic voltammetry (CV). The compounds **4a** and **4b** exhibited the characteristic double reduction peak of the perylene bisimide unit, the first reduction occurring at -1.07 V and the second at -1.25 V versus ferrocene (Fc). The oxidation of TPA occurred at 0.53 V versus Fc. This results in a LUMO value of PerAcr of 3.73 eV and a HOMO value of TPA of 5.34 eV, assuming the HOMO of Fc to be 4.8 eV. The HOMO value of 5.29 eV of the pure dendron **3** and the LUMO of 3.63 eV of the reference polymer **6** match well with the values of the hybrid block copolymer. Table 1 summarizes the CV data of the polymers.

Conclusion

In conclusion, we have shown that a TPA bearing second generation polyether dendron can be successfully converted into a macroinitiator suitable for nitroxide mediated radical polymerization of PerAcr to build up semiconductor dendritic-linear block copolymers [G2]-*b*-PPerAcr. Two such block copolymers with M_n of 4400 g/mol and 7200 g/mol were synthesized with strikingly low PDIs around 1.11. ^{1}H NMR, SEC and UV-Vis spectroscopy showed the successful synthesis of [G2]-*b*-PPerAcr and the photoluminescence was quenched completely in both hybrid block copolymers, indicating charge transfer between the perylene bisimide block and TPA segments. This novel architecture of semiconductor block copolymers has potential applications in organic photovoltaics, as well as ambipolar organic field effect transistors, if a desired microphase separation can be achieved. The use of dendritic blocks helps to introduce one of the blocks in amorphous state, so that a crystallization of the second block can be well-tuned in an amorphous matrix.

Experimental Part

General

Monomer PerAcr was prepared as described previously.[11] The initiator N-tert-Butyl-O-[1-(4-chloromethylphenyl)ethyl]-N-(2-methyl-1-phenylpropyl)hydroxylamine (Cl-BzEt-TIPNO) **1** and the free nitroxide **7** were prepared according to literature procedure.[21] NaH (60% in oil dispersion), *o*-DCB were purchased from Aldrich. Dry THF over mole sieve and 18-crown-6 were purchased from Fluka.

^{1}H NMR Spectra were recorded on a Bruker AC 250 spectrometer (250 MHz) and calibrated to the chloroform signal. SEC measurements were carried out in THF using UV (WATERS model 486) and refractive index (WATERS model 410) detectors. Polystyrene standards and *o*-DCB as an internal standard were used for calibration. UV-Vis spectra were recorded on a Hitachi 3000 spectrophotometer and photoluminescence spectra were acquired on a Shimadzu RF 5301 PC spectrofluorophotometer upon excitation at 493 nm. Films were spin cast onto quartz glass

substrates from chloroform. Differential scanning calorimetry experiments were conducted at heating rates of 10 K/min between 30 °C and 200 °C under N_2 with a Perkin Elmer Diamond DSC. Thermogravimetry measurements were conducted on a Mettler Toledo TGA/SDTA 851^e. Cyclic voltammetry measurements were conducted under nitrogen in dry DCM with tetrabutylammonium hexafluorophosphate as conducting electrolyte using a three-electrode assembly with a glassy carbon working electrode. Each measurement was calibrated to ferrocene/ferrocenium. The scan speed was 50 mV/s.

Synthesis of dendritic initiator [G2]-TIPNO 3.

To a solution of **2** (500 mg, 0.381 mmol) and 4.8 mg (0.018 mmol) 18-crown-6 in dry THF (2.5 mL) was added sodium hydride (76 mg, 80% dispersion in oil, 1.9 mmol) and the reaction mixture was stirred under argon at room temperature for 1 h. The initiator **1** (1140 mg, 3.050 mmol) was then added portionwise and the reaction mixture was stirred at room temperature for 24 h under argon. The crude product was purified by column chromatography. Exceeding TIPNO-Cl was washed from the column with CH_2Cl_2, the dendritic initiator was obtained with ethyl acetate to yield **3** as a slightly yellow powder after evaporation of the solvents (505 mg, 80%): ^{1}H NMR ($CDCl_3$): δ = 0.21 (d, *J* = 6.60 Hz),0.53 (d, *J* = 6.60 Hz), 0.76 (s), 0.92 (d, 5.97 Hz), 1.02 (s), 1.14 (t, *J* = 7.19 Hz), 1.26 (t, *J* = 7.20 Hz), 1.29 (d, *J* = 6.28 Hz), 1.50 (d, *J* = 5.30 Hz), 1.58 (d, *J* = 6.44 Hz) 1.75-1.95 (m), 2.15-2.36 (m), 3.29 (d, *J* = 10.79 Hz), 3.40-3.63 (m), 4.12 (q, *J* = 14.41, *J* = 7.33), 4.38 (s), 4.81-4.95 (m), 6.88-7.27 (m), 7.33-7.48 (m). IR (KBr): 3059, 3031, 2916, 2858, 1589, 1509, 1492, 1361, 1326, 1315, 1277, 1089, 819, 753, 695, 622, 510, 502 cm^{-1}.

Procedure for hybrid block copolymer 4a.

A mixture of dendritic initiator **3** (140 mg, 0.0679 mmol), free Nitroxide **5** (1.50 mg, 0.00679 mmol) and perylene bisimide acrylate, PerAcr **6** (416 mg, 0.504 mmol) was degassed by three freeze-pump-thaw cycles and then heated at 125 °C under argon for 880 min. The crude polymerization mixture was then dissolved in chlorobenzene and precipitated in methanol. To remove left over dendron and exceeding perylene bisimide monomer the precipitate was extracted in a soxhlet apparatus with hexane/acetone for 3 days to yield [G2]-*b*-PPerAcr **4a** as red powder (97 mg, 23%): ^{1}H NMR ($CDCl_3$): δ = 0.39 (d, *J* = 6.2 Hz), 0.83 (s), 0.91-1.05 (m), 1.10-1.50 (m), 1.69-1.83 (m), 1.68-2.00 (m), 1.98-2.14 (m), 2.15-2.31 (m), 3.40-3.60 (m), 3.88-4.22 (m), 4.38 (s), 5.02-5.23 (m), 6.88-7.27 (m), 7.86-8.60 (m). IR (KBr): 2925, 2854, 1697, 1657, 1596, 1405, 1342, 1247, 1176, 811, 745 cm^{-1}.

Procedure for hybrid block copolymer 4b.

A mixture of dendritic initiator **3** (200 mg, 0.0970 mmol) free Nitroxide **5** (2.14 mg, 0.0097 mmol) and perylene bisimide acrylate, PerAcr **6** (2515 mg, 3.04 mmol) was degassed by three freeze-pump-thaw cycles and then heated at 125 °C under argon for 1920 min. The crude polymerization mixture was then dissolved in chlorobenzene and precipitated in methanol. To remove left over dendron and exceeding perylene bisimide monomer the precipitate was extracted in a soxhlet apparatus with hexane/acetone for 5 days to yield [G2]-PPerAcr **4b** (500

mg, 20%): ^{1}H NMR ($CDCl_3$): δ = 0.39 (d, *J* = 6.2 Hz), 0.83 (s), 0.91-1.05 (m), 1.10-1.50 (m), 1.69-1.83 (m), 1.68-2.00 (m), 1.98-2.14 (m), 2.15-2.31 (m), 3.40-3.60 (m), 3.88-4.22 (m), 4.38 (s), 5.02-5.23 (m), 6.88-7.27 (m), 7.86-8.60 (m) ppm. IR (KBr): 2925, 2854, 1697, 1658, 1595, 1405, 1342, 1248, 1176, 811, 747 cm^{-1}.

Acknowledgements

The financial support for this research work from German Research Council (DFG/SFB 481-Project B4) and SPP 1355 (DFG) is gratefully acknowledged.

Supporting Information

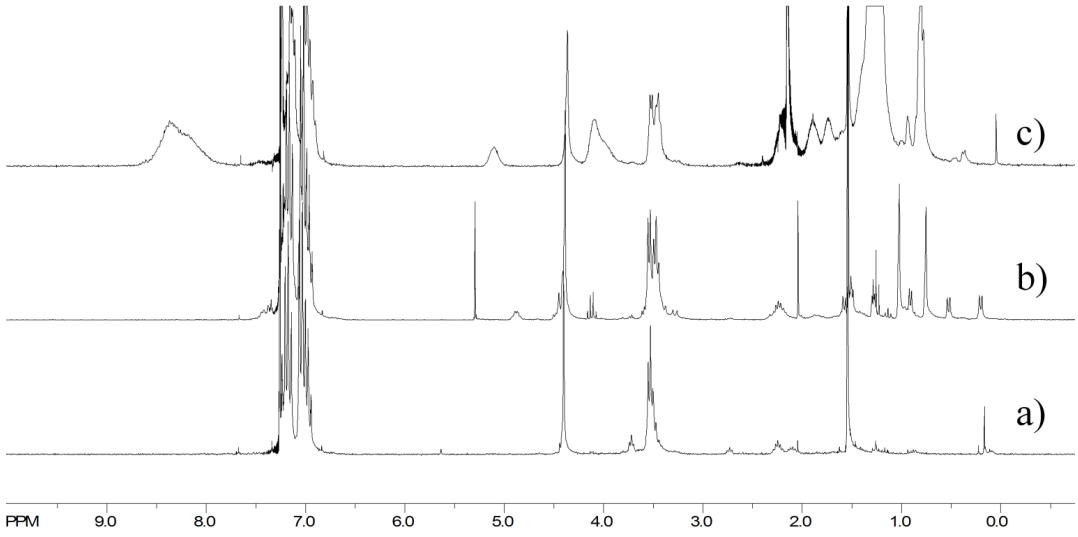

Figure 4: *^{1}H NMR (250 MHz, $CDCl_3$) of a) [G2]-OH **2** b) [G2]-TIPNO **3** and c) [G2]-b-PPerAcr-TIPNO **4a**.*

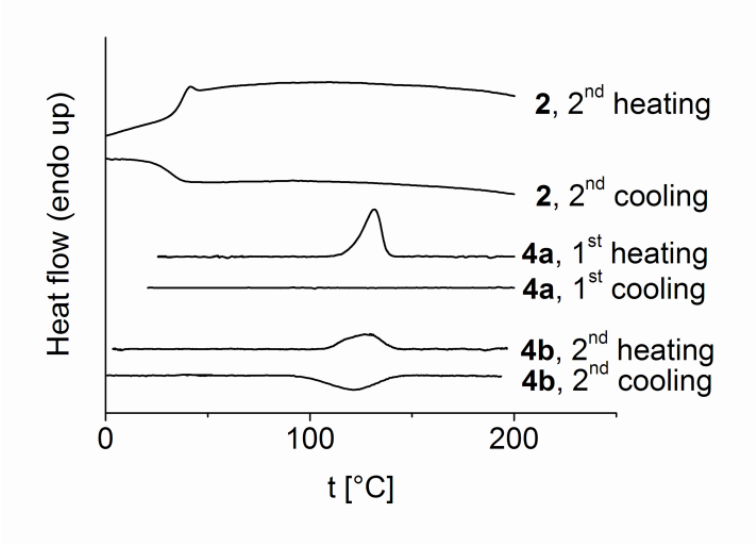

Figure 5: *DSC curves of [G2]-OH 2 and [G2]-b-PPerAcr 4a and 4b. The T_g of 2 cannot be observed in* ***4a*** *or* ***4b*** *any more, showing melting points of 112 °C and 109 °C respectively.*

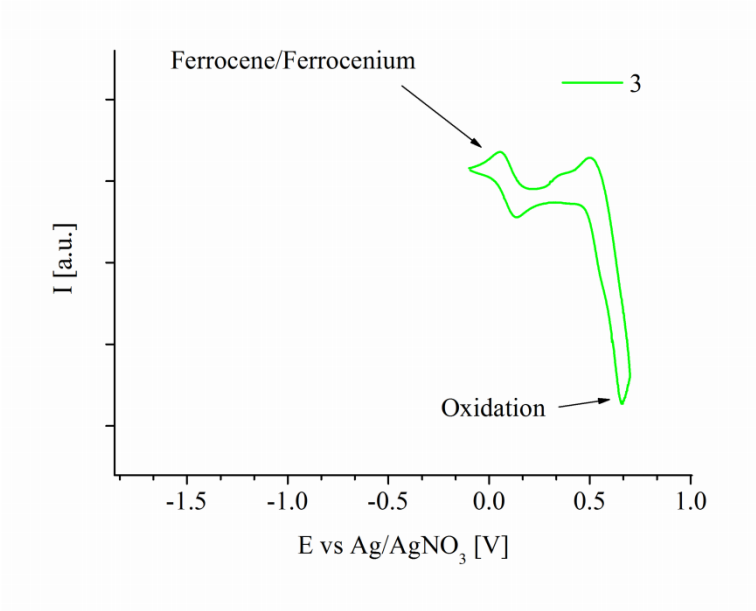

Figure 6: Cyclic voltammetry of dendron **3**.

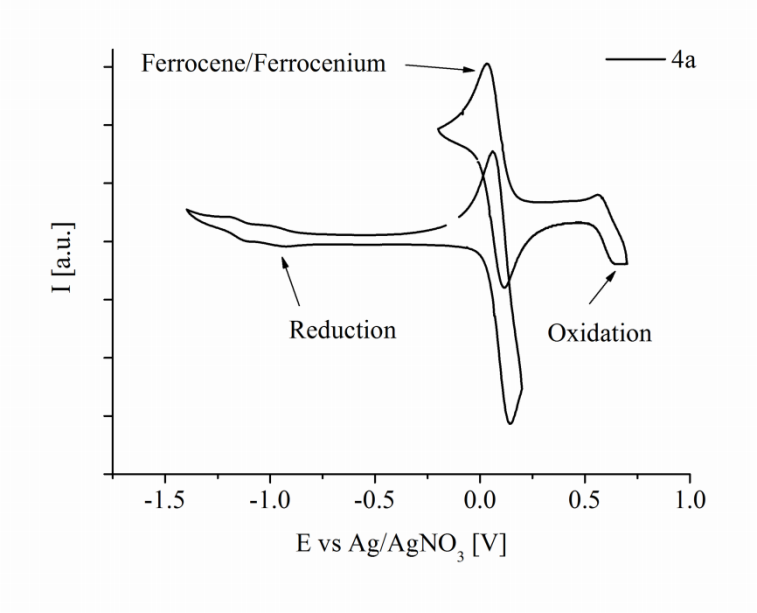

Figure 7: *Cyclic voltammetry of hybrid block copolymer* ***4a****.*

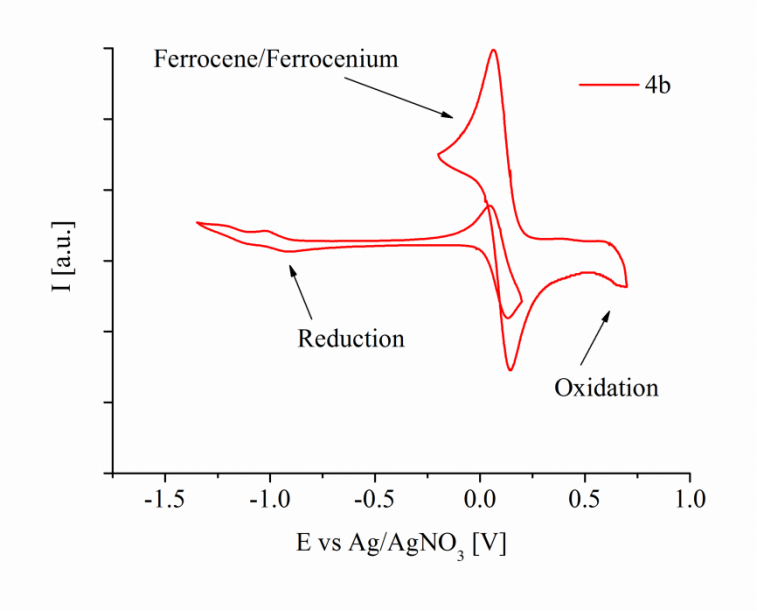

Figure 8: *Cyclic voltammetry of hybrid block copolymer* ***4b****.*

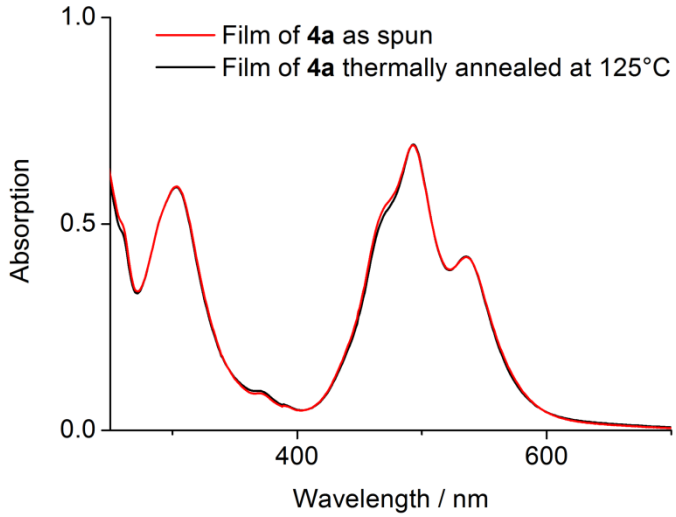

Figure 9: *Absorption spectrum of polymer* ***4a*** *of the film as spun and thermally annealed at 125°C for 5h.*

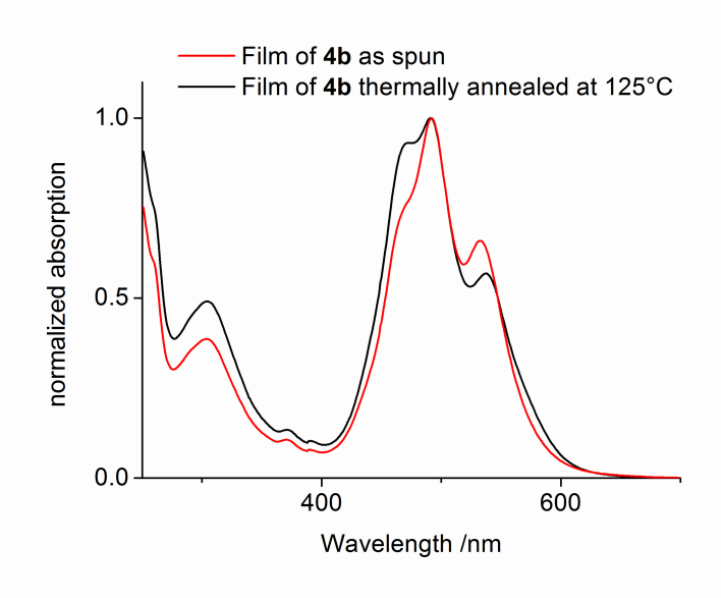

Figure 10: *Comparison of absorption spectrum of polymer* ***4b*** *of the film as spun and thermally annealed at 125°C for 5h (the intensities are normalized with respect to 493 nm).*

Bibliography

1. M. Jaiswal, R. Menon, *Polym Int* **2006**, *55*, 1371

2. S. Hüttner, M. Sommer, M. Thelakkat, *Applied Physics Letters* **2008**, *92*, 093302

3. M. C. Iovu, C. R. Craley, M. Jeffries-EL, A. B. Krankowski, R. Zhang, T. Kowalewski, R. D. McCullough, *Macromolecules* **2007**, *40*, 4733
4. S. M. Lindner, S. Hüttner, A. Chiche, M. Thelakkat, G. Krausch, *Angew. Chem. Int. Ed.* **2006**, *45*, 3364
5. M. Sommer, A. S. Lang, M. Thelakkat, *Angew. Chem. Int. Ed.* **2008**, *47*, 7901
6. H. Yan, Z. Chen, Y. Zheng, C. Newman, J. R. Quinn, F. Dötz, M. Kastler, A. Facchetti, *Nature* **2009**, *5*, 679
7. J. Zaumseil, H. Sirringhaus, *Chem. Rev.* **2007**, *107*, 1296
8. T. Kietzke, *Advances in OptoElectronics* **2007,** *2007***,** 40285
9. B. C. Thompson, J. M. J. Fréchet, *Angew. Chem. Int. Ed.* **2008**, *47*, 58
10. G. A. Buxton, N. Clarke, *Physical Review B* **2006**, *74*, 085207
11. M. Sommer, S. M. Lindner, M. Thelakkat, *Adv. Funct. Mater.* **2007**, *17*, 1493
12. S. M. Lindner, M. Thelakkat, *Macromolecules* **2004,** *37*, 8832
13. L. Wang, Z. Meng, Y. Yu, Q. Meng, D. Chen, *Polymer* **2008**, *49*, 1199
14. Y. Gao, X. Zhang, M. Yang, X. Zhang, W. Wang, G. Wegner, C. Burger, *Macromolecules* **2007**, *40*, 2606
15. B. K. Cho, A. Jain, S. M. Gruner, U. Wiesner, *Science* **2004**, *305*, 1598
16. M. E. Mackay, Y. Hong, M. Jeong, B. M. Tande, N. J. Wagner, S. Hong, S. P. Gido, R. Vestberg, C. J. Hawker, *Macromolecules* **2002**, *35*, 8391
17. J. J. Apperloo, R. A. J. Janssen, P. R. L. Malenfant, L. Groenendaal, J. M. J. Fréchet, *J. Am. Chem. Soc.* **2000**, *122*, 7042
18. N. Watanabe, C. Mauldin, J. M. J. Fréchet, *Macromolecules* **2007**, *40*, 6793
19. X. Chen, B. Gao, J. Kops, W. Batsberg, *Polymer* **1998**, *4*, 911
20. M. R. Leduc, C. J. Hawker, J. Dao, J. M. J. Fréchet, *J. Am. Chem. Soc.* **1996**, *118*, 11111
21. D. Benoit, V. Chaplinski, R. Braslau, C. J. Hawker, *J. Am. Chem. Soc.* **1999,** *121*, 3904
22. M. Sommer, S. Hüttner, M. Thelakkat, *Advanced Materials* **2008**, *20*, 2523
23. S. M. Lindner, N. Kaufmann, M., Thelakkat *Organic Electronics* **2007**, *8*, 69

Chapter 10

„Click" Chemistry for p-Type Semiconductor Materials

*Andreas S. Lang and Mukundan Thelakkat**

Applied Functional Polymers, Department of Macromolecular Chemistry I, University of Bayreuth, Universitätsstr. 30, 95440 Bayreuth, Germany

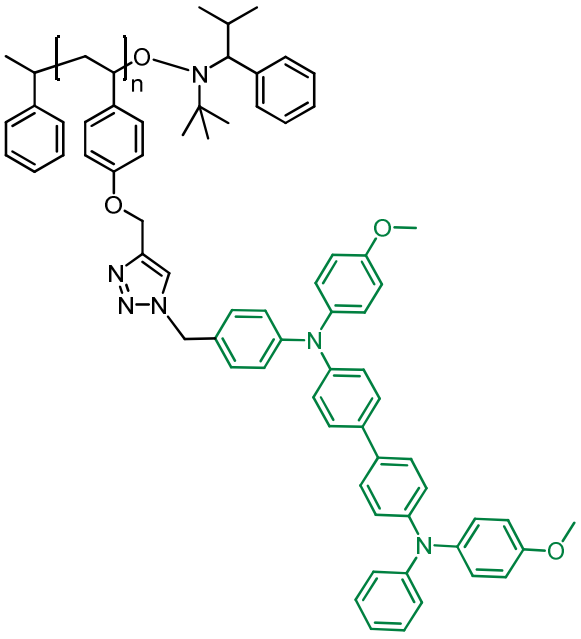

Abstract

The synthesis of a p-type semiconductor side-chain polymer with narrow molecular weight distribution and well defined molecular weight is presented here. The polymer (poly(*N*,*N*'-bis(4-methoxyphenyl)-*N*-phenyl-*N*'-4-triazolylphenyl-(1,1'-biphenyl)-4,4'-diamine), PDMTPD was synthesized successfully by a combination of nitroxide mediated polymerization of protected propargyl oxystyrene and copper catalyzed azide alkyne "click" chemistry of DMTPD-azide. The scaffold polymer poly(propargyl oxystyrene) had a PDI of 1.1. The click reaction between the two compounds was monitored by ^{1}H NMR and was found to proceed quantitatively. The final polymer could be obtained very easily by a single precipitation step. SEC shows that the resulting "clicked" polymer has a monomodal distribution, a narrow PDI of 1.09 and a molecular weight of 17 000 g/mol. The PDMTPD was also analyzed by ^{1}H NMR, DSC, UV/Vis and PL.

Introduction

Semiconductor polymers constitute an intensive research topic at present. Regarding their application in organic light emitting diodes (OLED),[1, 2] organic field effect transistors (OFET)[3, 4] or organic photovoltaic (OPV),[5, 6] these materials have the potential to revolutionize the technology of the future. For OPV applications, material requirements are versatile. They have to be thermally stable, have a low tendency to oxidize, have the required electronic levels for the photovoltaic application and have ideally a broad absorption. Taking these facts into account, it is clear that only tailor-made molecules stand a chance as a material for future applications. Semiconductor polymers can be divided into p-type and n-type polymers (i.e. donor and acceptor polymers). While n-type polymers are relatively rare (e.g. poly(perylene bisimide)[7]), p-type polymers are available in a wide variety, poly(3-hexylthiophene) being the most prominent at the moment.[8] A well known class of p-type semiconductors are polymers carrying triphenylamine (TPA) or tetraphenyl benzedine (TPD) units. Such polymers can be synthesized by polycondensation reactions as main chain polymers[9, 10] or as side chain polymers by controlled radical polymerization methods.[11-13] The latter can lead to polymers with narrow molecular weight distribution, controlled molecular weight and additionally offer the possibility to synthesize block copolymers. Such block copolymers were already synthesized by nitroxide mediated radical polymerization (NMRP) for the application in photovoltaic devices[12] and as block copolymers with poly(4-vinyl pyridine) to assemble nanoparticles.[13] Although these block copolymers could be achieved, the polymerization sequence of the monomers was always an issue because of incomplete initiation using macroinitiators carrying TPD moieties. Recent synthetic developments in polymer science such as the combination of controlled radical polymerization (CRP) and copper-catalyzed azide-alkyne cycloaddition (CuAAC, "click" chemistry)[14] have given scientists an elegant tool to create polymers in a diversity never known before. Generally, in this concept, an alkyne or azide functionalized monomer is polymerized using CRP followed by a subsequent polymer analogous copper-catalyzed "click" reaction with a respective azide or alkyne derivative. This allows the synthesis of manifold complex polymers out of functional "building bricks". Atom transfer radical polymerization (ATRP),[15, 16] reversible

Scheme 1: *Synthesis of an azide carrying DMTPD-N_3* ***4*** *starting from the DMTPD-mono aldehyde.*

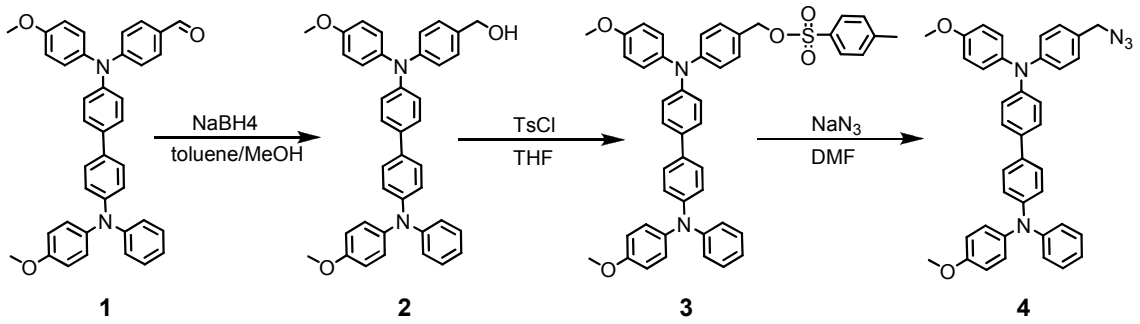

Scheme 2: *"Click" reaction between alkyne polymer, poly(propargyl oxystyrene)* ***5*** *and DMTPD-N_3* ***4*** *to synthesize the polymer PDMTPD* ***6****.*

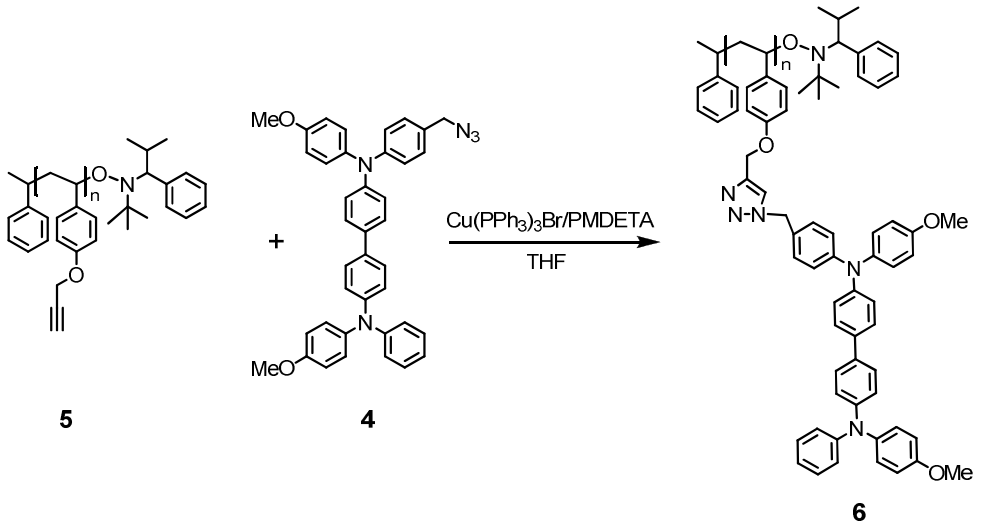

addition-fragmentation chain transfer polymerization (RAFT)[17, 18] and nitroxide mediated radical polymerization (NMRP)[19-21] have been applied in such concepts. Recently, the synthesis of different n-type poly(perylene bisimides) by a modular approach was shown by us.[22] Encouraged by the successful preparation of these n-type polymers we want to widen the "click" chemistry concept to p-type semiconductors and present the synthesis of a side chain polymer with pendant DMTPD by a combination of NMRP and "click" chemistry.

Results and Discussion

The synthetic route towards azide carrying *N*,*N*'-bis(4-methoxyphenyl)-*N*-phenyl-*N*'-4-azidophenyl-(1,1'-biphenyl)-4,4'-diamine, dimethoxy triphenyl diamine (DMTPD-N_3) is shown in Scheme 1. The synthesis starts from the DMTPD-aldehyde which was synthesized according to literature procedures published elsewhere.[12, 23] First, the aldehyde **1** was reduced to the alcohol with $NaBH_4$ as a reducing agent with high yields. The resulting alcohol DMTPD-OH **2** was activated

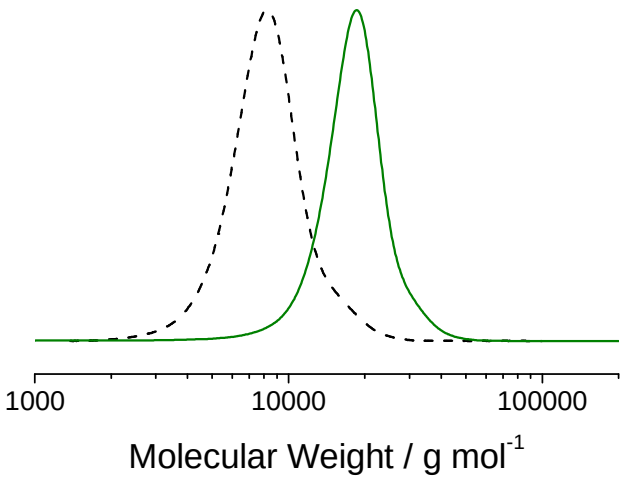

Figure 1: *SEC traces of scaffold polymer poly(propargyl oxystyrene)* ***5*** *(dashed line) and “clicked” semiconductor polymer PDMTPD* ***6*** *(green solid line). It can be seen that the molecular weight of the “clicked” polymer is significantly increased while the shape of the curve is preserved.*

with 4-toluenesulfonyl chloride to form a good leaving group in **3**. The subsequent exchange with NaN_3 gave the desired azide DMTPD-N_3 **4**.The poly(propargyl oxystyrene) **5** with an M_n of 7 400 g/mol (44 repeating units) and a PDI of 1.11 was synthesized according to literature procedure published elsewhere.[22] For the “click” reaction between DMTPD-N_3 **4** and poly(propargyl oxystyrene) **5** the pre-complexed copper catalyst Cu$(PPh_3)_3$Br was chosen. Such catalysts have the advantage that they are convenient in use and highly soluble in organic solvents. Also the stability of the Cu(I)$(PPh_3)_3$Br is much higher compared to easily oxidizable copper complexed by nitrogen ligands.[24] Standard catalyst systems as CuBr/PMDETA have to be formed in situ and are therefore not completely dissolved sometimes, if not formed prior to use and can contain Cu(II) species. An excess of DMTPD-N_3 **4** and poly(propargyl oxystyrene) **5** were dissolved in THF and the solution was degassed by purging with nitrogen for 10 min. The Cu$(PPh_3)_3$Br and one equivalent of PMDETA were added to the mixture to start the reaction (Scheme 2). After 24 h the reaction was stopped and purified by precipitation of the solution in acetone to remove the unreacted **4**. The pure “clicked” polymer could be obtained by this one simple precipitation and filtration step.

The polymer was studied by ^{1}H NMR to determine the conversion of the “click” reaction. After the “click” reaction, the signals of the prominent alkyne proton at 2.5 ppm, as well as that of the O*C*H_2 group at 4.6 ppm of alkyne polymer **5** disappear. In the “clicked” polymer **6**, the O*C*H_2 signals are shifted to 5.26 ppm. The signal of the newly formed triazole proton can be observed as broad signal at 7.66 ppm. The *C*H_2N_3 protons of the DMTPD-N_3 **4** at 4.46 ppm cannot be observed any more in polymer **6**, proving the absence of remaining DMTPD-N_3 **4**. The corresponding protons in the “clicked” polymers are now located adjacent to the newly-built

triazole unit and occur at 4.98 ppm. These facts prove the quantitative conversion of the alkyne groups to triazole.

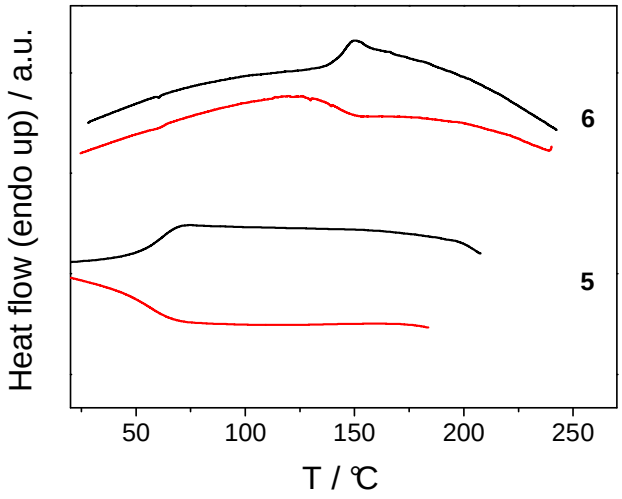

Figure 2: *DSC traces of scaffold polymer **5** and semiconductor "click" polymer PDMTPD **6** measured at 40 K/min. Both polymers show only one T_g at 59 °C and 144 °C, respectively, but no melting peaks.*

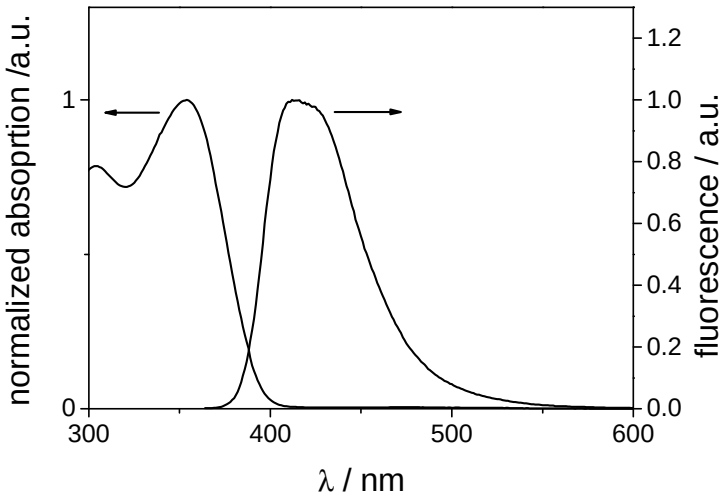

Figure 3: *Normalized UV/Vis absorption and fluorescence of PDMTPD **6** in THF solution.*

The semiconductor polymer PDMTPD **6** was studied by size exclusion chromatography (SEC). Figure 1 shows clearly that the molecular weight of the "clicked" polymer increases strongly after the "click" reaction while the PDI and the shape of the curve are well preserved compared to the scaffold polymer **5**. The "clicked" polymer PDMTPD exhibits a PDI of 1.09 and a molecular weight of 17 000 g/mol. This value is underestimated by SEC, if a degree of polymerization of 44 units is considered for polymer **5** and with 100% yield for the "click" reaction. Thus a theoretical molecular weight of 34 000 g/mol would be expected. Of course, the SEC is calibrated to

polystyrene, explaining this difference in molecular weight. The polymers were also studied by DSC. Figure 2 shows the DSC traces of scaffold polymer **5** and “clicked” semiconductor polymer **6** in comparison. Alkyne polymer **5** exhibits a T_g at 59 °C. After the “click” reaction to PDMTPD **6**, the T_g of the polymer is shifted to 144 °C. This value is very similar to the published T_g (148 °C) of (poly(*N*,*N*’-bis(4-methoxyphenyl)-*N*-phenyl-*N*’-4-vinylphenyl-(1,1‘-biphenyl)-4,4‘-diamine PvDMTPD polymerized by direct NMRP.[12] This means that the phase behavior of PDMTPD is not altered very much by the additional triazol unit. UV/Vis absorption measurement (Figure 3) of semiconductor polymer PDMTPD **6** in THF solution shows absorption up to 400 nm with a maximum at 354 nm. Exited at 354 nm the compound exhibits a strong blue fluorescence at 410 nm.

Conclusion

We have shown that the synthesis of a side chain p-type semiconductor polymer by the combination of nitroxide mediated radical polymerization and “click” chemistry is possible. The successful synthesis led to a polymer with narrow molecular weight distribution of 1.09 and a molecular weight of 17 000 g/mol. Quantitative conversion in the copper catalyzed azide-alkyne cycloaddition between the scaffold polymer **5** and the azide DMTPD-N_3 **4** could be proven by ^{1}H NMR. Polymers synthesized by this approach can be introduced as one block in fully functionalized block copolymers for organic photovoltaic or as homopolymer in blend systems or bilayer architectures. Also this work opens the general field of polymer analogous functionalization with p-type semiconductors.

Experimental

General

The synthesis of poly(propargyl oxystyrene) was shown elsewhere.[22] Dimethylformamide (99.8%) were purchased from Sigma-Aldrich. PMDETA (≥98%) was purchased from Fluka. All reagents were used without further purification unless otherwise noted. ^{1}H NMR (300 MHz) spectra were recorded on a Brucker AC 300 spectrometer in $(CD_3)_2SO$ and calibrated to $(CH_3)_2SO$ signal (2.54 ppm for ^{1}H). UV-vis spectra of solutions in THF with a concentration of 10^{-5} mol·L^{-1} were recorded on a Hitachi 3000 spectrophotometer and photoluminescence spectra were acquired on a Shimadzu RF 5301 PC spectrofluorophotometer upon excitation at 490 nm. SEC measurements were carried out in THF with two Varian MIXED-C columns (300x7.5 mm) at room temperature and at a flow rate of 0.5 mL/min using UV (Waters model 486) with 254 nm detector wavelength and refractive index (Waters model 410) detectors. Polystyrene in combination with *o*-DCB as an internal standard was used for calibration. Differential scanning calorimetry experiments were conducted at heating rates of 40 K·min^{-1} under N_2 atmosphere with a Perkin Elmer Diamond DSC, calibrated with indium. Thermogravimetry measurements were conducted on a Mettler Toledo TGA/SDTA 851^e under N_2 atmosphere at a heating rate of 10K/min.

Synthesis

N,*N*'-bis(4-methoxyphenyl)-*N*-phenyl-*N*'-4-carbonylphenyl-(1,1'-biphenyl)-4,4'-diamine (DMTPD-CHO) 1

DMF (6 mL) was cooled to 0 °C, freshly distilled $POCl_3$ (153.3 g, 0.91 mL) was added and stirred for 30 min at 0 °C. Then the mixture was brought to RT and stirred until a red complex was built. DMTPD (5.48 g, 10.0 mmol) was dissolved in DCM and cooled to 0 °C. The preformed complex was added and the reaction was stirred at 0 °C for 15 min. Subsequently the temperature was risen to 80 °C and the reaction was stirred for 3 h. The reaction was cooled to RT and 5 g Na acetate in 25 mL of H_2O and ice were added carefully under vigorous stirring. The mixture was stirred over night. The organic phase was separated and the water phase was extracted with DCM twice. The organic phases were combined, dried over Na_2SO_4, filtered and evaporated. The product was purified by column chromatography over silica with CH_2Cl_2 as eluent. The obtained product weighed 3.0 g (52 %). ^{1}H NMR (300 MHz, DMSO): δ (ppm) 9.72 (s, 1H, C*H*O), 7.40-6.70 (m, 24 H, Ar*H*), 3.70 (s, 6H, CH_3),

N,*N*'-bis(4-methoxyphenyl)-*N*-phenyl-*N*'-4-hydroxylphenyl-(1,1'-biphenyl)-4,4'-diamine (DMTPD-OH) 2

DMTPD-CHO (0.72 g, 1.3 mmol) was dissolved in 15mL of a 1:1 mixture of dry toluene and dry ethanol under inert gas atmosphere. $NaBH_4$ (95 mg, 2.50 mmol) was added and the reaction was stirred for 2h at RT. The progress of the reaction was controlled by thin film chromatography. The solvents were evaporated, the residue was washed with H_2O two times, filtered and dried. The light yellow powder weighed 720 mg (99.5 %).^{1}H NMR (300 MHz, DMSO): δ (ppm) 7.52-6.83 (m, 24 H, Ar*H*), 5.11 (t, 1 H, *J* = 5.2 Hz, CH_2O*H*), 4.43 (d, 2H, *J* = 4.0 Hz, CH_2OH), 3.74 (s, 6H, OCH_3).

N,*N*'-bis(4-methoxyphenyl)-*N*-phenyl-*N*'-4-tosylphenyl-(1,1'-biphenyl)-4,4'-diamine (DMTPD-Tos) 3

DMTPD-OH (579 mg, 1.00 mmol) was dissolved in 15 mL of THF under inert gas atmosphere. Triethylamine (0.7 mL) was added to the solution which was stirred for 10 min. Subsequently, tosylchloride (1.91 g, 10.0 mmol) was added and the reaction was stirred for 24 h at RT. The solvents were evaporated, the solid dissolved in $CHCl_3$ and washed with a solution of NH_4Cl in H_2O. The organic phase was dried with Na_2SO_4, filtered and evaporated. The raw product was further purified by column chromatography over silica cyclohexane:ethyl acetate 2:1 to remove side products. The pure fraction was flushed from the column with DCM:MeOH 1:1 afterwards. The fractions containing the product were evaporated. The light yellow powder weighed 558 mg (76.1 %). ^{1}H NMR (300 MHz, DMSO): δ (ppm) 7.61-6.83 (m, 28H, ArH_{TPD}, ArH_{Tosyl}), 4.36 (s, 2H, CH_2OTos), 3.76 (s, 6H, OCH_3), 2.10 (s, 3H, ArCH_3).

_N_,_N_'-bis(4-methoxyphenyl)-_N_-phenyl-_N_'-4-azidylphenyl-(1,1'-biphenyl)-4,4'-diamine (DMTPD-N_3) 4

DMTPD-Tos (550 mg, 0.75 mmol) was dissolved in dry DMF under inert gas atmosphere. NaN_3 (97 mg, 1.50 mmol) was added and the reaction was heated to 100 °C for 3 h. After cooling to RT the reaction was quenched with 10 mL of H_2O. The product was extracted with $CHCl_3$, the organic phase was dried with Na_2SO_4, filtered and evaporated. For further purification, the compound was cleaned by column chromatography over silica with a gradient of hexanes:ethyl acetate 9:1 to 5:1. The product was obtained as a light yellow powder and weighed 330 mg (72.8 %).^{1}H NMR (300 MHz, DMSO): δ (ppm) 7.56-6.88 (m, 24H, Ar*H*), 4.36 (s, 2H, C*H*$_2$N$_3$), 3.75 (s, 6H, OC*H*$_3$).

Click reaction of DMTPD-N_3 and poly(propargyl oxystyrene) to (PDMTPD) 6

DMTPD-N_3 (100.0 mg, 0.166 mmol) and poly(propargyl oxystyrene) (21.8 mg, 0.140 mmol) were dissolved in 2 mL of THF. The solution was degassed by purging with nitrogen for 10 min and sealed with a septum. To start the reaction, $Cu(PPh_3)_3Br$ (12.8 mg, 0.014 mmol) and PMDETA (2.4 mg, 0.014 mmol) were added under inert gas atmosphere. The reaction was stirred for 24 h, precipitated from acetone and filtered. The pure product was a slightly yellow powder. ^{1}H NMR (300 MHz, $CDCl_3$): δ (ppm) 7.66 (br s, 1H, Triazol-*H*), 7.42-6.14 (m, 24 H, Ar*H*), 5.26 (br s, 2H, OC*H*$_2$), 4.98 (br s, 2H, N-C*H*$_{2,triazol}$), 3.81-3.57 (m, 6H, OC*H*$_3$), 1.82-1.00 (br s, 3H, polymer backbone).

Acknowledgement

Financial support from DFG (GRK 1640 and SPP 1355) are kindly acknowledged

Bibliography

1. Tang, C. W.; VanSlyke, S. A. *Applied Physics Letters* **1987,** 51, (12), 913-915.
2. Burroughes, J. H.; Bradley, D. D. C.; Brown, A. R.; Marks, R. N.; Mackay, K.; Friend, R. H.; Burns, P. L.; Holmes, A. B. *Nature* **1990,** 347, (6293), 539-541.
3. Drury, C. J.; Mutsaers, C. M. J.; Hart, C. M.; Matters, M.; Leeuw, D. M. d. *Applied Physics Letters* **1998,** 73, (1), 108-110.
4. Sirringhaus, H.; Tessler, N.; Friend, R. H. *Science* **1998,** 280, (5370), 1741-1744.
5. Tang, C. W. *Applied Physics Letters* **1986,** 48, (2), 183-185.
6. Yu, G.; Gao, J.; Hummelen, J. C.; Wudl, F.; Heeger, A. J. *Science* **1995,** 270, (5243), 1789-1791.
7. Lindner, S. M.; Hüttner, S.; Chiche, A.; Thelakkat, M.; Krausch, G. *Angewandte Chemie International Edition* **2006,** 45, (20), 3364-3368.
8. Lohwasser, R. H.; Thelakkat, M. *Macromolecules* **2011,** 44, (9), 3388-3397.

9. Thelakkat, M.; Hagen, J.; Haarer, D.; Schmidt, H. W. *Synthetic Metals* **1999,** 102, (1-3), 1125-1128.

10. Ishikawa, M.; Kawai, M.; Ohsawa, Y. *Synthetic Metals* **1991,** 40, (2), 231-238.

11. Zorn, M.; Weber, S. A. L.; Tahir, M. N.; Tremel, W.; Butt, H.-J. r.; Berger, R. d.; Zentel, R. *Nano Letters* **2010**, 10, (8), 2812-2816.

12. Sommer, M.; Lindner, S. M.; Thelakkat, M. *Advanced Functional Materials* **2007,** 17, (9), 1493-1500.

13. Maria, S. b.; Susha, A. S.; Sommer, M.; Talapin, D. V.; Rogach, A. L.; Thelakkat, M. *Macromolecules* **2008,** 41, (16), 6081-6088.

14. Binder, W. H.; Sachsenhofer, R. *Macromolecular Rapid Communications* **2008,** 29, (12-13), 952-981.

15. Gao, H.; Matyjaszewski, K. *Journal of the American Chemical Society* **2007,** 129, (20), 6633-6639.

16. Ladmiral, V.; Mantovani, G.; Clarkson, G. J.; Cauet, S.; Irwin, J. L.; Haddleton, D. M. *Journal of the American Chemical Society* **2006,** 128, (14), 4823-4830.

17. Quémener, D.; Hellaye, M. L.; Bissett, C.; Davis, T. P.; Barner-Kowollik, C.; Stenzel, M. H. *Journal of Polymer Science Part A: Polymer Chemistry* **2008,** 46, (1), 155-173.

18. Zhang, X.; Lian, X.; Liu, L.; Zhang, J.; Zhao, H. *Macromolecules* **2008,** 41, (21), 7863-7869.

19. Lang, A. S.; Neubig, A.; Sommer, M.; Thelakkat, M. *Macromolecules* **2010,** 43, (17), 7001-7010.

20. Malkoch, M.; Thibault, R. J.; Drockenmuller, E.; Messerschmidt, M.; Voit, B.; Russell, T. P.; Hawker, C. J. *Journal of the American Chemical Society* **2005,** 127, (42), 14942-14949.

21. Fleischmann, S.; Komber, H.; Voit, B. *Macromolecules* **2008,** 41, (14), 5255-5264.

22. Lang, A. S.; Thelakkat, M. *Polymer Chemistry* **2011,** 10.1039/C1PY00191D.

23. Schmitz, C.; Thelakkat, M.; Schmidt, H.-W. *Advanced Materials* **1999,** 11, (10), 821-826.

24. Lal, S.; Diez-Gonzalez, S. *The Journal of Organic Chemistry* **2011,** 76, (7), 2367-2373.

Chapter 11

Semiconductor Block Copolymers: The Influence of Polar Substitution on Microphase Separation

*Andreas S. Lang,[1] Guo-Dong Fu[1,2] and Mukundan Thelakkat[1]**

[1]Applied Functional Polymers, Department of Macromolecular Chemistry I, University of Bayreuth, Universitätsstr. 30, 95440 Bayreuth, Germany

[2]School of Chemistry and Chemical Engineering, Southeast University, Nanjing, China 211189

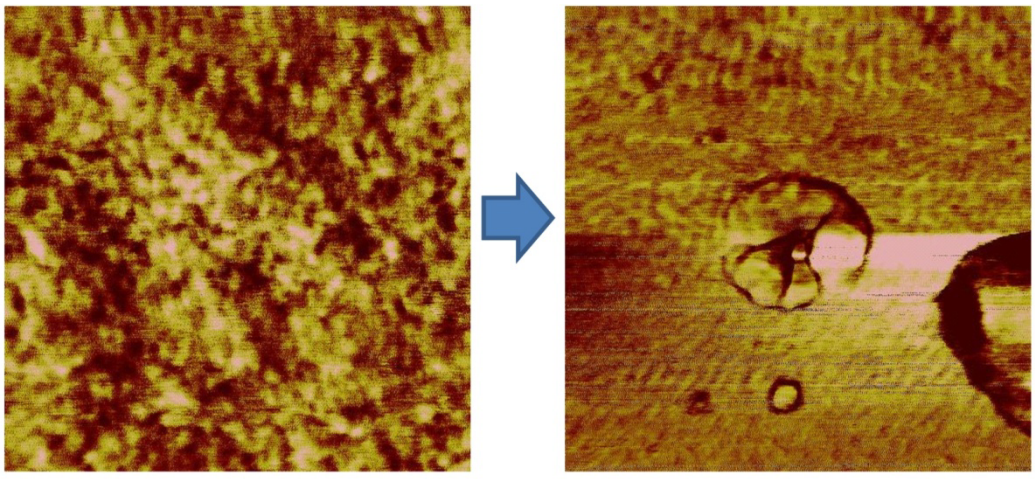

Abstract

To understand the role of hydrophilic-hydrophobic interactions on microphase separation in donor-acceptor (D-A) block copolymers, a comparative study is presented here. Four different donor-acceptor (D-A) block copolymers were synthesized using a combination of RAFT and "click" chemistry. Two block copolymers with an identical poly(propargyl acrylate) block length and different poly(dimethoxy triphenylamine) block length were first synthesized. Finally, the alkyne bearing propargyl acrylate block was "clicked" with hydrophobic or hydrophilic substituted perylene bisimides by copper-catalyzed azide-alkyne cycloaddition. The resulting semiconductor D-A block copolymers with hydrophilic or hydrophobic perylene bisimide blocks were compared regarding their optical properties and phase separation behavior. The compared block copolymers exhibit similar volume fractions and differ only in the substitution of the pending perylene bisimides.

Introduction

Organic photovoltaic (OPV) is currently under intensive research.[1, 2] This innovative concept could revolutionize the market for photovoltaic if efficiency and long term stability can be solved. The possibility to print photovoltaic cells on flexible substrates would allow roll-to-roll printing and thereby lead to low production costs.[3] Established OPV uses usually blend systems out of two components.[4] These components have to phase separate in such a way, that on the one hand a high interface is generated, which governs the generation of charges, and on the other hand, structures in the regime of 10s of nanometers have to be produced, so that excitons can travel to this interface before they recombine. Because binary mixtures tend to macrophase separate in their equilibrium structure, big effort is driven to produce films in a certain time, temperature and from special solvents or solvent mixtures, so that non-equilibrium structures can be "frozen in" to obtain fine percolating structures of certain size. The long term stability of such structures can be problematic due to a certain diffusion of the components, especially at elevated temperatures which are inevitable in outdoor application, in the bright sun. To avoid this problem, a solution can be the use of donor-acceptor block copolymers.[5-9] Here, one block is the acceptor and the other block the donor component. Due to the intrinsic tendency of block copolymers to phase separate into nanometer sized microstructures, an equilibrium structure of block copolymers as lamella or cylinder would be the ideal setup for organic photovoltaic devices, since a phase separation in the regime of 10s nanometers can be accomplished. Ideally, these phases have to phase separate in strict compartments of the respective material because otherwise recombination of the charges would take place. To get this, the material has to fulfill certain requirements. On the one hand, the volume fractions of the blocks have to be in the right ratio to each other to allow the desired geometry.[10] On the other hand, the χN factor has to be high enough so that phase separation can occur.[10, 11] Here, N is the number of repeating units and

Scheme 1: *Synthetic scheme of the synthesis of hydrophobic-hydrophobic block copolymers* ***9a,b*** *and hydrophilic-hydrophobic block copolymers* ***10a,b****.*

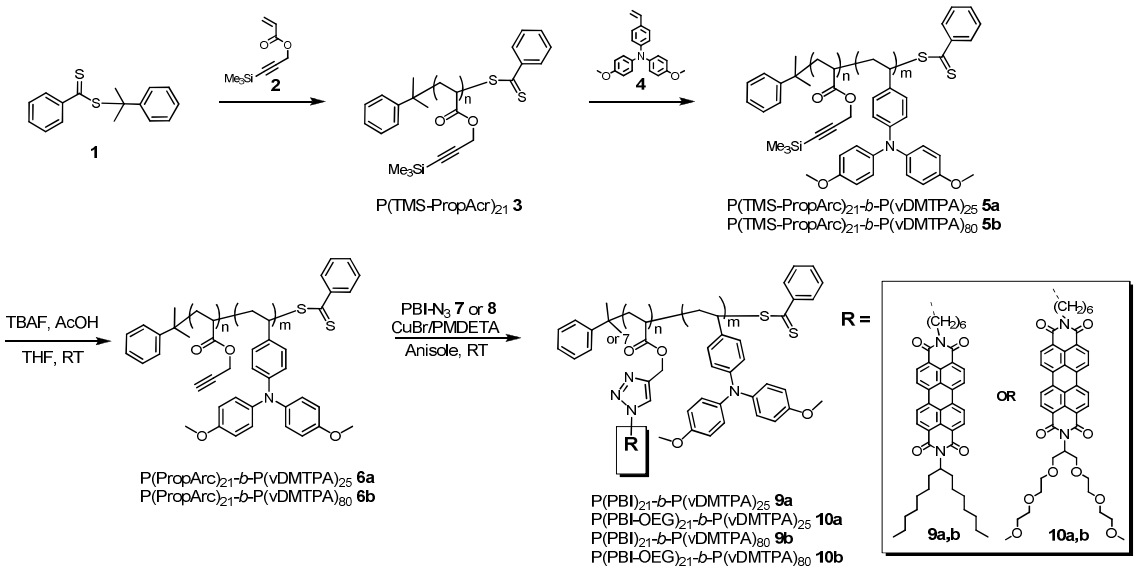

Table 1: *SEC data and theoretical calculated molecular weights of the synthesized polymers.*

polymer	M_n [g/mol] (SEC)[a]	M_w/M_n (SEC)[a]	M_n [g/mol] (^{1}H NMR)[b]	wt% Perylene Bisimide (^{1}H NMR)[c]	notes
3	4 200	1.09	-	-	$P(TMS\text{-}PropAcr)_{21}$
5a	12 600	1.11	12 500	-	$P(TMS\text{-}PropArc)_{21}$-*b*-$P(vDMTPA)_{25}$
5b	34 000	1.20	30 600	-	$P(TMS\text{-}PropArc)_{21}$-*b*-$P(vDMTPA)_{80}$
6a	9 800	1.11	11 000	-	$P(PropArc)_{21}$-*b*-$P(vDMTPA)_{25}$
6b	30 000	1.20	29 100	-	$P(PropArc)_{21}$-*b*-$P(vDMTPA)_{80}$
9a	56 000	1.12	27 200	69	$P(PBI)_{21}$-*b*-$P(vDMTPA)_{25}$
10a	64 000	1.18	28 600	70	$P(PBI\text{-}OEG)_{21}$-*b*-$P(vDMTPA)_{25}$
9b	98 000	1.13	45 300	41	$P(PBI)_{21}$-*b*-$P(vDMTPA)_{80}$
10b	93 000	1.09	46 700	43	$P(PBI\text{-}OEG)_{21}$-*b*-$P(vDMTPA)_{80}$

χ describes the Flory-Huggins interaction parameter which is influenced by the miscibility of the two polymer blocks. Thus, to enhance phase separation, either N can be increased or χ or both. A typical example of high χ block copolymers are polymers with one polar and one apolar block e.g. PS-*b*-PEO.[12-14] In this manuscript, we compare a donor-acceptor block copolymer with one polar and one apolar block with a D-A block copolymer with two apolar blocks to elucidate if phase separation in these polymers can be enhanced by increasing the hydrophobic-hydrophilic interactions. To achieve maximal comparability the modular approach of "click" chemistry[15, 16] was chosen, which allows the synthesis of such block copolymers with exactly the same degree of polymerization but a variable modification of one block. Besides the synthesis, preliminary results of the phase separation studies are shown here.

Results and discussion

The scheme of synthesis of the block copolymers is shown in Scheme 1. The RAFT method was chosen because of its wide applicability and easy control.[17-19] For the block copolymer synthesis, we chose a subsequent polymerization of trimethylsilyl protected propargyl acrylate and vinyl dimethoxy triphenylamine (vDMTPA). The poly(TMS-propargyl acrylate) block **3** was synthesized with a $M_{n,SEC}$ of 4 200 g/mol corresponding to 21 repeating units. This block was used as macro-RAFT agent for the two block copolymers **5a** and **5b** with different lengths of PvDMTPA as second block. Block copolymer **5a** exhibits a $M_{n,SEC}$ of 12 600 g/mol and a PDI of 1.11 while block copolymer **5b** has a higher molecular weight of 34 000 g/mol and a PDI of 1.20. Both block copolymers exhibit shoulders at approximately double molecular weight. This could be due to coupling reactions upon the quenching of the polymer. The composition of the block copolymers could be determined by ^{1}H NMR by comparing aromatic signals of triphenylamine and the OC*H*$_2$ protons of the poly(TMS-propargyl acrylate). From this, the theoretical molecular weights of all following polymers could also be determined by calculation and are shown as $M_{n,NMR}$ (Table 1). After deprotection of the alkyne group with tetrabutylammoniumfluoride, the block copolymers **6a** and **6b** with $M_{n,SEC}$ of 9 800 g/mol and 30 000 g/mol and with PDIs of 1.12 and 1.18, respectively, were obtained. The complete deprotection was proven by ^{1}H NMR where no protons of the $SiMe_3$ group at 0.20 ppm could be observed any more. Each of these two block copolymers was now "clicked" with either hydrophobic perylene bisimide (PBI) azide **7** with alkyl swallow-tail substituent or hydrophilic PBI azide **8** with oligo ethylene glycol swallow-tail substituent. Thus, out of the resulting four new block copolymers, two have hydrophobic-hydrophobic blocks (**9a** and **9b**) while the other two have hydrophilic-hydrophobic (**10a** and **10b**) blocks. The "clicked" polymers were purified in a soxhlet apparatus by extraction with acetone to wash out the excess of PBI-N_3. All PBI-N_3 could be removed by this way. Table 1 shows an overview of the SEC data and the calculated molecular weights of the synthesized polymers.

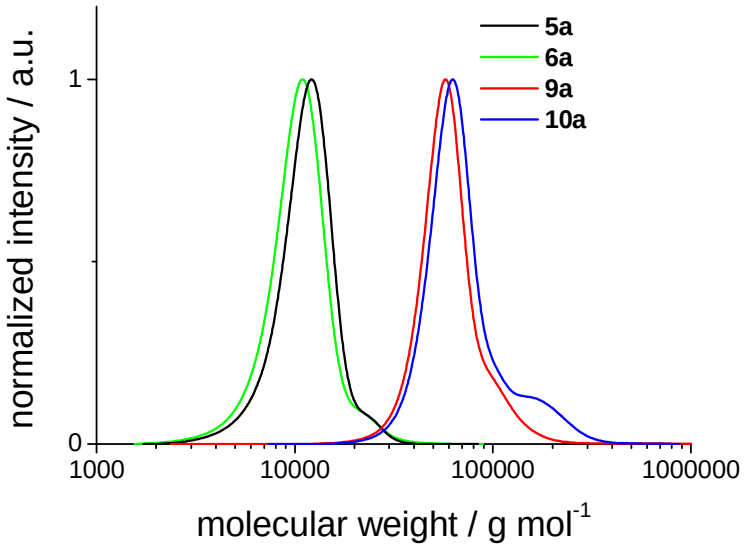

Figure 1: *SEC traces of protected block copolymer P(TMS-PropArc)$_{21}$-b-P(vDMTPA)$_{25}$* ***5a****, deprotected block copolymer* ***6a*** *and the two final "clicked" block copolymers* ***9a*** *(hydrophobic-hydrophobic) and* ***10a*** *(hydrophilic-hydrophobic).*

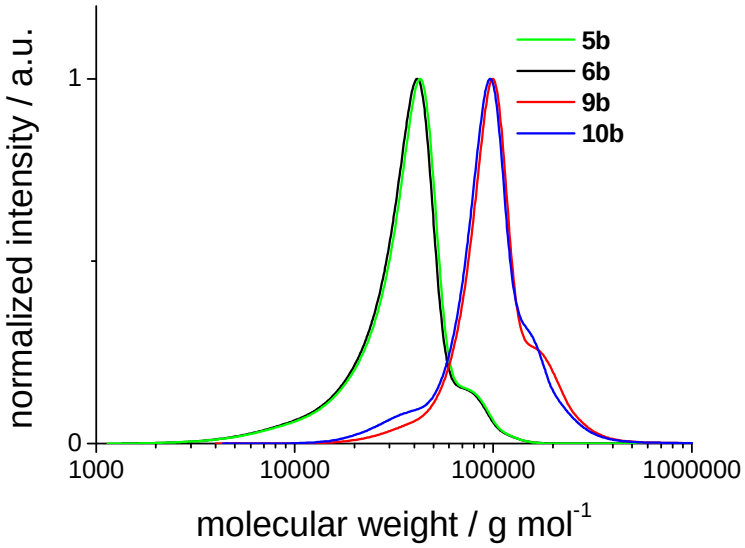

Figure 2: *SEC traces of protected block copolymer P(TMS-PropArc)$_{21}$-b-P(vDMTPA)$_{80}$* ***5b****, deprotected block copolymer* ***6b*** *and the two resulting "clicked" block copolymers* ***9b*** *(hydrophobic-hydrophobic) and* ***10b*** *(hydrophilic-hydrophobic).*

All polymers were analyzed by size exclusion chromatography (SEC) in THF. Figure 1 shows the SEC traces of the protected precursor block copolymer **5a**, the deprotected precursor block copolymer **6a** and of the "clicked" block copolymers **9a** with $M_{n,SEC}$ of 56 000 g/mol and **10a** with $M_{n,SEC}$ of 64 000 g/mol with PDIs of 1.12 and 1.18, respectively. The curves are clearly shifted to higher molecular weight after the "click" reaction. As can be seen from Figure 1 both block copolymers exhibit a shoulder which was also present in the precursor block copolymers **5a** and **6a**. Figure 2 shows the SEC traces of the protected precursor block copolymer **5b**, the deprotected precursor block copolymer **6b** and of the "clicked" block copolymers **9b** with $M_{n,SEC}$ of 98 000 g/mol and **10b** with $M_{n,SEC}$ of 93 000 g/mol with PDIs of 1.13 and 1.09, respectively. The curves are clearly shifted to higher molecular weight after the "click" reaction. As can be seen from Figure 2 both block copolymers exhibit a small shoulder at lower molecular weight and a stronger shoulder at higher molecular weight. Both were also present in the precursor block copolymers **5b** and **6b**. The main molecular weight peaks of **9b** and **10b** are quite similar in shape as expected.

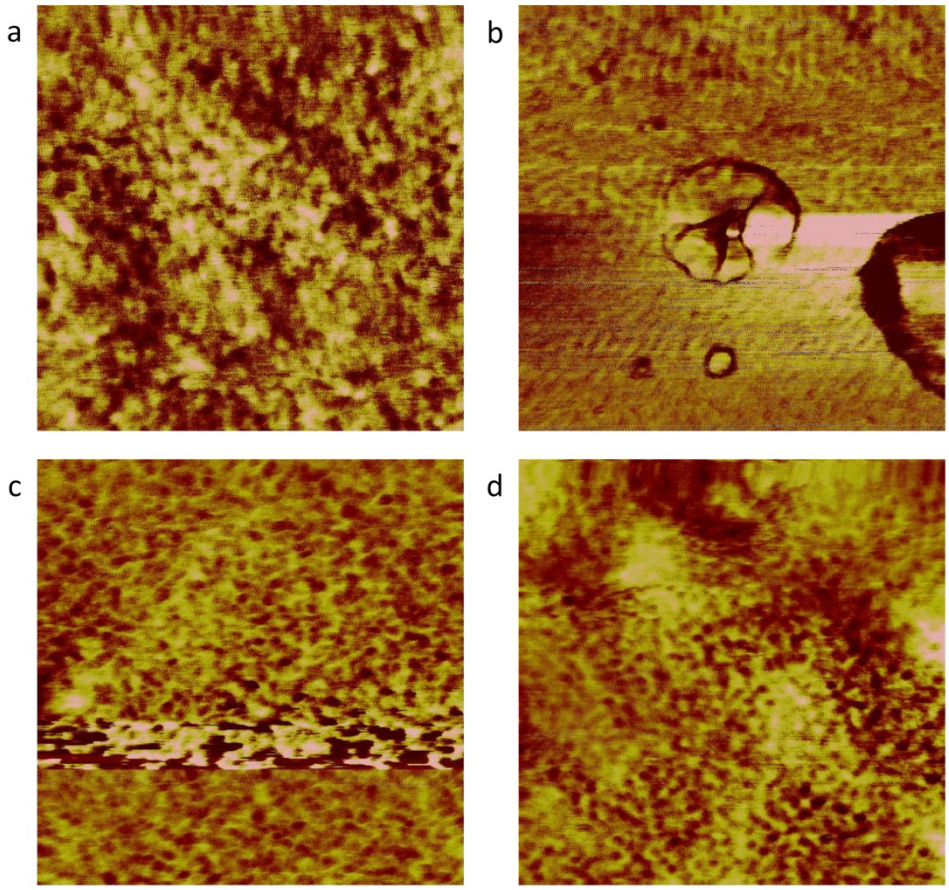

Figure 3: *AFM micrographs of annealed samples of polymers **9a**, **10a**, **9b** and **10b**. Comparing hydrophobic-hydrophobic block copolymer **9a** in a) and hydrophilic-hydrophobic block copolymer **10a** in b) clearly shows a change in phase behavior from disordered to lamellar ordering. The difference in the higher molecular weight polymers **9b** and **10b** is not so clear. The structures are similar and only a bit more clearly seen in d).*

Atomic force microscopy (AFM) was used to visualize the topography and surface of thin films of the block copolymers. The samples were prepared by spin-coating chloroform solutions of the block copolymers on ITO. The films were thermally annealed for 4 h at 250 °C under inert gas atmosphere to enhance the microphase separation. Figure 3 shows AFM phase images of the hydrophobic-hydrophobic block copolymers **9a,b** (Figure 3a, 3c) and hydrophilic-hydrophobic block copolymers **10a,b** (Figure 3b, 3d) with different weight fractions. Comparing the hydrophobic-hydrophobic block copolymer **9a** and the hydrophilic-hydrophobic block copolymer **10a** with similar perylene bisimide block weight fractions around 69% shows that no clear structure can be observed in **9a** (Figure 3a), but a lamellar structure in **10a** (Figure 3b). It is evident, that the morphology observed on the surface of the films is strongly dependent on the substitution. This could be explained by the relatively short block copolymers. In **9a** the χN parameter is not sufficient to form a proper phase separation. By the additional hydrophilic-hydrophobic driving force in **10a**, which increase χ, the χN parameter is high enough to let the block copolymer phase separate.

The higher molecular weight polymers **9b** and **10b** with perylene bisimide block weight fractions around 41% both exhibit a grainy wormlike structure on the film surface (Figure 3c) and d)). These structures are quite similar to each other and appear only a bit more clearly in d). We assume that in these higher molecular weight block copolymers, the χN parameter is high enough for phase separation in both block copolymers because of a higher N. The increase in χ in block copolymer **10b** does not make any visual difference anymore. It is possible, that the phase

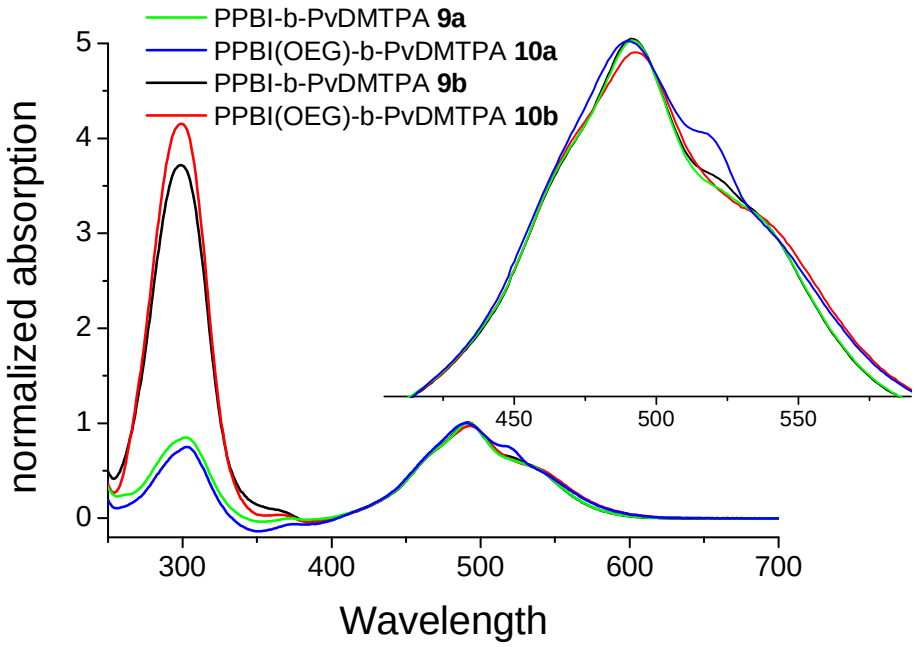

Figure 4: *UV/Vis absorption spectra of the "clicked" block copolymers, normalized to the absorption maximum of perylene bisimide at 490 nm.*

separation in **10b** builds purer phases, but this cannot be proven from the present data. Further analyses of bulk and thin film morphology using SEM and TEM have to be carried out. It is noted that similar published block copolymers show similar phase morphologies at comparable weight fractions.[5]

The absorption spectra of the four block copolymers **9a**, **9b**, **10a** and **10b** in THF solution (0.02 mg/mL) are shown in Figure 4. All polymers exhibit the TPA absorption at 300 nm and the perylene bisimide absorption between 400 and 600 nm. The smaller block copolymers **9a** and **10a** show identical absorption intensity for both TPA and PBI, indicating an identical composition of the two blocks. The higher molecular weight block copolymers **9b** and **10b** show a small difference in the intensity of their TPA absorption. Block copolymer **10b** exhibits a higher absorption of TPA compared to block copolymer **9b**, indicating a higher content of TPA compared to perylene bisimide, to which the spectra are normalized. This could be an indication that the "click" reaction in high molecular weight block copolymer **10b** was not 100% complete.

Conclusion

The presented results are only preliminary but give a first impression of how the introduction of polar oligoethylene glycol groups in the perylene bisimide block can enhance the phase separation in semiconductor block copolymers. Further, utilizing RAFT and "click" chemistry, comparable D-A block copolymers were obtained with ease, compared to earlier sequential synthesis of similar block copolymers. "Click" chemistry allows the introduction of any perylene moieties to a scaffold polymer.

Experimental part

General

Vinyl dimethoxy triphenylamine 4 was synthesized according literature.[5] *N*-(1-Heptyloctyl)-perylene-3,4,9,10-tetracaboxylic acid bisimide **7** and *N*-(1,3-bis(2-(2-(2-methoxyl)ethoxyl)ethoxyl)propyl) perylene-3,4,9,10-tetracaboxylic acid bisimide **8** were prepared according to a published procedure.[20] Tetrabutylammonium fluoride (>98%), and PMDETA (≥98%) were purchased from Fluka. CuBr (98%) was bought from Acros. All other chemicals were purchased from Sigma-Aldrich. All reagents were used without further purification unless otherwise noted.

^{1}H NMR (300 MHz) spectra were recorded on a Brucker AC 300 spectrometer in $CDCl_3$ and calibrated to $CHCl_3$ signal (7.26 ppm for ^{1}H). UV-vis spectra of solutions in $CHCl_3$ with a concentration of 10^{-5} mol·L^{-1} were recorded on a Hitachi 3000 spectrophotometer and photoluminescence spectra were acquired on a Shimadzu RF 5301 PC spectrofluorophotometer upon excitation at 490 nm. SEC measurements were carried out in THF with 0.25% tetrabutylammoniumbromide with two Varian MIXED-C columns (300x7.5 mm) at room temperature and at a flow rate of 0.5 mL/min using UV (Waters model 486) with 254 nm detector

wavelength and refractive index (Waters model 410) detectors. Polystyrene in combination with *o*-DCB as an internal standard was used for calibration.

Synthesis

Poly(trimethyl silyl propargyl acrylate) (PTMSPA) (1)

Trimethyl silyl propargyl acrylate (1.85 g, 10.0 mmol), 2-phenylpro-2-yl dithiobenzoate (53 mg, 0.2 mmol), AIBN (8.2 mg, 0.05mmol) and 0.5 mL of toluene were introduced into a 10 mL schlenk tube. The solution was degassed by three freeze-pump-thaw cycles. The tube was placed in a preheated oil bath with 60 °C for 20 h. Then the reaction was quenched in an ice bath. The polymer solution was put in a large amount of methanol and kept at -35 °C for 24 h. Then the top solvent was removed carefully and more methanol was added. After three cycles of freezing, removal of top solvent and addition of more methanol, the polymer was kept under high vacuum overnight to remove the residual solvent. About 1.2 g of red polymer was obtained. M_n=4.2x10^3 g/mol, PDI = 1.09. ^{1}H NMR (300 MHz, $CHCl_3$): δ (ppm) 4.68 (s, 2H, OC$H_{2,\text{acrylate}}$), 2.40 (br s, 1H, CHC$H_{2,\text{acrylate}}$), 2.07-1.56 (m, 2H, CHCH_2), 0.20 (s, 9H, $SiMe_3$).

Poly(TMS-propargyl acrylate)-*b*-PvDMTPA 5a,b

PTMSPA (0.20 g, 1.1 mmol) (M_n = 4.2x10^3), vinyl dimethoxy triphenyl amine (1.00 g, 3.0 mmol) AIBN (0.70 mg, 4.0 μmol) and 1.5 mL of toluene were added into a 10 mL schlenk tube. The reaction was degassed by three freeze-pump-thaw cycles. Then, the tube was put into a preheated oil bath at 60 °C under stirring. The reaction was quenched in an ice bath and precipitated in MeOH. (**5a**: M_n = 12.6x10^3 g/mol, PDI = 1.11; **5b**: M_n = 34x10^3 g/mol, PDI = 1.20). ^{1}H NMR (300 MHz, $CHCl_3$): δ (ppm) 7.00-6.22 (m, 12H, ArH), 4.71 (s, 2H, OCH_2) 3.62 (s, 6H, OCH_3), 2.54-1.12 (m, 3H, CHC$H_{2,\text{ acrylate}}$, 3H, CHC$H_{2,\text{styrene}}$), 0.20 (s, 9H, $SiMe_3$).

General Procedure for Deprotection to Poly(propargyl acrylate)-*b*-PvDMTPA 6a,b

Polymer **5a,b** (250 mg) was dissolved in 2 mL of THF. Acetic acid (15 mg, 0.25 mmol) and TBAF trihydrate (75 mg, 0.24 mmol) where added. The reaction was stirred over night, precipitated in methanol and filtered. (**6a**: M_n = 9.8x10^3 g/mol, PDI = 1.11; **6b**: M_n = 30x10^3 g/mol, PDI = 1.20). ^{1}H NMR (300 MHz, $CHCl_3$): δ (ppm) 7.07-6.24 (m, 12H, ArH), 4.71 (s, 2H, OCH_2), 3.63 (s, 6H, OCH_3), 2.64-2.36 (m, 2H, CHC$H_{2,\text{acrylate}}$, alkyne$H$), 2.15-1.24 (3H, CHC$H_{2,\text{styrene}}$).

Poly(perylene bisimide alkyl triazol acrylate)-*b*-PvDMTPA 9a,b

Poly(propargyl acrylate)-*b*- PvDMTPA (70 mg) and perylene **7** (50 mg, 0.07 mmol) were dissolved in 2 mL of anisole. The solution was degassed by purging with nitrogen for 10 minutes. Subsequently a preformed complex of PMDETA/CuBr was added through a septum to start the reaction. The mixture was stirred at RT over night, precipitated in methanol and cleaned further by soxhlet extraction with acetone. (**9a**: M_n = 56x10^3 g/mol, PDI = 1.12; **9b**: 18M_n = 98x10^3 g/mol, PDI = 1.13). ^{1}H NMR (300 MHz, $CHCl_3$): δ (ppm) 8.29-7.33 (m, 9H, ArH_{perylene}, triazole-H), 7.00-6.12

(m, 12H, ArH_{TPA}), 5.30 (br s, 2H, OC_2), 5.03 (br s, 2H, N-C*H*), 4.51 (br s, 2H, N-C$H_{2,perylene}$), 3.94 (br s, 2H, N-C$H_{2,triazol}$), 3.61 (br s, 6H, OCH_3), 2.59-1.00 (35H, 17CH_2, C$H_{backbone}$), 0.86 (s, 6H, CH_3).

"Click" Reaction to Poly(perylene bisimide OEG triazol acrylate)-*b*-PvDMTPA 10a,b

Poly(propargyl acrylate)-*b*- PvDMTPA (70 mg) and perylene **8** (55 mg, 0.07 mmol) were dissolved in 2 mL of anisole. The solution was degassed by purging with nitrogen for 10 minutes. Subsequently a preformed complex of PMDETA/CuBr was added through a septum to start the reaction. The mixture was stirred at RT over night, precipitated in methanol and cleaned further by soxhlet extraction with acetone. (**10a**: M_n = 64x10^3 g/mol, PDI = 1.18; **10b**: M_n = 93x10^3 g/mol, PDI = 1.09). ^{1}H NMR (300 MHz, $CHCl_3$): δ (ppm) 8.28-7.12 (m, 9H, Ar$H_{perylene}$, triazole-*H*), 7.00-6.15 (m, 12H, ArH_{TPA}), 5.71 (br s, 2H, OC_2), 5.58 (br s, 2H, N-C*H*), 4.52 (br s, 2H, N-C$H_{2,perylene}$), 4.31-3.92 (m, 4H, CHCH_2O), 3.84-3.40 (m, OCH_2OCH_2O, N-C$H_{2,triazol}$), 3.61 (br s, 6H, OCH_3), 3.32 (m, 6H, OCH_3), 2.31-1.13 (m, 6H, C$H_{2,backbone}$, C$H_{backbone}$).

Bibliography

1. Hains, A. W.; Liang, Z.; Woodhouse, M. A.; Gregg, B. A. *Chemical Reviews* **2010,** 110, (11), 6689-6735.
2. Armstrong, N. R.; Wang, W.; Alloway, D. M.; Placencia, D.; Ratcliff, E.; Brumbach, M. *Macromolecular Rapid Communications* **2009,** 30, (9-10), 717-731.
3. Espinosa, N.; García-Valverde, R.; Urbina, A.; Krebs, F. C. *Solar Energy Materials and Solar Cells* **2011,** 95, (5), 1293-1302.
4. Dennler, G.; Scharber, M. C.; Brabec, C. J. *Advanced Materials* **2009,** 21, (13), 1323-1338.
5. Sommer, M.; Lindner, S. M.; Thelakkat, M. *Advanced Functional Materials* **2007,** 17, (9), 1493-1500.
6. Sommer, M.; Lang, A. S.; Thelakkat, M. *Angewandte Chemie International Edition* **2008,** 47, (41), 7901-7904.
7. Sommer, M.; Hüttner, S.; Wunder, S.; Thelakkat, M. *Advanced Materials* **2008,** 20, (13), 2523-2527.
8. Lindner, S. M.; Hüttner, S.; Chiche, A.; Thelakkat, M.; Krausch, G. *Angewandte Chemie International Edition* **2006,** 45, (20), 3364-3368.
9. Lindner, S. M.; Thelakkat, M. *Macromolecules* **2004,** 37, (24), 8832-8835.
10. Matsen, M. W.; Bates, F. S. *Macromolecules* **1996,** 29, (4), 1091-1098.
11. Leibler, L. *Macromolecules* **1980,** 13, (6), 1602-1617.
12. Zhu, L.; Chen, Y.; Zhang, A.; Calhoun, B. H.; Chun, M.; Quirk, R. P.; Cheng, S. Z. D.; Hsiao, B. S.; Yeh, F.; Hashimoto, T. *Physical Review B* **1999,** 60, (14), 10022.

13. Reining, B.; Keul, H.; Höcker, H. *Polymer* **2002,** 43, (25), 7145-7154.

14. Huang, P.; Guo, Y.; Quirk, R. P.; Ruan, J.; Lotz, B.; Thomas, E. L.; Hsiao, B. S.; Avila-Orta, C. A.; Sics, I.; Cheng, S. Z. D. *Polymer* **2006,** 47, (15), 5457-5466.

15. Binder, W. H.; Sachsenhofer, R. *Macromolecular Rapid Communications* **2007,** 28, (1), 15-54.

16. Binder, W. H.; Sachsenhofer, R. *Macromolecular Rapid Communications* **2008,** 29, (12-13), 952-981.

17. Moad, G.; Rizzardo, E.; Thang, S. H. *Australian Journal of Chemistry* **2005,** 58, (6), 379-410.

18. Chiefari, J.; Chong, Y. K.; Ercole, F.; Krstina, J.; Jeffery, J.; Le, T. P. T.; Mayadunne, R. T. A.; Meijs, G. F.; Moad, C. L.; Moad, G.; Rizzardo, E.; Thang, S. H. *Macromolecules* **1998,** 31, (16), 5559-5562.

19. Moad, G.; Rizzardo, E.; Thang, S. H. *Accounts of Chemical Research* **2008,** 41, (9), 1133-1142.

20. Lang, A. S.; Thelakkat, M. *Polymer Chemistry* **2011**, 10.1039/C1PY00191D.

List of Publications

Manuscripts

Fu, G.-D.; **Lang**, **A. S.;** Zheng, Z.; Yao, F.; Zhang, W.; Müller, A. H. E.; Thelakkat, M.: **Semiconductor Nanoparticles from Donor-Acceptor Dual Brush Block Copolymers**, *Angewandte Chemie Int. Ed.* **2011***, submitted.*

Lang, A. S.; Thelakkat, M.: **Modular Synthesis of Poly(perylene bisimides) using "Click" Chemistry: A Comparative Study**, Polymer Chemistry **2011**, DOI: 10.1039/c1py00191d.

Lang, A. S.; Neubig, A.; Sommer, M.; Thelakkat, M.: **NMRP versus "Click"-Chemistry for the Synthesis of Semiconductor Polymers Carrying Pendant Perylene Bisimides**, *Macromolecules* **2010,** *43*, 7001-7010.

Wicklein, A.; **Lang, A. S.**; Muth, M. A.; Thelakkat, M.: **Swallow-Tail Substituted Liquid Crystalline Perylene Bisimides: Synthesis and Thermotropic Properties**, *Journal of the American Chemical Society* **2009**, *131*, 14442–14453.

Lang, A. S.; Kogler, F. R.; Sommer, M.; Wiesner, U.; Thelakkat, M.: **Semiconductor Dendritic-Linear Block Copolymers by Nitroxide Mediated Radical Polymerization**, *Macromol. Rapid Comm.*, **2009**, *30*, 1243-1248.

Sommer, M.; **Lang, A. S.**; Thelakkat, M.: **Crystalline-Crystalline Donor-Acceptor Block Copolymers**, *Angewandte Chemie Int. Ed.* **2008**, *47*, 7901-7904.

Attended National and International Conventions

12.-16.04.11	*"Controlled/Living Polymerization"*, Antalya, Türkei, **Talk** (Best Oral Presenter Award)
24.-26.02.11	*"Makromolekulares Kolloquium"*, Freiburg, **Poster**
03.-06.10.10	*"Polymers in Biomedicine and Electronics"*, Berlin, **Poster**
24.-25.08.09	*"IRTG Tagung"*, Mainz, **Poster**
31.04.-04.05.09	*"EUPOC 2009"*, Gargnano, Italy
21.-25.07.08	*"8th International Symposium on Functional π-Electron Systems",* Graz, Austria, **Poster**
06.-08.02.08	*International Workshop "Towards Organic Photovoltaics"*, Linz, Austria, **Poster**

Danksagung

Ich möchte mich bei allen herzlichst bedanken, die auf vielfältige Art und Weise zum Gelingen dieser Arbeit beigetragen haben.

Ein besonderer Dank gilt meinem Doktorvater, Prof. Dr. Mukundan Thelakkat der stets Geduld mit mir hatte. Ich danke für die Möglichkeit, unter seiner Leitung mit einem hohen Grad an Freiheit forschen zu dürfen. Auch danke ich für die vielen Diskussionen, die viele Ideen und Anregungen brachten. Die Teilnahme an nationalen und internationalen Fachtagungen, die mir ermöglicht wurde, war eine große Bereicherung, sowohl fachlich als auch kulturell.

Prof. Dr. Hans-Werner Schmidt danke ich für einen sehr gut ausgestatteten Lehrstuhls.

Allen Mitarbeitern der MCI danke ich für die stete Hilfsbereitschaft, die Unterstützung in fachlichen Angelegenheiten, die super Organisation des Lehrstuhls und für die tolle Arbeitsatmosphäre in all den Jahren.
Danke vor allem an diejenigen, die Messgeräte betreut und am Laufen gehalten haben und so verlässliche Messungen ermöglicht haben. Für die Unterstützung bei organisatorischen Angelegenheiten bedanke ich mich besonders bei Petra Weiß.

Danke an meine Praktikanten, Julia Singer, Isabelle Haas, Manuela May, Annika Eckert und Steven Czich, die ich während meiner Doktorarbeit betreuen durfte und die mir bei der einen oder anderen Synthese helfend zur Seite standen.

Vielen Dank an André Wicklein, ohne den die Arbeit am Lehrstuhl um einiges langweiliger gewesen wäre. Wir hatten immer viel zu lachen und haben den Humor des anderen immer gut ergänzt. Danke auch für die vielen fachlichen Diskussionen über Synthesen und Perylene in jeglicher Couleur.

Ein besonderes Dankeschön an meine Laborkollegin Anne Neubig, die all meine ab und zu aufkeimenden Launen ohne zu murren ertragen hat und immer versucht hat mich aufzubauen wenn es mal wieder nicht so lief (oft). Mit dir das Labor zu teilen hat viel Spaß gemacht.

Katharina Neumann danke ich für stete gute Laune die sie mit in die Gruppe gebracht hat. Mit dir zusammen habe ich immer viel Spaß gehabt. Danke auch für die fachlichen Diskussionen mit dir, egal ob ich dir helfen konnte oder du mir, wir haben beide dabei immer was dazugelernt.

Helga Wietasch danke ich für die Hilfe bei einigen Reaktionen und literweise destillierte Lösemittel.

Michael Sommer möchte ich für seine Gesellschaft während meiner ersten Zeit im Labor danken und für die Hilfe bei den ersten wackeligen Schritten im Gebiet der NMRP.

Prof. Dr. Guo-Dong Fu danke ich für die Zusammenarbeit vom Dezember 2009 bis November 2010.

Neben allem Fachlichen möchte ich mich ebenso bei meinen Studienfreunden, insbesondere dem „harten Kern“ der sich nach all den Jahren immer noch gut versteht, für viele frohe Stunden herzlich bedanken.
Kathrin Inzenhofer danke ich dafür, dass sie mir immer eine gute Freundin war. Wir haben so viele Praktika während des Studiums zusammen bestritten und auch sonst so einiges zusammen durchgemacht. Danke, dass ich mich immer mit allem an Dich wenden konnte!
Andreas Hanisch und Matthias Dötterl danke ich dafür, dass die beiden immer etwas mit mir unternommen haben. Danke dafür, dass ihr immer super Ideen hattet!

Martina, dir danke ich für deine Unterstützung, dass du mir immer Mut machst, mich angetrieben und in den richtigen Momenten abgelenkt hast. Ohne dich wäre das letzte Jahr sehr hart geworden.

Den größten Dank schulde ich meinen lieben Eltern und Großeltern, die mich auf jede erdenkliche Art und Weise unterstützt haben und mir während des Studiums und meiner Doktorarbeit den nötigen Rückhalt gegeben haben, ohne welchen ich nie so weit gekommen wäre. Euch ist diese Arbeit gewidmet. DANKE!!!

Erklärung

Die vorliegende Arbeit wurde selbstständig von mir verfasst. Ich habe keine anderen als die angegebenen Hilfsmittel verwendet. Ferner habe ich nicht versucht, woanders eine Doktorarbeit einzureichen.

Bayreuth, August 2011

(Andreas Lang)